



HAL
open science

Développement de nouveaux matériaux d'emballage à partir de micro- et nano-fibrilles de cellulose

Céline Guezenec

► **To cite this version:**

Céline Guezenec. Développement de nouveaux matériaux d'emballage à partir de micro- et nano-fibrilles de cellulose. Autre. Université de Grenoble, 2012. Français. NNT: 2012GRENI067 . tel-00870839

HAL Id: tel-00870839

<https://theses.hal.science/tel-00870839>

Submitted on 8 Oct 2013

HAL is a multi-disciplinary open access archive for the deposit and dissemination of scientific research documents, whether they are published or not. The documents may come from teaching and research institutions in France or abroad, or from public or private research centers.

L'archive ouverte pluridisciplinaire **HAL**, est destinée au dépôt et à la diffusion de documents scientifiques de niveau recherche, publiés ou non, émanant des établissements d'enseignement et de recherche français ou étrangers, des laboratoires publics ou privés.

THÈSE

Pour obtenir le grade de

DOCTEUR DE L'UNIVERSITÉ DE GRENOBLE

Spécialité : Matériaux, Mécanique, Génie Civil, Electrochimie

Arrêté ministériel : 7 août 2006

Présentée par

Céline GUEZENEC

Thèse dirigée par **Alain DUFRESNE** et
codirigée par **Florence GIRARD**

préparée au sein du **Laboratoire du Génie des Procédés
Papetiers**

dans l'**École Doctorale Ingénierie – Matériaux, Mécanique,
Énergétique, Environnement, Procédés de Production**

Développement de nouveaux matériaux d'emballage à partir de micro- et nano- fibrilles de cellulose

Development of new packaging materials
based on micro- and nano-fibrillated
cellulose

Thèse soutenue publiquement le «**20 décembre 2012**»,
devant le jury composé de :

Pr. Hamid KADDAMI

Professeur de l'université de Marrakech, Président

Pr. Nathalie GONTARD

Directrice de recherche à l'INRA, Rapporteur

Pr. Marie-Pierre LABORIE

Professeur de l'université de Freiburg, Rapporteur

Dr. Noël CARTIER

Manager project R&D, Ahlstrom, Membre

Pr. Alain DUFRESNE

Professeur de Grenoble INP, Membre

Dr. Florence GIRARD

Ingénieur de recherche au Centre Technique du Papier, Membre



A mon grand père Henri,

Remerciements

Si on devait établir la formulation de ces trois années de thèse, elle serait composée de dur labeur, d'enrichissements, de curiosité, de persévérance, de belles rencontres, de réussite mais aussi de déceptions, de doutes et de nombreuses remises en questions. Tout au long de ce parcours, de nombreuses personnes ont de près ou de loin apporté leur contribution et il est temps à présent de les remercier.

Tout d'abord, je remercie Véronique Morin au CTP, Naceur Belgacem et Evelyne Mauret au LGP2 pour m'avoir accueillie dans leur équipe de recherche et m'avoir apporté les conditions et les moyens techniques nécessaires à la réalisation de mes travaux.

Je tiens à remercier Alain Dufresne, mon directeur de thèse pour m'avoir encadrée et suivie tout au long de la thèse ainsi que pour ses conseils scientifiques, sa réactivité et sa zénitude. De plus, la liberté qu'il m'a laissée dans mon travail a également contribué à ma progression. Cette thèse n'aurait pas eu lieu si Florence Girard, mon encadrante au CTP, ne m'avait pas confié ce travail et donné sa confiance. Alors merci profondément pour cette belle opportunité. Merci également pour m'avoir accompagnée au cours de ce projet, pour tous tes conseils pratiques, ta rigueur et ton sens du travail carré et précis ainsi que pour ta gentillesse.

A présent, je tiens à adresser toute ma reconnaissance à tous les membres du jury pour le temps qu'ils ont consacré à évaluer mon travail et les échanges intéressants qui ont eu lieu lors de la soutenance. Ainsi, merci au Professeur Hamid Kaddhami d'avoir accepté de présider ce jury, merci aux Professeurs Nathalie Gontard et Marie Pierre Laborie d'avoir été les rapporteurs de ce mémoire, enfin merci au Dr Noël Cartier pour avoir examiné ces travaux et apporté son point de vue industriel à la discussion.

Je tiens à remercier l'agence nationale de la recherche et des technologies (ANRT) pour son support financier. Merci également à l'équipe du projet européen SUNPAP, pour avoir financé une partie de ma thèse et pour les nombreux échanges que nous avons eu avec les différents partenaires lors de nos rencontres.

J'ai partagé ces trois années avec l'équipe de l'UST8 au CTP que je remercie du fond du cœur. En premier lieu, un grand merci à son manager David Guérin pour m'avoir accueillie au sein de son équipe et m'avoir permis de m'y investir. Je tiens aussi à lui exprimer ma sincère reconnaissance pour avoir participé à ces travaux, pour nos divers échanges lors de la rédaction et pour avoir contribué à mon enrichissement scientifique et professionnel durant ces 3 ans. Enfin, merci de m'avoir permis de poursuivre mon chemin au sein de l'UST8 et de continuer notre collaboration.

Merci également à Philippe, alias mon frère, pour sa disponibilité, ses conseils de jeune docteur, son amitié et sa grinta. A présent, je t'attends au 10 km!

L'UST8 ne serait pas ce qu'elle est sans les deux comparses Bernard et Franck que je remercie pour leur bon accueil, leurs conseils pratiques et leur bonne humeur me permettant de passer une agréable journée au laboratoire bien qu'après toute une journée de travail je n'avais toujours pas obtenu les bons réglages à l'endupap. Je tiens également à les

remercier ainsi que Claude et Max pour leur investissement et leur professionnalisme lors des essais pilote, qui a permis la réalisation et la production d'un démonstrateur ce qui n'était pas forcément gagné d'avance. Ainsi merci beaucoup à vous 4.

Enfin merci à Laurent, le roi de l'enduction pour sa disponibilité, tous ses conseils techniques et sa sympathie.

Je n'oublierai pas de remercier Catherine Decroux pour m'avoir permis de boucler la fin de mes manip grâce à sa rigueur exemplaire et à son investissement.

A présent, merci à Valérie et Sandra ainsi qu'à Arthur, Caroline et Christelle pour les diverses productions de MFC et les images de microscopie optique.

Merci également à toute l'équipe de l'UST4, pour m'avoir offert la possibilité de travailler dans leur labo quand j'en avais besoin et m'avoir appris le fonctionnement des différents appareils de mesure.

J'allais également souvent chiner au sein des équipes UST1, UST6 et UST7 qui m'ont toujours bien accueillie, écoutée et aidée comme ils le pouvaient, alors merci.

Merci également à Elisa et Olivier pour m'avoir fait découvrir le CTP et sans qui je ne serais sans doute pas là à vous remercier.

Merci à toute la SUNPAP Team du CTP pour tous nos échanges sur les MFC/NFC et avec qui les déplacements étaient toujours très sympas.

L'entourage a également son importance pour le bon déroulement d'une thèse, ainsi je tiens à remercier Priscilla et son franc parlé, Zizou pour sa convivialité, Olivier et sa tranquillité, Tiphaine et sa gentillesse pour leur soutien, leur camaraderie et les petites pauses café.

Je tiens aussi à remercier ma camarade de bureau Françoise-Stéphanie Ketep. Faisant notre thèse en même temps, on a partagé les hauts et les bas, les réussites comme les déceptions et la période de rédaction où l'on pouvait toujours compter l'une sur l'autre pour se motiver. Merci pour ta joie de vivre, pour m'avoir ouvert l'esprit avec ta culture africaine, pour ton caractère très exigeant et pour nos fous rires. Je serai toujours là pour t'aider en informatique.

Je tiens à faire un gros clin d'œil à toute l'équipe du LGP2, bien que vous ne m'ayez pas beaucoup vu, vous m'avez toujours bien accueillie et aidée dès que j'en avais besoin. Alors merci à tous les doctorants, à Berthine ainsi qu'à Cécile. J'aimerais également remercier Julien Bras pour son investissement dans la vie de l'équipe transfo afin d'offrir de bonnes conditions de travail à tous.

Merci à Stéphane Coindeau du CMTc pour les analyses XRD et pour ses connaissances dans ce domaine.

Je tiens à remercier Lydia Martinez pour sa gentillesse et son aide à la finalisation du mémoire avec ses corrections d'anglais .

Nos petits rendez-vous footing m'ont toujours permis de décompresser alors je tiens à vous dire merci. Merci à Malou, Fred, Laurence, Dominique et Païlan pour ces bons moments passés ensemble malgré des séances de fractionné parfois très difficiles.

Malou, je tiens également à te faire une petite dédicace pour ta gentillesse, tous tes petits tuyaux et tous tes conseils.

Je tiens à remercier tous mes amis bretons qui m'ont toujours soutenue dans ce projet et pour tous les supers moments que nous passons ensemble lors de nos retrouvailles, alors merci à Claudie, Lucie, Adèle, Anne-So, Manon, Virginie, Célia, Ju, Pipo, Gillou, Fanch, Mamat, Yves-Ma et Matthieu.

Pour terminer, je voudrais remercier toute ma famille. Un grand merci à mes parents pour m'avoir soutenue tout au long des mes études, leurs encouragements, leur confiance et leur amour. Merci à ma sœur lillie et mon frère Jérónimo pour votre écoute, votre réconfort et toute la motivation que vous m'avez donnée. Merci à mes grand parents et ma grand-mère pour m'avoir suivie et toujours été derrière moi. Merci tata pour cette grande surprise la veille de ma soutenance, je suis contente que tu ais pu être là le jour J. Merci également pour tous nos échanges qui comptent beaucoup pour moi et qui m'ont un peu guidé dans mes choix.

Enfin, merci à toi Cédric. Je te remercie de partager ma vie depuis 8 ans et ainsi de m'avoir soutenue dans cette belle aventure de la thèse. Merci pour ton écoute toujours très attentionnée, pour ta compréhension, tes conseils, tes encouragements et ta confiance en moi. Merci également d'avoir géré toute la logistique et les petites choses du quotidien durant ma période de rédaction. Les mots ne seront jamais assez fort pour exprimer ma reconnaissance envers toi et je tiens à partager cette réussite avec toi.

Table of contents

General introduction	- 19 -
I - Chapter I : Literature review	- 25 -
I.1. - Introduction.....	- 27 -
I.2. - Introduction to barrier packaging.....	- 27 -
I.2.1. - Packaging definitions.....	- 27 -
I.2.1.1. - Materials used for the packaging.....	- 27 -
I.2.1.2. - Main functions of packaging	- 28 -
I.2.1.3. - Packaging end of life/Recycling.....	- 29 -
I.2.2. - Barrier packaging	- 29 -
I.2.2.1. - Mass transport properties.....	- 29 -
I.2.2.1.1. - Diffusion.....	- 30 -
I.2.2.1.2. - Solubility	- 31 -
I.2.2.1.3. - Permeation	- 31 -
I.2.2.2. - Barrier properties of polymers	- 31 -
I.2.2.2.1. - Influencing factors.....	- 31 -
I.2.2.2.2. - Permeability values for synthetic polymers.....	- 32 -
I.2.3. - Paper&board packaging.....	- 32 -
I.2.3.1. - Coating techniques.....	- 34 -
I.2.3.1.1. - Extrusion coating and lamination	- 34 -
I.2.3.1.2. - Classical coating processes.....	- 35 -
I.2.3.2. - Barrier properties of paper & board packaging	- 37 -
I.3. - Microfibrillated cellulose	- 38 -
I.3.1. - Fibres, nanocrystals and microfibrillated cellulose	- 38 -
I.3.2. - Overview of the production routes of nanocelluloses	- 41 -
I.3.2.1. - Production of cellulose nanocrystals (CNC).....	- 41 -
I.3.2.2. - Production of MFC/NFC	- 42 -
I.3.3. - MFC production	- 43 -
I.3.3.1. - From various sources.....	- 43 -
I.3.3.2. - Pre-treatments	- 44 -
I.3.3.2.1. - Mechanical pretreatment.....	- 44 -
I.3.3.2.2. - Chemical pretreatment.....	- 45 -
I.3.3.2.3. - Enzymatic pretreatment	- 45 -
I.3.3.2.4. - Conclusion	- 46 -
I.3.3.3. - Mechanical treatments	- 46 -
I.3.3.3.1. - Homogenizer	- 47 -
I.3.3.3.2. - Microfluidizer.....	- 48 -
I.3.3.3.3. - Grinder.....	- 48 -
I.3.3.3.4. - Other methods	- 49 -
I.3.4. - Morphology of MFC/NFC	- 49 -
I.3.4.1. - Transmission electron microscopy	- 49 -
I.3.4.2. - Scanning electron microscopy.....	- 52 -
I.3.4.3. - Atomic force microscopy	- 52 -
I.3.5. - Degree of polymerization of cellulose.....	- 53 -

I.3.6. - Rheology of MFC suspensions.....	- 54 -
I.3.7. - MFC films	- 58 -
I.3.7.1. - Production of MFC films	- 58 -
I.3.7.2. - Properties of MFC films	- 59 -
I.3.7.2.1. - Density and porosity	- 59 -
I.3.7.2.2. - Transparency	- 61 -
I.3.7.2.3. - Mechanical properties.....	- 62 -
I.3.7.2.4. - Barrier properties	- 64 -
I.3.7.2.5. - Biodegradability	- 68 -
I.3.7.3. - Conclusion	- 68 -
I.4. - MFC based nanocomposites.....	- 68 -
I.4.1. - Starch matrix.....	- 69 -
I.4.1.1. - Introduction	- 69 -
I.4.1.2. - Mechanical properties	- 70 -
I.4.1.3. - Barrier properties.....	- 71 -
I.4.2. - Poly(vinyl alcohol) matrix.....	- 71 -
I.4.2.1. - Introduction	- 71 -
I.4.2.2. - Mechanical properties	- 72 -
I.4.2.3. - Barrier properties.....	- 73 -
I.4.3. - Conclusion	- 74 -
I.5. - MFC based paper & board materials.....	- 74 -
I.5.1. - Introduction of MFC into pulp.....	- 74 -
I.5.2. - MFC in coating colours	- 75 -
I.6. - Conclusion	- 78 -
II - Materials and methods.....	- 79 -
II.1. - Introduction.....	- 81 -
II.2. - Materials.....	- 81 -
II.2.1. - Microfibrillated cellulose (MFC).....	- 81 -
II.2.1.1. - Commercial MFC	- 82 -
II.2.1.2. - Production of enzymatically pretreated MFC	- 82 -
II.2.1.2.1. - General protocol	- 82 -
II.2.1.2.2. - Enzymatic pretreatment	- 83 -
II.2.1.2.3. - Mechanical treatments.....	- 83 -
II.2.1.3. - Production of TEMPO oxidized MFC	- 84 -
II.2.1.3.1. - General protocol	- 84 -
II.2.1.3.2. - TEMPO oxidation.....	- 84 -
II.2.1.3.3. - Mechanical treatment.....	- 85 -
II.2.2. - Starch	- 86 -
II.2.3. - PVOH	- 86 -
II.2.4. - Sorbitol	- 86 -
II.2.5. - Poly(ethylene oxide).....	- 86 -

II.2.6. - Base boards	- 86 -
II.3. - Experimental methods (for material production)	- 87 -
II.3.1. - Production of MFC films.....	- 87 -
II.3.1.1. - Casting-evaporation technique	- 87 -
II.3.1.2. - Handsheet method	- 87 -
II.3.2. - Development of MFC based composites.....	- 89 -
II.3.3. - MFC based paper & board materials	- 90 -
II.3.3.1. - Increase of MFC solids.....	- 90 -
II.3.3.1.1. - Centrifugation	- 90 -
II.3.3.1.2. - Inverted dialysis	- 90 -
II.3.3.2. - Coating trials at lab scale	- 90 -
II.3.3.2.1. - PVOH solubilisation in MFC suspension	- 90 -
II.3.3.2.2. - Production of coated board at lab scale	- 91 -
II.3.3.3. - Coating trials at pilot scale.....	- 91 -
II.3.3.3.1. - PVOH solubilisation in MFC suspension at pilot scale.....	- 91 -
II.3.3.3.2. - Production of coated board at pilot scale.....	- 91 -
II.4. - Characterisation techniques	- 92 -
II.4.1. - Chemical composition analysis.....	- 92 -
II.4.2. - Microscopic techniques	- 93 -
II.4.2.1. - Optical microscopy	- 93 -
II.4.2.2. - Scanning Electron Microscope (SEM)	- 93 -
II.4.2.3. - Field Emission Gun Scanning Electron Microscope (SEM-FEG)	- 93 -
II.4.2.4. - Transmission electron microscope (TEM).....	- 93 -
II.4.2.5. - Atomic force microscope (AFM)	- 93 -
II.4.2.6. - TOPO 3D	- 93 -
II.4.3. - Viscosity measurements	- 94 -
II.4.3.1. - Brookfield viscosimeter.....	- 94 -
II.4.3.2. - Rheometer	- 94 -
II.4.4. - Transparency properties	- 95 -
II.4.5. - Surface roughness testing.....	- 95 -
II.4.6. - Density of materials.....	- 96 -
II.4.6.1. - Basis weight.....	- 96 -
II.4.6.2. - Coat weight measurements.....	- 96 -
II.4.6.3. - Thickness	- 96 -
II.4.7. - Mechanical properties	- 96 -
II.4.7.1. - Tensile tests	- 96 -
II.4.7.2. - Burst measurements	- 97 -
II.4.7.3. - Tear measurements	- 97 -
II.4.8. - Barrier properties.....	- 97 -
II.4.8.1. - Water absorption capacity (Cobb measurements).....	- 97 -
II.4.8.2. - Grease absorption capacity (Cobb measurements).....	- 98 -
II.4.8.3. - Sorption behaviour of paper at several relative humidities.....	- 98 -
II.4.8.4. - Bendtsen air permeability	- 98 -
II.4.8.5. - Water vapour transmission rate.....	- 98 -

II.4.8.6. - Oxygen transmission rate.....	- 99 -
II.4.9. - Mercury porosimetry	- 99 -
II.4.10. - X-ray diffraction	- 100 -
II.4.11. - Thermal properties	- 100 -
II.4.11.1. - DSC	- 100 -
II.4.11.2. - TGA.....	- 100 -
III - Study of microfibrillated cellulose suspensions/films	- 101 -
III.1. - Introduction	- 103 -
III.2. - Characterisation and comparison of several grades of MFC suspensions-	104 -
III.2.1. - Visual aspect of MFC suspensions	- 105 -
III.2.2. - Influence of the fibrillation process on the MFC morphology	- 105 -
III.2.3. - Optical microscopy.....	- 105 -
III.2.3.1. - SEM-FEG.....	- 108 -
III.2.3.2. - TEM	- 110 -
III.2.3.3. - Conclusion	- 110 -
III.2.4. - Chemical composition analysis of MFC.....	- 111 -
III.2.5. - Influence of the fibrillation state on the rheological behaviour of MFC	suspensions.....
III.2.5.1. - Viscosity of MFC produced by enzymatic pretreatment	- 112 -
III.2.5.1.1. - Conditions of viscosity measurements	- 112 -
III.2.5.1.2. - Influence of the degree of fibrillation.....	- 113 -
III.2.5.1.3. - Determination of flow behaviour.....	- 115 -
III.2.5.1.4. - Comparison of MFC suspensions	- 116 -
III.2.5.1.5. - Influence of the production scale.....	- 117 -
III.2.5.2. - Viscosity of MFC produced by TEMPO oxidation pretreatment	- 118 -
III.2.5.3. - Conclusion	- 119 -
III.2.6. - Conclusion	- 119 -
III.3. - Development of MFC films	- 120 -
III.3.1. - Production of MFC films.....	- 120 -
III.3.1.1. - Film production by casting/evaporation	- 120 -
III.3.1.2. - Films production by the Handsheet method.....	- 121 -
III.3.1.3. - Comparison between the two techniques	- 123 -
III.3.2. - Properties of enzymatic MFC films: Influence of the fibrillation and process-	124 -
III.3.2.1. - Physical properties and morphology of MFC films	- 124 -
III.3.2.1.1. - SEM-FEG images	- 124 -
III.3.2.1.2. - Film density.....	- 125 -
III.3.2.1.3. - Determination of the roughness by topography.....	- 126 -
III.3.2.1.4. - Mercury porosimetry	- 127 -
III.3.2.1.5. - Bendtsen permeability.....	- 129 -
III.3.2.1.6. - XRD diffraction: Determination of the crystallinity index	- 130 -
III.3.2.2. - Measurement of transparency	- 131 -

III.3.2.3. - Mechanical properties of MFC films.....	- 132 -
III.3.2.3.1. - Tensile tests.....	- 132 -
III.3.2.3.2. - Burst index.....	- 135 -
III.3.2.3.3. - Tear resistance	- 135 -
III.3.2.3.4. - Conclusion	- 136 -
III.3.2.4. - Barrier properties of MFC films.....	- 136 -
III.3.2.4.1. - Grease resistance.....	- 136 -
III.3.2.4.2. - Water resistance	- 137 -
III.3.2.4.3. - Water vapour transmission rate (23°C-50% RH).....	- 138 -
III.3.2.4.4. - Oxygen transmission rate (23°C-0% RH).....	- 140 -
III.3.2.5. - Conclusion	- 141 -
III.3.3. - Influence of the TEMPO pretreatment on MFC film properties.....	- 142 -
III.3.3.1. - SEM-FEG images	- 142 -
III.3.3.2. - Roughness measurement by topography	- 143 -
III.3.3.3. - Mercury porosimetry.....	- 143 -
III.3.3.4. - Properties of TEMPO oxidized MFC films.....	- 145 -
III.3.3.5. - Conclusion	- 147 -
III.3.4. - Conclusion	- 147 -
III.4. - Addition of sorbitol in MFC films	- 148 -
III.5. - Conclusion	- 148 -
IV - Development of MFC based nanocomposites.....	- 151 -
IV.1. - Introduction.....	- 153 -
IV.2. - Manufacture protocol of MFC composites	- 154 -
IV.3. - Influence of MFC addition on the starch matrix properties.....	- 157 -
IV.3.1. - Introduction	- 157 -
IV.3.2. - Structure of starch/MFC composites	- 157 -
IV.3.2.1. - Visual aspect	- 158 -
IV.3.2.2. - Thickness and density of films	- 159 -
IV.3.2.3. - Polarized light microscopy	- 160 -
IV.3.2.4. - SEM-FEG	- 161 -
IV.3.3. - Mechanical properties of starch/MFC composites.....	- 162 -
IV.3.4. - Barrier properties of starch/MFC composites	- 165 -
IV.3.4.1. - Water vapour transmission rate	- 165 -
IV.3.4.2. - Oxygen permeability	- 167 -
IV.3.5. - Influence of MFC addition on the structure of starch film.....	- 168 -
IV.3.5.1. - X-ray diffraction.....	- 168 -
IV.3.5.2. - DSC measurements.....	- 168 -
IV.3.5.3. - TGA experiments	- 169 -
IV.3.6. - Study of the influence of sorbitol addition	- 170 -
IV.3.6.1. - Structure of starch/S/MFC films	- 171 -
IV.3.6.1.1. - Visual aspect	- 171 -
IV.3.6.1.2. - Thickness and density	- 172 -

IV.3.6.1.3. - SEM-FEG	- 172 -
IV.3.6.2. - Mechanical properties	- 172 -
IV.3.6.2.1. - Tensile properties	- 172 -
IV.3.6.2.2. - TGA analysis	- 174 -
IV.3.6.2.3. - Conclusion.....	- 175 -
IV.3.6.3. - Barrier properties	- 175 -
IV.3.7. - Conclusion.....	- 177 -
IV.4. - Influence of MFC addition on the PVOH matrix properties	- 177 -
IV.4.1. - Introduction	- 177 -
IV.4.2. - Structure of PVOH/MFC composites.....	- 178 -
IV.4.2.1. - Visual aspect	- 178 -
IV.4.2.2. - Thickness and density of films	- 179 -
IV.4.2.3. - SEM-FEG images	- 179 -
IV.4.3. - Mechanical properties of PVOH/MFC composites	- 180 -
IV.4.4. - Barrier properties of PVOH/MFC composites.....	- 184 -
IV.4.4.1. - Water vapour transmission rate at 23°C-50% RH	- 184 -
IV.4.4.2. - Water vapour transmission rate at 38°C-90% RH	- 185 -
IV.4.4.3. - Water sorption of PVOH/MFC films.....	- 186 -
IV.4.4.4. - Oxygen transmission rate at 23°C-0% RH	- 187 -
IV.4.5. - Thermal behaviour of PVOH/MFC composites	- 187 -
IV.4.5.1. - Differential scanning calorimetry	- 187 -
IV.4.5.2. - Thermogravimetric analysis (TGA).....	- 189 -
IV.4.6. - Effect of thermal treatment on the PVOH/MFC films.....	- 189 -
IV.4.6.1. - DSC analysis	- 190 -
IV.4.6.2. - Water solubility.....	- 190 -
IV.4.7. - Conclusion.....	- 191 -
IV.5. - Comparison of the properties of starch/MFC and PVOH/MFC nanocomposite properties.....	- 191 -
IV.6. - Conclusion.....	- 192 -
V - Development of barrier packaging board based on MFC	- 193 -
V.1. - Introduction	- 195 -
V.2. - Optimisation of the formulation and coating parameters at lab scale-	196 -
V.2.1. - Introduction	- 196 -
V.2.2. - Matrix selection	- 196 -
V.2.3. - Preparation of coating colours.....	- 196 -
V.2.3.1. - Influence of MFC addition on the coating colour solids.....	- 196 -
V.2.3.2. - Methods tested to increase the concentration of MFC based coating colour ..	- 198 -
V.2.3.2.1. - Increase of MFC concentration by centrifugation	- 198 -
V.2.3.2.2. - Increase of MFC concentration by inverted dialysis	- 200 -
V.2.3.2.3. - Direct solubilization of PVOH in MFC suspension.....	- 200 -

V.2.3.3. - Preparation of PVOH/MFC coating colour.....	- 202 -
V.2.4. - Viscosity measurement and choice of the coating technology	- 202 -
V.2.5. - Production of coated board samples using rod meyer coating.....	- 203 -
V.2.6. - Characterisation of PVOH/MFC coated boards	- 204 -
V.2.6.1. - Observation of the surface by SEM.....	- 204 -
V.2.6.2. - Properties of coated board samples.....	- 205 -
V.2.6.2.1. - Thickness and coat weight	- 205 -
V.2.6.2.2. - Mechanical properties.....	- 205 -
V.2.6.2.3. - Barrier properties.....	- 206 -
V.2.7. - Comparison with PVOH/MFC composite results.....	- 208 -
V.2.8. - Conclusion.....	- 209 -
V.3. - Development of PVOH/MFC barrier layer from lab to pilot scale.....	- 209 -
V.3.1. - Introduction	- 209 -
V.3.2. - Formulation of the grease/O₂ barrier layer	- 209 -
V.3.3. - Runnability.....	- 210 -
V.3.3.1. - Parameters to control.....	- 210 -
V.3.3.2. - Rheological behaviour of PVOH/MFC coating colours	- 211 -
V.3.3.3. - Brookfield viscosity of formulations	- 212 -
V.3.4. - Sample production	- 213 -
V.3.5. - Characterisations of coated boards.....	- 215 -
V.3.5.1. - Thickness and basis weight	- 215 -
V.3.5.2. - Surface observation	- 216 -
V.3.5.2.1. - SEM images	- 216 -
V.3.5.2.2. - AFM.....	- 218 -
V.3.5.3. - Mechanical properties.....	- 219 -
V.3.5.4. - Barrier properties	- 221 -
V.3.5.4.1. - Grease resistance	- 221 -
V.3.5.4.2. - Cobb index 60s measurements	- 222 -
V.3.5.4.3. - Cobb index 300s measurements	- 223 -
V.3.5.4.4. - Water vapour permeability	- 225 -
V.3.5.4.5. - Oxygen permeability (23°C-0% RH)	- 228 -
V.3.6. - Discussion	- 229 -
V.3.6.1. - Study of drying rate.....	- 229 -
V.3.6.2. - Influence of MFC on PVOH viscosity	- 230 -
V.3.7. - Conclusion.....	- 231 -
V.4. - Production of barrier packaging materials using MFC at pilot scale .-	- 232 -
V.4.1. - Production of demonstrator with additional top coating layer	- 232 -
V.4.1.1. - Production of samples.....	- 232 -
V.4.1.2. - Mechanical properties	- 232 -
V.4.1.3. - Barrier properties	- 233 -
V.4.1.3.1. - Water resistance.....	- 233 -
V.4.1.4. - Water vapour transmission rate	- 233 -
V.4.1.5. - Oxygen transmission rate at 23°C-0% RH.....	- 234 -
V.5. - Comparison with other packaging materials.....	- 235 -

V.5.1. - Comparison with the literature values	- 235 -
V.5.2. - Comparison with existing materials	- 235 -
V.6. - Converting	- 236 -
V.7. - Biodegradability	- 236 -
V.7.1. - Biodegradability of paper board samples	- 237 -
V.7.2. - Degradation tests in simulated composting conditions	- 237 -
V.7.3. - Ecotoxicity effects of final compost	- 238 -
V.7.4. - Conclusion.....	- 239 -
V.8. - Conclusion.....	- 239 -
General conclusion and perspectives.....	- 241 -
Literature cited	- 247 -
List of abbreviations	- 261 -
Résumé étendu	- 263 -

General introduction

The packaging industry is an industrial sector in constant evolution. The new regulations as well as the societal, economic and technological trends encourage industry to seek lighter, more performing, more eco-friendly and more competitive products.

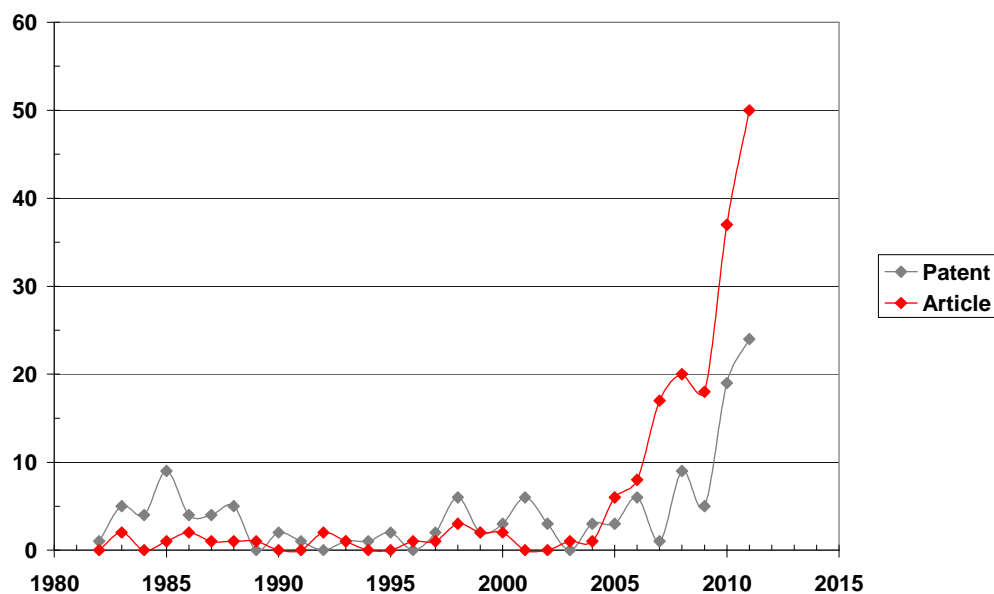
Most food contact packaging materials are currently manufactured either from plastic or from a combination of paper/board with petroleum based polymers. Indeed, these synthetic polymers offer good barrier and mechanical properties so far associated with a low cost. However, these materials derived from petroleum have major drawbacks:

- Their non-renewable origin,
- Their cost-index linked to oil prices,
- Their poor recyclability,
- Their environmental impact.

With today's view toward sustainable development, there is an increasing interest in replacing these polymers with materials derived from renewable resources. Moreover, the use of nanoparticles is promising for the development of lighter and stronger materials with improved functions. One of these new nanoscale renewable alternatives [1] is the micro/nanofibrillated cellulose (MFC/NFC).

MFC results from the disintegration of cellulose fibres by a mechanical shearing treatment. Several studies have shown that this material is highly interesting because it offers good barrier properties coupled with mechanical resistance.

There is a growing interest in microfibrillated cellulose, as represented by the increase of the number of publications [2] on this topic as shown below.



Annual number of scientific publications and patents with the term "microfibrillated cellulose" [2]

Here, the trend was only reported for the publications with the term "microfibrillated cellulose". However, the nomenclature for this material is not clearly defined yet and authors use various terminologies for the same product.

Therefore, microfibrillated cellulose can also be described by other terms such as:

- Cellulose nanofibrils
- Cellulose microfibrils
- Cellulose nanofibers
- Nanocellulose

This list is not exhaustive and a more extensive description can be found elsewhere [3]. The number of articles would thus be more important if all these terms had been taken into account. A project of standard is currently being investigated to clarify and define terms for nanoparticles produced from cellulosic material [4]. The term “microfibrillated cellulose (MFC)” is used throughout this memory and is referring to the first term defined in the literature by Turbak *et al.* [5].

In 2009, the studies concerning MFC were totally focused on their production and application at the lab scale. A European project called SUNPAP (NMP4-LA-2008-228802) started thus to scale up the nanoparticles in modern papermaking. Twenty three partners were associated in this project for a period of 3 years. The main objectives of this project were:

- Development and up-scaling of novel processes for the energy-efficient production of nanomaterials, namely MFC, at the pilot scale.
- Exploitation of innovative sustainable solutions for the whole paper industry value chain by integrated sustainability assessment approaches based on economical, social and environmental impact assessments.
- To enable the introduction of NFC based processes to various types of applications in the papermaking value chain.

This thesis was achieved in the frame of an international research programme at the CTP (NanoMat) and forms part of this SUNPAP European project. More particularly, this work was associated with the work package application, dealing with the application of MFC to modern papermaking in bulk or in standard and advanced coating systems. The main objective was to develop a barrier packaging board material using MFC. The thesis was divided into three main phases with the study of the intrinsic properties of MFC, the development of MFC based composites as model films and then the introduction of MFC in coating colour to develop a barrier layer at the board surface.

This thesis has thus been organized in five chapters: from the characterization of MFC materials to their use in coating processes.

The first chapter corresponds to the literature review giving an overview of the production of MFC, their characterisation and their properties. Then the influence of MFC addition in a polymer matrix and its reinforcing effect were detailed before the use of MFC in papermaking process. This allows the identification of different challenges to take up for the up-scaling of MFC use.

The second chapter describes the materials and methods with an overview of the different types of MFC used and their production methods. The experimental protocols to develop films and paper & board materials and the characterisation methods are also reported.

The three following chapters focus on the results obtained throughout the project. Therefore, the third chapter firstly describes the influence of the fibrillation process on the properties of MFC suspensions. The morphology of the nanoparticles and the viscosity of the suspensions

were characterised using respectively microscopic observations and rheological measurements. A second part is dedicated to the development of MFC films in order to study their intrinsic properties. A comparison of the film properties was established according to the technique employed for the film production and to the pulp pretreatment. Eventually, the addition of sorbitol is a suggested strategie to improve the MFC film properties.

Chapter four is devoted to the development of MFC composites from starch or poly(vinyl-alcohol) matrix. The influence of MFC on the mechanical and barrier properties was evaluated and the effect on the film structure was analysed. In the case of starch, the influence of plasticizer addition was also assessed, and the final properties were compared with those of unplasticized composite films. To conclude, the best matrix was selected for the development of barrier packaging material by coating process.

The last chapter reports the potential of MFC to develop a barrier layer at the board surface. After a preliminary study at lab scale, trials were carried out at pilot scale with the production of a final packaging demonstrator. The barrier efficiency was measured and compared with packaging materials existing on the market. Converting ability and biodegradability were tested in order to explore the possible industrial application of this final product.

Finally, after the general conclusion, some perspectives are proposed.

I - Chapter I : Literature review

I.1. - Introduction

The packaging manufacturing sector needs a constant innovation and researches to develop biosourced materials with high barrier performances. The objective of this study is to propose an alternative to petroleum based polymers and to develop a technological and economical competitive barrier material using microfibrillated cellulose (MFC). The research focus on several aspects such as:

- The characterisation of MFC suspensions according to their production process.
- The mechanical and barrier properties of films produced from pure microfibrillated cellulose or from the combination of a polymer matrix and MFC.
- The development of MFC barrier layers by a coating process.

This chapter firstly gives an overview on the actual packaging market and its needs. The MFC production techniques are then described as well as the improvements carried out to reduce the production energy costs. The techniques for MFC characterisation are also detailed and their limits discussed. Lastly, the use of MFC in composites or in paper&board materials is tackled equally with its advantages and its drawbacks.

I.2. - Introduction to barrier packaging

I.2.1. - Packaging definitions

I.2.1.1. - Materials used for the packaging

The last 200 years have seen the packaging evolving from being a simple container for the product to becoming an important element of total product design. The extension from packing tomato ketchup in glass bottles to squeezable co-extruded multi-layer plastic bottles with oxygen barrier materials for long shelf life [6] is an example.

Indeed, with the consumer society, the human evolution and innovation and the way of life changes, packaging materials have significantly advanced and became highly efficient. In the 21th century, the consuming packaging materials are thus more and more present and diversified in the life of consumers [7].

In 2008, 12.8 millions tons of packaging materials were put on the market in France [8]. This corresponds to 200kg/inhabitant/year. On a European Union scale, the average quantity reached 166kg/inhabitant/year corresponding to 83.6 millions tons [9]. The packaging materials are divided into 5 main sections: papers & boards, plastics, glass, wood and metals.

Figure I-1 details the ton distribution of materials used for packaging application. Papers & boards represent the most used material in tons with a part of 35% in France and 42% in Europe [8,10].

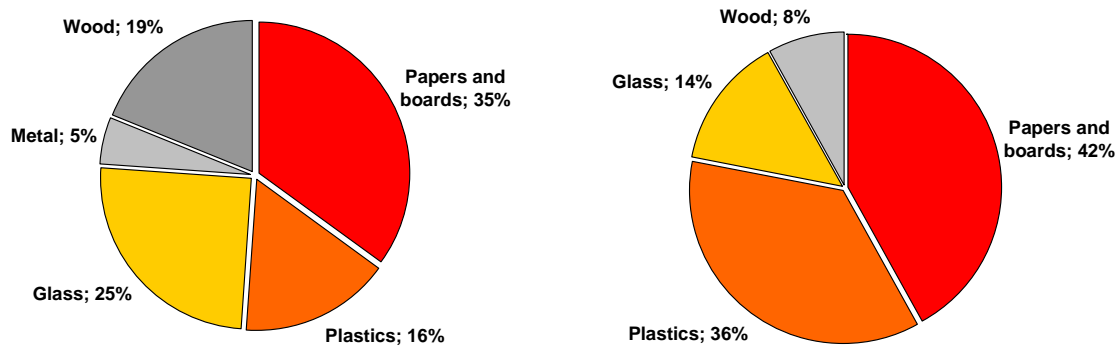


Figure I-1: Materials used in France (left) and in Europe (right) for packaging [8, 10].

I.2.1.2. - Main functions of packaging

Packaging materials are manufactured according to the packed product. Their main functions are [11]:

- To transport,
- To contain (food, goods),
- To protect products from the environment, or environment from products,
- To identify and to inform on the product,
- To attract for the promotion of sales, for advertising,
- To express the brand values.

High mechanical strength is required to provide the transportation. The required properties for the material used are thus: good breaking length, sufficient tearing resistance, and high burst index.

In order to carry out the storage, interactions between the product, the package and the environment must be assessed. Three kinds of interactions are possible:

- The migration corresponding to the transfer of package components to the packed product.
- The sorption is an opposite phenomenon with the transfer of product components to the package.
- The permeation is the transfer of components through the packaging material from inside to outside or from outside to inside.

These interactions can lead to undesirable effects as for example:

- An increase or a loss of humidity,
- Oxidation phenomenon,
- Gas loss,
- Degradation of active elements,
- Alteration of food flavour.

To limit the interactions between the inside and the outside of the package and preserve the food quality, the matter transfers should be reduced by the development of barrier properties. Different types of barrier may be required including gas (O_2 , CO_2 , N_2 , ethylene), water vapour, aroma, light or grease.

Barrier properties are adapted according to the packed product.

I.2.1.3. - Packaging end of life/Recycling

Packaging has many advantages such as food loss reduction, health protection and making life easier. However, their use also showed drawbacks like the use of raw material and energy, difficulties to reuse and recycle, and voluminous waste. That's why, the package end of life must be considered during the development of new materials.

Table I-1 shows the different ways used in Europe for the paper&cardboard packaging waste treatment. Recycling is mainly used for these materials with a percentage reaching 80%.

Largest consumers	Paper&cardboard packaging waste	Recycling		Incineration		Landfill	
		[%]	[Mt/a]	[%]	[Mt/a]	[%]	[Mt/a]
Germany	7.1	80%	5.7	18%	1.3	2%	0.1
Italy	4.6	70%	3.2	8%	0.4	22%	1.0
France	4.5	89%	4.0	8%	0.4	3%	0.1
United Kingdom	3.8	79%	3.0	8%	0.3	13%	0.5
Total	20	80%	15.9	12%	2.3	9%	1.8

Table I-1: Paper&cardboard packaging waste treatments [12, 13].

The data for the plastic packaging waste, collected in Table I-2, presents a different assessment. The recycling of plastic packaging waste is only 29% with a higher percentage of 43% in Germany. An equivalent repartition is observed between recycling, landfill and incineration. Contrary to recycling, the landfill and incineration processes have more impact on the environment.

Largest consumers	Plastic packaging waste	Recycling		Incineration		Landfill	
		[%]	[Mt/a]	[%]	[Mt/a]	[%]	[Mt/a]
Germany	2.6	43%	1.1	52%	1,4	5%	0.1
Italy	2.2	28%	0.6	30%	0,7	42%	0.9
France	2.1	21%	0.4	32%	0,7	47%	1.0
United Kingdom	2.1	22%	0.5	9%	0,2	69%	1.4
Total	9	29%	2.6	32%	2,9	39%	3.5

Table I-2: Plastic packaging waste treatments [12, 13].

During the development of new packaging boards, the end of life must be considered in order to reduce the waste treatment and use of raw material. For a good recycling rate, the use of paperboard materials in packaging must be favoured and the one of plastics limited.

I.2.2. - Barrier packaging

The aim of barrier packaging is to reduce the mass transport properties in order to limit their undesirable effects and increase the shelf life duration of the food and beverage.

I.2.2.1. - Mass transport properties

The mass transport (transfer) is performed by diffusion mechanisms depending on the nature of the permeant molecule (liquid or gas) and on the nature of the packaging material

(homogeneous or porous) [14]. Three coefficients are used to describe the transport properties through a package: diffusion (motion speed), solubility, and permeation (molecule transport speed) [15,16,17].

I.2.2.1.1. - Diffusion

The diffusion is induced by the random motion of small molecules through a material from a highly concentrated side to a less concentrated side until reaching an equilibrium. This phenomenon is generally described in three steps: the molecules are firstly adsorbed at the membrane surface, secondly the diffusion through the material takes place, and finally the desorption occurs on the opposite side. Figure I-2 describes this mechanism.

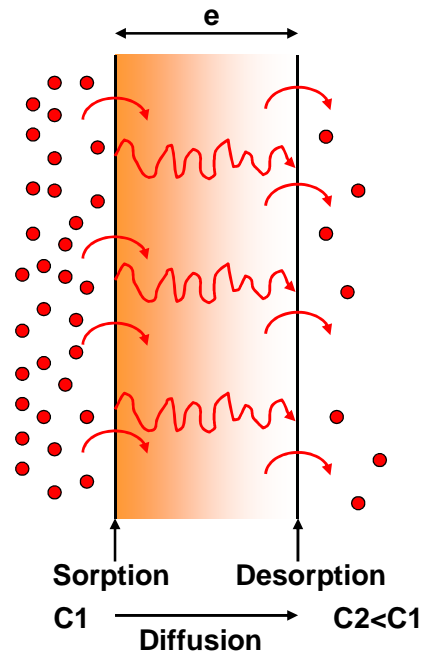


Figure I-2: Schematic representation of permeation [14].

The diffusion is defined by the Fick's law, based on the proportionality between the rate of transfer of the diffusing substance through a unit area and the concentration gradient. In the case of unidirectional diffusion, this corresponds to the following equation [16]:

$$J = -D \frac{\partial C}{\partial x} \quad (\text{Eq.1})$$

Where: - J is the mass flux ($\text{kg}/\text{m}^2 \cdot \text{s}$),
 - D the diffusion coefficient (m^2/s),
 - C the concentration of the diffusing molecule (kg/m^3),
 - x the diffusion axis.

In the case of compact (dense) materials, the flux can be expressed by:

$$J = D \frac{(C_1 - C_2)}{e} \quad (\text{Eq.2})$$

where e is the membrane thickness, C_1 and C_2 are the permeant concentration on both sides of the membrane.

However, for porous materials it is likely that molecules pass through large, non adsorbing pores [18]. From the Matthews and Spearing formula [19], the porosity (ϵ) and the tortuosity (ζ) must be included in the calculation:

$$J = \frac{\varepsilon}{\tau} D \frac{(C_1 - C_2)}{e} \quad (\text{Eq.3})$$

I.2.2.1.2. - Solubility

Adsorption and desorption characterize the affinity of a given substance for two media with which it comes into contact [17].

Henry's law is applied to link the surface concentration of a gas component with the partial pressure in the atmosphere in which the material is in contact:

$$C = S.p \quad (\text{Eq.4})$$

where C is the concentration of the solute (mol/m³), S is Henry's solubility (mol/m³/Pa) and p is the partial pressure of the solute (Pa).

From this equation, the flux can thus be expressed as:

$$J = DS \frac{(P_1 - P_2)}{e} \quad \text{or} \quad J = \frac{\varepsilon}{\tau} DS \frac{(P_1 - P_2)}{e} \quad (\text{Eq.5, Eq.6})$$

where P₁ and P₂ are the partial pressure of each side of the membrane.

I.2.2.1.3. - Permeation

Permeation is the ability of permeates to penetrate and pass right through an entire material in response to a difference in partial pressure.

Permeability includes both kinetic (diffusion) and thermodynamic (solubility) properties of the polymer/permeate system. The permeability (Pe) is thus expressed in kg/m.s.bar by the combination of the diffusion coefficient and the solubility coefficient:

$$Pe = D.S \quad \text{or} \quad Pe = \frac{\varepsilon}{\tau} DS \quad (\text{Eq.7, Eq.8})$$

$$J = \frac{Pe(p_1 - p_2)}{e} \quad (\text{Eq.9})$$

I.2.2.2. - Barrier properties of polymers

I.2.2.2.1. - Influencing factors

For polymers, various parameters can influence the barrier properties of the material. Indeed, the diffusion and solubility coefficients depend on physical and physico-chemical parameters such as:

- The polymer morphology:

The crystalline part of the polymer strongly reduces the permeability rates of gases contrary to the amorphous part. The free volume influences the permeant mobility.

- The nature and concentration of the diffusing substance:

The molecule size influences the diffusion. The molecule affinity with the polymer influences the solubility.

- The temperature:

Pe increases with temperature according to the Arrhenius law: $D = D_0 \exp\left(-\frac{E_a}{RT}\right)$

where D₀ is the maximum diffusion coefficient at infinite temperature, E_a the activation energy of molecules, R the gas constant, and T the temperature.

- The humidity:

The relative humidity has very significant effects on the permeability of flexible films. The permeability increases with the increase of relative humidity for hygroscopic material. For example, the barrier properties of nylon, poly(vinyl alcohol) or cellophane are reduced when increasing the relative humidity [20].

The storage conditions (temperature, humidity & light) have an influence on the barrier properties of packages and it is essential to adapt the choice of the material according to these parameters.

I.2.2.2.2. - Permeability values for synthetic polymers

In the barrier packaging industry, aluminium foil is widely regarded as the standard material [11]. To reduce the cost and the weight of packages, various systems have been developed by lamination of high barrier polymers such as poly(vinylidene chloride), ethylene vinyl alcohol copolymer, and poly(vinyl alcohol). These synthetic polymers have a very low oxygen transmission rate but only in the dry state as shown in Table I-3 [21].

Polymer	Oxygen permeability at 23°C-50% or 23°C-0% RH (cm³.µm/m².day.bar)	Water vapour permeability at 23°C-85% RH (g.µm/m².day)
Poly(ethylene terephthalate) (PET)	987- 4935	500 – 2000
Polypropylene (PP)	49350-98700	200 - 400
Polyethylene (PE)	49350-197400	500 – 2000
Polystyrene (PS)	98700-148050	1000 – 4000
Poly(vinyl chloride) (PVC)	1974-7896	1000 – 2000
Poly(ethylene naphtalate) (PEN)	493	700
Polyamide (PA)	99 – 987 (dry)	500 – 10000
Poly(vinyl alcohol) (PVAL)	20 (dry)	30000
Ethylene vinyl alcohol (EVOH)	0.99 – 9.9 (dry)	1000-3000
Poly(vinylidene chloride) (PVDC)	9.9 – 296 (dry)	100

Table I-3: Gas barrier properties of synthetic polymers [21].

Nevertheless, the use of plastics has an environmental impact and there is a growing interest to replace petrochemical polymers by more environmentally friendly materials.

I.2.3. - Paper&board packaging

Paper & boards are used for many applications such as graphic paper, sanitary & household, newsprint and packaging application (Figure I-3). The production of case material is 26.3% corresponding to more than half of the production of paper&board packaging [22].

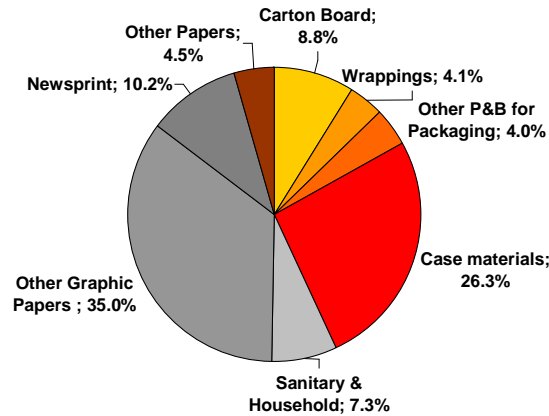


Figure I-3: Paper consumption according to market segment [22].

Concerning the use of papers&boards for barrier and functional packaging, boards are mainly converted into liquid packages as shown Figure I-4 [23].

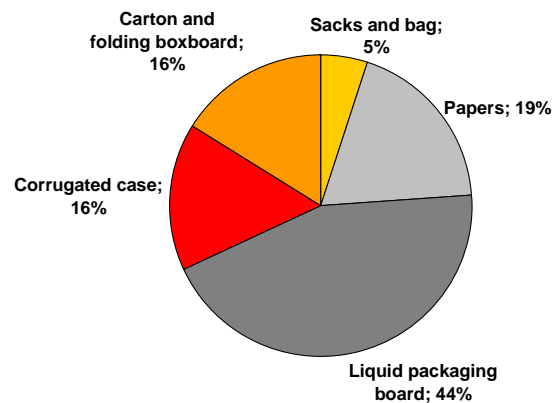


Figure I-4: Market for functional and barrier coatings by grade of paper or board [23].

From the environmental point of view, paper and board materials have a lower impact compared to other packaging materials [24]. However, paper&board materials have some drawbacks (Table I-4) such as low barrier properties (water and grease resistance, water vapour and gas permeability).

Advantages	Disadvantages
Low density Good stiffness Can be creased and folded Can be glued with adhesives Not brittle, but not as strong as many plastics, metals or glasses Several grades have inherent grease resistance Excellent surface for inexpensive printing Many products are approved for direct food contact Repulpable and amenable to recycling processes Better resistance to high and low temperatures than many plastics Low cost	Permeable to water, water vapour, aqueous solutions, emulsions, organic solvents, gases, volatile flavours and aromas Most grades are not resistant to grease or fatty substances Not heat-sealable by itself but it can be glued

Table I-4: Advantages and disadvantages of paper packaging [11].

To improve the paper properties, several treatments can be used [14]:

- A chemical or physical reaction at the paper surface to improve its water or grease resistance. The vegetal parchment, used for packed cheese for instance, is an example. This paper is formed from blotter paper by acid hydrolysis and possesses a good grease resistance [14].
- Treatment of the pulp with a barrier solution before or after the sheet formation.
- The production of complex materials by lamination, extrusion or both of barrier films. The combination of a paper/board, an aluminium foil and a polymer film is often used to obtain a rigid, barrier and thermo sealable materials.
- The application of barrier materials by coating process. This online process presents the advantage of being in-line compared to the off-line extrusion or laminating processes. The deposited products are generally waxes and paraffins, fluorinated products or water based polymer dispersions.

I.2.3.1. - Coating techniques

I.2.3.1.1. - Extrusion coating and lamination

Two major off-line processes are used to produce complexes, by combining board with polymer films. Figure I-5 presents one of these techniques, i.e. the extrusion coating. The major polymers used are: polyethylene, polypropylene, polyamide, or polyethylene terephthalate.

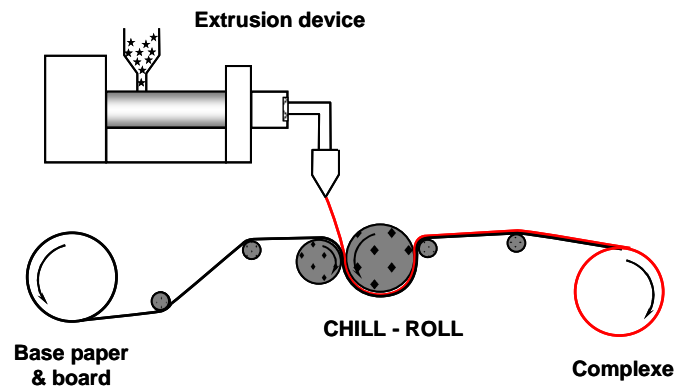


Figure I-5: Extrusion coating process [14].

The second technique is the lamination process (Figure I-6). In this case, the paper&board base is combined to the polymer or aluminium foil using an adhesive.

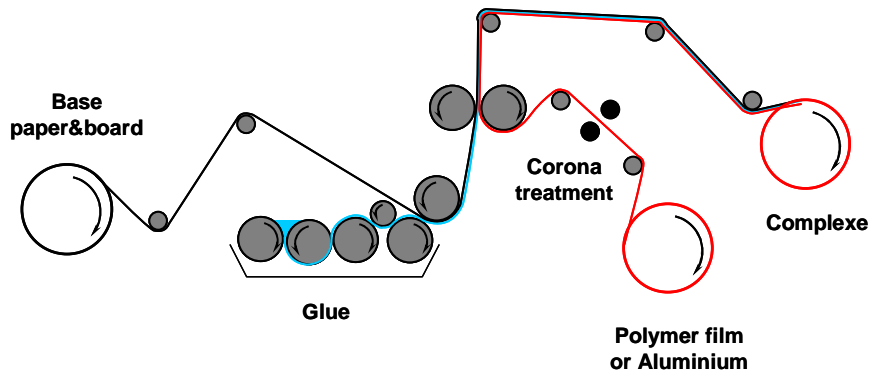


Figure I-6: Lamination process [14].

I.2.3.1.2. - Classical coating processes

The three main coating techniques used for the paper surface treatment are illustrated in the followed figures (Figure I-7, Figure I-8, Figure I-9). Firstly, Figure I-7 presents the metering size press coating. This technique is the most commonly used process in the paper industry and generally used for low coat weight.

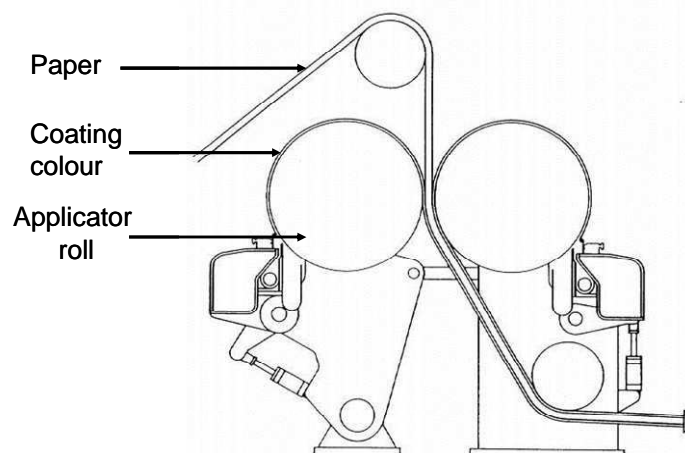


Figure I-7: Scheme of metering size press [25].

The blade coating is described in Figure I-8. The rod coating is based on the same principle; the blade is replaced by the wire-wound rod. The blade and rod coatings produce a level coating layer at the surface. A large range of coat weight is available with these systems.

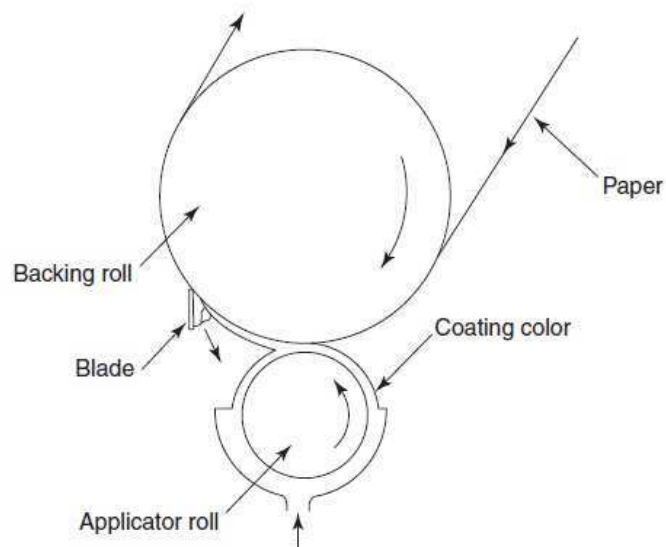


Figure I-8: Scheme of blade/rod coating [26].

Curtain coating, Figure I-9, offers the possibility to deposit several layers in one pass. Moreover, the contour coating allows to obtain a homogeneous layer thickness.

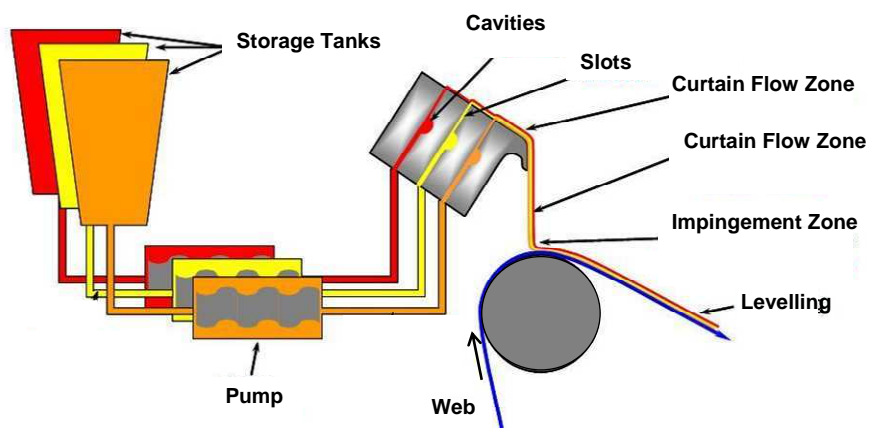


Figure I-9: Scheme of curtain coater [27].

Parameters for each coating technique are summarized in Table I-5. Each technique has its specific parameters such as coating colour viscosity and the coat weight deposited.


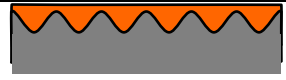
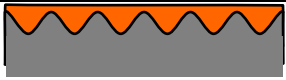
Coating process	Speed (m/min)	Solids (%)	Viscosity (mPa.s)	Coat weight (g/m ²)		
Metering size Press	1000	5-20	20-100	0,5 – 8	One layer	 Contour coating
Blade/Rod	1500	50-70	500-3000	5 – 20	One layer	 Level coating
Curtain	1800	40-70	500-1500	7-20	Multilayer	 Ideal contour coating

Table I-5: Parameters of coating techniques.

I.2.3.2. - Barrier properties of paper & board packaging

Several possibilities are available to produce packaging from paper & board materials. Table I-6 summarizes some examples.

	Application	Barrier properties	Use
Complex with Polymer (PE, PP, PA, PET...)	Extrusion coating	PE : Water and water vapour barrier	Paper/PE : flexible packaging for meat, fish PE/Board/PE: freeze product, milk box Board/PET: basket for fresh foods
Wax and paraffin	Applicator roll, impregnation, curtain coater, spray	Excellent water resistance, good grease and water vapour barrier	Paper mould, cup, board box, cheese paper, bakery bag...
Fluorinated product	Wet end, coating (size press, coating, printing)	Excellent grease resistance, moderate water barrier	Fat food packaging, pet food, fast foods
Water based polymer dispersion	Size press, blade rod coating, printing	According to the dispersion use	Flexible or rigid packaging, fat, dry, fresh product...

Table I-6: Examples of paper & board packaging [14].

Currently, the use of petroleum based polymers is common for the paper&board packaging production. Paper&board having poor barrier properties, they are generally associated with petroleum-based polymer films with excellent barrier properties. However, the implementation of these polymers by extrusion or lamination needs offline processes which increase the production costs. Moreover, their recycling possibilities are always low compared to paper&board packaging.

The use of bio-sourced products is thus one of the priorities of this study in order to preserve the biodegradability and recycling properties of the paper&board materials. Extrusion involves specific temperature and viscosity values for the successful film production. Bio-sourced materials are generally not adapted for the extrusion, hence coating process was studied here.

I.3. - Microfibrillated cellulose

Biopolymers are currently more and more studied to replace synthetic polymers. There are three categories of biopolymers [28]:

- Polymers directly extracted from natural materials such as: polysaccharides (cellulose, starch for example), proteins and lipids,
- Polymers produced by classical chemical synthesis from renewable bio-derived monomers,
- Polymers produced by microorganisms or genetically transformed by bacteria.

The development of nanoparticles from cellulose has been extensively studied over the last decade. Large improvements were carried out for their production method and their yield. A growing interest was observed for the use of nanocelluloses in composites and in papermaking.

I.3.1. - Fibres, nanocrystals and microfibrillated cellulose

Cellulose fibres are available in large amount on Earth. Indeed, between 10^{10} and 10^{11} tons of cellulose are synthesized each year [29]. They are derived from wood as well as from higher plants, a wide variety of bacteria, algae and fungi, and some animals such as tunicates.

Figure I-10 shows the structure of wood from macro to molecular level. Cellulose fibres are generally 20 to 40 μm in diameter and about one millimetre long. However, the size of fibres depends above all on the type of wood: hardwood or softwood. Hardwood mainly consists of small fibres with length 0.4-1.6 mm and width 10-40 μm . Fibres of softwood are longer with length 1.4-6 mm and width 20-50 μm [30].

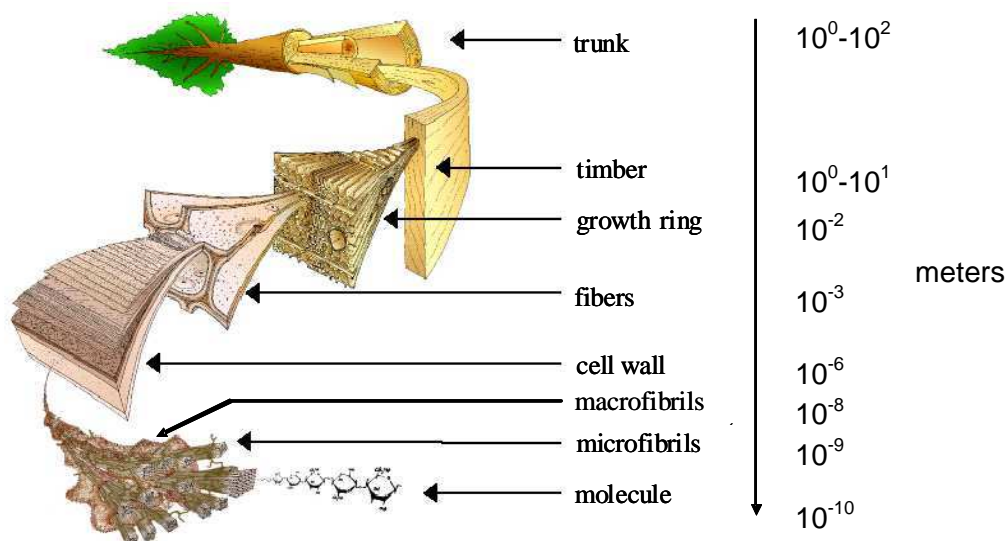


Figure I-10: Detailed structure of a tree from macro to molecular level [30].

The cell wall is a multilaminar composite (Figure I-11) [31]. In the individual cell wall, layers differ each other by the orientation of the crystalline cellulose microfibrils within each layer.

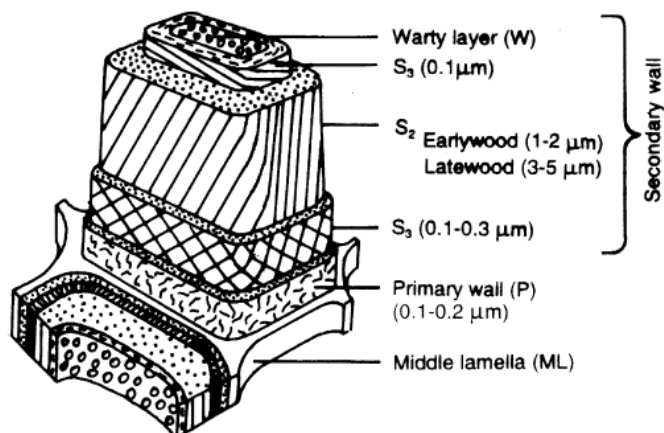


Figure I-11: Scheme of general structure of the tracheid cell wall of a fibre and the dominant helical orientation of the microfibrils [31].

The external layer of the fibre or middle lamella with a thickness of 0.5-2 μm mainly consists of lignin (70%) associated to hemicelluloses and pectin. This layer ensures the adhesion of the cell with its neighbours.

The primary cell wall is very thin (0.03-1 μm) and is made up of several layers of microfibrils which are embedded in a lignin, hemicellulose and pectin mixture.

The secondary cell wall is the thickest layer and accounts for 60-90% of the volume of the whole cell wall. This cell wall is divided into three different layers (S₁, S₂ and S₃) which are composed of microfibrils aligned in an ordered and parallel arrangement which differs from S₁ layer to S₃ layer. S₁ is only 0.1-0.3 μm thick and the microfibril angle with respect to the cell axis is 60° to 80°. S₂ layer is the most important with a thickness of 1-5 μm. In this layer the microfibril angle is 5° to 30° to the cell axis. S₃ is a relatively thin layer of 0.1 μm and the microfibril angle is 60° to 90° to the cell axis [32, 33].

Therefore, fibres are composed of an assembly of microfibrils which have nanometer size and which can be isolated by fibrillation.

At the molecular level, cellulose is a polydisperse linear polymer of poly-β(1,4)-D-glucose residues, whose molecule is shown in Figure I-12.

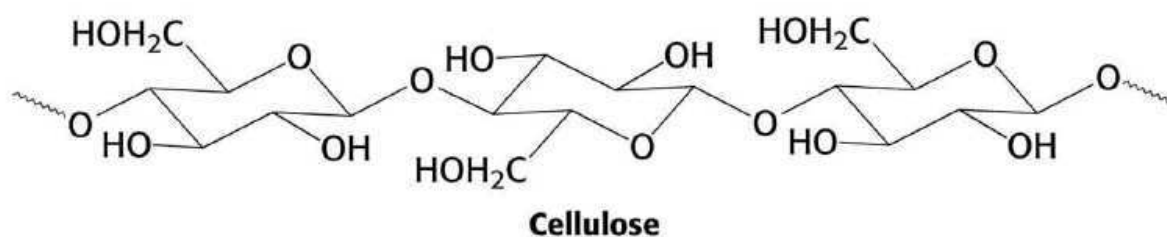


Figure I-12: Cellulose molecule [34].

Cellulose exists under several crystalline forms corresponding to allomorphs called: I, II, III, III_{II}, IV_I, IV_{II}. Cellulose I is the native cellulose which could be converted into the other forms by chemical or thermal treatments.

Cellulose is a very stiff material among natural materials thank to its crystalline regions which have a very high elastic modulus evaluated to 140 GPa (cf. Figure I-13). Its mechanical resistance competes with engineering materials too (Figure I-14). The crystalline regions could thus bring interesting reinforcing effect.

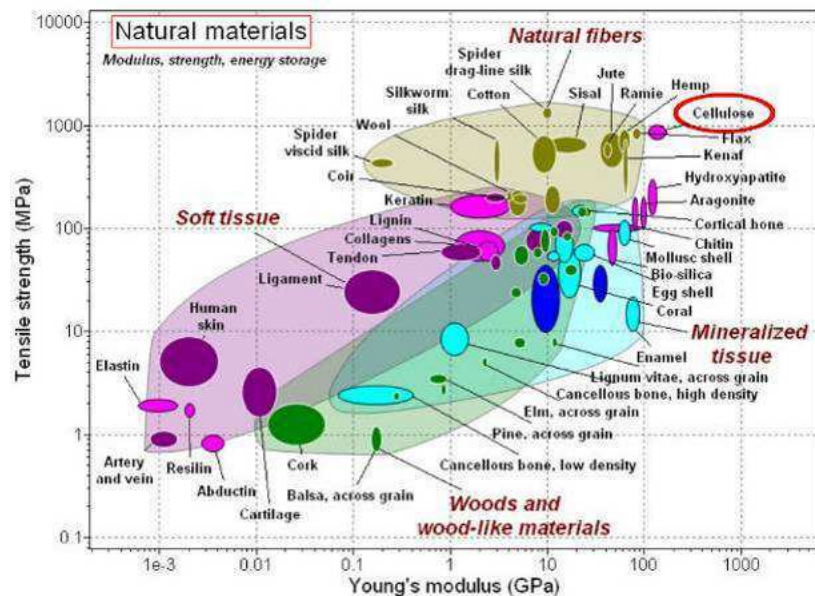


Figure I-13: Mechanical properties of natural materials [35].

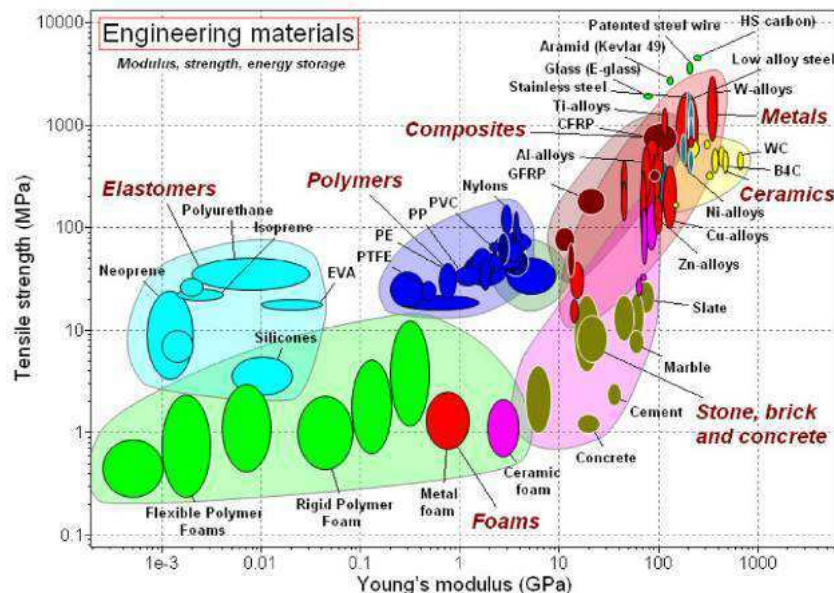


Figure I-14: Mechanical properties of engineer materials [35].

In order to exploit the mechanical properties of crystalline cellulose, fibres can be decomposed into nanocelluloses with higher crystalline ratio. Among nanoparticles that can be obtained from cellulose fibres, two types can be distinguished: whiskers (or cellulose nanocrystals) and cellulose microfibrils (or microfibrillated cellulose). Figure I-15 shows the

morphology of these nanoparticles and the different corresponding names generally used in the literature.

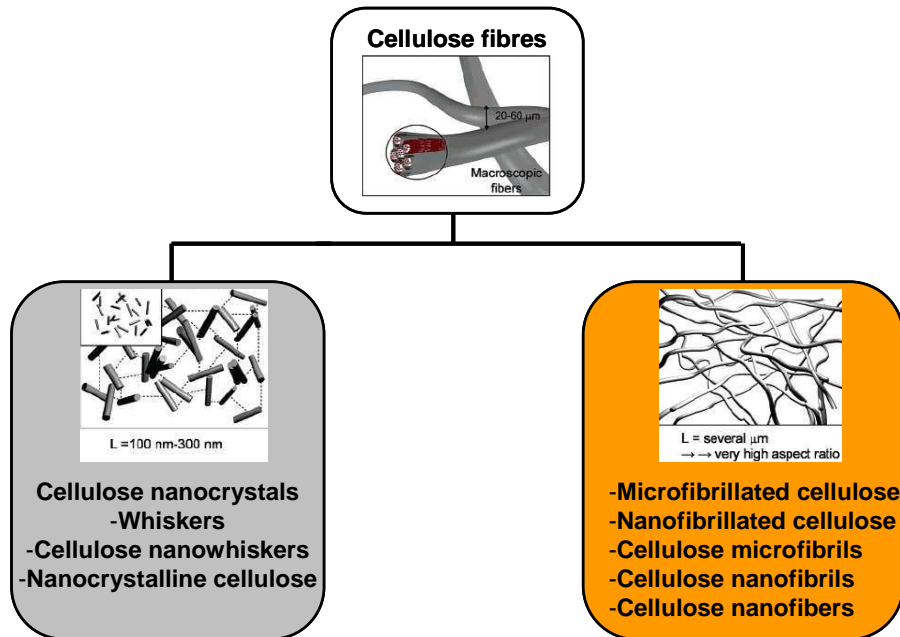


Figure I-15: Nanoparticles obtained from cellulose with their terminologies.

I.3.2. - Overview of the production routes of nanocelluloses

Whiskers and cellulose microfibrils have different shapes and aspect ratios. This results from the different methods employed for their production. This part gives thus a short overview of these production routes.

I.3.2.1. - Production of cellulose nanocrystals (CNC)

Whiskers are only composed of the crystalline part of cellulose. They consist of highly crystalline rod-like particles with a high specific area [36]. Stable aqueous suspensions of cellulose nanocrystals are generally produced by a strong acid hydrolysis treatment allowing the disruption of amorphous region (cf. Figure I-16).

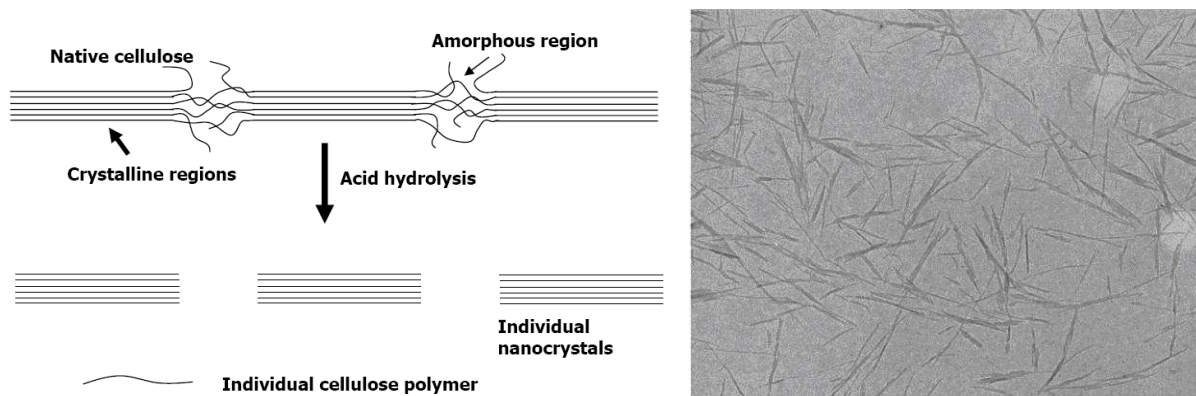


Figure I-16: Acid hydrolysis of cellulose [34] and TEM image of cellulose whiskers [30].

The structure and properties, specially the size of whiskers depend on the source of the original material [37] and the hydrolysis conditions. The length of cellulose whiskers is

generally around 100-300 nm and their aspect ratio (length/diameter) is typically between 10 and 30 [38].

A pilot production plan was recently built by FpInnovation and Domtar in Canada. The production can reach one ton nanocrystals per day with a yield of 60%. The product is for the moment designed for the high added value market with an announced cost between 10 and 100€/kg.

I.3.2.2. - Production of MFC/NFC

Cellulose microfibrils, presented in Figure I-17, are an assembly of linear glucan chains of cellulose. The whole structure is stabilized by hydrogen bonds. Cellulose microfibrils are extracted from wood or plants by mechanical processing or homogenisation [38].

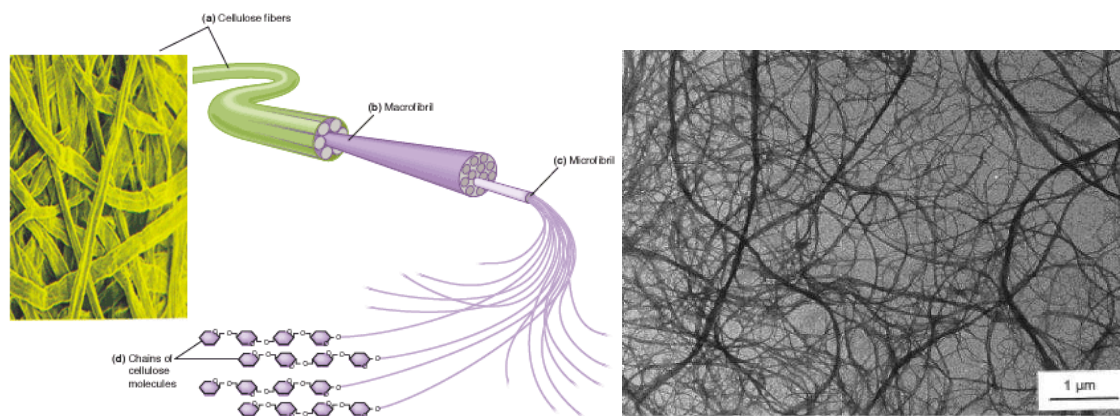


Figure I-17: Structure [39] and TEM image of cellulose microfibrils [40].

Aggregates of microfibrils consist of both monocrystalline regions and amorphous regions. Their length is few micrometers and their diameter is generally around 5-30 nm leading to a very high aspect ratio.

Figure I-18 describes and summarizes the methods used to obtain these cellulose nanoparticles and their size.

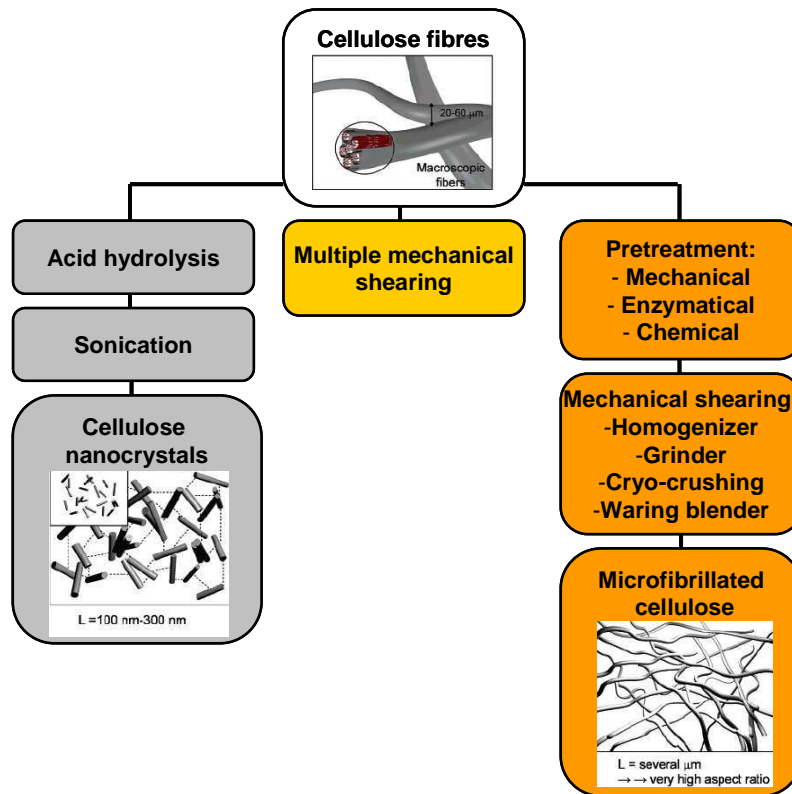


Figure I-18: Methods of fibre treatment (adapted from Pääkkö) [41].

This project was only focused on microfibrillated cellulose for several reasons: firstly their aspect ratio is higher and this could be more profitable for the development of barrier materials. Secondly, MFC is more appropriate for the papermaking market with lower cost. Indeed, the yield of the mechanical process is of 100%. Spence *et al.* [18] described energy & materials cost between 0.75 and 1.9 €/kg. Partners in the SUNPAP european project have also evaluated production costs of this order.

The following literature review details thus the production of microfibrillated cellulose (MFC) as well as the development of MFC films, MFC based composites and MFC based paper&board materials.

I.3.3. - MFC production

I.3.3.1. - From various sources

MFC is prepared as an aqueous suspension under the form of nanofibril aggregates with a lateral dimension in the range of ten nanometers and a high aspect ratio.

Several studies on this subject showed that it is possible to produce MFC from various cellulose sources. Wood is the first source used but other sources were also investigated and are summarized in Table I-7.

Sources	
Wood	Non wood
Pinus sylvestris/Picea abies [41]	Potato tubers [49]
Picea Abies [42]	Sugar beet pulp [29, 40, 50, 51, 52, 53]
Pinus pinaster [43]	Swede root [54]
Northern black spruce [44, 45]	Peel of Opuntia ficus-indica [55]
Radiata Pine [46]	Algae [56]
Eucalyptus [47]	Sugar cane bagasse [57]
Hardwood softwood [48]	Sisal [58, 59]
	Rachis of date palm tree [60]
	Banana rachis [61]

Table I-7: Cellulose sources used to prepare MFC.

I.3.3.2. - Pre-treatments

Over the years, several procedures were developed for the fibre delamination [62]. The first MFC suspensions were produced by the method developed by Turbak *et al.* [5] and Herrick *et al.* [63]. This method consisted in passing a dilute cellulose wood pulp fibre/water suspension through a mechanical homogenizer where a large pressure drop facilitated microfibrillation. However, about 27000 kWh per ton of MFC were necessary to produce a suspension from a sulphite pulp with high hemicellulose content [62].

To promote a good fibrillation, it is generally needed to repeat the mechanical shearing several times. The processing cost is thus very high using these mechanical processes. To reduce the energy need, three categories of pretreatments were developed in order to facilitate the disintegration [2]:

- Mechanical treatment with a mechanical cutting,
- Chemical treatment with acid hydrolysis, TEMPO-mediated oxidation or carboxymethylation,
- Enzymatic pre-treatment with cellulases.

I.3.3.2.1. - Mechanical pretreatment

One solution can be to reduce the fibre length by mechanical cutting in a first step. Indeed, cutting the fibres into shorter lengths increases the rate of homogenisation by exposing increased fibre cross section area to fibrillation [63].

Nakagaito *et al.* [64] developed a combination of repeated mechanical forces to promote the fibrillation of cellulose fibres with 30 passes through a refiner and then 14 passes in a homogenizer. Recently, Zimmermann *et al.* [65] developed a general mechanical method convertible for a later industrial up-scaling. First, a mechanical pre-treatment was conducted in a thermostatic reactor with on line dispersing system. To reduce the fibre dimensions and improve the swelling capacity in water, the pulp was milled in a preliminary step. After cooling to 15°C and dispersion at 20.000 rpm, cellulose fibril bundles were obtained. Then, these suspensions were introduced in a microfluidizer high shear processor. The mechanical treatment was done until observation of a highly viscous and homogeneous suspension with no solid residue.

The mechanical technique has limits and the energy consumption is always high. For this reason, another solution has been proposed with the pre-treatment of the fibre cell wall prior

to homogenization. Firstly, a chemical way was tested with acid hydrolysis, TEMPO-mediated oxidation or carboxymethylation.

I.3.3.2.2. - Chemical pretreatment

The use of acid hydrolysis as pre-treatment showed that the molecular weight of cellulose polymer was lower with this technique and resulted in short, fibrous crystallites with a low aspect ratio [66]. However, three other pre-treatments can lead to a more efficient process and lower processing cost. First, Wågberg *et al.* [67] described the carboxymethylation procedure followed by homogenization. The carboxymethylation consists in the substitution of hydroxyl groups by carboxymethyl groups (CH_2COOH). This method produces highly charged MFC material and this charging of the pulp allows an easier fibrillation. Indeed, the introduction of charged groups into the fibre pulp has long been known to enhance delamination of the fibre walls [68]. The fibrils liberated had a diameter of 5-15 nm and a length of more than 1 μm with a charge density about 0.5 meq.g^{-1} .

Saito *et al.* [43] studied the efficiency of 2,2,6,6-tetramethylpiperidine-1-oxyl (TEMPO)-mediated oxidation of cellulosic fibres used prior the mechanical treatment. This reaction, described Figure I-19, provides a negative charge at the microfibril surface [69,70]. The electrostatic repulsion caused by anionic carboxylate groups between the TEMPO-oxidized cellulose nanofibers (TOCN) decreases the number of hydrogen bonds present in the wood cell walls. This combination presents the advantage of disintegrating fibres into microfibrils with lower width (10-20 nm wood MFC) using a much lower energy input. Several authors have also chosen this technique to produce MFC [71, 72, 73].

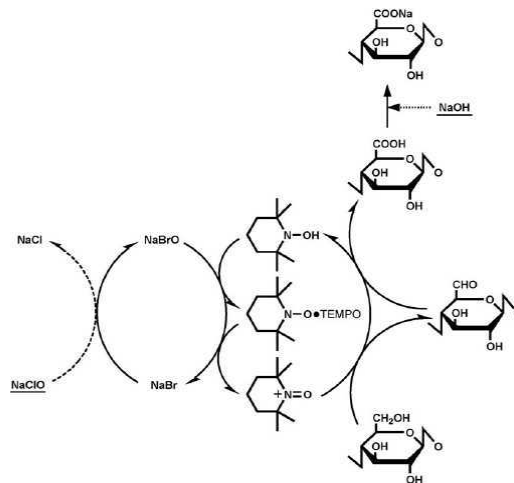


Figure I-19: TEMPO-mediated oxidation of cellulose to form C6-carboxylate group [70].

These last two methods lead thus to a modification of cellulose molecule with addition of carboxymethyl group for the first one and an oxidation that is to say the substitution of CH_2OH groups by carboxyl groups for the second one. The last pre-treatment method is an enzymatic hydrolysis.

I.3.3.2.3. - Enzymatic pretreatment

The use of cellulases for applications in the pulp and paper industry has been extensively reported, mainly for paper recycling or fiber refining [3]. Cellulases can be divided into three groups [74,75]:

- Endoglucanases or β -1,4-endoglucanases which randomly hydrolyze accessible intramolecular β -1,4-glucosidic bonds in cellulose chains, generating oligosaccharides of various lengths and consequently new chain ends,
- Exoglucanases (cellobiohydrolases) acting on the chain termini to release soluble cellobiose (cellobiohydrolase) or glucose (glucanohydrolase) as major products,
- β -glucosidases which hydrolyze cellobiose to glucose, in order to eliminate cellobiose inhibition.

The endoglucanases are generally used for the MFC production [42] and lead to the cellulose degradation through breaking glucosidic bonds to weaken microfibril surface.

Pääkkö *et al.* [41] achieved an enzymatic hydrolysis treatment combined with mechanical shearing and high pressure homogenization. Compared to aggressive acid hydrolysis, this concept of soft enzymatic hydrolysis allowed to reach a higher aspect ratio of MFC. Moreover, the constriction chambers of the homogenizer quickly became blocked and the resulting material was non homogeneous and contained a large amount of intact fibres. The use of enzymatic treatment improved the suspension homogeneity. At last, the use of enzymatic pre-treatment shows advantages from the environmental point of view, compared to chemical methods. This method of enzymatic pre-treatment followed by mechanical shearing, was also used by Janardhnan and Sain [44] and Henriksson *et al.* [76] and patented by Ankerfors [77] in 2009.

I.3.3.2.4. - Conclusion

The pretreatment of pulp before the mechanical shearing improved the suspension homogeneity and reduced the energy consumption. Some data are summarized in Table I-8.

Pretreatment	Pulp type, bleached	Energy requirement (kWh ^t ⁻¹)
None	Kraft	12000-70000
None	Sulphite	27000
Carboxymethylation (DS=0.1)	Kraft/Sulphite	500
Enzymatic/Refining	Sulphite	1500

Table I-8: Energy requirement for the MFC production [62].

Therefore, the use of enzyme pretreatment decreased by a factor 20 the energy needs compared to unpretreated pulp. The carboxymethylation once again reduced by three times the energy requirements compared to enzymatic pretreatments.

I.3.3.3. - Mechanical treatments

Currently, several technologies are available for the MFC production such as described in the Table I-9.

Technologies	Supplier
Homogenizer	Manton - Gaulin GEA
Microfluidizer Grinder	Microfluidics Masuko

Table I-9: Technologies for the MFC production.

I.3.3.3.1. - Homogenizer

The homogenizer used by Turbak *et al.* [5] was a Manton-Gaulin 15MR homogenizer. The slurries of cellulose fibres at 1-2 wt% were subjected to a high pressure (55 MPa) homogenizing action. In this process, the fibre pulp was passed through a thin slit where it was subjected to large shear forces. Figure I-20 illustrates the forces performed by the valve opening and closing in rapid succession leading to high shearing of the pulp [3]. This procedure has to be generally repeated several times (10-20 times) in order to increase the degree of fibrillation. According to the number of passes, suspensions became more viscous and translucent.

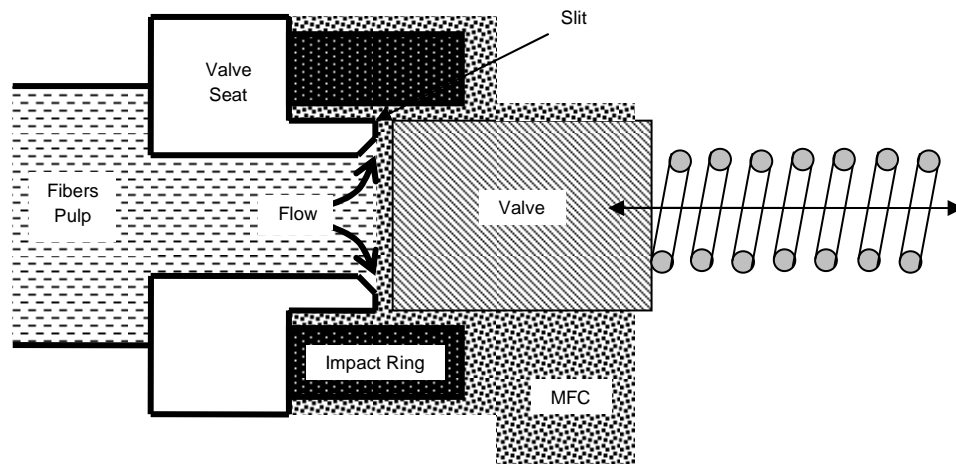


Figure I-20: Scheme of the slit Gaulin homogenizer [3].

Several researchers have then followed this procedure for NFC production. Dufresne *et al.* [49] used, for example, 15 passes through a laboratory homogenizer at 500 bars and 90-95°C to produce MFC from potato tubers. Andresen *et al.* [78] produced MFC from spruce sulphite pulp using 10 passes at 600 bars in a Gaulin M12 homogenizer. The main disadvantage of this device is the clogging of the system by the long fibres and particularly in the in-line valve [18]. The number of cycles is important leading to an excessive energy requirement and very high processing costs.

More recently, a homogenizer, supplied by GEA, allowed the production of MFC at pilot scale (Figure I-21). The process is similar to the one of Gaulin homogenizer but the pressure can reach 1500 bars with a higher flow rate.



Figure I-21: Scheme of a high pressure homogenizer (GEA Niro Soavi) [79].

I.3.3.3.2. - Microfluidizer

An alternative to the homogenizer is the microfluidizer (Microfluidics Inc, USA). The fluid slurry is pumped through z-shaped interaction chambers where it is submitted to high shear forces (Figure I-22). Indeed, the combination of high pressure (2760 bars) and interaction chambers defibrillates the fibres by shear forces and impacts against the channel walls and colliding streams. Plugging issues are reduced using reverse flow through the chamber compared to the homogenizer system. Several passes are required once again to perform a good fibre fibrillation.

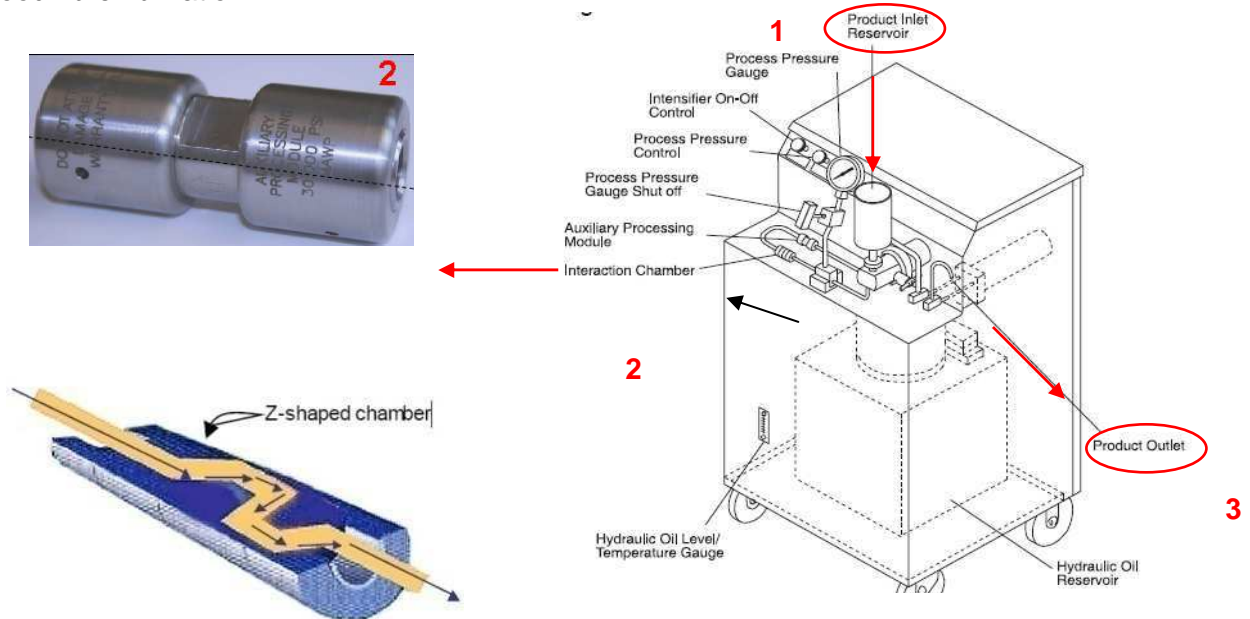


Figure I-22: Microfluidizer device [80].

I.3.3.3.3. - Grinder

Other researchers performed the mechanical treatment using a friction grinding process by grinding discs (Figure I-23). Wood fibres are forced through a gap between a rotor and a stator disk. These disks have bursts and grooves that contact the fibres to disintegrate them into the sub-structural components [18]. The upper grinding disc is fixed and the lower one is rotated at a high speed 1500 rpm. For example, Taniguchi and Okurama [81] obtained MFC with a diameter of 20-90 nm after 10 passes through the super grinding machine.

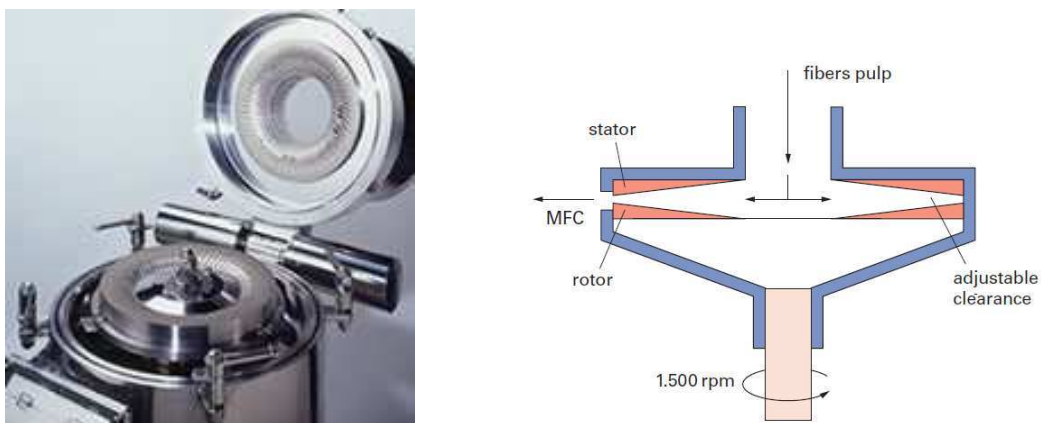


Figure I-23: Masuko grinder [3,82].

I.3.3.3.4. - Other methods

Another method of preparation using high shear refining and cryocrushing was studied by Chakraborty *et al.* [45]. This technique, seldom used, consisted in the combination of severe shearing in a refiner and high-impact crushing under liquid nitrogen. Liquid nitrogen was used to freeze the water in the refined pulp and a mortar and pestle were used to produce a high impact force to liberate the fibrils [18]. The diameter of microfibrils ranged between 0.1 and 1 μm , larger elements compared to the other techniques.

Lastly, the use of simple blender can be sufficient to homogenize TEMPO oxidized pulp. Saito *et al.* [43] reached 90% of thin elements from pulp oxidized with 2.5 or 3.8 mmol NaClO/g cellulose and homogenization in a Waring blender.

This part summarized the different methods used for the mechanical fibrillation of cellulose. Several equipments such as homogenizer, microfluidizer and grinder are available for the production of MFC. Mechanical, chemical or enzymatic pretreatments are generally associated to mechanical shearing in order to reduce the energy requirements. It is important to note that these different processes influence the final MFC properties.

I.3.4. - Morphology of MFC/NFC

One of the main techniques currently used to characterise cellulose microfibrils is a combination of microscopic techniques such as for example SEM, TEM, AFM. Allowing the study of surface samples, these techniques provide information concerning the MFC morphology.

I.3.4.1. - Transmission electron microscopy

Transmission electron microscopy (TEM) is a high-resolution microscopic technique often used to characterise MFC. The principle is that an electron beam is going through the sample. Electrons are transmitted to the detector according to the interactions between electrons and atoms of the sample. An image is thus obtained with a resolution around 0.1 nm. For this technique, a drop of dilute MFC suspension is deposited on a substrate. The drying can lead to MFC aggregation, it is thus difficult to observe individualized MFC. Therefore, Pääkkö *et al.* [41] have suppressed the drying using the cryo-TEM procedure to obtain images such as in Figure I-24. The sample was thus studied at cryogenic temperature in a frozen-hydrated state.

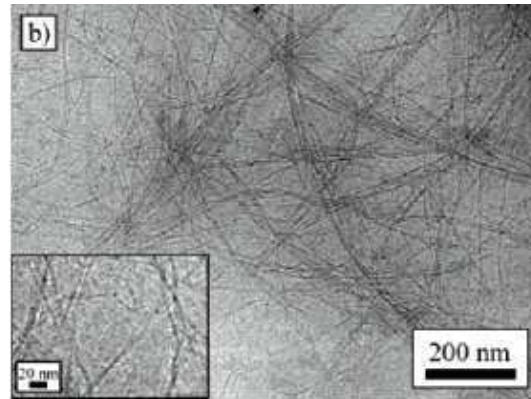


Figure I-24: Cryo-TEM image of MFC [41].

Figure I-24 shows long, well-defined and distinct cellulose microfibrils which are mostly of a diameter around 5 nm as well as thicker fibrils of a diameter of up to 10-20 nm. However, the length was not easily evaluated with this technique.

Table I-10 summarizes the diameter ranges and the TEM images of MFC obtained from various sources and techniques.

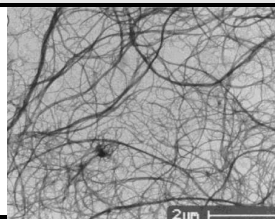
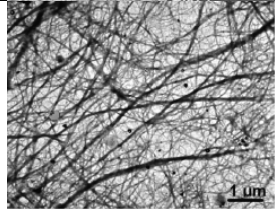
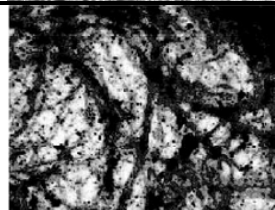
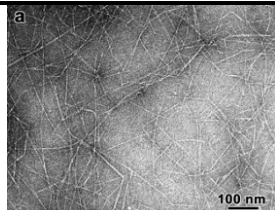
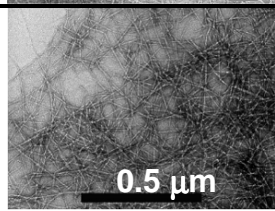

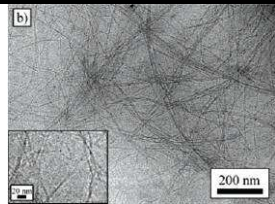
Method	Reference	Vegetal source	MFC width	TEM image
Mechanical shearing	[49]	Potato pulp	5 nm	
	[55]	<i>Opuntia ficus-indica</i> parenchyma cell	5 nm	
	[45]	Bleached kraft pulp	0.1-1 μm	
	[65]	Softwood sulphite pulp, Wheat straw pulp, Beech wood	< 100 nm	
TEMPO oxidation + mechanical shearing	[43]	Bleached sulphite pulp	few nm	
Carboxymethylation + mechanical shearing	[67]	Softwood sulphite pulp	5-15 nm	
Enzymatic pre-treatment + mechanical shearing	[44]	Bleached Kraft pulp	10-250 nm	
	[42,76]	Bleached sulphite pulp	15-30 nm	
	[41]	Bleached sulphite softwood pulp	5-20 nm	

Table I-10: MFC suspensions obtained from various sources and methods.

I.3.4.2. - Scanning electron microscopy

Scanning electron microscopy (SEM) uses an electron beam which scans the surface of the sample. The resolution reaches the range of the nanometer when a field emission gun (FEG) is coupled with SEM. This technique was used by Taniguchi *et al.* [81] for MFC films. Figure I-25 shows the network formation with MFC. The MFC suspension is an entangled network: the MFC size is thus very difficult to measure exactly. Indeed, the extremities of individual MFC were not observed because of the aggregation and entanglement. Moreover, the scale used to observe the diameter ($\sim 10\text{-}30\text{ nm}$) was too small to measure the length ($\sim 1\text{-}3\ \mu\text{m}$).

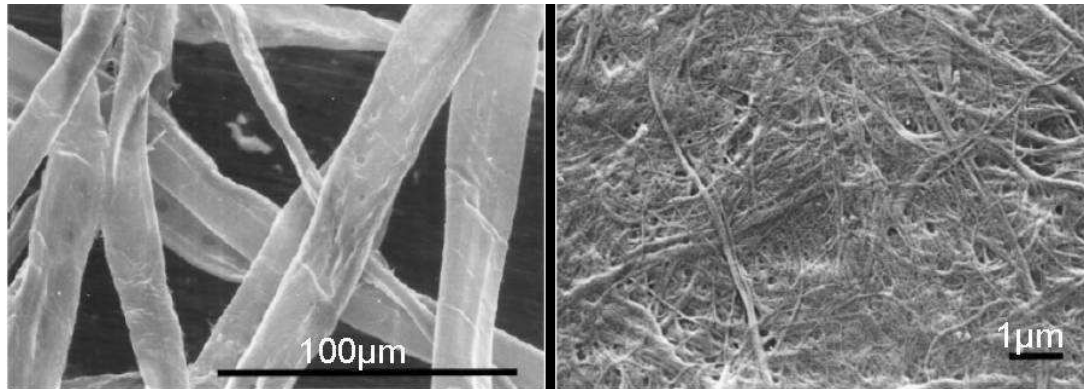


Figure I-25: SEM photos of wood pulp (left) and MFC from wood pulp (right) [81].

I.3.4.3. - Atomic force microscopy

Atomic force microscopy (AFM) consists in scanning a cantilever with a sharp tip at its end across a sample surface with a small constant force. The topography of the sample is determined by measuring the interactions between the sharp tip and the sample surface which depend on attraction or repulsion between atoms present at the surface and the tip. A piezoelectric scanner drives the tip to scan the sample. Using this technique, Pääkkö *et al.* [41] dried the MFC on a mica substrate.

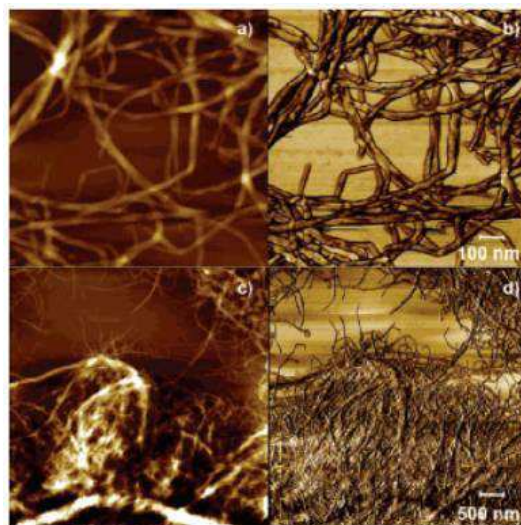


Figure I-26: AFM analysis of MFC dried on mica substrate [41].

The AFM micrographs shown in Figure I-26, present a network of objects whose width is 20-30 nm. The larger widths of fibrils compared to those of the cryo-TEM images can be due to the drying of fibrils or fibril aggregates.

Therefore, the microscopic techniques give qualitative information on the MFC morphology. Only the diameter was clearly defined. Most of the MFC consists of nanofibrils with a diameter ranging between 5 nm and 30 nm and a length around several micrometers.

I.3.5. - Degree of polymerization of cellulose

This intrinsic viscosity measurement is currently used to determine the degree of polymerisation of cellulose according to the standard ISO 5351. The nanofibrillated cellulose suspension is firstly dried for 24h at 50°C and then a given amount is dissolved in a cupri-ethylenediamine (CED) solution. The running time through a marked distance of a capillary tube viscometer is determined. The limiting viscosity can be calculated from the equation:

$$[\eta] = \lim_{c \rightarrow 0} \frac{\eta_{sp}}{c} = \lim_{c \rightarrow 0} \frac{\eta - \eta_0}{\eta_0 c} \quad (Eq. 10)$$

η_{sp} corresponds to the intrinsic viscosity, η to the solution viscosity, η_0 to the viscosity of the pure solvent and c to the concentration of the polymer in solution. The Mark-Houwink equation gives the relation between the intrinsic viscosity and the molecular weight M :

$$[\eta] = KM^a \quad (Eq. 11)$$

The parameters a and K depend on the particular polymer/solvent system. For cellulose dissolved in CED, $K=0.42$ and $a=1$ for $DP < 950$ and $K=2.28$ and $a=0.76$ for $DP > 950$ [83].

Table I-11 presents the results obtained by Zimmermann *et al.* [65] for five types of fibres and their corresponding MFC obtained from softwood sulphite pulp, wheat straw pulp and beech wood pulp. The degree of polymerization of cellulose microfibrils allowed to evaluate the efficiency of high shear fibrillation. For example, the degree of polymerization of softwood sulphite pulp decreased from 2249 to 825 upon fibrillation process.

Cellulose material	Intrinsic Viscosity η (ml/g)	Degree of polymerization (DP)
Softwood sulphite pulp (SSP)	800	2249
SSP fibrillated	350	825
Wheat straw pulp (WPS1)	570	1433
WSP1 fibrillated	320	749
Wheat straw pulp (WSP2)	441	1025
WSP2 fibrillated	280	674
Beech wood pulp (BWP1)	460	1088
BWP1 fibrillated	390	930
Beech wood pulp (BWP2)	120	291
BWP2 fibrillated	100	230

Table I-11: Intrinsic viscosity and degree of polymerization of several pulps and their corresponding MFC [65].

In this study, the authors also showed that the homogeneity of the MFC material was more important for its reinforcement potential than the degree of polymerization of cellulose. The

quality of fibrillation as well as the network formation influences strongly the final properties. FEG-SEM micrographs (cf. Figure I-27) show less homogeneous and bigger aggregates for beech wood pulp compared to this pulp after fibrillation process. However, they had almost the same degree of polymerisation. The mechanical properties obtained for films produced with the two sources of cellulose are linked to the quality of the suspension. Indeed, films achieved with the commercial source have an elastic modulus 4 times lower and a tensile strength 2.5 times lower than those of films obtained from MFC produced from this source.

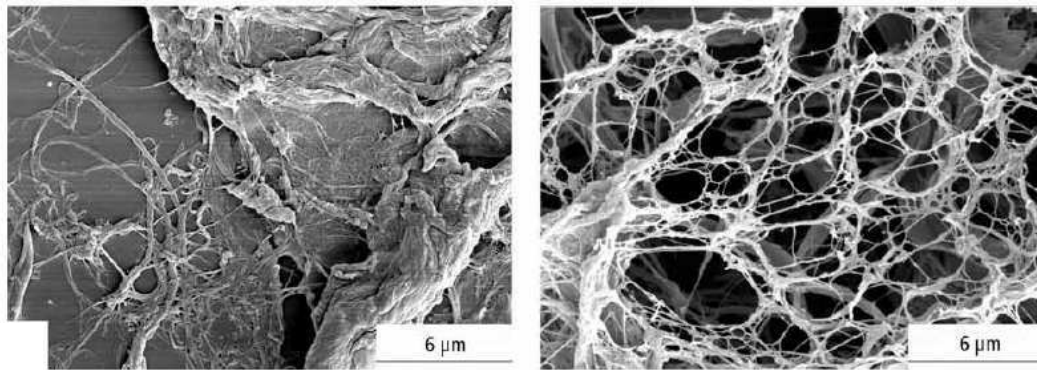


Figure I-27: FE-SEM micrograph of commercial refined beech wood pulp (left) and laboratory isolated nanofibrillated cellulose out of refined beech wood pulp (right) [65].

I.3.6. - Rheology of MFC suspensions

The rheological behaviour is an important characteristic of MFC. Indeed, after homogenization, MFC suspensions generally have a gel-like behaviour even for low concentration (2%). Figure I-28 shows MFC gels corresponding to carboxymethylated MFC and oxidized MFC.



Figure I-28: Photos of carboxymethylated MFC gel [84] (left) and of TEMPO oxidized MFC gel [38] (right).

The viscosity increases with the fibrillation rate. Rheological study can thus give good information concerning the fibrillation state. The increase of particle aspect ratio is directly related to the viscosity. The viscosity of fluids made of particles in suspension depends on the particle volume fraction. This is described by the Einstein equation for low concentration suspensions of rigid spherical particles [85]:

$$\eta = \eta_s (1 + 2.5\phi) \quad (\text{Eq. 12})$$

where η is the viscosity of the fluid, η_s the viscosity of the solvent and Φ the percentage volume fraction of particles.

Clarke *et al.* [86] have described the viscosity according to the percentage volume concentration for four shapes of particles (cylinder, disc, grain, sphere) (Figure I-29).

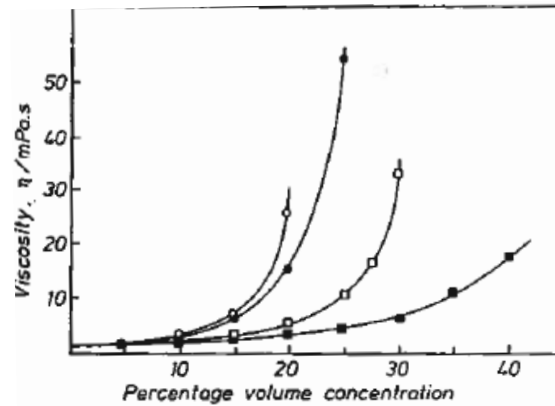


Figure I-29: Viscosity according to the percentage volume concentration; ○ cylinder, ● disc, □ grain, ■ sphere [86].

MFC has a very high aspect ratio leading to low percolation threshold. Therefore, the viscosity quickly increases with the volume concentration. The study of dynamic viscosity allows thus a better understanding of the behaviour of MFC suspensions and of their viscoelastic properties.

Lewis *et al.* [87] carried out one of the first studies on this topic. The rheological behaviour of cellulose microfibril suspensions from sugar beet pulp was characterised using a stress-imposed rheometer. Two different geometries were used, cone-plate for flow measurements and plate-plate for dynamic measurements.

The influence of MFC concentration was assessed. The existence of a critical microfibril concentration was demonstrated for $C=3$ g/L. From this concentration, the viscosity increased rapidly and a gel-like behaviour was obtained. Therefore, for MFC concentrations above 3 g/L, MFC forms a physical network (Figure I-30).

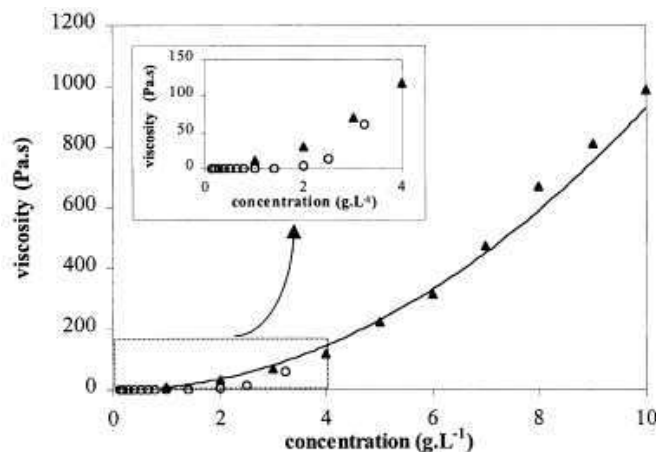


Figure I-30: Viscosity of MFC suspensions as a function of MFC concentration (▲) compared with zero shear rate viscosity for xanthan solutions (○) [87].

The influence of the energy applied during dispersion on the quality of the suspension was also demonstrated in this study. Ultrasonic dispersion was more efficient than mechanical stirring, with higher values of yield stress. The rheological study was achieved with oscillatory measurements as a function of temperature. There was no variation of storage modulus for the three studied temperatures (25, 40 and 60°C).

Pääkkö *et al.* [41] studied the rheological behaviour of MFC suspensions from wood. A controlled strain rheometer was used with two geometries: cone-plate for the 1-3 % (w/w) samples and plate-plate for the 0.125-0.5 % (w/w) samples. The shear viscosity was evaluated according to the shear rate from 0.1 to 1000 1/s (Figure I-31).

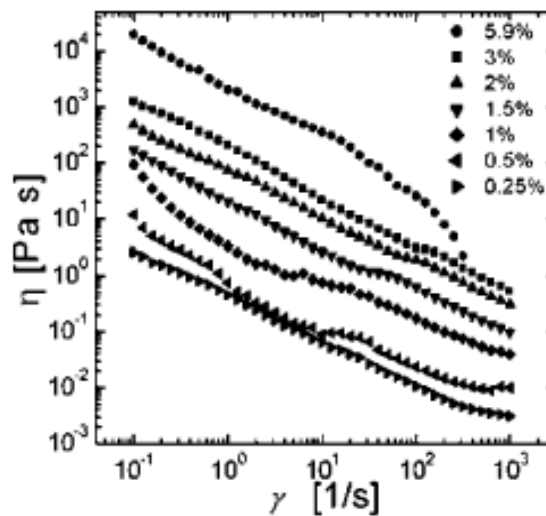


Figure I-31: Viscosity of MFC suspensions at various MFC concentrations (left) [41].

As reported in Figure I-31, the viscosity of the suspension increases with the MFC concentration. Moreover, a shear thinning behaviour was observed: the viscosity decreased when the shear rate increased. This shear thinning behaviour was also observed for TEMPO oxidized MFC, obtained from pine sulphite pulp [88] (Figure I-32).

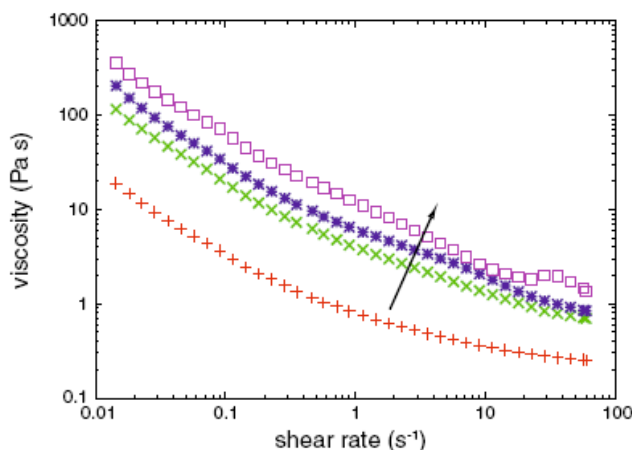


Figure I-32: Viscosity of TEMPO-oxidized MFC during the Waring-blendor treatment as a function of shear rate. The arrow shows the increase in treatment time [88].

The range of viscosity was higher for this kind of MFC. Indeed, the viscosity at 100 s⁻¹ for the 0.4% oxidized MFC suspension was the same as for the 2% MFC suspension from the same

pulp treated with 10 homogenizing passes at 55 MPa [88]. This was probably due to the higher charge surface of MFC after TEMPO-mediated oxidation.

More recently, two articles described the rheological behaviour of MFC suspensions according to the shear rate. Iotti *et al.* [89] reported the presence of shear rate-viscosity hysteresis loop. The study used a rotational rheometer with shear rates ranging between 0 and 1000 s^{-1} . The viscosity evolution was described according to the shear rate (Figure I-33).

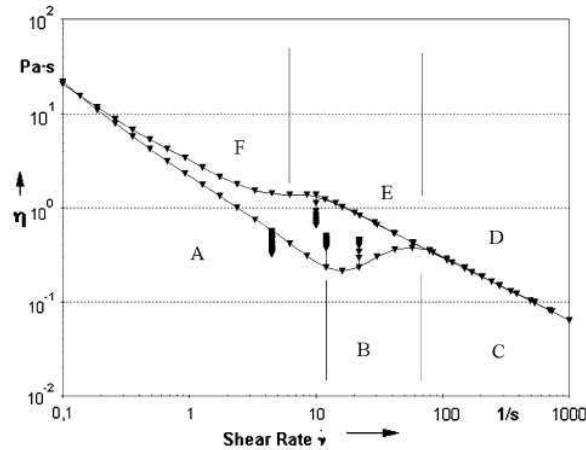


Figure I-33: Rheological measurements of MFC at 25°C with the increasing shear rate curve (0-1000 s^{-1}) and the decreasing shear rate curve (1000-0 s^{-1}) [89].

The curve was divided into six different areas. The A and F areas correspond to the no-shear structure. Under shear, the fibrils were oriented along the flow line leading to the viscosity decrease. In the C and D areas, the high-shear structure was formed and a shear thinning behaviour was observed due to the stability and the orientation of the structure. For the intermediate areas, B and E, low shear structure was induced with the reorganisation and the network formation by temporary hydrogen bonds or Van der Waals interactions.

Saarikoski *et al.* [90] used an imaging approach to put in relation the rheological behaviour and the flocculation of the cellulose fibrils. The study showed that MFC suspensions form a gel structure consisting of sintered flocs. Upon shearing, the flocculated network structure was firstly deformed elastically until a limit where the flocs break loose from each other. Figure I-34 shows the images of flocs state according to the shear rate. The size of flocs was inversely proportional to the shear rate.

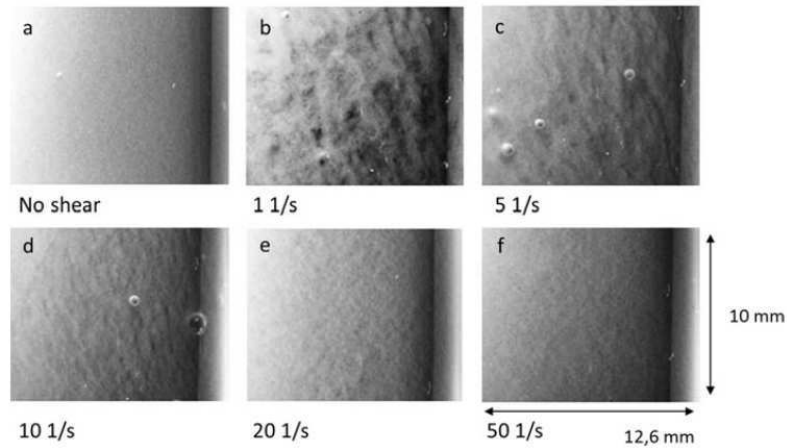


Figure I-34: Flocculated flow at several shear rates [90].

The influence of the presence of ions was also studied here. The addition of sodium chloride decreased the repulsions between microfibrils and increased the aggregation effects.

The MFC suspensions had a gel-like behaviour and their viscosity was related to their degree of fibrillation. Viscosity measurements were reported by several researchers but no standard procedure was described. Moreover, few measurements with imposed strain rheometer were described in the literature. Several studies reported a high viscosity of MFC suspension at low concentrations which can limit their use in industrial applications. The chemical modification of the fibril surface could be a solution to reduce the interfibril interactions and thus the suspension viscosity.

I.3.7. - MFC films

I.3.7.1. - Production of MFC films

Several researchers [49,81] have developed techniques to produce MFC films. The most used technique is casting/evaporation. Indeed, this method is very simple. The MFC suspension (0.1% up to 1%) is poured into a mould (Teflon or polystyrene) and then stored, generally at room temperature, until total water evaporation. For example, Aulin *et al.* [91] achieved MFC films by pouring MFC suspension at 0.13% into polystyrene Petri dishes and storing at 23°C/50% RH.

Another technique used is the suction filtration. Syverud *et al.* [92] used a suspension at 0.1 wt% poured into a cylindrical mould containing at bottom a polyamide filter cloth (top), a filter paper (middle) and a supporting Cu wire (bottom). The water was removed by free suction through the polyamide film into the filter paper. The films were dried by water evaporation at room temperature.

Henriksson *et al.* [76] filtered the MFC suspension in a glass filter funnel using filter paper. Films were then stacked between filter papers and dried at 55°C for 48h under about 10 kPa applied pressure.

Large and flat films were produced by Sehaqui *et al.* [93] using a rapid Khöten sheet former. This procedure, described in Figure I-35, is a faster technique than casting and the drying under constrain prevented the shrinkage and avoided the wrinkling.

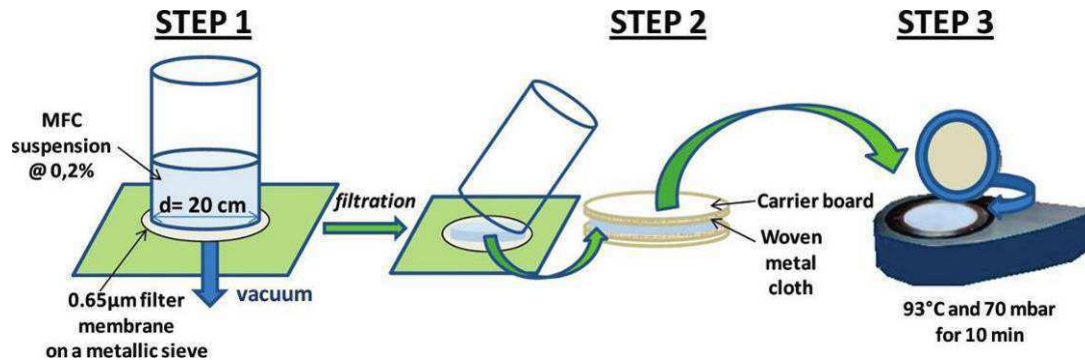


Figure I-35: Preparation procedure of MFC films using a semiautomatic sheet former [93].

I.3.7.2. - Properties of MFC films

It is important to emphasize that the properties of MFC films are related to the kind of MFC used and production technique. For example, the properties of carboxymethylated MFC are different from those of unmodified MFC.

I.3.7.2.1. - Density and porosity

The physical properties of MFC films are related to their porosity and density. These parameters strongly depend on the structure of the nanoparticles, the presence of residual components and the technique used to prepare the films [3].

The MFC film density can be calculated from the thickness and the basis weight of samples. Spence *et al.* [48] compared the density of MFC cast films produced from several pulp types. After homogenization, films showed a densification. The packing was more important with thin elements and when using a homogeneous suspension. Densities of MFC films were between 0.514 and 0.972 g/cm³ for the thermo-mechanical pulp (TMP) and unbleached hardwood (UBHW) pulp, respectively. These values are lower than the ones reported by Syverud *et al.* [92] ranging from 0.8 to 1.1 g/cm³. The observed difference resulted in the use of vacuum filtration to produce MFC films in the latter study. Nogi *et al.* [94] obtained films from wood flour with very high density of 1.53 g/cm³ thanks to a drying under pressure of 15 kPa. The density of crystalline cellulose is 1.59 g/cm³ whereas that of pure natural fibre cellulose reaches 1.55 g/cm³ [95]. The cavities in the sheet were thus almost completely removed. Figure I-36 summarizes the different density values reported for MFC films in the literature.

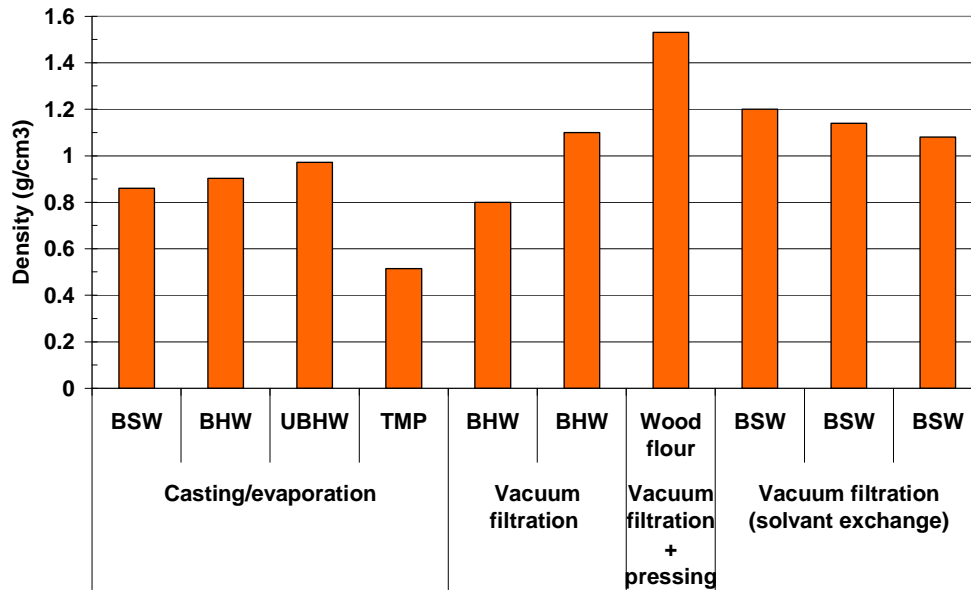


Figure I-36: Density values reported in literature for MFC films.

An Archimedes scale was also used to determine the density for MFC films [76,96]. The density was calculated from the displacement of the sample when immersed in mercury using the Archimedes scale. The porosity was then deduced from the density with the formula:

$$porosity = \frac{1 - \rho_f}{\rho_c} \quad (Eq. 13)$$

where ρ_f corresponds to the density of the film and ρ_c corresponds to the density of the cellulose, which is assumed to be 1500 kg/m^3 .

Henriksson *et al.* [76] studied the density and the porosity of MFC films prepared in different solvents. The porosity increased when the films were produced in less hydrophylic liquid. The values were thus of 28% for films produced in water and of 40% for films produced in acetone. FEG-SEM images of MFC film surface (Figure I-37) shows the cellulose microfibril network formed by interfibrillar hydrogen bonding. The surface of the film was very closed with pore diameters in the range of 10-50 nm.

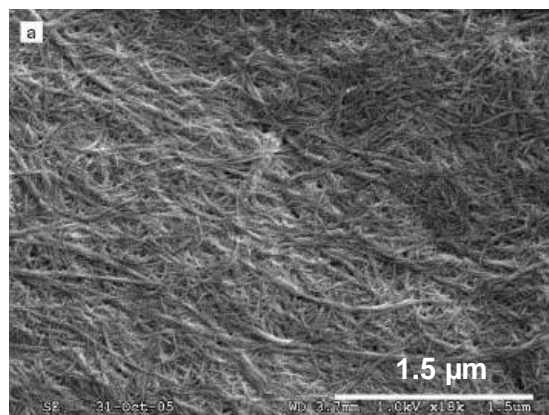


Figure I-37: FEG-SEM micrographs of cellulose microfibril film surface [76].

Missoum *et al.* [97] determined the pore size of MFC films by mercury porosimetry. The size obtained ranged from 4 nm to 20 nm. Fukuzumi *et al.* [98] analyzed the pore size of wood and tunicin TEMPO-oxidized MFC films at 0% RH using positron annihilation lifetime spectroscopy (PALS). This technique is used to study voids and defects in solids. PALS analysis revealed a pore size around 0.47 nm from the film surface to the interior of the film explaining the very high oxygen barrier of films. The AFM image, Figure I-38, gave an overview of the dense structure consisting of thin nanofibril elements.

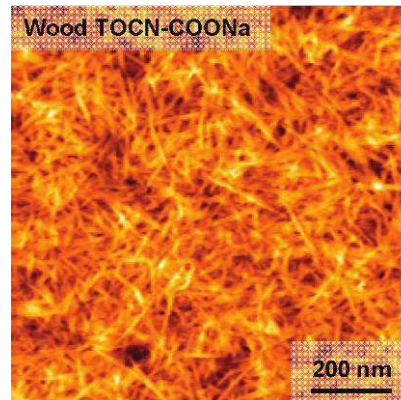


Figure I-38: AFM image of the surface of a TEMPO oxidized cellulose nanofibril film [98].

The literature studies showed the large range of MFC film densities. Indeed, the film density is determined by fibril interactions and film process. The porosity also plays a role in the MFC film properties. In most cases, the porosity was determined from the density and the theoretical density of cellulose. Few studies details the pore size measurement. However the values obtained are generally very low.

I.3.7.2.2. - Transparency

Elements with diameters less than one tenth of visible light wavelengths are not expected to cause light scattering [99]. MFC being in this size range, most of MFC films displayed an important transmittance value under visible light. For example, films formed by filtration in Nogi *et al.* study [94], presented a good transparency thanks to a polishing step with emery paper. The transparency of this nanofibre sheet (thickness 55 μm) reached 71.6% at a wavelength of 600 nm (cf. Figure I-39).

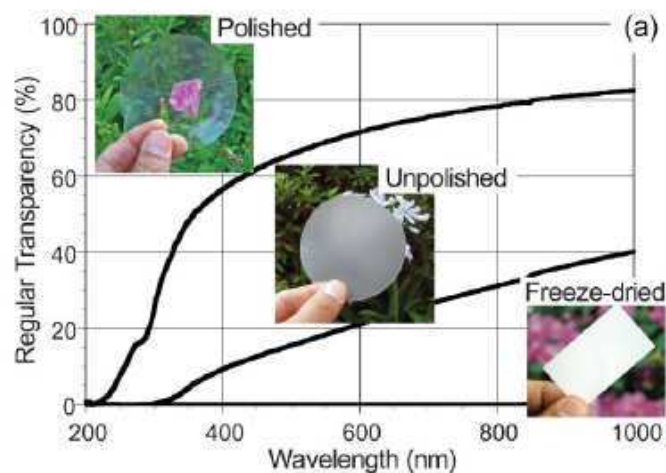


Figure I-39: Transparency of cellulose nanofibre sheets [94].

I.3.7.2.3. - Mechanical properties

Many authors evaluated the mechanical properties of MFC films having a thickness between 20 and 200 μm and demonstrated their high stiffness.

For example, Henriksson *et al.* [76] showed the reinforcement potential of MFC. Indeed, MFC films with a thickness of 70 μm presented high strength properties with an average Young's modulus equal to 10 GPa despite high porosity (20-28%). These results are reported in Figure I-40.

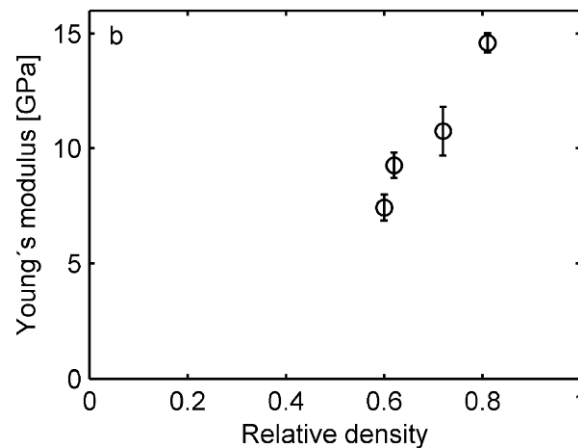


Figure I-40: Young's modulus of MFC films [76].

Using cellulose nanofibrils from sugar beet pulp, Leitner *et al.* [53] obtained a material with an elastic modulus of 9.3 GPa and a tensile strength of 104 MPa. The authors observed a clear increase of mechanical properties after high pressure homogenisation. Indeed, the unhomogenised pulp had values of 4.6 GPa for the elastic modulus and 73 MPa for the tensile strength.

MFC films prepared by Syverud *et al.* [92] had the same tensile strength value of 104 MPa for a thickness of 21 μm . However, the elastic modulus of 15.7 GPa was significantly higher. Similar results were reported by Svagan *et al.* [96] with MFC films having an elastic modulus and a tensile strength of 13 GPa and 180 MPa, respectively. The differences observed could be explained by the various sources of cellulose, or by the process used to produce MFC films. For example, Syverud *et al.* [92] produced MFC films from spruce by vacuum filtering while Svagan *et al.* [96] prepared films from a blend of spruce and pine by casting.

Chun *et al.* [100] obtained ultrastrength nanopaper with a potential for various industrial applications. Microfibrillated cellulose was produced from cellulose powder and 12 passes through the homogenizer at 1400 bars. Nanopaper with a thickness of 20 μm had a tensile modulus of 10.6 GPa. After the consecutive chemical modification with NaOH and tetramethoxy orthosilicate (TMOS), the tensile strength increased from 135 to 212 MPa.

Taniguchi and Okamura [81] evaluated the mechanical properties of MFC films obtained from wood pulp and tunicin. The values were compared with those of commercial print paper, hybrid composite (from wood pulp, tunicin and collagen) and low-density polyethylene. The results show that films from wood pulp had a tensile index 2.4 times higher than print paper and 2.7 times than polyethylene.

Nogi *et al.* [94] obtained films with good mechanical properties with a Young's modulus and a tensile strength of 13 GPa and 223 MPa, respectively.

Fukuzumi *et al.* [71] developed transparent and high gas barrier films from cellulose nanofibres prepared by TEMPO-mediated oxidation. Two sources were used: never-dried softwood and hardwood bleached kraft pulp fibres. From 0.1% (w/v) TEMPO oxidized cellulose nanofibres (TOCN)/water dispersion, films about 20 μm thick presented a good transparency, with a transmittance value of 90% at 600 nm for the film prepared from softwood cellulose and of 78% for the MFC film from hardwood cellulose. A high tensile strength was observed. MFC films from softwood had a tensile strength and Young's modulus of 233 MPa and 6.9 GPa, respectively, and MFC films from hardwood had values of 222 MPa and 6.2 GPa.

Figure I-41 compares the mechanical properties of MFC films obtained in the literature. Values have thus generally a Young's modulus value higher than 10 GPa and a tensile strength higher than 100 MPa. The mechanical properties of wood and crystalline cellulose were also reported on the graph for comparison. The MFC films have higher mechanical properties than wood but the values are also very far from crystalline cellulose properties.

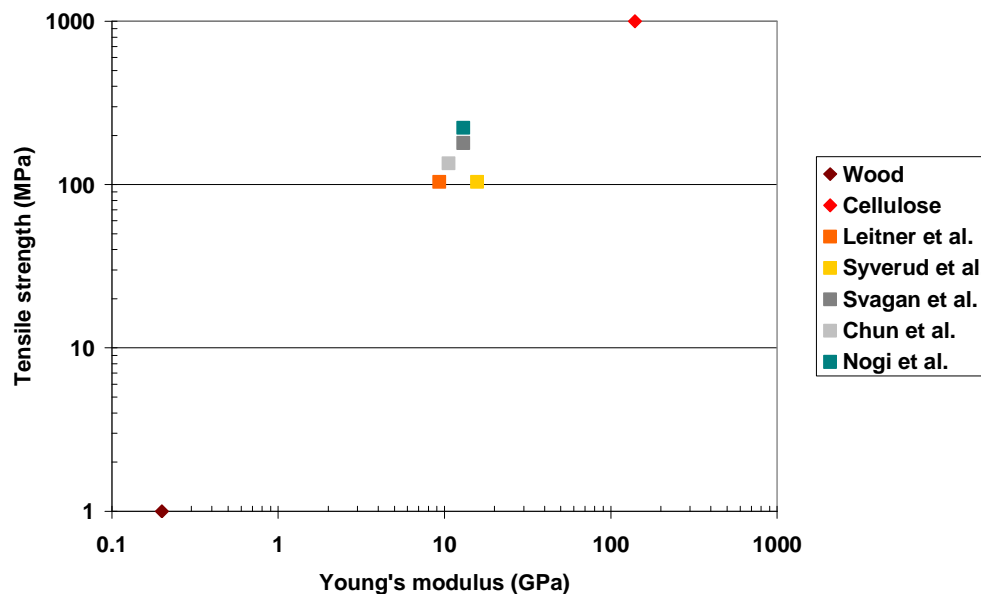


Figure I-41: Comparison of mechanical properties of MFC films in the literature review.

A comparison of mechanical properties for MFC films produced by several techniques was established by Sehaqui *et al.* [93] (Figure I-42). MFC films produced using the sheet former had the highest Young's modulus with a value of 13.4 GPa compared to 10.3 GPa for the cast MFC film.

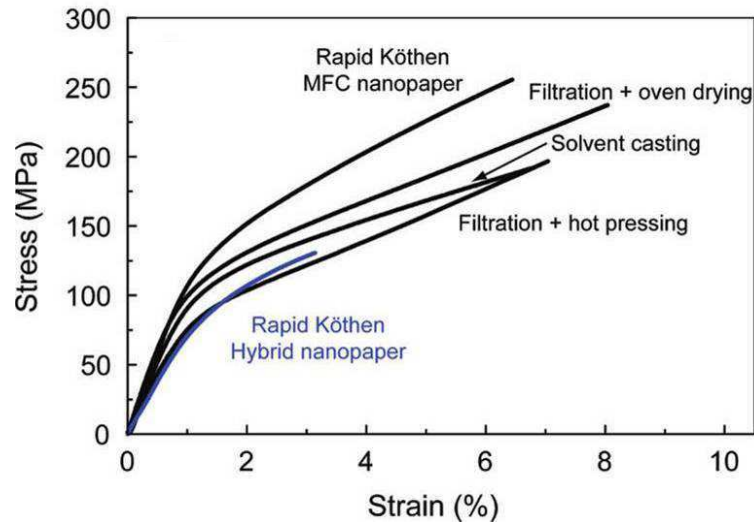


Figure I-42: Mechanical properties of MFC films produced with different techniques [93].

The difference observed between the mechanical properties of MFC films were often due to the variation of density. Therefore, techniques used to produce more compact films will be preferentially chosen to produce MFC films.

I.3.7.2.4. - Barrier properties

MFC has a high ability to form web structures and an important crystalline part, which are favourable criteria for the development of barrier materials.

- Pure MFC films

Barrier properties of MFC films were evaluated by Syverud *et al.* [92]. The air permeability values of MFC films with thickness between 20 μm and 33 μm was around 10 $\text{nm}/\text{Pa}\cdot\text{s}$. The oxygen transmission rate (OTR) of MFC films was around 17 $\text{cm}^3/\text{m}^2\cdot\text{day}$. From these results, the authors demonstrated that MFC films have a good applicability in packaging because the usual recommended OTR for modified atmosphere packaging is below 10-20 $\text{cm}^3/\text{m}^2\cdot\text{day}$.

Oxygen barrier properties of carboxymethylated MFC films were also reported by Aulin *et al.* [91]. Indeed, the cast MFC films (8 g/m^2 ; thickness 5.1 μm) presented a low value of oxygen permeability equal to 0.06 $\text{cm}^3\cdot\mu\text{m}/\text{m}^2\cdot\text{day}\cdot\text{bar}$ at 23°C 0% RH and 85 $\text{cm}^3\cdot\mu\text{m}/\text{m}^2\cdot\text{day}\cdot\text{bar}$ at 23°C-50% RH. These values were very promising compared with values for other materials used in packaging as indicated in Table I-12.

Material	Oxygen permeability ($\text{cm}^3 \mu\text{m}/\text{M}^2 \cdot \text{day} \cdot \text{bar}$)	Source and conditions
MFC (Carboxymethylated)	0.06	[91], 0% RH
MFC (Carboxymethylated)	85	[91], 50% RH
MFC (not pre-treated)	352-503	[92], 50% RH
TEMPO-oxidized nanocellulose	0.4	[71], 0% RH
<i>O</i> -acetylgalactoglucomannan	200	([101], [102]), 50% RH
<i>O</i> -acetylgalactoglucomannan-alginate (7:3)	55	([101], [102]), 50% RH
<i>O</i> -acetylgalactoglucomannan-CMC (7:3)	128	([101], [102]), 50% RH
Whey protein-glycerol (3:1-0.8:1)	4000-33000	[103], 50% RH
Whey protein-sorbitol (1.5:1)	103	([104], [105]), 30% RH
Amylose-glycerol (2.5:1)	700	[106], 50% RH
Amylopectin-glycerol (2.5:1)	1400	[106], 50% RH
Cellophane	41	[107], 0% RH
Cellophane-glycerol	950	[108], 50% RH
Chitosan-glycerol (4:1)	1-4	[109], 0% RH
Chitosan-glycerol (2:1)	4-8	[109], 0% RH
65% Glucuronoxylan/35% xylitol	21	[110], 50% RH
Arabinoxylan	200	[111], 50% RH
Collagen	120	([104],[105]), 0% RH
Microcrystalline wax	154	([104],[105]), 0% RH
Carnauba wax	15700	([104],[105]), 0% RH
Poly(vinylidene chloride) (PVDC)	10-300	[21], 50% RH
Poly(vinylalcohol) (PVOH)	20	[21], (0% RH
Polyamide (PA)	100-1000	[21], 0% RH
Poly(ethylene-terephthalate) PET	1000-5000	[21], 50% RH
Poly(vinyl chloride) PVC	2000-8000	[21], 50% RH
Poly(lactic acid) PLA	18400	[71], 0% RH
Polypropylene (PP)	49400-98700	[21], 50% RH
Polystyrene (PS)	98700-148700	[21], 50% RH
Low density polyethylene (LDPE)	190000	([104],[105]), 50% RH
Ethylene vinyl alcohol (EVOH)	1-10	[21], 0% RH

Table I-12: Oxygen permeability data for MFC films and literature values for some renewable and synthetic polymers [91].

For example, ethylene vinyl alcohol (EVOH) copolymer, a highly efficient barrier material often used in food packaging, has an oxygen permeability value of 1-10 $\text{cm}^3 \cdot \mu\text{m}/\text{m}^2 \cdot \text{day} \cdot \text{bar}$ at 23°C-0% RH. It is 41 $\text{cm}^3 \cdot \mu\text{m}/\text{m}^2 \cdot \text{day} \cdot \text{bar}$ at 23°C-0%RH for cellophane.

This study also showed the effect of water and relative humidity (RH) on barrier properties (Figure I-43). At a RH higher than 70%, the OTR value increased dramatically. According to the authors [91], the explanation would be that water present in the amorphous part acts as a plasticizer, reducing the intermolecular interaction between MFC fibrils thus reducing the stiffness of the material.

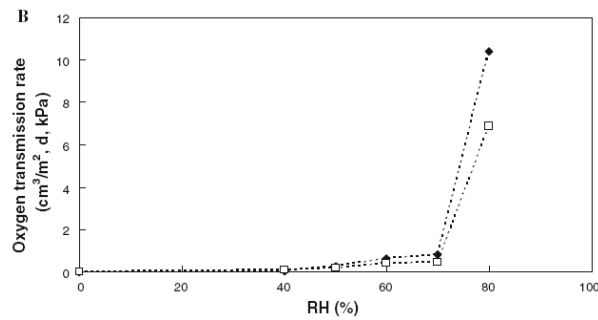


Figure I-43: Effect of relative humidity on OTR of MFC films [91].

The mass transport properties of MFC films were investigated in two publications. Firstly, Minelli *et al.* [112] analyzed the sorption and the permeation of neat MFC films or in combination with glycerol. The water sorption of two kinds of MFC films was determined for a water activity ranging between 20% and 80% (Figure I-44). Carboxymethylated MFC (MFC G2) films showed higher water uptake than MFC produced by enzymatic pre-treatment (MFC G1). Moreover, the addition of plasticizer decreased the porosity of materials but increased the diffusion coefficient. The presence of plasticizer enhanced thus the water sorption at higher water activity. The oxygen permeability of films was very low in dry conditions. However, a significant increase was observed with the increase of water activity as already observed with hydrophilic membranes.

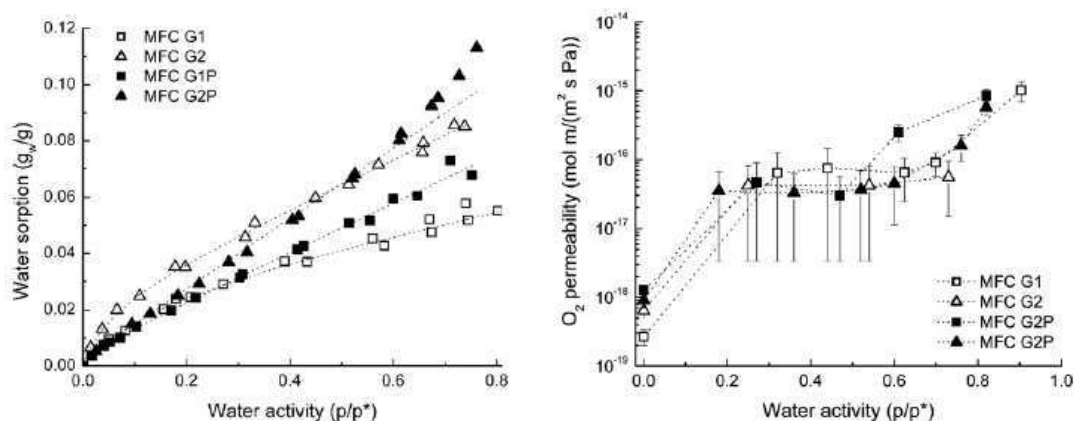


Figure I-44: Water sorption and oxygen permeability of MFC films as a function of water activity (MFC G1 and MFC G2 corresponded to films produced with microfibrils having a diameter of 17-30nm and of 5-15 nm respectively; MFC G1P and MFC G2P were plasticized MFC films with glycerol) [112].

Secondly, the water sorption behaviour and the gas permeation of MFC films were compared to cellulose nanocrystal films obtained from sisal fibres. Belbekhouche *et al.* [113] notified that both films have similar water sorption isotherms but that the water diffusion coefficient was higher for the nanocrystal films. The possible explanation was the presence of residual lignin and other extractive substances present at the MFC surface. Films of cellulose nanocrystals had also the highest gas permeability probably due to the shorter diffusion pathway compared to the one of MFC films.

Water vapour barrier properties of MFC films were determined by Spence *et al.* [18]. The value for pure MFC films reached 0.0215 (g/m².day)/m corresponding to 21500 g.μm/m².day.

This value was not sufficient for the development of packaging. Two techniques were thus employed to improve this property: the addition of filler and the coating of MFC films.

- Addition of filler

Four different fillers were tested and added to the slurry before the film formation: kaolin clay, calcium carbonate, cooked starch and uncooked starch. Only the kaolin clay and the calcium carbonate had a positive effect with a decrease of water vapour transmission rate value. An improvement of 51.6% was obtained with the addition of 7.5% kaolin clay (cf. Figure I-45).

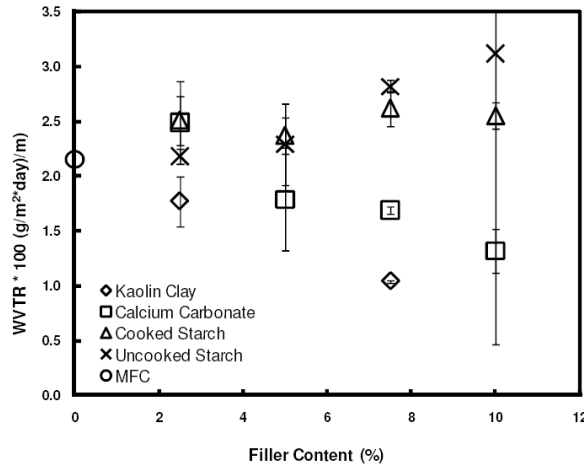


Figure I-45: Water vapour transmission rate of filled MFC films [18].

- Coating of MFC films

In a second step, MFC films were coated with beeswax, paraffin or cooked starch using a dipping technique. This second method was more efficient to reduce the water vapour transport of MFC films. Beeswax coating resulted in the lowest value, with a 1g/m^2 layer the water vapour value was much smaller than LDPE value (Figure I-46).

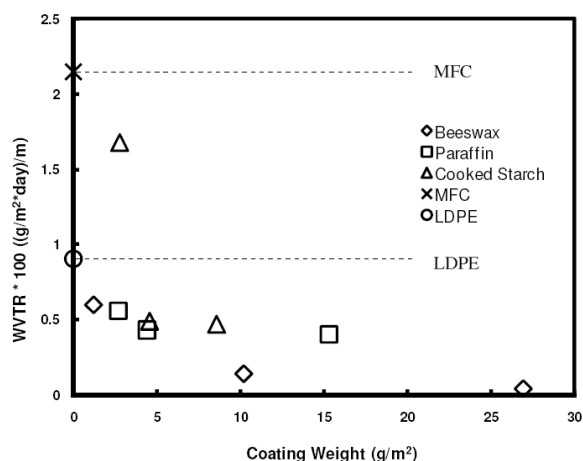


Figure I-46: Water vapour transmission rate of coated MFC films [18].

- Surface coating with MFC

Fukuzumi *et al.* [71] developed transparent and high gas barrier films from cellulose nanofibres prepared by TEMPO-mediated oxidation. Indeed, the coating of a polylactic acid (PLA) film ($20\ \mu\text{m}$) with a $0.4\ \mu\text{m}$ thick nanofibre layer led to a decrease of oxygen permeance from $74600000\ \text{cm}^3/\text{m}^2\cdot\text{day}\cdot\text{bar}$ to $10000\ \text{cm}^3/\text{m}^2\cdot\text{day}\cdot\text{bar}$ at 23°C -0% RH. A

second study on the barrier properties of TEMPO MFC from softwood bleached kraft pulp was published by Isogai team. Indeed, Fujisawa *et al.* [72] compared the properties of TOCN-COOH films with TOCN-COONa films corresponding to TEMPO-oxidized cellulose with free carboxyl groups. The oxygen transmission rate was determined for poly(ethylene terephthalate) (PET) films and PET films coated with 1 μ m thick TOCN-COONa or TOCN-COOH layer at 23°C-0% RH. The value of PET film coated with TOCN-COONa was improved from 1550 to 0.17 cm³. μ m/m².day/bar.

Lately, the properties of TEMPO MFC films were determined according to the starting pulp and the reaction conditions by Rodionova *et al.* [73]. The lowest oxygen permeability was obtained from spruce pulp and the highest carboxylate content (1.4 mmol/g). The OTR of PET film coated with TEMPO oxidized MFC reached 4 cm³/m².day.

I.3.7.2.5. - Biodegradability

Taniguchi *et al.* [81] studied the biodegradability of MFC films from several sources such as wood (spruce and poplar bleached kraft pulp), tunicin, and chitosan. For this, MFC films with a thickness of 3-100 μ m were buried in humus soil for several days. The degradation was evaluated by the degree of enzyme decomposition due to micro-organisms. The results, summarized in Table I-13, reported that films disappeared after 40 days in soil.

Time after burial (days)	Biodegradation step
10	Surface swelling
15-17	Surface softening
20-22	Development of pores on surface
30-33	Corruption of part of surface
40	Disappearance

Table I-13: Biodegradation of MFC films [81].

I.3.7.3. - Conclusion

MFC is a very interesting material for its good mechanical and barrier properties and its good biodegradability. However, due to its very low solid content, it is very difficult to use it alone. Embedding in a polymer matrix can be a good way to take full advantage of its properties.

I.4. - MFC based nanocomposites

Nanocomposites in general are two-phase materials in which one of the phases has at least one dimension in the nanometer range (1–100 nm) [114]. The use of MFC as reinforcement filler in nanocomposites has many advantages such as the low cost of the raw material, low density, renewable origin, large availability, high mechanical properties, biodegradability...

MFC was already introduced in several matrices as described in Figure I-47.

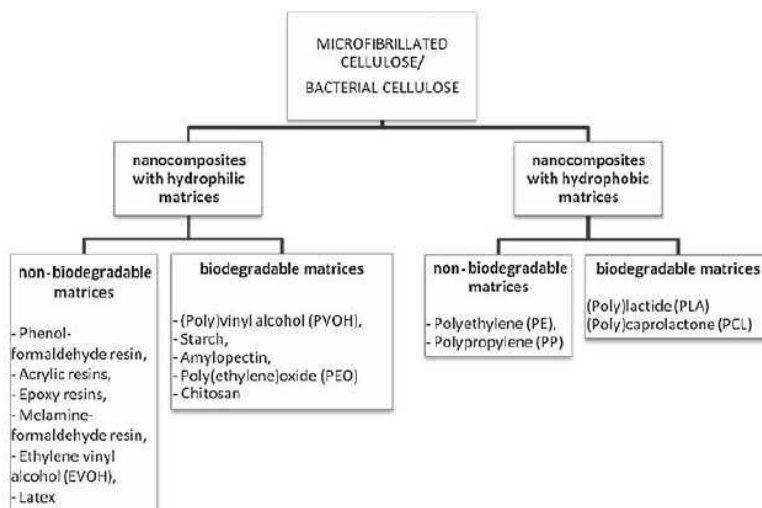


Figure I-47: Nanocomposites based on nanocellulosic materials [114].

Starch and poly(vinyl alcohol) were studied in the present work for the development of nanocomposites. These hydrophilic and biodegradable matrices were chosen for their good compatibility with MFC and their biodegradability properties.

I.4.1. - Starch matrix

I.4.1.1. - Introduction

Starch is a natural, renewable, biodegradable polymer produced as a storage polysaccharide from various sources of seed endosperm and plant tubers such as maize, wheat and potato. Starch consists of two glucosidic macromolecules of general formula $(C_6H_{10}O_5)_n$: amylose and amylopectin. The ratio of these two macromolecules depends on the starch origin. Their structures are presented Figure I-48.

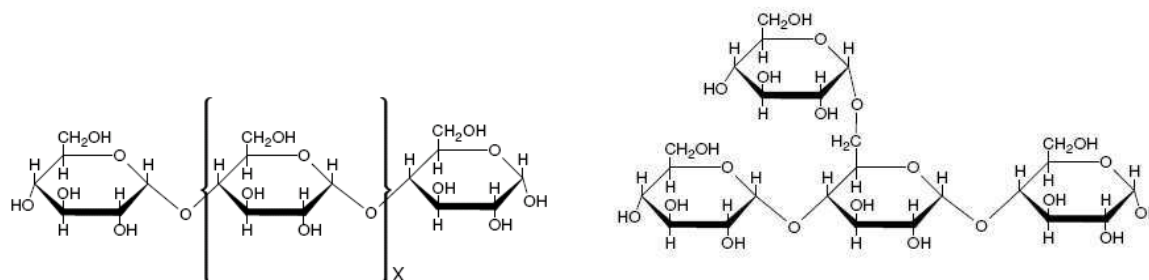


Figure I-48: Chemical structure of amylose (left) and amylopectin (right) [115].

The dissolution of the starch powder in water at high temperature leads to the release of polymer chains and to starch gelatinization. A rearrangement of polymer chains occurs. Many studies reported the preparation of starch cast films from starch solutions [116,117]. There is a continuous development of environmentally friendly biodegradable plastic films from starch to compete with and replace synthetic polymers in different applications [118]. Starch is promising because of its low cost and its natural abundance [119]. However, starch films are generally too brittle, and plasticizers such as glycerol or sorbitol are currently used for the production of starch films. In their study, Dole *et al.* [120] showed that the use of such additives decreases the barrier properties and unfortunately no good compromise can be

found between mechanical and barrier properties. Indeed, the best barrier properties are obtained for low plasticizer contents, giving too brittle films. The oxygen permeability was increased from 0.53 to 4.66 mol/Pa.m.s for films with 12% and 25% glycerol, respectively. Nano-biocomposites are a new class of hybrid materials composed of nano-sized filler incorporated into a bio-based matrix [121]. According to their shape and their nature, nano-fillers can improve the starch properties such as the mechanical stiffness and the gas barrier properties [122]. Park et al. [123] have for example developed biodegradable thermoplastic starch/clay nanocomposites. The interactions between starch and cloisite clay led to improved tensile properties with an increase of tensile strength value from 2.6 to 3.3 MPa with addition of 5% clay. Moreover, a reduction of 40% of water vapour transmission rate value was observed with 10 wt% cloisite compared to neat starch.

I.4.1.2. - Mechanical properties

Many authors have also used MFC as filler to reinforce starch films. The main method to produce MFC/starch composite is casting/evaporation. Dufresne *et al.* [49,124] produced composite materials with MFC from potato tuber cells, starch and glycerol. They reported that the mechanical properties of composites increase with the increase of MFC content. Moreover, the MFC content influenced the water diffusion coefficient. Table I-14 presents this decrease of water diffusion coefficient with the increase of MFC content.

Celulose content (%)	D (cm ² /s)	
	0% Glycerol	30% Glycerol
0	5.04 x 10 ⁻¹⁰	1.10 x 10 ⁻¹⁰
10	3.53 x 10 ⁻¹⁰	8.39 x 10 ⁻¹¹
30	1.65 x 10 ⁻¹⁰	5.25 x 10 ⁻¹¹
40	1.72 x 10 ⁻¹⁰	2.08 x 10 ⁻¹¹

Table I-14: Water diffusion coefficients in MFC/starch composites conditioned at 95% RH [124].

In Lopez-Rubio *et al.* study [125], the MFC suspensions were mixed with solutions of starch and casted in mould. The glycerol content varied between 0 and 38 wt%. The stirring led to microbubble formation which had a negative impact on the film preparation. They were removed by degasification before casting. The authors thus obtained high quality films even without glycerol. Glycerol-free amylopectin film reinforced with 10% MFC had a Young's modulus around 2 GPa and a tensile strength of 40 MPa at 23°C 50%RH. The increase in glycerol content increased the ductility of films but decreased their stiffness and strength. Indeed, films with 10% MFC and 20% glycerol had values two times lower with a Young's modulus and a stress at break of 1.1 GPa and 16 MPa, respectively, at 23°C 50% RH.

Homogeneous films were obtained by Svagan *et al.* [96]. The concentration of MFC in composites reached up to 70 wt%, thanks to a good compatibility between MFC and starch. A reinforcement effect of the starch/glycerol (50/50) matrix was observed with the increase of MFC content. The Young's modulus increased from 1.6 MPa for pure starch to 6.2 GPa when adding 70 wt% of MFC within the starch matrix. All the values for several MFC contents are given in Table I-15.

MFC (wt %)	Young's modulus (MPa)	Tensile strength (MPa)	Strain-to-failure (%)	Work of fracture (MJ/m ³)
0	1.6	0.35	80	0.18
10	180	5.0	25	0.94
20	780	15	22	2.7
30	1600	31	18	4.
40	3100	58	15	6.2
50	4300	80	11	6.5
60	4800	120	9.3	7.8
70	6200	160	8.1	9.4
100	13000	180	2.1	2.4

Table I-15: Mechanical properties of Starch/MFC composites [96].

I.4.1.3. - Barrier properties

Svagan *et al.* [126] also demonstrated that MFC had a strong reducing effect on the moisture uptake of starch. Indeed, with 70 wt% of MFC, the moisture uptake was halved compared to neat starch films.

The introduction of MFC in starch films allowed to reinforce these films and to decrease their water sensitivity. Plackett *et al.* [127] also studied the introduction of MFC from 0% to 75% in the amylopectin matrix with or without glycerol. The reinforcement effect was only visible for MFC contents higher than 20%. For the oxygen permeability at 23°C 50% RH, the increase of MFC content decreased the value. However, it was impossible to determine the value for the unfilled matrix due to the brittleness of the films. No significant difference between pure MFC films and starch/MFC 50/50 films was observed. This could be a good compromise to obtain good barrier properties from a suspension with higher solid contents. Indeed, the values obtained in this study were of the same order of magnitude as the gas permeability of PVOH.

I.4.2. - Poly(vinyl alcohol) matrix

I.4.2.1. - Introduction

Poly(vinyl alcohol) (PVOH) is the most important synthetic water-soluble polymer produced in the world [128]. PVOH is prepared from the hydrolysis of poly(vinyl acetate) as presented in Figure I- 49 and Figure I- 50:

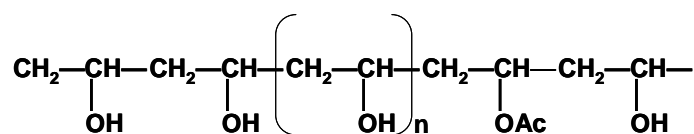


Figure I- 49: General molecular structure of PVOH.

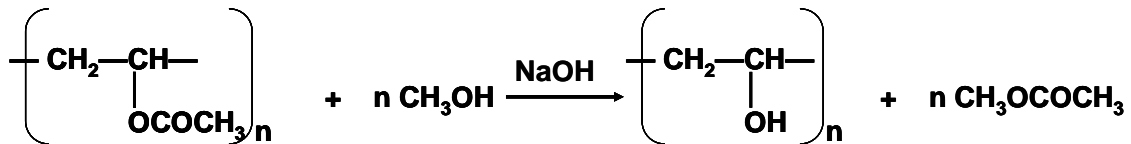


Figure I- 50: Hydrolysis of poly(vinyl acetate).

PVOH properties depend strongly on its degree of polymerisation (molecular weight) and degree of hydrolysis (Figure I-51). The maximum degree of hydrolysis is 99%, a 1% acetate remaining thus after hydrolysis.

Low viscosity Increased solubility Increased flexibility	High viscosity Tensile strength Pigment binding
Molecular weight Low \longleftrightarrow High Hydrolysis degree	
Increased solubility Water sensitivity Flexibility Tackiness Adhesion to hydrophobic surface	Water resistance Barrier properties Tensile strength Solvent resistance Adhesion to hydrophilic surface

Figure I-51: Effect of molecular weight and degree of hydrolysis on PVOH properties [129].

Many studies have developed a large variety of nanocomposites using PVOH as matrix [130]. For example, clay introduction was studied for PVOH by Strawhecker *et al.* [131]. The hybrid polymer/silicate systems had mechanical, thermal and water vapour transmission properties which were superior to that of the neat PVOH matrix for low loading. Moreover, the thermal stability was slightly enhanced and the optical clarity was retained. Carbon nanotubes were also introduced in PVOH matrix leading to the nucleation of crystalline phase for very low weight fractions. However, the carbon nanotube filler also promoted the degradation rate of the matrix [132].

I.4.2.2. - Mechanical properties

With the growing interest in fibrous biopolymers, MFC was also introduced in PVOH. For example, Lu *et al.* [133] produced composites with MFC contents ranging from 1 to 15 wt%. PVOH is water-soluble, which allows a good dispersion of MFC in polymer matrix due to the high stability of MFC in water. MFC had a reinforcement effect on this matrix: the Young's modulus of the composite increased from 3.7 to 5.2 GPa when adding 15% MFC. Another study achieved by Leitner *et al.* [53] presented the reinforcement of PVOH matrix by MFC. MFC was introduced at high concentrations from 50% to 90% giving composites with tensile strengths of 60-80 MPa and elastic moduli of 6-8 GPa. For comparison, neat PVOH has a tensile strength of 17 MPa and an elastic modulus of 0.25 GPa at room temperature.

Poly(vinyl alcohol) nanocomposites reinforced with cellulose fibrils were studied by Cheng *et al.* [134]. Several kinds of fibrils (and not MFC) were used and compared to commercial MFC. Fibrils from microcrystalline cellulose, regenerated cellulose fibres and pure cellulose fibres were obtained by high intensity ultrasonication. In this study, the introduction of fibrils

once again increased the mechanical properties of PVOH and the reinforcement effect was still more important with the small fibrils. The composites made of PVOH and the smallest fibrils (6%) reached a Young's modulus of 7 GPa and a tensile strength of 113 MPa.

Bruce *et al.* [54] reported the development of high performance composites from low-cost plant primary cell walls. Two kinds of cellulose were used, purified cell wall fragments (PCWF) and fibrillated cell wall materials (FCWM). Composites were produced from 4 types of matrices (poly(vinyl alcohol), acrylic polymer, epoxy, and hemicellulose). The composites PVOH and cellulose microfibrils offered the highest mechanical properties (tensile strength of 145 MPa and tensile modulus of 6 GPa) compared to other cellulose based composites in this study.

All results are summarized in Figure I-52. The reinforcement potential of MFC was clearly observed for the PVOH matrix in each study.

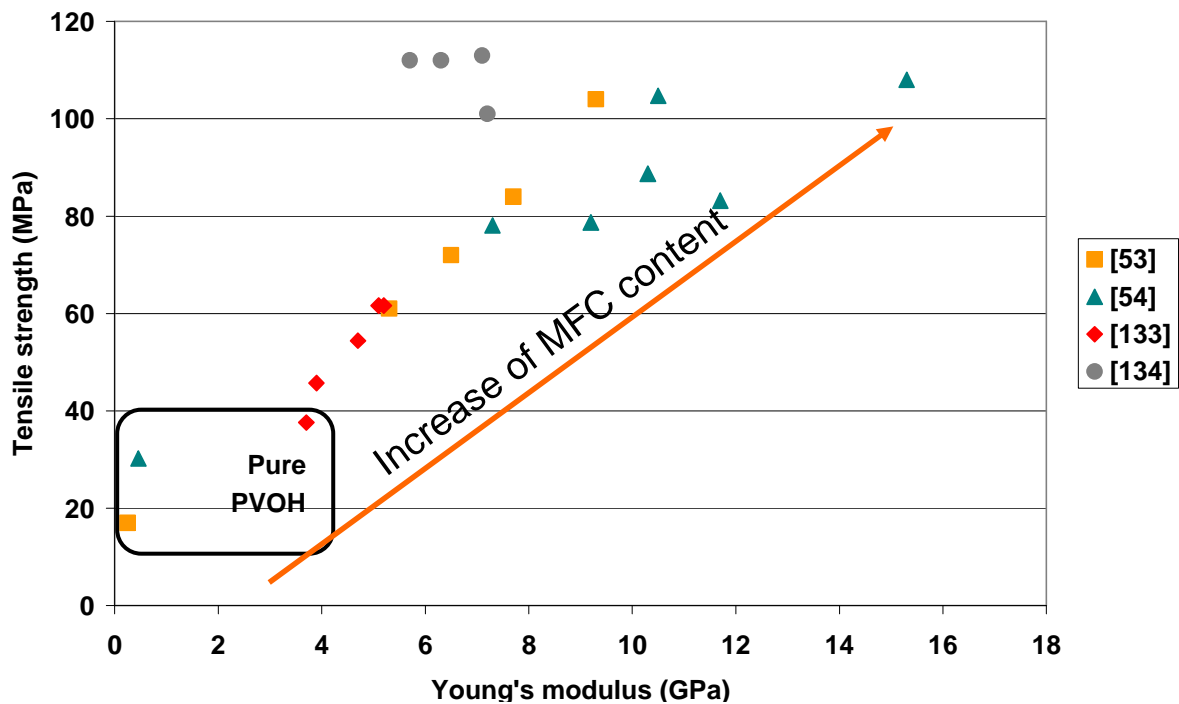


Figure I-52: Comparison of mechanical properties values for PVOH/MFC composite films.

I.4.2.3. - Barrier properties

Paralikar *et al.* [135] developed PVOH/cellulose nanocrystal barrier nanocomposite films. PAA, Poly(acrylic acid) was used as a cross linking agent to provide water resistance to PVOH. A heat treatment improved the cross linking density. The barrier properties of the films were evaluated from water vapour transmission rate measurements and chemical vapour transmission rate measurements. The films prepared with 10% cellulose nanocrystal and 10% PAA presented a good potential for the development of barrier membranes. Indeed, these films were three times more water vapour resistant than 100% PVOH films. The water vapour transmission rate (WVTR) of composites reached 240 g/m².day instead of 720 g/m².day for PVOH film at 30°C and 30% RH.

Cellulose nanocrystals were added to poly(vinyl alcohol) and poly(vinyl acetate) copolymers by Roohani *et al.* [130]. Results showed stronger interactions between the matrix and the filler for fully hydrolyzed PVOH compared to partially hydrolyzed PVOH. Indeed, the reinforcement effect was found to be higher for the highest degree of hydrolysis of PVOH.

The relative tensile modulus reached 1.2 and 2.2 for a composite filled with 12% nanocrystals and PVOH hydrolyzed at 80% and 99%, respectively.

I.4.3. - Conclusion

The literature survey on MFC nanocomposites showed that the addition of MFC has a positive effect on starch and PVOH matrix properties. Most studies focused on the mechanical properties and detailed the reinforcement potential of MFC. The enhancement of mechanical properties was due to the strong interaction between MFC and hydrophilic matrix.

The barrier properties of these materials were little detailed although they are essential for the development of packaging materials.

I.5. - MFC based paper & board materials

In spite of a strong interest for cellulose microfibrils, their use in papermaking process is still less studied compared to composite materials. Indeed, up to now few studies were realized on the introduction of MFC in coating colour or on the production of paper & board materials with MFC. First studies on the reinforcement of bulk are firstly described and the introduction in coating colour is treated in the second part.

I.5.1. - Introduction of MFC into pulp

Eriksen *et al.* [136] studied the fabrication of thermo-mechanical pulp (TMP) with MFC addition. The authors evaluated the effect on physical properties of TMP handsheets with MFC at various concentrations between 1 and 8 %. An increasing tensile index with decreasing average particle size was observed in this study. The tensile index increased at the 95% confidence level compared to the reference sheet. Moreover, the addition of MFC reduced the light scattering and the light absorption coefficients, also decreased the brightness but decreased the air permeability. The authors observed that the energy consumption for the MFC production was very high and this may be a major objection against the use of MFC for industrial application although its positive effect on the paper strength was proved.

Ahola *et al.* [137] used microfibrillated cellulose as a paper strength additive. The ability of MFC to improve the wet-strengthening was studied in order to reduce the amount of poly(amideamine) epichlorohydrin (PAE) used in papermaking. A preliminary adsorption study with quartz crystal microbalance (QCM) showed that a uniform and viscous layer of MFC could be adsorbed using a bi-layer system with a preliminary layer of PAE. The treatment with PAE and MFC of pulp slurries resulted in an increase of wet and dry strengths even at low added amounts of PAE (*cf. Figure I-53*).

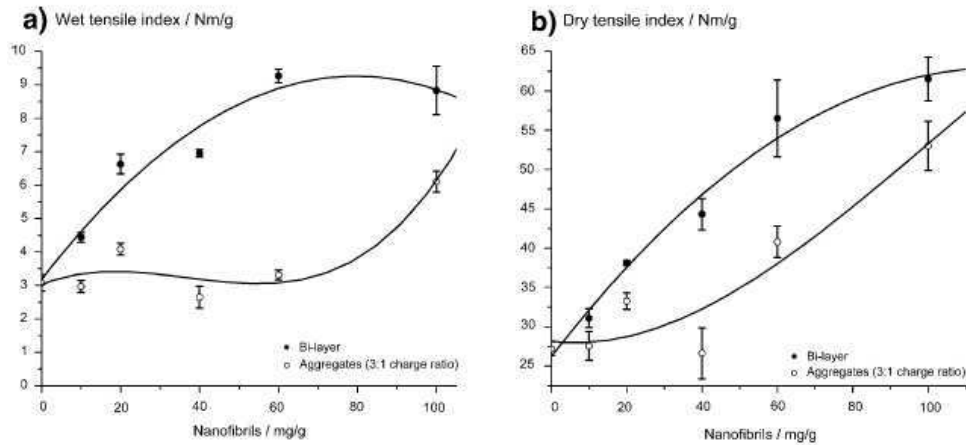


Figure I-53: Wet and dry tensile index of paper treated with PAE according to the addition of cellulose nanofibrils [137].

Mörseburg *et al.* [138] developed a new concept of layered sheets using thermo-mechanical pulp (TMP), clays and MFC. Several compositions were tested (cf. Table I-16) and the strength and optical properties were evaluated for each sample. The best sheets (N3) were composed of fillers and TMP in the top layer and MFC and refined TMP in the centre of the sheets. The use of MFC in top and wire layer led to worse results. The quality index, represented in Figure I-54, shows the results obtained.

Sheet structure	T1	T2	F1	F2	N1	N2	N3
Wire layer	TMP A	TMP A	TMP A + Clay	TMP A + Clay	TMP A + Clay + 0.5 NFC	TMP A + Clay + 0.25 NFC	TMP A + Clay
Interface						0.25 NFC	
Centre layer	TMP R	TMP R + BSK	TMP R + BSK	TMP R + BSK	TMP R	TMP R	TMP R + NFC
Interface						0.25 NFC	
Top layer	TMP A	TMP A	TMP A + Clay	TMP A + Clay	TMP A + Clay + 0.5 NFC	TMP A + Clay + 0.25 NFC	TMP A + Clay
BSK/NFC content (%)	0	9.6	8.8	8.8	2.8	2.6	2.9
Filler content (%)	0	0	30.4	37.3	33.7	33.6	34.6

Table I-16: Composition of the layered sheets [138].

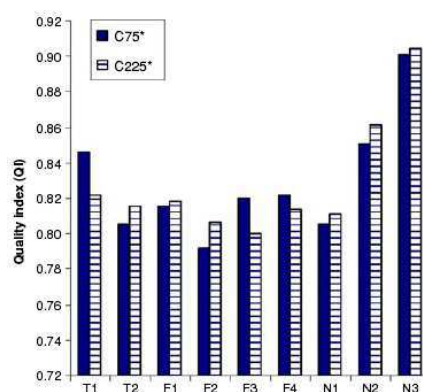


Figure I-54: Quality index of layered sheets [138].

I.5.2. - MFC in coating colours

Concerning the coating with MFC suspensions, the objective of the studies was to improve the barrier properties or the printing quality.

Syverud *et al.* [92] worked on the spraying of MFC as a surface layer on paper. First, oriented sheets were prepared using a dynamic sheet former and then MFC suspension was deposited on the top of the wet base paper. The results showed that the strength of the base paper increased significantly upon coverage with a layer of less than 10 g/m² of MFC and the air permeability decreased dramatically (cf. red ring in Figure I-55). The addition of MFC layer with a coat weight between 2 and 8 g/m² allowed decreasing the air permeability from 40000 to 300 nm/Pa.s. The value is thus divided by 2 for a 2 g/m² coating and by 300 for a 8 g/m² coating compared to the uncoated base paper.

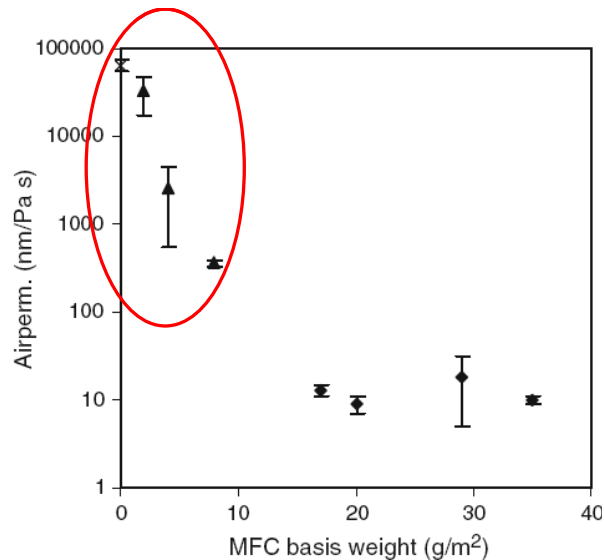


Figure I-55: Air permeability of the base paper (x), MFC coated papers (▲) and MFC films (◆) [92].

A kraft paper and a greaseproof paper were coated with an aqueous carboxymethylated MFC suspension in a study carried out by Aulin *et al.* [91]. In this case, the oxygen transmission rate of the paper decreased dramatically even with a thin MFC layer. The values for the two papers are presented in Figure I-56. The coverage of MFC on paper fibres is observed on E-SEM micrographs in Figure I-57.

However, the concentration of the suspension was very low and the deposited coat weight was thus limited. To reach higher coat weights, higher solid contents should be used.

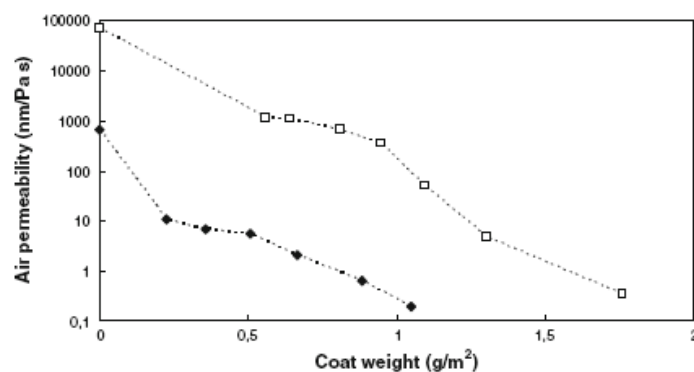


Figure I-56: Air permeability as a function of MFC-coat weight for an unbleached (□) and a greaseproof paper (◆) [91].

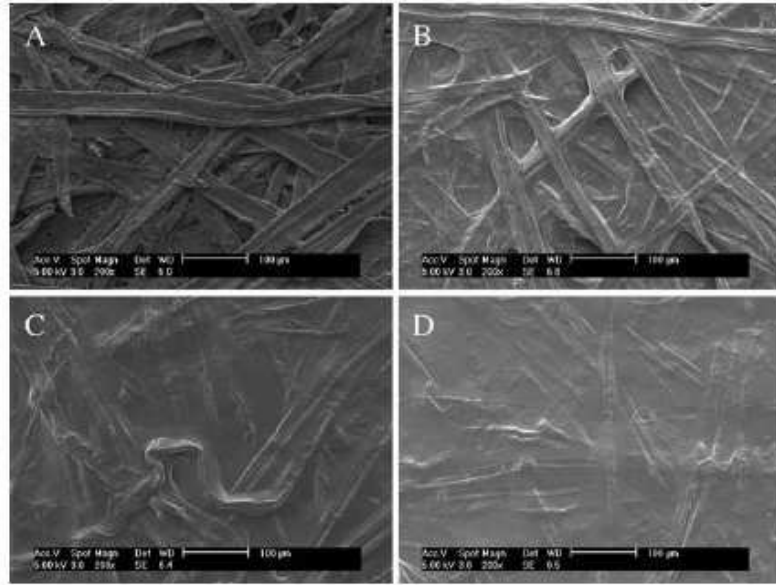


Figure I-57: E-SEM micrographs of uncoated (A) and MFC coated with coat weights of 0.9 g/m² (B), 1.3 g/m² (C) and 1.8 g/m² (D), Scale bar 100 µm [91].

Hult *et al.* [1] presented another approach to high barrier packaging using MFC and shellac. Shellac is a natural hydrophobic resin. The suspension was prepared in ethanol and used in two coating processes: rod coating and spray coating. The coating was achieved on three base papers (A/B/C). The results obtained were a reduction of air, water and oxygen permeability. As shown in Table I-17, the air permeability value decreased with MFC coating (series AM/BM/CM), from 49 nm/Pa.s to 0.752 nm/Pa.s at 25°C-50% RH for the base paper. A new decrease was obtained with shellac coating (series AMS/BMS/CMS) and the air permeability of AMS sample reached 0.150 nm/Pa.s at 25°C-50% RH. The same trend was observed as other barrier properties. The authors observed in this study that a multi-layer system gave better barrier properties than one layer with a MFC/Shellac blend. Although a sufficient oxygen barrier for high barrier packaging was not achieved, the reduction of OTR was significant.

Series	Air permeance (nm/Pa s)	OTR (cm ³ /m ² 24 h)	WVTR (g/m ² 24 h)	Fmax (kPa)
A	49 ± 14	–	53.29 ± 3.25	815,2 ± 38,1
B	184 ± 92	–	64.58 ± 2.14	807,4 ± 41,1
C	813 ± 97	–	72.38 ± 0.58	819,6 ± 23,5
AM	0.752 ± 0.031	34578 ± 1227	52.89 ± 2.27	–
BM	0.482 ± 0.054	35034 ± 1287	64.24 ± 1.72	–
CM	0.671 ± 0.042	35275 ± 1197	70.89 ± 1.41	–
AMS	0.150 ± 0.003	4466 ± 103	6.54 ± 1.12	822,3 ± 49,5
BMS	0.054 ± 0.007	5090 ± 94	7.68 ± 0.54	808,6 ± 77,9
CMS	0.073 ± 0.004	5438 ± 165	8.14 ± 0.43	812,0 ± 20,2

Table I-17: Barrier properties of untreated papers and coated samples [1].

Hamada and Bousfield [139] reported the coating of thin MFC layer on a PVA synthetic sheet. The aim was to improve the printability. Three coat weights, namely 0.5, 1.5 and 3 g/m² were deposited at the sheet surface using various wire wound rods. The 3 g/m² layer

gave a good coverage and improved the printing quality. Indeed, the presence of MFC on the surface allowed to capture the ink pigments improving the ink density (Figure I-58).

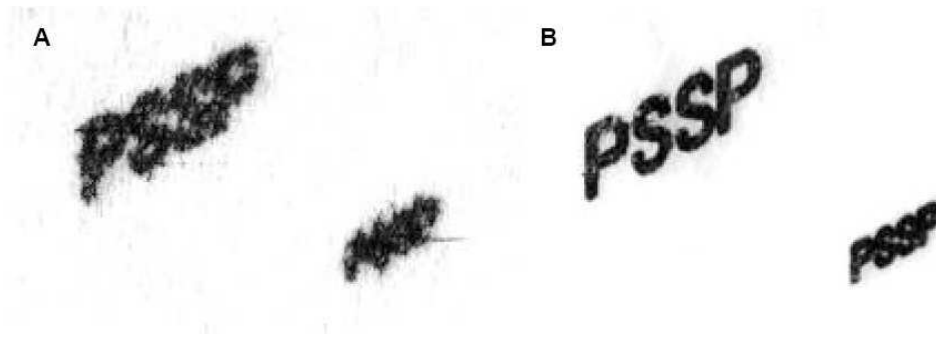


Figure I-58: Images of inkjet printed samples: uncoated synthetic fibre sheet (A), coated sheet of MFC with 3 g/m^2 (B) [139].

A Patent was also deposited by Ankerfors *et al.* [77] in 2009, relating to compositions for coating of printing papers. This coating colour combining MFC and one or more polysaccharide hydrocolloids could reduce the linting and dusting propensity of paper during printing. The polysaccharide can be starch for example. The use of polysaccharide hydrocolloid presents three advantages; it offers a coating that holds the linting particles in place, partially anchors particles internally in the sheet and anchors the MFC layer to the sheet. This invention can alleviate the linting tendency via surface sizing treatment with MFC, starch or a mixture of the two additives.

I.6. - Conclusion

First, the production of MFC has been improved these past years with more efficient and less energy-consuming processes. MFC can be obtained from several cellulose sources and MFC properties depend directly on this source and mainly on preparation conditions.

MFC films, produced by different techniques, presented good mechanical and barrier properties, promising for the development of packaging.

Several investigations have demonstrated the reinforcement potential of MFC in different matrices such as starch or poly(vinyl alcohol) for example. However, few studies detailed the barrier properties of these MFC based composites.

The use of MFC in coating colours has just started to be studied. From results obtained so far, coating offers good resulting properties in spite of very low coat weights. However, higher solid contents of MFC suspensions are necessary to increase the coat weight.

The use of MFC has thus a great interest in packaging area. However, more research has to be conducted to solve the current drawbacks, mainly their low concentration and their high viscosity.

II - Materials and methods

II.1. - Introduction

This chapter describes the raw materials, the experimental protocols and the characterisation methods employed throughout the project. The first part deals with the raw materials and mainly the microfibrillated cellulose (MFC). Several sources of MFC were studied. Their methods of production are thus detailed for each kind of suspension. Moreover, a codification was used to clearly define the MFC suspensions and to improve the understanding. Subsequently, the experimental protocols are described with the developed techniques to produce MFC or composite films and the coating methods used to manufacture the MFC based paper & board materials. The last part of the chapter is devoted to the characterisation techniques such as microscopy, viscosity measurements, mechanical and barrier properties, thermal properties....

II.2. - Materials

II.2.1. - Microfibrillated cellulose (MFC)

MFC is the main material of this study and it is very important to clearly define it. Indeed, the terminology used for this material is not clearly defined yet and authors use various nomenclature for the same product. Therefore, microfibrillated cellulose can also be described by other terms such as: Cellulose nanofibrils, Cellulose microfibrils, Cellulose nanofibers or Nanocellulose. Here, a codification is employed to describe the kind of MFC according to the production method that is to say the pretreatment and the mechanical shearing treatment. This codification is detailed in Figure II-1.

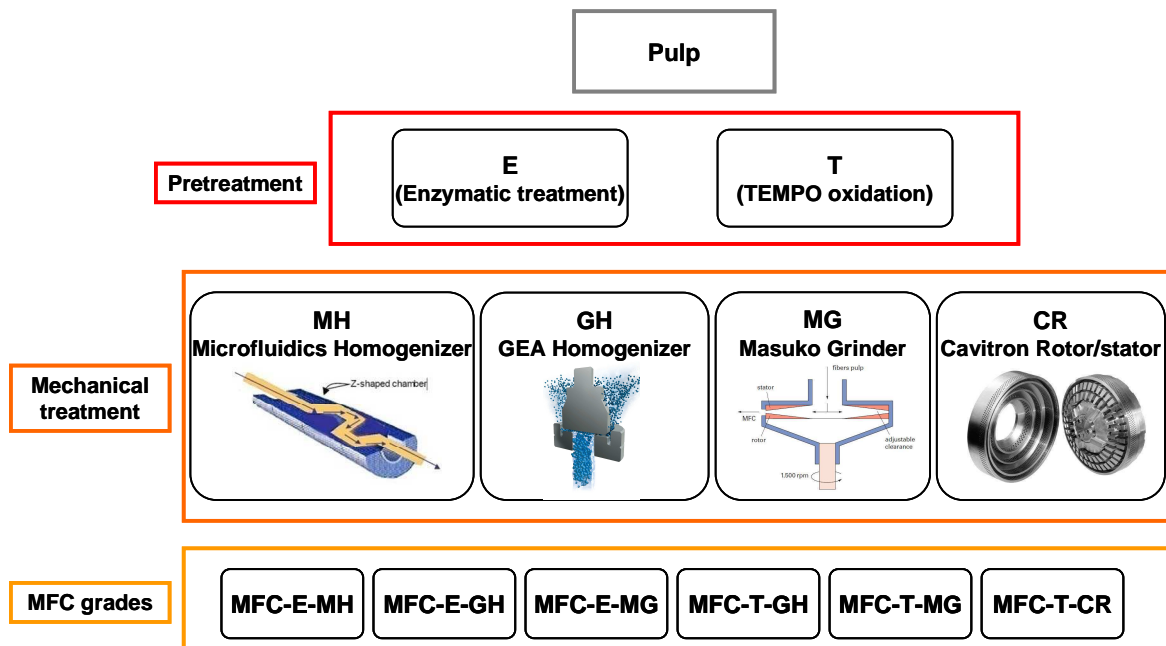


Figure II-1: Codification used to define MFC.

MFC was produced at different scales to allow the achievement of trials. Three sources were thus obtained from laboratory productions (MH and MG) and three others from pilot

productions (GH and CR). In addition to the six MFC grades, a commercial source, called MFC-Arbo, was also studied as reference and compared with other MFC suspensions. Each MFC source is detailed thereafter with its supplier or the method used for the production.

II.2.1.1. - Commercial MFC

MFC-Arbo corresponds to the material called Arbocel, a commercial fine cellulose supplied by JRS company (Germany). This MFC was delivered with a concentration of 13%. Figure II-2 shows its visual aspect which looks like a fine pulp. Morphological investigation showed a diameter of $\sim 30 \mu\text{m}$ and a length of $\sim 500 \mu\text{m}$.

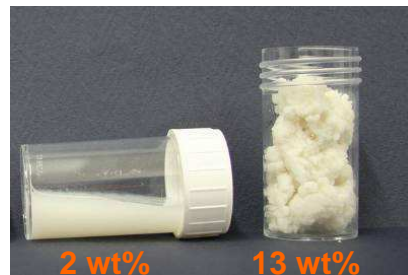


Figure II-2: MFC-Arbo.

All other MFC suspensions were produced at lab or pilot scale using an enzymatic or chemical pretreatment followed by a mechanical shearing treatment. All productions were carried out from the spruce/pine (60/40) dissolving pulp delivered by the Domsjö company (Sweden).

II.2.1.2. - Production of enzymatically pretreated MFC

II.2.1.2.1. - General protocol

The production of MFC was performed in several steps: refining, enzymatic pretreatment and mechanical shearing of the pulp. The general protocol is described in Figure II-3.

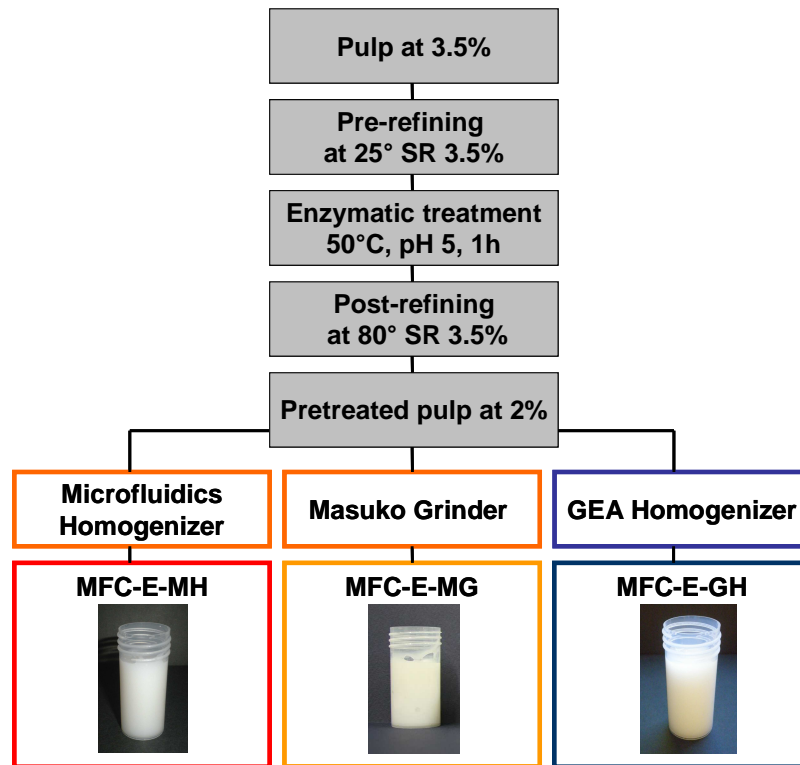


Figure II-3: General protocol to produce enzymatically pretreated MFC.

II.2.1.2.2. - Enzymatic pretreatment

To improve the accessibility to enzymes, the pulp, disintegrated at 3.5%, was firstly pre-refined using a 12" single-disc pilot refiner system. The pre-refined pulp at 25°SR was then treated with enzymes (Novozym 476; 0.1 kg/t) at 50°C, pH 5 for 1 hour. A second refining, until 80°SR, was then carried out to cut the fibres and then improve the cellulose fibrillation [140].

II.2.1.2.3. - Mechanical treatments

Three devices were used to perform the mechanical shearing on the enzymatic pretreated pulp in order to produce microfibrillated cellulose:

- Microfluidizer M-110EH (Microfluidics Corp.) (MH) is a high-pressure homogenizer equipped with 3 Z-like chambers with internal diameters of 400 μm , 200 μm or 100 μm . The suspension pulp at 2% flowed at 350 mL/min corresponding to an applied pressure of 1500 bar for the 400 μm chamber, 2000 bar for the 200 μm chamber and 2500 bar for the 100 μm chamber. The pulp fibre slurry was passed once through the 400 μm diameter chamber, 3 times through the 200 μm diameter chamber and 5 times in the last 100 μm diameter chamber.
- Supermasscolloider (Masuko Sangyo Co) (MG) is an ultra-fine grinder using a rotor/stator technology; pulp suspension around 2% was thus only passed 5 times in the device at 1500 rpm.
- Ariete homogenizer (GEA Niro Soavi) (GH) allowed MFC production at pilot scale with a flow rate of 1000 l/h. The production was performed into three steps: a first pass at 500 bars, a second pass at 1000 bars followed by four passes at 1500 bars.

Table II-1 summarizes the main parameters for each technique.

Mechanical treatment	Microfluidics Homogenizer	Masuko Grinder	GEA Homogenizer
Scale	Lab	Lab	Pilot
Parameters	1 pass 400 μm 3 passes 200 μm 5 passes 100 μm	5 passes 1500 rpm	1 pass 500 bar 1 pass 1000 bar 4 passes 1500 bar

Table II-1: Mechanical shearing used after enzymatic pretreatment.

II.2.1.3. - Production of TEMPO oxidized MFC

II.2.1.3.1. - General protocol

TEMPO oxidation is a chemical modification treatment of fibres. Here MFC was produced in only two main steps: fibres were pretreated by TEMPO oxidation before the mechanical shearing as shown in Figure II-4.

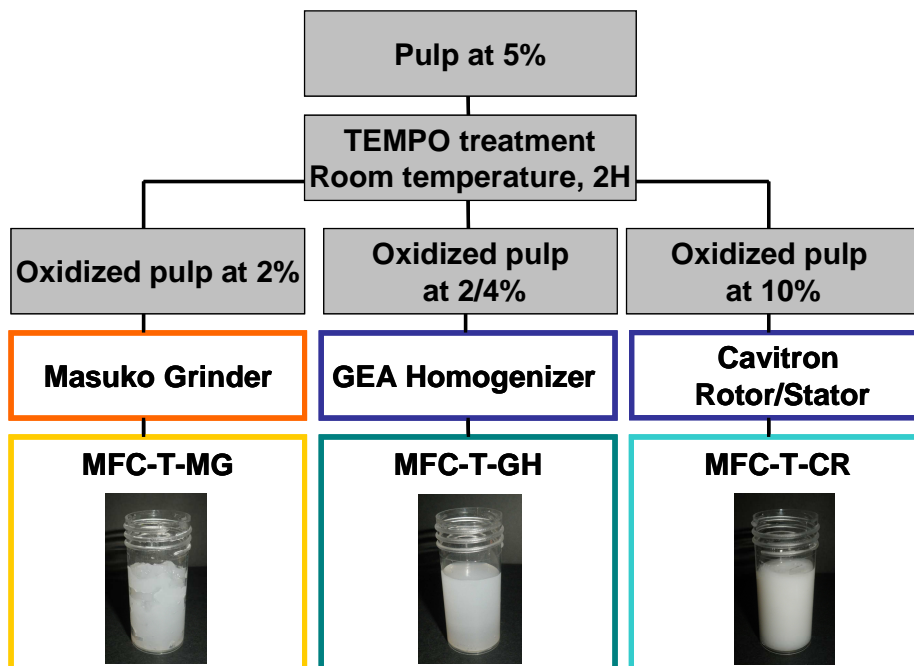


Figure II-4: General protocol of TEMPO oxidized MFC production.

II.2.1.3.2. - TEMPO oxidation

The TEMPO oxidation step was performed in the redox system TEMPO (2,2,6,6-Tetramethyl-piperidin-1-oxyl) / NaBr / NaOCl. The TEMPO molecule is observed in Figure II-5.

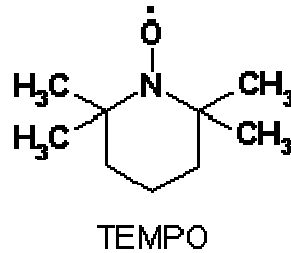


Figure II-5: Molecule of TEMPO.

The oxidation rate was defined to 1.1 mmol/g in order to preserve a yield around 70%. Pulp at 5% consistency was stirred with TEMPO reagent, NaBr and NaOCl during 2 hours. Ethanol was then added to stop the reaction. Four washing cycles were then carried out by centrifugation leading to an oxidized pulp with a concentration between 5-10 wt%.

II.2.1.3.3. - Mechanical treatment

Three types of mechanical shearing were also used to fibrillate the oxidized pulp.

- Supermasscolloider (Masuko Sangyo Co) (MG): the oxidized pulp was passed 3 times in the device at 1500 rpm in order to obtain the fibrillation.
- Ariete homogenizer (GEA Niro Soavi) (GH): two passes at 1500 bar were sufficient to reach a good fibrillation state.
- Cavitron rotor/stator: during the SUNPAP project, another device was developed and used to produce TEMPO MFC. It consists of concentric rings of rotor and stator with nozzle geometry (Figure II-6). The homogenization occurred by shear forces in the rotor-stator gap and by pressure pulsation in the nozzle. Its capacity was 0.2-120 m³/h.

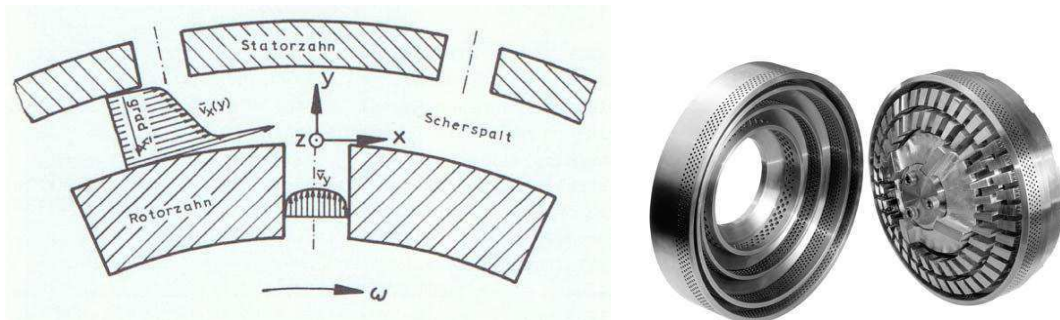


Figure II-6: Rotor-stator device developed in SUNPAP project [140].

As observed in Table II-2, the mechanical shearing was less intensive (severe) after the TEMPO pretreatment compared to enzymatic reference. Indeed, the fibrillation was easier after this pretreatment. The TEMPO oxidation replaces the hydroxyl groups by carboxyl groups. This modification of fibres increases the space between fibrils, decreases the degree of polymerization as well as the fibre length.

Mechanical treatment	Masuko Grinder	GEA homogenizer	Cavitron rotor/stator
Scale	Lab	Pilot	Pilot
Parameters	3 passes 1500 rpm	2 passes 1500 bar	22 runs

Table II-2: Mechanical shearing used after TEMPO pretreatment.

II.2.2. - Starch

A modified waxy corn starch was provided by Cargill. This starch mainly consisted of amylopectin at 98%. The modification was performed by hydrophobic octenyl succinic groups.

II.2.3. - PVOH

Poly(vinyl alcohol) (PVOH) was the Mowiol 4-98 delivered by Kuraray. The degree of hydrolysis of the polymer was 98% and its molecular weight was 27000 g/mol.

PVOH is a product already used in paper for several applications such as:

- Carrier for optical brightening agents, co-binder and water retention aid in the coating colour.
- In silicon based papers and oil grease and fat-proof papers as surface treatment
- In tissue and cigarette papers for high mechanical values [141].

II.2.4. - Sorbitol

The sorbitol D-Sorbit (98 wt%) provided by Carl Roth GmbH was used as plasticizer for the matrix to develop composites.

II.2.5. - Poly(ethylene oxide)

A poly(ethylene oxide) from Sigma Aldrich was used for the inverted dialysis procedure. Its molecular weight was 100000 g/mol to avoid any diffusion through the dialysis membrane.

II.2.6. - Base boards

Two base boards provided by Stora Enso (SUNPAP partner) were used for the coating trials during the project.

- An uncoated kraftboard of 220 g/m² dry
- Ensocoat board of 182 g/m² dry: a coated solid bleached sulphate (SBS) board with light pigment coating on reverse side (Figure II-7).

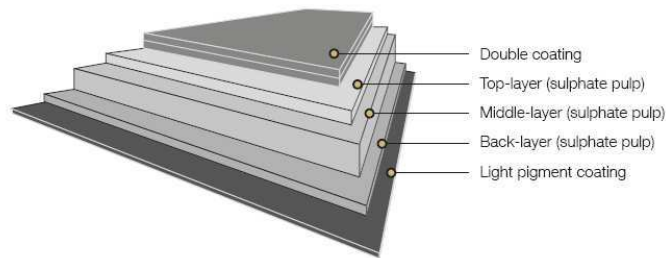


Figure II-7: Sketch of Ensocoat board 182 g/m².

II.3. - Experimental methods (for material production)

II.3.1. - Production of MFC films

Two techniques were employed to produce the MFC films:

- The casting-evaporation technique, also simply called casting.
- The handsheet technique.

II.3.1.1. - Casting-evaporation technique

In order to obtain a homogeneous suspension, MFC was preliminary diluted at 1 wt% and magnetically stirred for 1 hour. Then, 43 g of suspension were poured into polystyrene petri dishes with a diameter of 13.5 cm. MFC films of 30 g/m² were obtained after a few days of drying in conditioned room at 23°C-50% RH (Figure II-8).

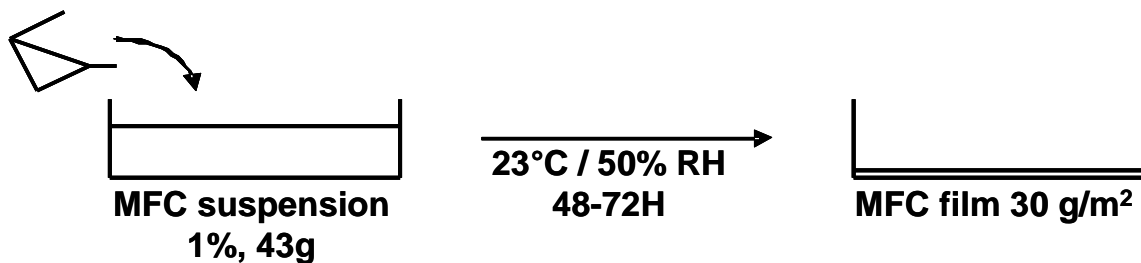


Figure II-8: Casting process.

All films were conditioned at 23°C-50% RH before the characterisation tests.

II.3.1.2. - Handsheet method

The handsheet method used a semi-automatic sheet former (Rapid-Khöten) to produce MFC films (Figure II-9). This device is currently used to produce model paper called handsheet at lab scale.



Figure II-9: Semi-automatic sheet former Rapid Khöten.

This method was adapted from the protocol described by Sehaqui *et al.* [93]. All steps are described in Figure II-10. A MFC suspension was firstly prepared at 0.5% and stirred using a disperser during 30 min. The diluted suspension was then poured into the bottom of a hollow cylinder containing a metallic sieve at its bottom covered with a mixed cellulose ester (nitrocellulose, cellulose acetate) membrane with 0.65 μm pore size (Milipore DAWP29325). After filtration, the gel cake was peeled off from the membrane and stacked between two cover papers and two carrier boards. Films were dried in a sheet dryer at 93°C and under vacuum for 10 min. At last, the films of 30 g/m^2 were separated from the cover papers. The diameter of the films reached 20 cm with this method. All samples were stored at 23°C-50% RH for at least one day before testing. As casting method, no preferential orientation of fibres in x and y direction occurred with this process, films was an orthotropic material.

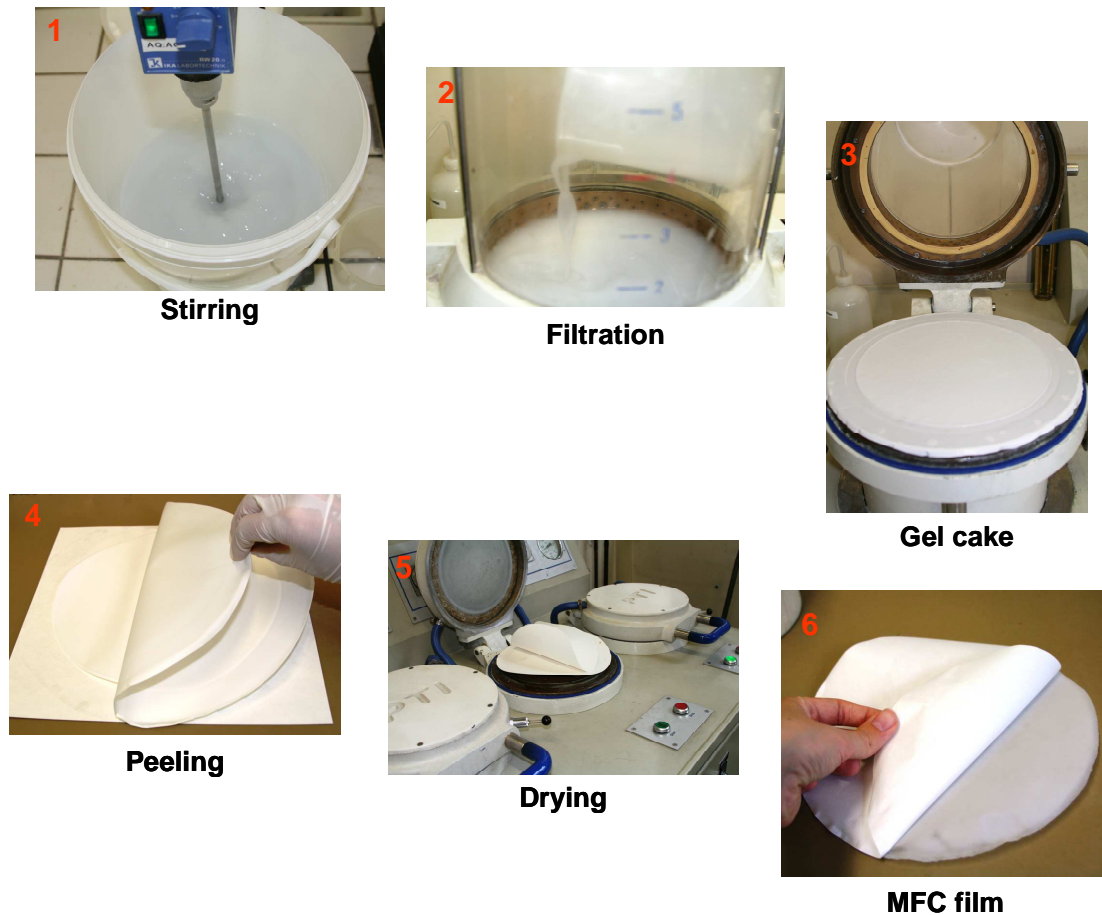


Figure II-10: Production of MFC films using a semi-automatic sheet former.

II.3.2. - Development of MFC based composites

All composites from PVOH or starch were produced with the same protocol (Figure II-11). The matrices were firstly solubilised in water at 95°C for one hour to obtain a 25% PVOH or starch aqueous solution. The MFC based composites were then prepared by addition of MFC suspension in the matrix aqueous solution to reach MFC contents in the dry film ranging from 0 wt% to 75 wt%. In order to obtain homogeneous composites, the concentration of matrix/MFC mixtures was adapted to obtain a good spreading and to avoid sedimentation. The suspensions were diluted according to the MFC content as follows Table II-3:

MFC content	Concentration
< 30 wt%	5 wt%
30 wt%	3 wt%
≥ 50 wt%	1 wt%

Table II-3: Concentration of the matrix/MFC mixture according to the MFC content.

After stirring for one hour, matrix/MFC suspensions were poured into petri dishes of 13.5 cm. Samples were stored and conditioned at 23°C-50% RH until complete water evaporation.

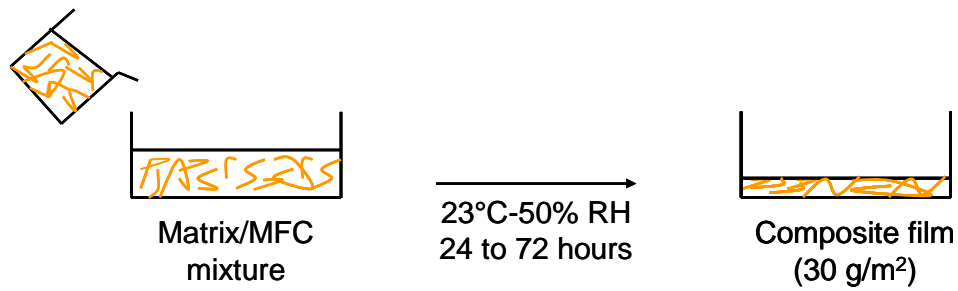


Figure II-11: General scheme for the preparation of matrix/MFC composites.

II.3.3. - MFC based paper & board materials

II.3.3.1. - Increase of MFC solids

II.3.3.1.1. - Centrifugation

Centrifugation was used to increase the MFC concentration in the suspension. MFC suspensions were introduced at 2% in test tubes of 175 ml. To do so, 5 cycles were performed with a centrifuge Sigma 3-16 (Fischer) at 4000 rpm.

II.3.3.1.2. - Inverted dialysis

A cellulose T4 tubular membrane made of regenerated cellulose (cylinder diameter 47.7 mm, wall thickness 40 μm) was used to carry out the inverted dialysis. The amount of introduced MFC suspension was 17.9 ml/cm of membrane. The membrane with a molecular weight cut off (MWCO) of 12000-14000 g/mol was firstly filled with the MFC suspensions and then immersed in a PEG solution at 15% with a molecular weight of 100000 g/mol. The dialysis lasted 22 hours.

II.3.3.2. - Coating trials at lab scale

II.3.3.2.1. - PVOH solubilisation in MFC suspension

The preparation of coating colour was carried out by PVOH solubilisation in MFC suspension (Figure II-12). The MFC suspension was firstly stirred using a disperser and the PVOH powder was slowly added. The mixture was stirred and heated at 95°C for 1 hour.



Figure II-12: Solubilisation of PVOH in MFC suspension.

II.3.3.2.2. - Production of coated board at lab scale

Coating lab trials were carried out using a laboratory rod coater (Figure II-13). This device is composed of a mobile coating plate, a fixing system of rod and a drying system. The coating colour was deposited at the surface of the substrate using the wire wound rod and dried using infra-red dryers.

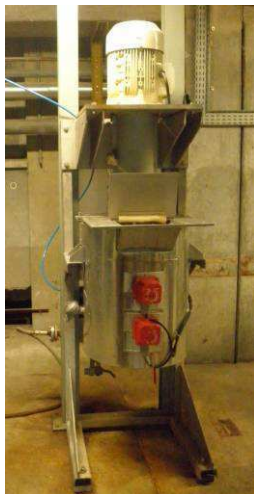


Figure II-13: Laboratory rod coater (left) and several wire wound rods (right).

After drying, the coated sheets were stored at 23°C-50% RH in a conditioned room before characterization.

II.3.3.3. - Coating trials at pilot scale

II.3.3.3.1. - PVOH solubilisation in MFC suspension at pilot scale



50 kg of coating colour were prepared by batch in the cooker using direct steam injection (Figure II-14). The suspension was stirred at 1000 rpm and 92°C for one hour.



Figure II-14: Preparation of coating colour at pilot scale.

II.3.3.3.2. - Production of coated board at pilot scale

Board reels were coated on the CTP pilot coater using a SoftTip blade (Figure II-15). During the trials, the machine speed was 70 m/min and the drying system used a combination of electric infra-red and forced hot air.



Figure II-15: CTP's pilot coater.

A coat weight between 10 and 20 g/m² was applied on the board. The applicator roll firstly deposited the coating colour at the surface and subsequently the blade adjusted the coat weight (Figure II-16).



Figure II-16: Wet paper after coating and applicator roll.

II.4. - Characterisation techniques

II.4.1. - Chemical composition analysis

The chemical composition analysis of samples was carried out according to the standard TAPPI T249 om-85 corresponding to "Carbohydrate composition of extractive-free wood and wood pulp by gas liquid chromatography". This technique involves two steps: an acid hydrolysis of sugars followed by a chromatography analysis which determines the kind of sugars which constituted the pulp. The hemicelluloses are thus determined following the presence of sugars. The analysis was carried out on MFC films. A sulphuric acid solution (24N) was added to the samples and after 1h the samples were put in an autoclave at 120°C for 1 hour. After autoclaving, the samples were filtered and analysed with gas liquid chromatography.

II.4.2. - Microscopic techniques

II.4.2.1. - Optical microscopy

Optical microscopy observations were performed using an optical microscope AXIO Imager M1m (Zeiss) in transmission mode. The observations were obtained with a natural source visible light or a polarised light.

II.4.2.2. - Scanning Electron Microscope (SEM)

SEM micrographs of surfaces were obtained from a FEI Quanta 200 ESEM with an acceleration voltage of 12.5 kV and a magnification of 1200x. Samples were cooled in liquid nitrogen and then fractured. The surface was sputter coated with a thin layer of gold prior to analysis.

II.4.2.3. - Field Emission Gun Scanning Electron Microscope (SEM-FEG)

The morphology and the average width of MFC were studied using a Zeiss Ultra 55 Field Emission Gun Scanning Electron Microscope (SEM-FEG). The acceleration voltage was 3 kV and the magnification reached 20000x. A thin Au-Pd conductive coating (ab.1nm) was deposited on top of the sample to reduce the charge effect.

II.4.2.4. - Transmission electron microscope (TEM)

Transmission electron microscopy (TEM) micrographs were obtained with a Philips CM200 transmission electron microscope using an acceleration voltage of 80 kV. The resolution was about one Angström. A drop of MFC suspension diluted 1000 times was deposited on a carbon-coated grid electrically polarized. Microfibrils were immediately adsorbed on the surface and the excess water was removed with a blotting paper. The grid was dried before putting in the microscope.

II.4.2.5. - Atomic force microscope (AFM)

Atomic Force Microscopy observations were performed on a Multimodal AFM (DI, Veeco, Instrumentation Group) with the tapping mode. The tip was a Multi130 with a radius of 10 nm and the scan rate for tapping was 1 Hz. The roughness of the samples was determined for an area of 10 μm^2 .

II.4.2.6. - TOPO 3D

The topography surface was observed and measured by TOPO 3D. As described on the Figure II-17, this measurement used light interferometry principle. The technical data of this data are detailed in Table II-4.

Technical data	
Vertical range	up to 500 μm
Vertical resolution	0.02 μm Ra
Measurement field	7.3 to 0.36 mm
Lateral resolution range	9.5 to 0.47 μm
Vertical scan speed	1 $\mu\text{m}/\text{sec}$
Acquisition time	1 to 2 minutes

Table II-4: Technical data of TOPO 3D.

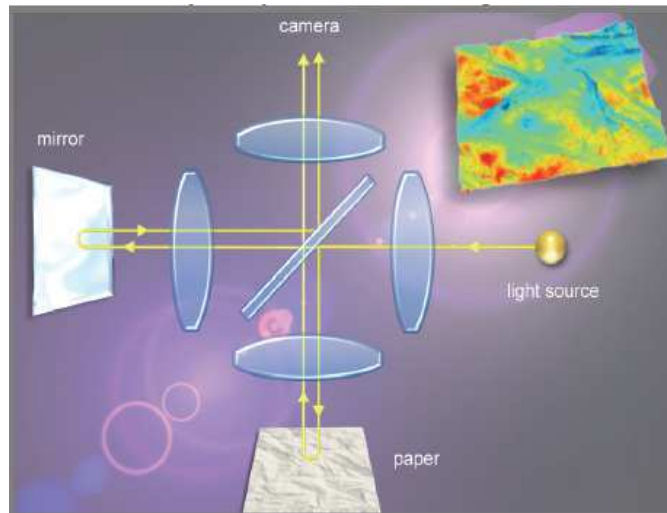


Figure II-17: Measurement principle: Interferometry.

II.4.3. - Viscosity measurements

II.4.3.1. - Brookfield viscosimeter

The Brookfield viscosimeter is an instrument used to measure the fluid viscosity using the principle of rotational viscosimetry (Figure II-18). The device measures the resulting torque on a spindle rotating at a definite and constant speed immersed in the fluid. The viscosity was calculated from the spindle size and rotational speed.



Figure II-18: Brookfield viscosimeter.

II.4.3.2. - Rheometer

During this study, the rheological behaviour of MFC suspensions was studied with a control stress rheometer AR-1000 (TA-instrument) using a plate-plate geometry. A 40 mm diameter quartz plate geometry was selected for the measurements with a gap of 1 mm. A representation of the rheometer is given in Figure II-19.

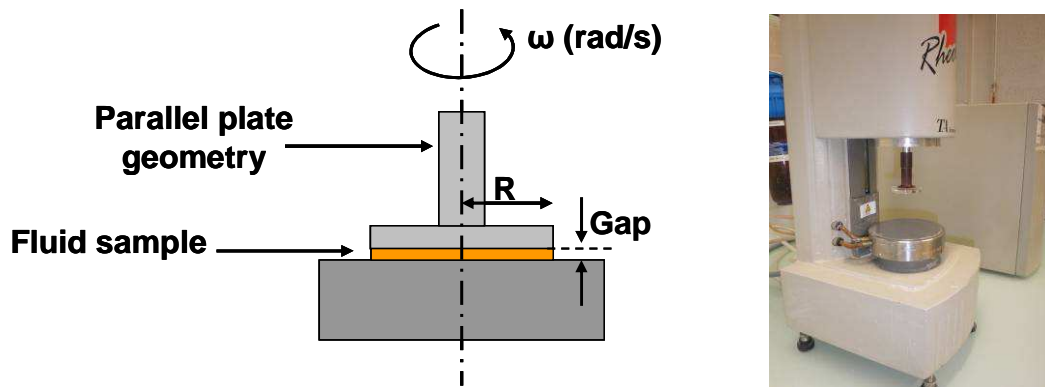


Figure II-19: Rheometer with plate-plate geometry.

The flow procedure mainly used for the measurements was:

- A conditioning step with a shear rate of 100 s⁻¹ for two minutes at 20°C followed by an equilibrium step for 1 minute.
- A steady state flow with a shear rate ramp from 1000 to 0.02 s⁻¹ with 10 points per decade and a maximum sample period of 1 min 30 s.
- A steady state flow with a shear rate ramp from 0.02 to 1000 s⁻¹ with 10 points per decade and a maximum sample period of 1 min 30 s.

This procedure allowed to determine the viscosity according to the shear rate as well as the thixotropy of the fluids.

II.4.4. - Transparency properties

The transmittance of MFC films was determined using a Hazemeter device for visible light. Three values represent the transparency of materials:

- Total transmittance of visible light corresponding to the fraction of the intensity of the incident radiation on the intensity of the radiation coming out from the sample. These measurements were evaluated according to the standard ASTM D1003-07.
- Haze corresponding to the percentage of light transmitted through the sample and diffused with an angle over than 2.5°. This was measured according to the standard ASTM D1003-07.
- Clarity which represents the percentage of light transmitted through the sample and diffused with an angle under than 2.5°. This value was determined according to the standard ISO 14782:1999.

II.4.5. - Surface roughness testing

The mean roughness (Ra) of film surface was measured using the perthometer M2 (Mahr) (Figure II-20). Roughness average Ra is the arithmetic average of the absolute values of the roughness profile ordinates. The roughness profil was determined with a traversing length of 56 mm and according to the standard DIN 4768. The top and reverse sides were tested during the measurements.



Figure II-20: Perthometer M2 (Mahr).

II.4.6. - Density of materials

All samples were stored for 24h in conditioned room at 23°C-50% RH before characterisation.

II.4.6.1. - Basis weight

The basis weight of the samples was determined for a 70 cm² area with a precision balance (0.0001g).

II.4.6.2. - Coat weight measurements

Coat weight was measured by the weight difference between the board before and after coating. For this, the thermobalance METTLER TOLEDO LJ16 was used. Five uncoated and coated sheets of 70 cm² were dried at 120°C for 5 minutes and weighted. The coat weight corresponds to the average value obtained from these measurements.

II.4.6.3. - Thickness

The thickness of films or boards was determined according to the standard ISO 534. Thickness measurements were carried out under a specific charge with a precision micrometer Adamel Lhomargy MI.20 (Figure II-21). Measurement was performed on a 16 mm² area under a pressure of 100 ± 10 KPa. An average thickness was determined from 10 measurements per sample and 5 sheets per series.



Figure II-21: Micrometer Adamel Lhomargy MI.20.

II.4.7. - Mechanical properties

II.4.7.1. - Tensile tests



Tensile tests were carried out at 23°C-50% RH with an Instron device equipped with a load cell of 500 N (Figure II-22). Measurements were done according to the standard ISO 1924-2 and performed with a crosshead speed of 10 mm/min on samples of 15 mm in width and 100 or 180 mm in length. At least 5 replicates were tested per reference.

Figure II-22: Tensile test with an Instron device.

II.4.7.2. - Burst measurements

Burst measurements were determined according to the standard NF EN ISO 2758. This measurement allowed to determine the interactions between fibres. The device used was a burst tester (Frank PTI). At least 5 replicates were tested per reference.

II.4.7.3. - Tear measurements

Tear measurements were evaluated by Elmendorf method according to the standard NF EN 21974. The test gives an overview of the entanglement fibres ability. A L & W Tearing tester SE009 was used for the tests. At least 5 replicates were tested per reference.

II.4.8. - Barrier properties

II.4.8.1. - Water absorption capacity (Cobb measurements)

This method, based on standard ISO 535: 1991, allowed to determine the water amount (Cobb index) absorbed at the surface of the substrate for a given time. The water absorption ability of the cellulosic substrate depends, among other parameters, on the porosity, and the sizing of the substrate.

Measurements were done on a rigid plate with a smooth and plane surface. The sample was fixed between the plate and a metallic cylinder (Figure II-23).



Figure II-23: Cobb equipment.

10 mm in height of water was poured inside the cylinder at the sample surface. After a given contact time, the water was removed and the water remaining at the sample surface was wrung with a blotter paper and a roll of 10 kg \pm 0,5 kg. Sheets were weighed before and immediately after the water exposition and wringing. The result was calculated from the mass difference divided by the area (g/m^2) with the formula:

$$Q = 10000 \cdot (m_1 - m_2) / S$$

Where Q is the Cobb index (g/m^2); m_1 and m_2 the sheet weight before and after the Cobb test (g) and S the sheet area in contact with water (cm^2).

Five replicates were tested for each series and the value corresponds to the average of these measurements. The measurement areas were 10 cm^2 or 25 cm^2 and the test durations 60s, 300s or 1800s.

II.4.8.2. - Grease absorption capacity (Cobb measurements)

Cobb measurements were also used to determine the grease resistance of materials. In this case, water was simply replaced by coloured peanut oil. The contact time was set at 24 hours.

II.4.8.3. - Sorption behaviour of paper at several relative humidities

A varimass or hygrosorption analyser was designed to measure the water sorption of paper in controlled humidity environment from 15 to 90% RH. Samples previously conditioned at 23°C-50% RH were weighted all along the humidity ramp from 50% RH to 85% RH. Eventually, the samples were dried to determine their dry weight and to calculate the water uptake of samples for each humidity level.

II.4.8.4. - Bendtsen air permeability

Bendtsen air permeability measurements were carried out with a Lorentzen and Wettre device according to the standard NF Q03-076. At least 5 replicates were tested per reference.

II.4.8.5. - Water vapour transmission rate

The water vapour transmission rate (WVTR) of samples was determined according to the standard ISO 2528. The water vapour transmission rate corresponds to the water vapour having passed through the sample per unit area for a given time and conditions. Samples were put on dishes containing CaCl_2 anhydrous salt and the system was hermetically closed by wax. Then dishes were stored at constant temperature and humidity (23°C-50% RH, 23°C-85% RH or 38°C-90% RH) (Figure II-24). Dishes were weighed at regular time intervals for one week. The increase of weight allowed determining the WVTR. Six replicates were tested by series and one of them was without CaCl_2 in order to determine the swelling of the material.

**Controlled atmosphere:
23°C-50% RH, 23°C-85%RH or 38°C-90% RH**

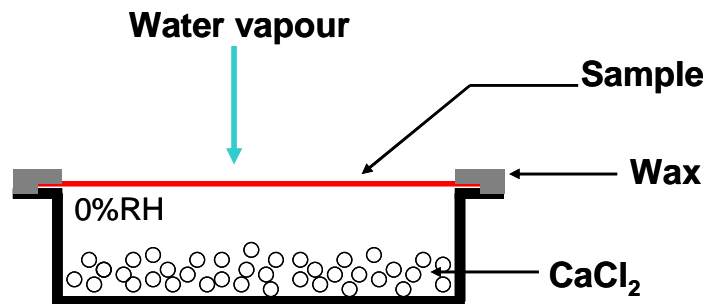


Figure II-24: Dish method to determine the WVTR of samples.

II.4.8.6. - Oxygen transmission rate

The oxygen transmission rate (OTR) of samples was measured with a MOCON OX-TRAN® 2/21 ML according to the standard ISO 15105-2:2003 Annexe A. The principle is described in Figure II-25. One side of the sample was exposed to an oxygen flux and the molecules, diffusing through the tested material, were measured by the oxygen detector. At least two replicates were analysed on the surface area ranging between 0.5 and 5 cm² according to the available samples.

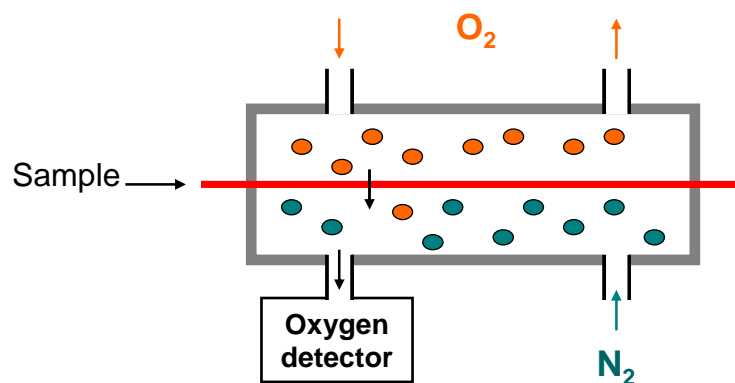


Figure II-25: Principle of oxygen transmission rate measurement.

II.4.9. - Mercury porosimetry

Samples, previously dried at 60°C for several days, were coiled and placed in a mercury penetrometer (Figure II-26). A vacuum was created before the mercury introduction at low pressure in penetrometer. Then, the pressure was progressively increased step by step. Each pressure increment corresponds to a volume which penetrates the sample pores. The mercury volume was measured according to the mercury pressure. The measurement gave thus the mercury volume per mass unit (mL/g).

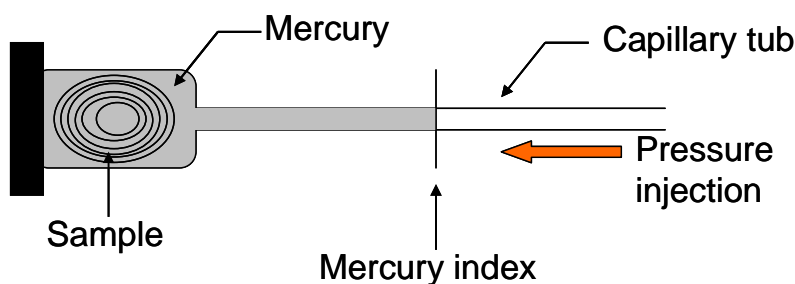


Figure II-26: Scheme of mercury penetrometer.

II.4.10. - X-ray diffraction

A wide angle X-ray diffraction analysis was generally used to determine the crystalline structure of the compounds. When the X-ray photon beam interacts with a crystalline sample, a radiation part is diffracted at angles defined according to the Bragg law:

$$2 * d_i * \sin \theta_i = n * \lambda \quad (\text{Eq.14})$$

Where d_i corresponds to the spacing between the planes in atomic lattices, θ_i is the angle between the incident ray and the scattering planes, λ is the wavelength of the incident wave, n is an integer.

The radial distributions and their magnitudes are characteristic of a lattice structure and atomic organisation.

Films were placed on a plate with tape and the measurements were performed with a PANanalytical, X'Pert PRO MPD diffractometer equipped with a X'celerator detector. The operating conditions for the refractometer were: Copper K α radiation, 2θ between 6 and 44°, step size 0.067°, counting time 90 s.

II.4.11. - Thermal properties

II.4.11.1. - DSC

Differential scanning calorimetry allows to determine the glass transition temperature (T_g), the melting temperature (T_m) of materials and also the degree of crystallinity of semicrystalline materials. For this, the sample was subjected to a heating rate and the changes of states were determined by the difference of heat flow between the sample and a reference. The measurements were performed using a DSC2920 CE modulated differential calorimeter from TA Universal analysis. Around 10-15 mg of samples were placed in an aluminium DSC cell. Each sample was heated from -50°C to 250°C with a heating rate of 10°C/min under nitrogen atmosphere. The melting temperature was determined at the peak temperature of the endothermic peak. A minimum of two replicates was analysed for each sample.

II.4.11.2. - TGA

The thermogravimetric analysis measures the sample weight according to the temperature giving the thermal stability of samples. The samples were heated from 30°C to 600°C with a heating rate of 10°C/min with a STA 6000 (Perkin Elmer Instruments model, USA). A minimum of two replicates was analysed for each sample

III - Study of microfibrillated cellulose suspensions/films

III.1. - Introduction

Investigating microfibrillated cellulose has dramatically increased over the past decade. Its ability to replace polymers coming from petrochemical resources was explored. Its reinforcement potential as well as its barrier properties are now well known. Microfibrillated cellulose (MFC) refers to mechanically treated cellulose fibres regardless the technique used for its production. However, MFC properties are related to the cellulose source and to the treatment applied to the pulp for the fibrillation.

Several grades of MFC, defined according to the production method, were characterized in this study. Besides commercial MFC, all MFCs were produced from only one wood source: spruce/pine dissolving bleached pulp. Commercial MFC was compared with MFC produced at laboratory and pilot scale. The influence of the pretreatment and the mechanical treatment implemented on the initial pulp was investigated by the study of MFC morphology and MFC properties.

One objective of this PhD was thus to characterise the MFC suspensions delivered by our partners in the European project SUNPAP. This allowed selecting the MFC with the best properties in order to develop composites and/or MFC based coating colour. This chapter consists of two major parts.

The first part concerns the characterisation of MFC suspensions. The techniques used to analyse the morphology of fibrils are described and their limits are discussed. Moreover, the rheological behaviour was characterized for each kind of MFC suspensions.

The second part deals with the study of MFC intrinsic properties. To carry it out, self-standing MFC films were firstly elaborated by two methods: casting-evaporation and handsheet method. Their visual aspect, their morphology, their mechanical and barrier properties were analysed according to the source and to the method of production.

III.2. - Characterisation and comparison of several grades of MFC suspensions

Different grades of MFC suspensions used during this work were studied and characterized. It is very important to clearly define each kind of MFC because the method of production strongly influences the final suspension behaviour. Concerning the codification used to describe the MFC samples, the first letter corresponds to the pretreatment (enzymatic (E) or chemical with the tempo oxidation (T)) applied to the pulp and the second letter to the mechanical shearing equipment (Microfluidics homogenizer (MH), Gea homogenizer (GH), Masuko grinder (MG), Cavitron rotor/stator (CR)) used for fibrillation as described in Figure III-1.

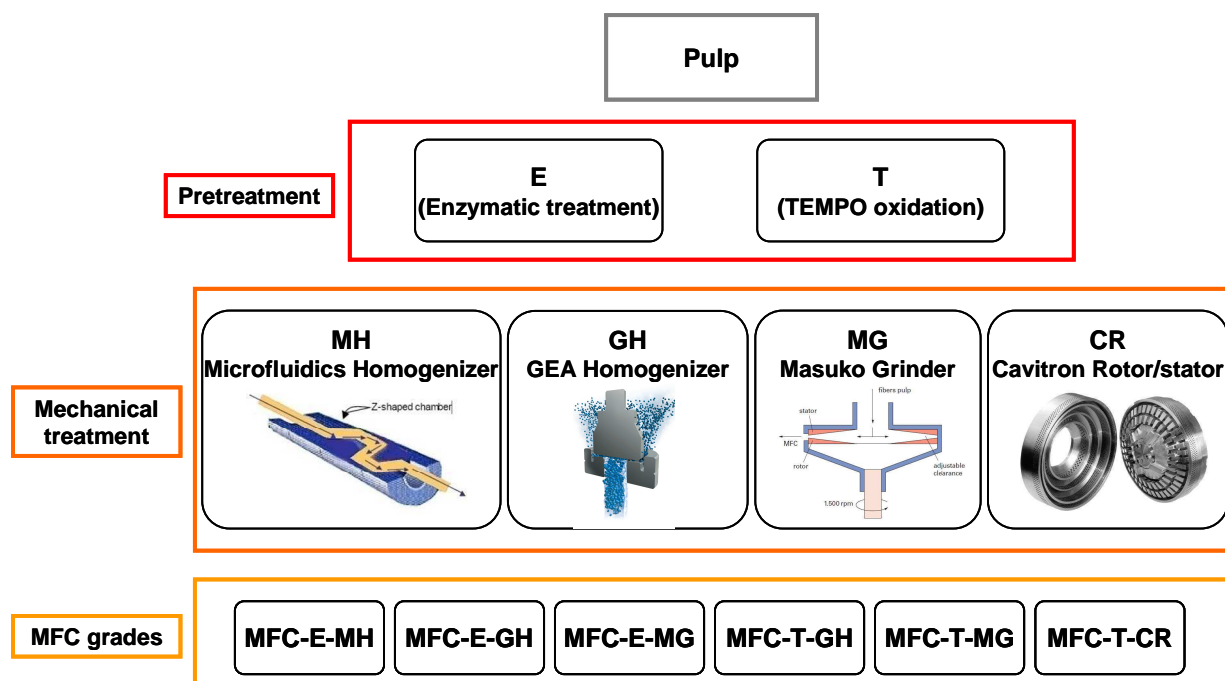


Figure III-1: Codification of the MFC samples.

Two ways were studied to pretreat the pulp and make the fibrillation easier during the mechanical shearing. First, the enzymatic treatment: it does not modify the surface chemistry of cellulose fibres and randomly hydrolyzes accessible intramolecular β 1-4 glucosidic bonds in order to improve the fibrillation. TEMPO-mediated oxidation was the second way used to pretreat the fibres before the mechanical shearing. The TEMPO-mediated oxidation of fibres substitutes the carboxyl groups for hydroxyl groups. This increases the space between the fibrils and facilitates the fibrillation. The aim of these two pretreatments was to reduce the energy input required for the fibrillation by decreasing the number of passes in the homogenizer. The number of passes was thus of five for enzymatic pulp and of two for TEMPO-oxidized pulp.

The morphology of MFCs and the viscosity of suspensions have been studied in this part and compared with those of commercial MFC source, called MFC-Arbo. Several aspects have thus been considered; the influence of the pretreatment, the homogeneity of the suspension, and the impact of the up-scaling of production.

III.2.1. - Visual aspect of MFC suspensions

Figure III-2 shows pictures of the three kinds of MFC in aqueous suspension. The visual aspect was very different according to the source. MFC-Arbo, corresponds to fine commercial cellulose, its initial concentration reached 13% and the suspension diluted at 2% flowed easily in the tube. At lab scale, MFC was produced at a concentration of 2% whatever the pretreatment. The suspensions appeared with a gel-like behaviour. The suspensions did not flow in the tube, thus revealing their high viscosity. The MFC obtained by using TEMPO-mediated oxidation pretreatment showed a lower turbidity and higher translucence.

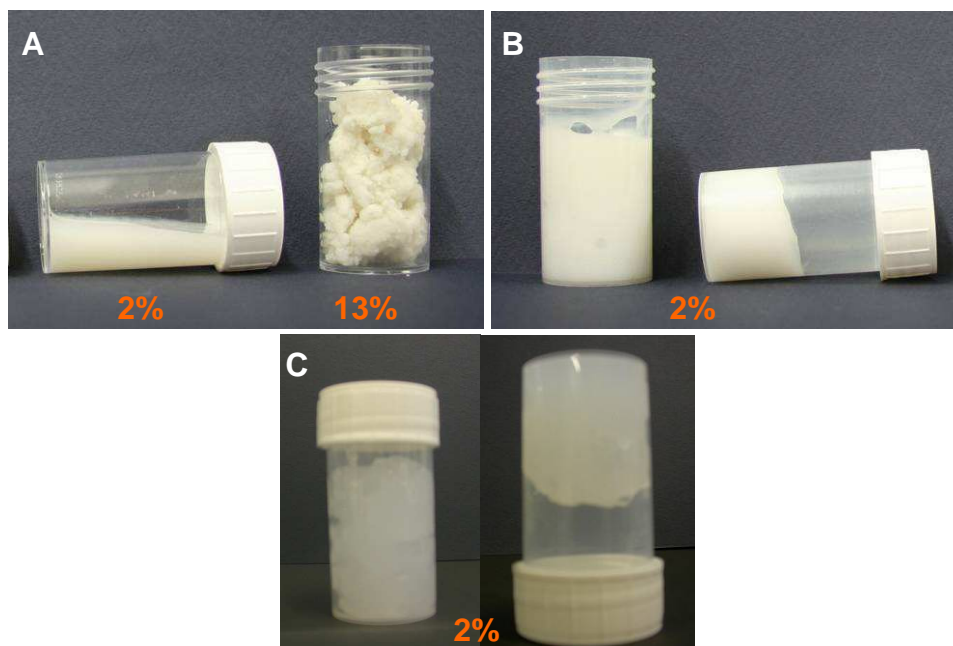


Figure III-2: Photos of MFC suspensions: MFC-Arbo (A), MFC-E-MG (B), MFC-T-MG (C).

The visual aspect is a first step of the characterisation because the apparent viscosity and the turbidity gave an overview of the MFC fibrillation state. Fibrillation is the production of nano-scale elements from the cellulose fibres. The fibrillation state, also called degree of fibrillation, defines the degree of disintegration of fibres into microfibrils.

In the following parts, methods used to characterize the MFC suspensions are detailed.

III.2.2. - Influence of the fibrillation process on the MFC morphology

The morphology of MFC plays an important role in the MFC properties because they are related to the degree of fibrillation. One of the main techniques used to characterize MFC suspensions is the microscopic observation and most particularly the combination of three techniques: optical microscopy, scanning electron microscopy (SEM) and transmission electron microscopy (TEM).

III.2.3. - Optical microscopy

Optical microscopy was firstly employed to investigate the quality of MFC suspensions. Photos gave an overview of the fibrillation state and the homogeneity of MFC suspensions linked to the treatment applied to the pulp. This is illustrated in Figure III-3 with the observation of the enzymatic pretreated wood pulp after several passes in the Gea

homogenizer. The increase of the number of passes in the homogenizer decreased the element size, improved the suspension homogeneity and the fibrillation state.

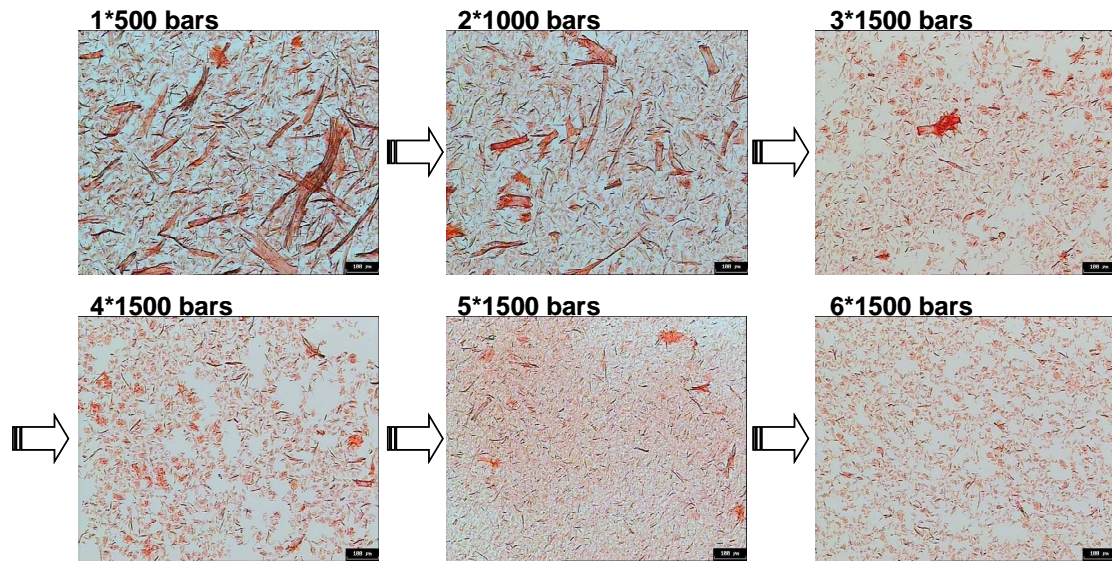


Figure III-3: Influence of the number of passes on the fibrillation state for the case of MFC obtained by enzymatic treatment and Gea homogenizer [140].

Figure III-4 shows images obtained for each suspension and the results were different according to the production method.

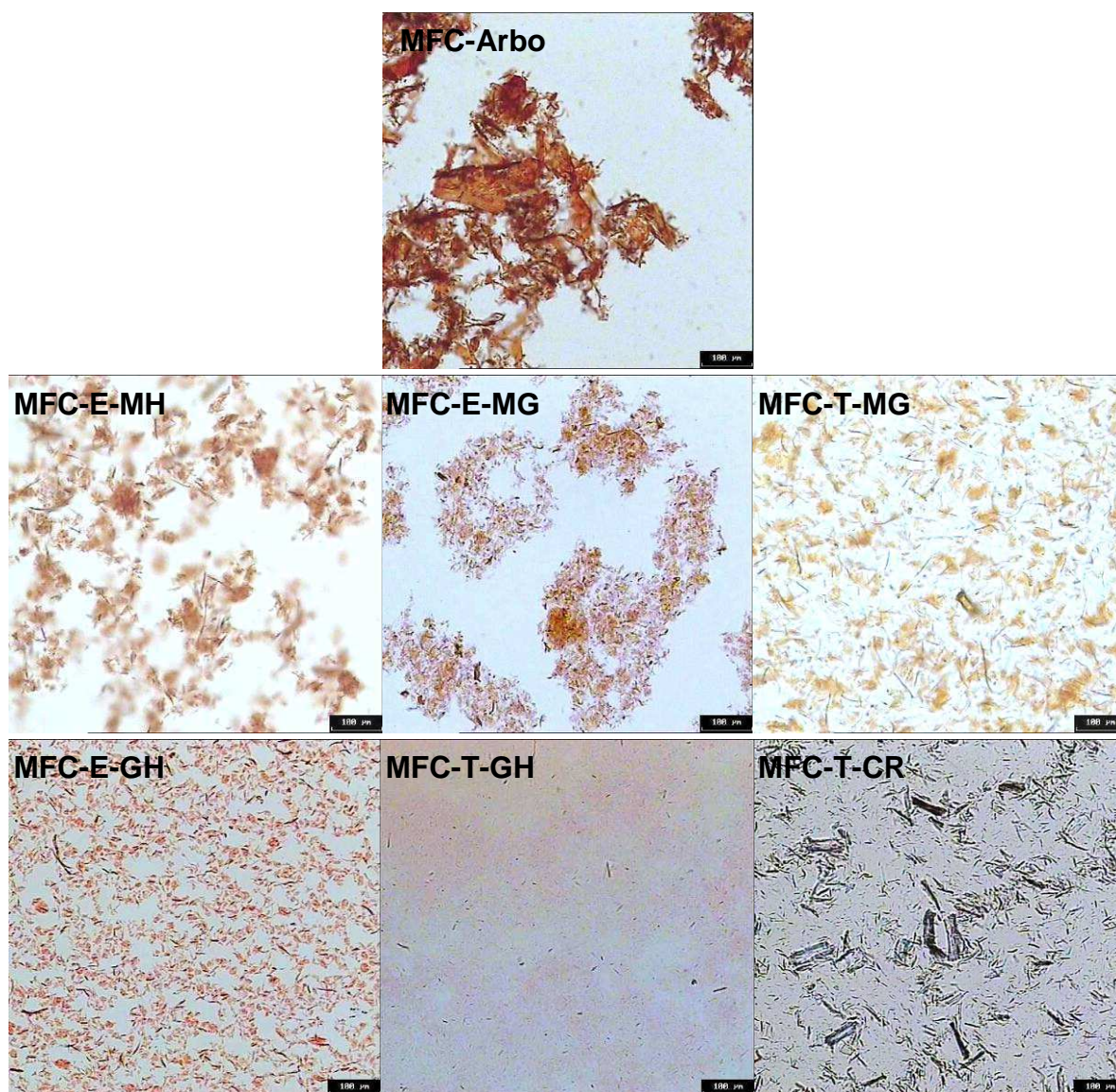


Figure III-4: Optical microscopy images of MFC suspensions used in this work.

The commercial fine cellulose (MFC-Arbo) had a low fibrillation state with the presence of big and large elements. The Morphi analysis confirmed this result with an estimated element size of 10-30 μm in width and 500 μm in length.

The other suspensions had large size distributions and were more or less made of thin elements. For example, MFC-E-MH suspension consisted of very thin elements but larger elements were also observed. The size distribution was thus very broad in this sample. The MFC-E-MG suspension shown was more homogeneous with a majority of thin fibrils. Due to the high thinness of the particles, they were not clearly seen when using this technique.

The production at pilot scale used other homogenisation techniques compared to lab scale production. The thinness of microfibrils MFC-E-GH, produced on a larger scale, seemed to be of intermediate sizes between the one of MFC-E-MH and MFC-E-MG (cf. Figure III-5). The homogeneity and the quality of the MFC suspension produced at pilot scale show that the fibrillation quality remained very good after the up-scaling of the production and the use of new equipment.

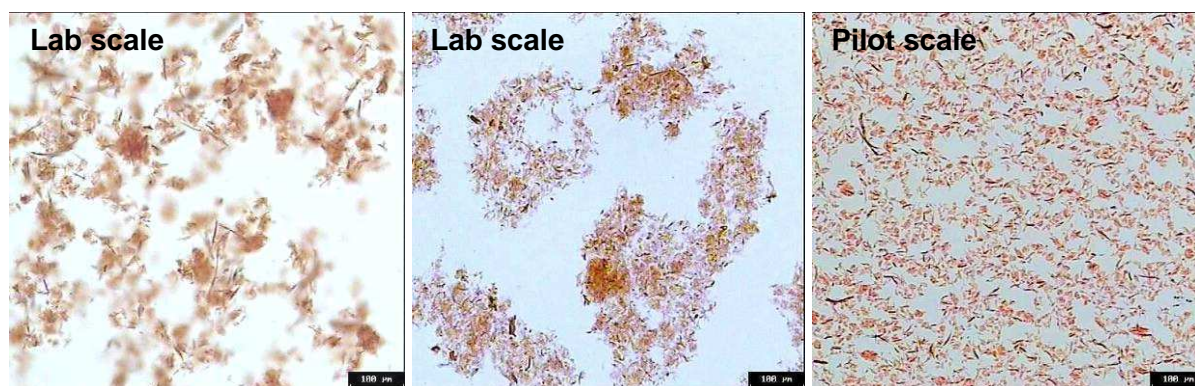


Figure III-5: Influence of scale production.

The influence of pretreatment is observed in Figure III-6. A higher degree of fibrillation was obtained after TEMPO pretreatment and two passes through the Gea homogenizer (MFC-T-GH) compared to the enzymatic pulp, which needed to be passed five times in the homogenizer (MFC-E-GH).

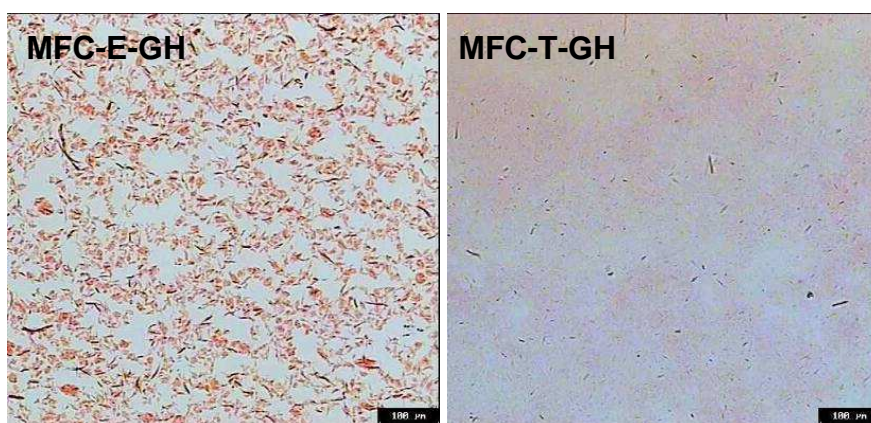


Figure III-6: Influence of pretreatment.

In spite of TEMPO pretreatment, the use of rotor stator, developed by cavitrion in SUNPAP project, showed a lower efficiency. Indeed, short fibres were always present in the suspension after the mechanical treatment demonstrating the bad homogenization of MFC-T-CR.

The visualisation of the suspension by light microscopy gave a good overview of the MFC suspensions. The quality of the suspension can be compared and most specifically the MFC size distribution. The commercial source showed very large elements compared to MFC suspensions produced in this project. These images proved that the state of fibrillation strongly depends on the treatment applied to the pulp. Moreover, the pretreatment made the fibrillation easier and influenced the morphology of MFC.

To complete the morphological characterization and to estimate the element sizes, SEM-FEG and TEM micrographs were analysed.

III.2.3.1. - SEM-FEG

The magnification of scanning electron microscopy with a field emission gun (SEM-FEG) gives a better visualisation of the fibril size. However, the suspension was dried during the preparation of the sample. This drying process led to strong aggregation of fibrils and it was

difficult to observe individualized fibrils. Figure III-7 shows micrographs of MFC observed by SEM-FEG. The micrograph of MFC-Arbo showed large elements slightly fibrillated at the surface. Here, the microscopic imaging showed that the commercial MFC suspension doesn't correspond exactly to microfibrillated cellulose suspension. This sample seemed to be an ultra-refined pulp.

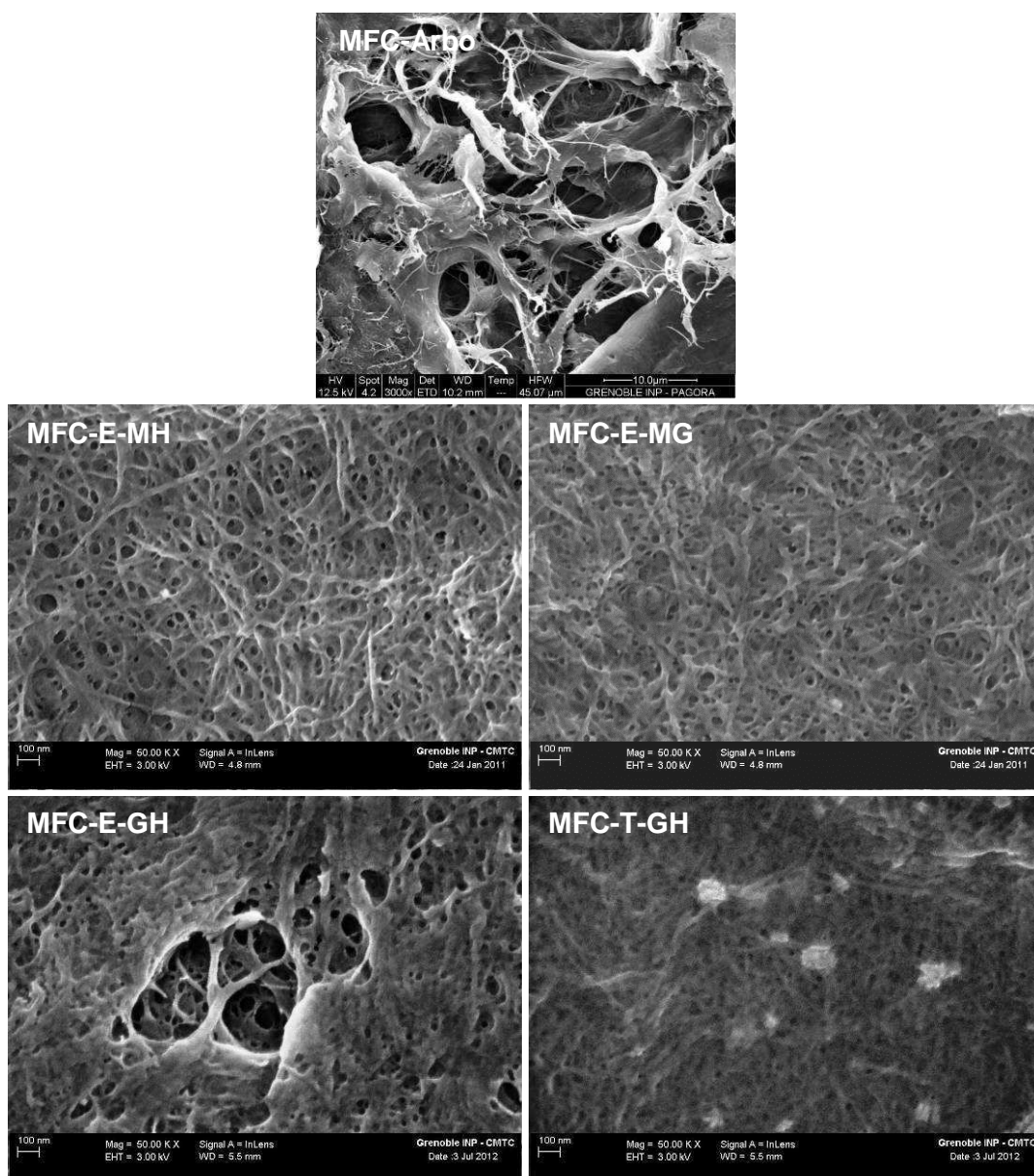


Figure III-7: SEM-FEG micrographs of dried MFC suspensions.

Concerning the others MFC, the diameter could be approximated in a 10-30 nm range. Due to entanglements and different scale observations, the length of the fibrils cannot be measured here; it is generally estimated to 1-3 μm .

The MFC-E-MG suspension was the thinnest fibril enzymatic suspension from the light microscopy images. It corresponded to a closer network showing the importance of particle's size on the network formation. The aggregation during the drying was more or less important according to the source. With the TEMPO oxidized suspension MFC-T-GH, the aggregation was very strong and it was very difficult to distinguish the elements.

III.2.3.2. - TEM

The visualisation of individualized microfibrils was made possible using the TEM technique. The preparation of samples allowed individualizing the fibrils thanks to a 1000 times dilution. In Figure III-8, single fibrils were well distinguished and the diameter was evaluated at 10 nm.

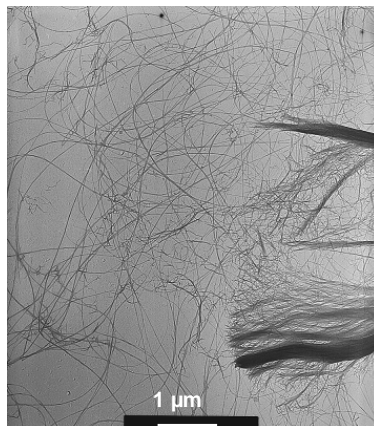


Figure III-8: TEM images of MFC-E-MG.

A comparison of MFC produced at pilot scale was made using TEM images (Figure III-9).

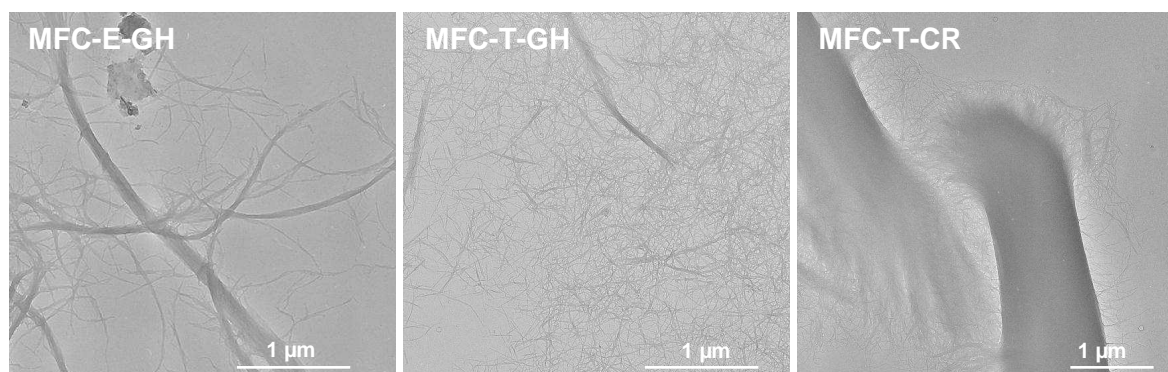


Figure III-9: TEM images of MFC produced at pilot scale:
MFC-E-GH, MFC-T-GH, MFC-T-CR (C).

The difference in MFC diameter was well observed here. MFC produced by TEMPO pretreatment followed by 2 passes in the homogenizer showed the thinnest elements. These images were scanned only a small part of the suspension and it was not always representative of the entire suspension.

III.2.3.3. - Conclusion

The combination of these three microscopic techniques allowed to partially characterise the morphology of MFC suspensions. The mechanical shearing and the increase of passes in the homogenizer led to the fibrillation and a homogeneous suspension. Enzymatic and TEMPO pretreatments were used in this study to pretreat the pulp; the images showed that the MFC morphology was impacted by these pretreatments. The transfer on a larger scale and the use of different techniques also influenced the fibril size.

Moreover, few appropriate techniques are currently available to determine the size distribution of MFC in suspension. In the SUNPAP project, some partners used fractionation techniques to separate the MFC particles according to their size. Six fractions were thus

obtained with particle size $>20\ \mu\text{m}$ for the first fraction and $<0.1\ \mu\text{m}$ for the last fraction. The studied suspensions in the project had between 60% and 80% of fibrils in the fraction 1-0.1 μm [142].

III.2.4. - Chemical composition analysis of MFC

The chemical composition of MFC was analysed using the sugar hydrolysis method and compared with the initial bleached pulp. According to the results (Table III-1), the commercial fine cellulose consisted of 85% glucose and 14% xylose. This carbohydrate composition is characteristic of a hardwood pulp.

	MFC-Arbo	Pulp	MFC-E	MFC-T [142]
Glucose	85.4%	96,5%	94.9%	71.4%
Xylose	14.1%	1.5%	2.2%	15.0%
Mannose	0.5%	2%	2.9%	12.1%
Galactose	$<0.05\%$	$<0.05\%$	$<0.05\%$	$<0.05\%$
Arabinose	$<0.05\%$	$<0.05\%$	$<0.05\%$	$<0.05\%$

Table III-1: Carbohydrate composition of pulp and MFC according to the pretreatment.

The composition of MFC produced at lab scale was compared with the initial pulp. It was composed of about 95% of glucose and traces of xylose and mannose. The enzymatic pretreatment and the mechanical shearing treatment did not impact the carbohydrate composition of the pulp. Conversely, TEMPO pretreatment influenced the chemical composition of the pulp. The degree of polymerization of cellulose was decreased and this explained the glucose content decrease and the increase of xylose and mannose corresponding to hemicelluloses.

Lignin is a fibre component which influences the surface properties and particularly the hydrophilic properties. Here, the starting pulp was a bleached pulp and no lignin residues were detected.

III.2.5. - Influence of the fibrillation state on the rheological behaviour of MFC suspensions

The rheological characterisation of MFC suspensions had two objectives. The first one was to obtain some information about the degree of fibrillation of samples and the second one was to evaluate their flow behaviour.

Indeed, the rheological behaviour of fluids is an important parameter for industrial processes. At each step, the viscosity could be modified by the process. During the coating process, for example, the range of shear rates applied to the coating colour is very high as shown in Figure III-10. Throughout the process, going from the stirring stage to the coating stage, the fluid is submitted from middle to high shear rates. The study of the rheological behaviour of coating colours allows to anticipate the behaviour of fluids during the trials and to adapt the most convenient coating process.

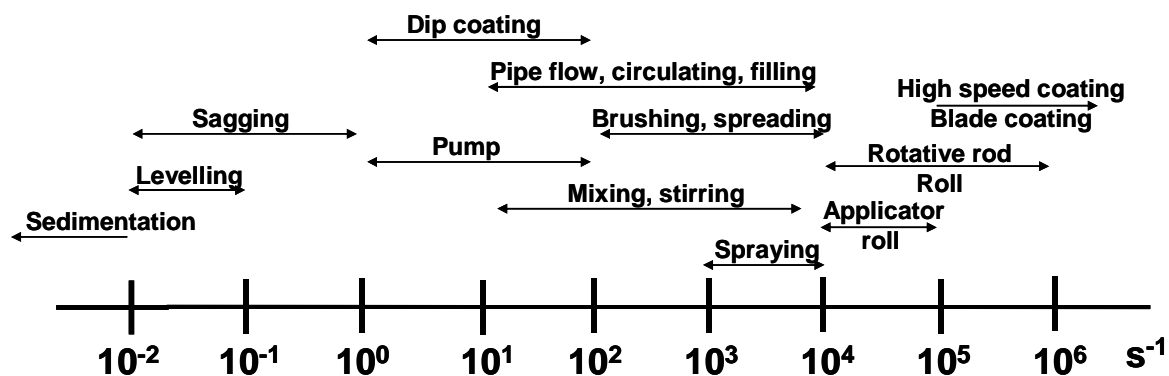


Figure III-10: Shear rate ranging in different coating process [25,143].

However, a MFC suspension is a particular fluid and the determination of its viscosity and its rheological behaviour is not obvious. Two main parameters could influence the rheological measurements of MFC suspensions. First, a MFC suspension is a heterogeneous fluid consisting of particles with a high aspect ratio and a high flexibility leading to possible entanglements, flocculation or phase separation. Secondly, colloidal interactions occur linked to electrostatic effects between fibrils due to the charge at the microfibril surface [90].

Conventional Brookfield measurements, currently used for coating processes, were not adapted for example. During the measurement, a film of water was formed between the spindle and the suspension which did not allow a valid measurement.

In our study, plate-plate measurements were chosen to determine the flow behaviour of MFC suspensions. This technique gave repeatable and reproducible results and no phase separation was observed after measurements.

III.2.5.1. - Viscosity of MFC produced by enzymatic pretreatment

III.2.5.1.1. - Conditions of viscosity measurements

As detailed in the introduction, the particularity of MFC suspensions leads to an adaptation of common rheological protocols. In order to obtain good rheological measurements, the rheometer geometry is selected according to the particle size. Indeed, the gap must be at least ten times greater than the particle size. The size of individualized fibrils is around 1-3 μm in length but it is difficult to evaluate the size of aggregates. Plate-plate geometry was thus selected instead of cone plate geometry. Indeed with the former, it is possible to set the gap between the parallel plate, thereby eliminating the problems due to the particle size.

Plate-plate measurements were thus carried out on suspensions for shear rates ranging from 10 s^{-1} to 1000 s^{-1} . Two curves were obtained, one for the increasing shear rate and one for the decreasing shear rate. To reduce potential history effects on the samples, a pre-shearing step was applied on all samples before the rheological characterisation. A preliminary study showed the need to apply a pre-shearing. MFC 1a and MFC 1b corresponded to the same MFC-E-GH suspension but the MFC 1a was freshly stirred before the measurement and MFC 1b was not. Figure III-11 showed different curves obtained for these two samples although this was the same suspension.

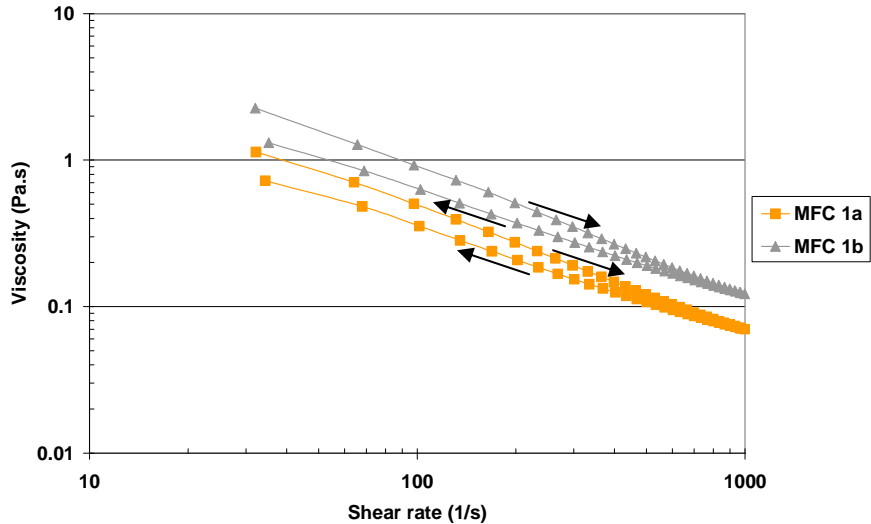


Figure III-11: Viscosity of MFC 1a and MFC 1b according to the shear rate.

The measurements were carried out once again on the two samples in the same conditions but using a preshearing at 100 s^{-1} for two minutes (Figure III-12). This time, similar curves were obtained for both samples proving the efficiency of a preshearing to reduce the history effect of MFC suspension.

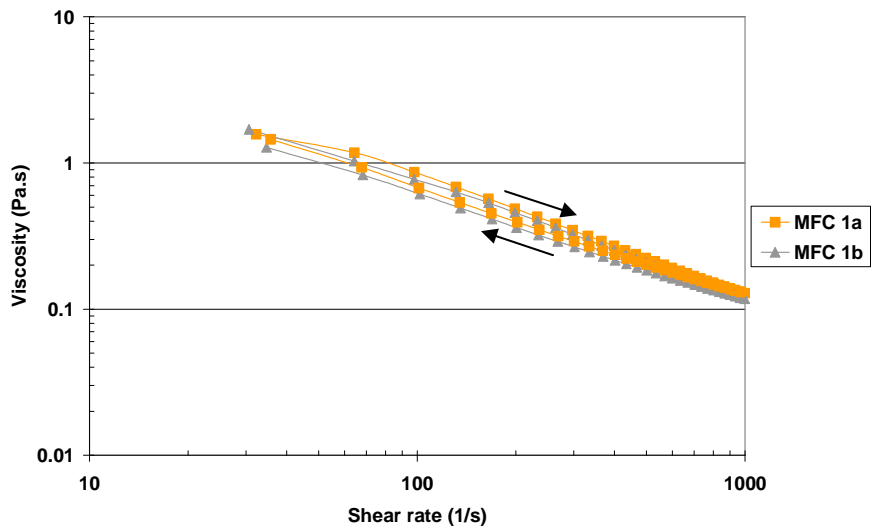


Figure III-12: Viscosity of MFC 1a and MFC 1b according to the shear rate after preshearing.

All viscosity measurements carried out with the rheometer were made with a parallel plate geometry and a shear rate range from 0.02 to 1000 s^{-1} after a preshearing (two minutes at 100 s^{-1}).

III.2.5.1.2. - Influence of the degree of fibrillation

The viscosity of MFC suspensions is a critical point for their use on a large scale. Indeed, a gel-like behaviour was observed for a low solid content (2%). Several reasons could explain this high viscosity.

Firstly, an increase of the specific surface area (SSA) was observed during the fibrillation process. Homogenized microfibrils have a higher SSA compared to the starting pulp. Spence

et al. [18] described an increase of SSA from 11 m²/g to 195 m²/g for a bleached softwood pulp after homogenisation using the Congo red adsorption method. These values corresponded to values for wet suspensions. The SSA values, determined on dry pulps by BET technique, are lower about 1.27 m²/g for whatman paper for example and 23 m²/g for MFC [144]. The SSA is related to the number of hydroxyl groups accessible on the surface. The fibrillation increases thus the number of OH groups on the surface and this favours the hydrogen bonding interactions between fibrils or between fibrils and water. This is why, in agreement with microscopic images, the viscosity of the pulp increased with the number of passes in the homogenizer or grinder.

Figure III-13 shows the evolution of the MFC viscosity as a function of the shear rate according to the number of passes in the homogenizer. The viscosity increases with the degree of fibrillation. This measurement gives thus an indication of the fibrillation state and allows to compare the homogeneity of different MFC suspensions.

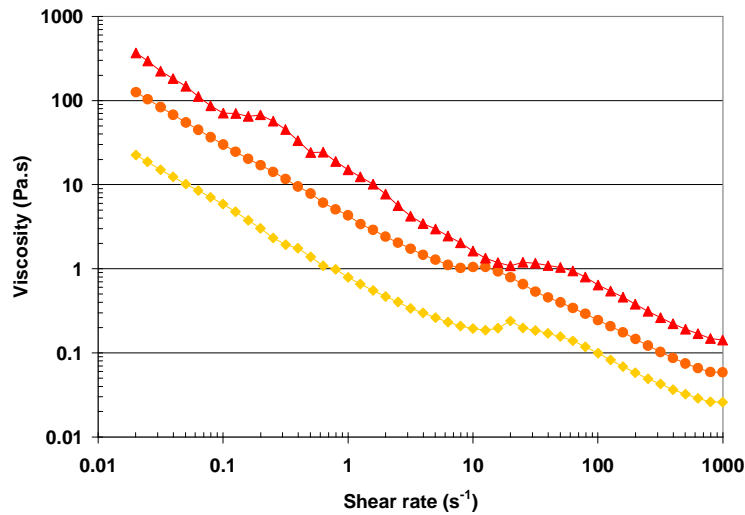


Figure III-13: Evolution of the viscosity of MFC-E-GH suspensions as a function of the shear rate after several passes in the homogenizer.

Secondly, MFC has a high ability to form a tight and entangled network due to its very high aspect ratio (L/D). The fibril dimensions were estimated to 10-30 nm in width (D) and 1-3 μm in length (L) corresponding approximately to a L/D ratio around 100. The maximum packing fraction is thus very low and this explained the high viscosity associated with the low solid content. Figure III-14 details the viscosity of a MFC-E-GH suspension according to the volume concentration and for several shear rates (1 s⁻¹, 10 s⁻¹, 100 s⁻¹ and 1000 s⁻¹).

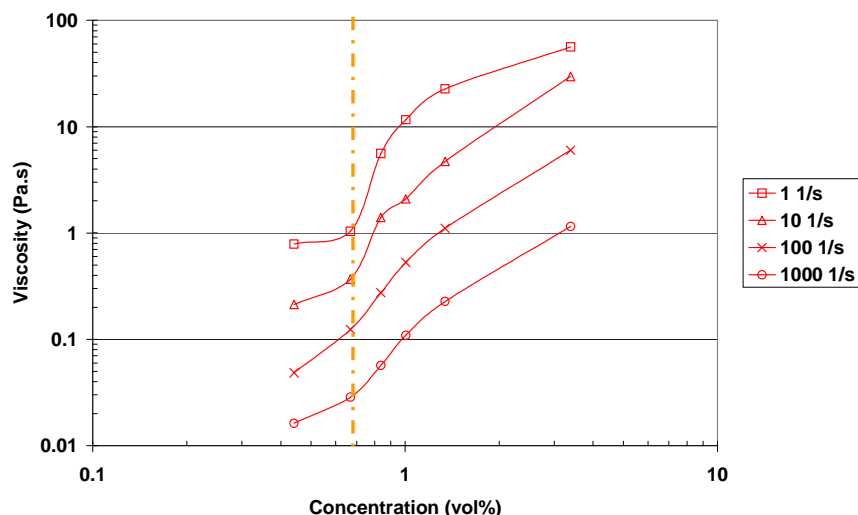


Figure III-14: Evolution of the viscosity of MFC-E-GH as a function of the concentration for different shear rates.

A strong increase of the viscosity was observed for concentrations higher than 0.67 vol%, corresponding to the percolation threshold. If the density of cellulose is assumed to be 1.5 g/cm³, this concentration corresponds to 1 wt%.

The percolation threshold (v_{Rc}) can be calculated for rigid rods such as whiskers from the equation [145]:

$$v_{Rc} = \frac{0.7}{L/d}$$

This equation is based on the statistical percolation theory for cylindrical-shaped rigid particles. MFC are flexible but if the aspect ratio of MFCs is estimated to 100, their theoretical percolation threshold is around 0.7 vol%. This is in agreement with the results obtained here. Therefore, from 0.67 %vol (1 %wt) of solid content, MFC formed a network in the suspension. From this concentration, the viscosity increased significantly with the concentration. [146, 147]

Therefore, the entanglement is probably one of the reasons leading to the high viscosity of MFC suspensions. However, the fibril charges also play a role on the physico chemical properties of suspensions and thus on the rheological properties. Complementary works will determine the real impact of the interactions between fibrils and between fibrils and water. For this, the rheological measurement must be coupled with a visual examination to observe the formation of aggregates according to the ionic charge in solvent.

Recently, Saarikoski *et al.* [90] characterized the flocculated network structure of MFC suspensions. The floc size was inversely proportional to the shear rate. Moreover, the addition of sodium chloride decreased the inter fibrillar repulsion encouraging the aggregation.

III.2.5.1.3. - Determination of flow behaviour

The thixotropic behaviour of MFC suspensions was determined using decreasing shear rates (1000-0 s⁻¹) followed by increasing shear rates (0-1000 s⁻¹). Figure III-15 shows the shear rate dependency of the MFC suspension viscosity.

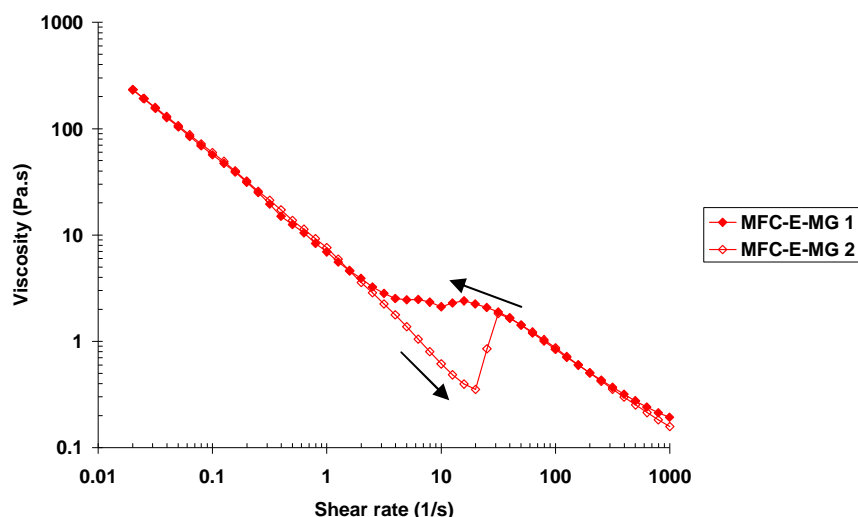


Figure III-15: Rheological behaviour of MFC suspension (MFC-E-MG).

The viscosity of MFC-E-MG could be described in three phases: firstly at low shear rate (between 0.02 and 5 s^{-1}) a shear thinning behaviour was observed due to the breakdown of the structure and to the orientation of MFC aggregates in the flow direction. The second phase showed a hysteresis loop, in this intermediate shear range ($3 - 50 \text{ s}^{-1}$). Iotti *et al.* [89] suggested that this phenomenon was due to the formation of a new structure and to a reorganisation. The third part once again showed a shear thinning behaviour due to the breaking of the MFC structure (network) under the highest shear rates.

The thixotropic behaviour of MFC suspensions was thus demonstrated by this measurement.

III.2.5.1.4. - Comparison of MFC suspensions

The influence of MFC properties on the viscosity was observed by the comparison of MFC suspensions. The suspension viscosities were measured for a solid content of 2 wt%. According to the size reduction and the homogeneity of the suspension, the viscosity differed from 11 to 100 Pa.s for a shear rate of 0.1 s^{-1} and from 0.03 to 0.2 Pa.s for a shear rate of 1000 s^{-1} . These results are in agreement with microscopic observations: the most homogeneous suspension (MFC-E-MG) had the highest viscosity (Figure III-16).

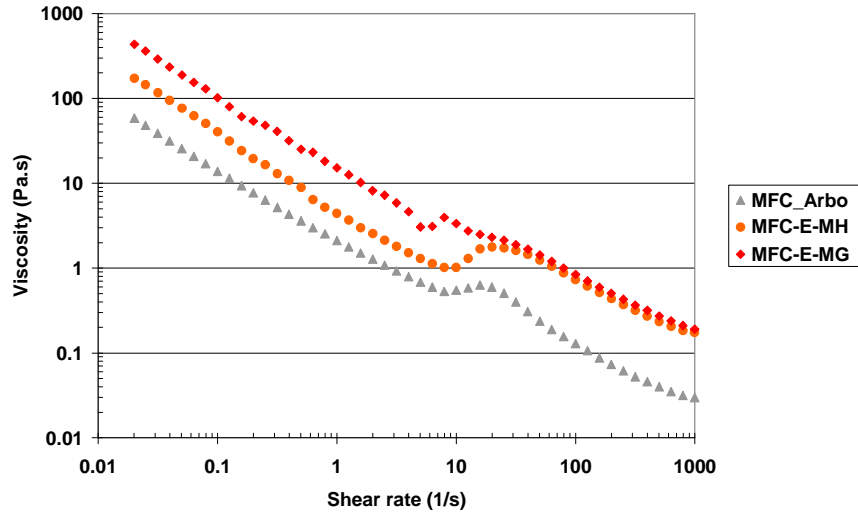


Figure III-16: Influence of the degree of fibrillation: Evolution of the viscosity as a function of the shear rate for different MFC suspensions.

III.2.5.1.5. - Influence of the production scale

The production of MFC at pilot scale was carried out with Gea homogenizer. This technique is different from the Microfluidic homogenizer or the Masuko grinder used at lab scale. The rheological properties give an indication of the quality of suspensions. Curves, Figure III-17, show quite similar viscosities for both MFC suspensions. This demonstrated the quality of suspensions produced on a larger scale.

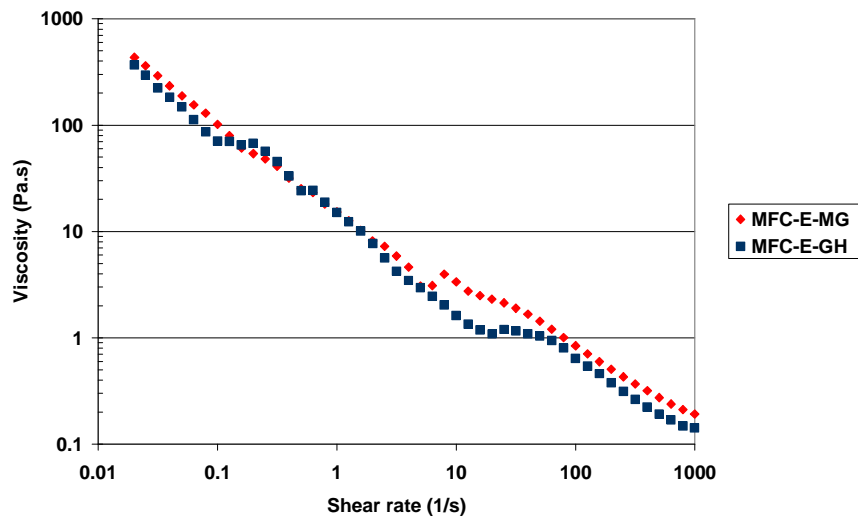


Figure III-17: Shear rate dependency on the viscosity for MFC suspensions produced at lab and pilot scale.

The comparison of the different kinds of MFC showed that the viscosity was related to the degree of fibrillation. Three main structures were described for the thin MFC suspensions, namely a structure at low shear rates with a shear thinning behaviour, an intermediate structure formed by hydrogen interactions in the range of 10-100 s⁻¹ and the broken structure at higher shear rates.

III.2.5.2. - Viscosity of MFC produced by TEMPO oxidation pretreatment

The viscosity of TEMPO-oxidized MFC was compared with enzymatically pretreated MFC at 2% (Figure III-18). Although TEMPO MFC had a lower aspect ratio, its viscosity was in the same range as the one obtained for enzymatic MFC. In this case, the high viscosity was established by the higher surface charge of TEMPO MFC leading to strong interactions. Indeed Missoum *et al.* [97] showed that the surface charge ($\mu\text{eq/g}$) determined using polyDADMAC was equivalent to the total charge of MFC measured by the Gramm method. The percentage of the surface charge in TEMPO MFC was thus around 100%. It was significantly higher than the one of enzymatically treated MFC around 30%. The shear thinning behaviour was also observed for the TEMPO MFC suspension and its viscosity was lower at high shear rates compared to the enzymatic MFC. It was supposed that the hydrogen bonds were totally broken under high shearing, thereby destroying the gel structure. The aspect ratio of these fibrils was lower and consequently this also reduced the entanglements between fibrils. Here, there probably was not the structural change observed previously. No thixotropy was revealed according to the shear rate contrary to enzymatic MFC.

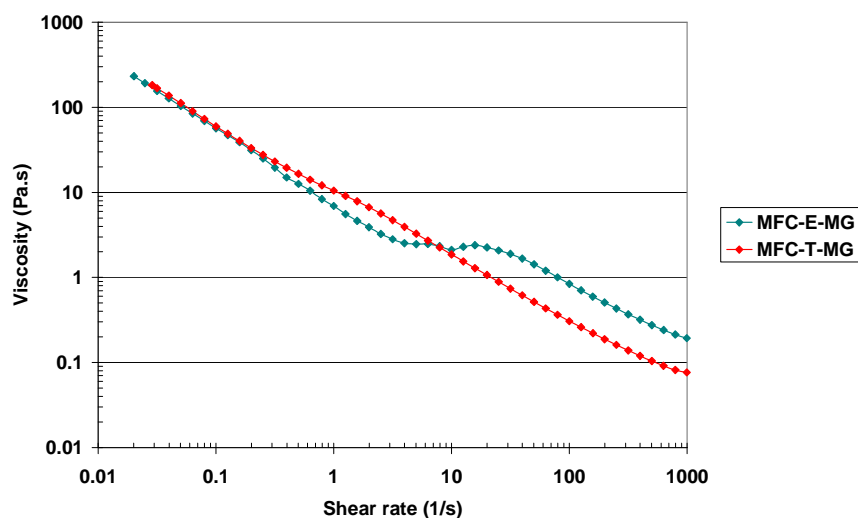


Figure III-18: Influence of pretreatment on the MFC viscosity as a function of the shear rate.

Figure III-19 shows the results obtained for the viscosity of TEMPO MFC suspensions produced at lab and pilot scale. Both curves exactly displayed the same trend and the viscosity was slightly higher for the MFC produced at pilot scale. The degree of fibrillation was thus similar whatever the production scale.

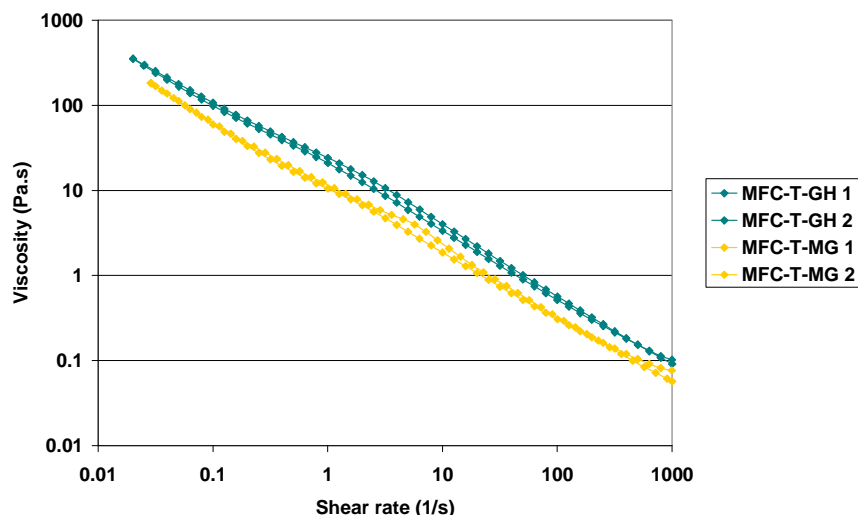


Figure III-19: Thixotropic behaviour of TEMPO MFC.

Here, no thixotropy effect was observed: the viscosity evolved in the same way during the decreasing shear rate and the increasing shear rate. The structure of the TEMPO system was thus not time dependent. The size of the elements of this MFC grade is lower and more homogeneously distributed.

III.2.5.3. - Conclusion

The characterisation using a rheometer was quite long and difficult to use during the production process. Sneek *et al.* [142], our partners in the SUNPAP project, have developed a routine method using a Brookfield viscosimeter. The use of vane spindles was required to reduce the disruption and keep a homogeneous mixture during the measurement. The viscosity was determined for several speeds and for one known concentration. Repeatable and reproducible results were obtained in a short time. This method was complementary to the rheometer and only allowed to evaluate the viscosity and thus the fibrillation quality.

The present rheological study had two objectives: firstly the comparison of MFCs according to the fibrillation state and their pretreatment, secondly the characterisation of their rheological behaviour.

MFC suspensions had a high viscosity for a concentration of 2% and it was found to increase with the degree of fibrillation. Moreover, the pretreatment also played a role on the viscosity value and the rheological characterisation. The shear thinning behaviour observed during the measurements is a positive point which favours their use in process. In the end, the study showed that viscosity measurements can also be a good method to check the quality of MFC suspensions.

III.2.6. - Conclusion

The characterisation of MFC suspensions is currently carried out using a combination of microscopic techniques and viscosity measurements. The visualisation at different magnifications allowed to observe the suspension homogeneity and the morphology of MFC. However, the size determination of individualized elements and more particularly the length is difficult due to the entanglement and the high aspect ratio. The quality of fibrillated on suspensions was very dependent on the pretreatment and on the homogenisation technique. Viscosity measurements are complementary studies giving an indication of the degree of

fibrillation. Moreover, the analysis of their rheological behaviour determined their future behaviour in coating processes. This work also showed the impact of the production process on the final MFC suspension viscosity.

This first part also showed that the MFC suspensions are very difficult to characterize. None of this measurement gives the size distribution of fibrils in MFC suspensions. Therefore, the definition of quality was currently impossible as well as the control of the reproducibility of MFC production. In the SUNPAP project, the size distribution was examined by a fractionation study giving interesting results although the characterization was long, around 1.5 day [142].

III.3. - Development of MFC films

To study the intrinsic properties of MFC, self-standing or 100% MFC films were produced and their mechanical and barrier properties were characterised. Two methods were used for the film production. The first method is casting/evaporation, a very easy technique to implement which is overused in the literature. The second one was adapted from Sehaqui *et al.* [93] using a semi-automatic sheet former. Only films prepared from MFC suspensions produced at lab scale were characterised. Firstly part, the two methods have been compared as well as the degree of fibrillation using enzymatic pretreated cellulose as source of MFC. Secondly, the properties obtained for films prepared from the TEMPO-oxidized source have been dealt with. Thirdly two possibilities to improve the MFC films properties and most particularly the water sensitivity have been presented.

III.3.1. - Production of MFC films

The comparison of the two methods, casting/evaporation and handsheet method was established with three kinds of MFC: MFC-Arbo, MFC-E-MH and MFC-E-GH. The aspect of the film was compared according to the degree of fibrillation and to the technique used.

III.3.1.1. - Film production by casting/evaporation

Films were firstly produced by the casting/evaporation technique. MFC suspensions were diluted at a concentration of 1% before being poured in a polystyrene petri dish. Water evaporation was performed at ambient conditions (23°C-50% RH) for 72 hours. Films of 30 g/m² for each suspension were obtained and are visually represented Figure III-20.

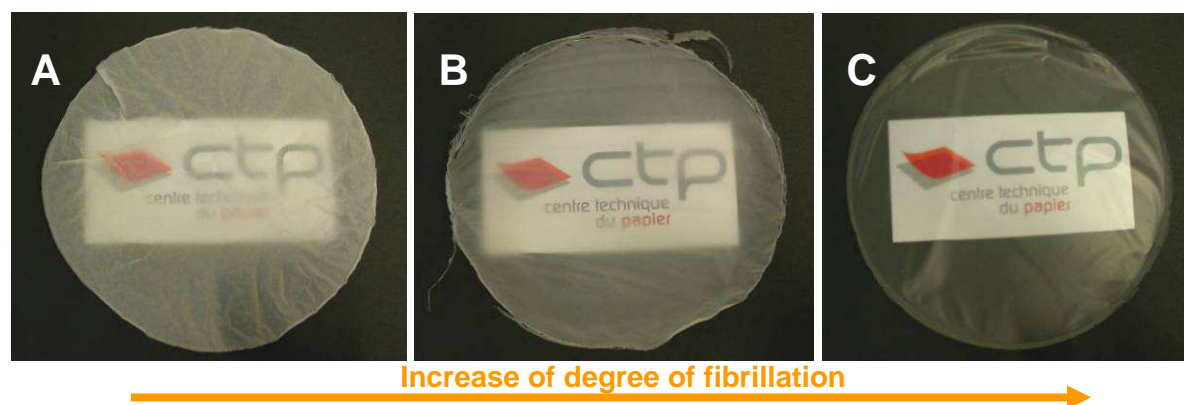


Figure III-20: Cast films produced from MFC-Arbo (A), MFC-E-MH (B), MFC-E-MG (C).

The visual aspect of MFC films was very different according to the sources. The main differences were most particularly observed for the homogeneity, the shrinking and the transparency of the films. The best film quality was thus obtained from the most homogeneous suspension and the thinnest elements previously observed in microscopy, i.e. MFC-E-MG.

III.3.1.2. - Films production by the Handsheet method

The casting/evaporation technique is a quite simple method to implement at lab scale. Nevertheless, this technique has some disadvantages such as a long drying time and the possible shrinkage of films. Sehaqui *et al.* [93] found a novel technique to limit these problems. Indeed, flat MFC films were quickly produced using a semi-automatic sheet former. The method is described in Figure III-21.

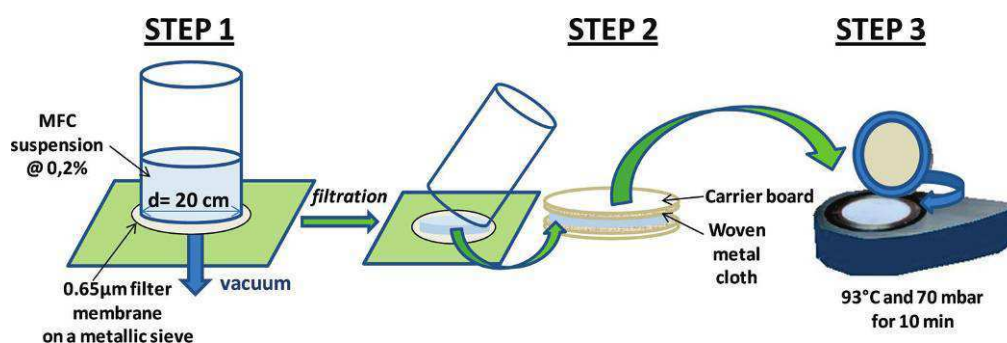


Figure III-21: Production of cellulose nanopaper using a semi automatic sheet former [93].

The first trials using this method were not satisfactory. Films produced were not homogeneous due to the presence of flocs clearly observed by a visual observation (Figure III-22).

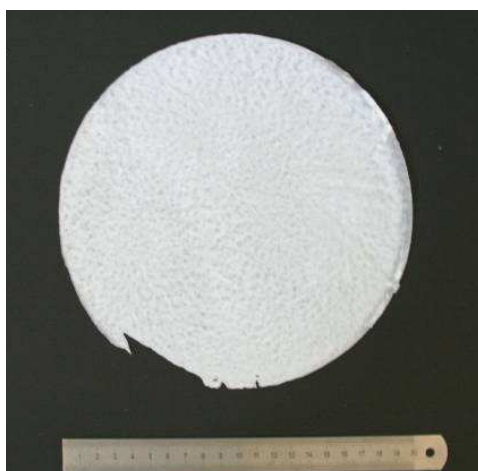


Figure III-22: First MFC films by Handsheet method.

The low transparency of the film indicated a high roughness. The microscope visualisation of the film surface revealed a high roughness due to the marks of woven metal cloth (Figure III-23). Due to this high roughness, the apparent density (determined from thickness) was only 0.46 g/cm^3 .

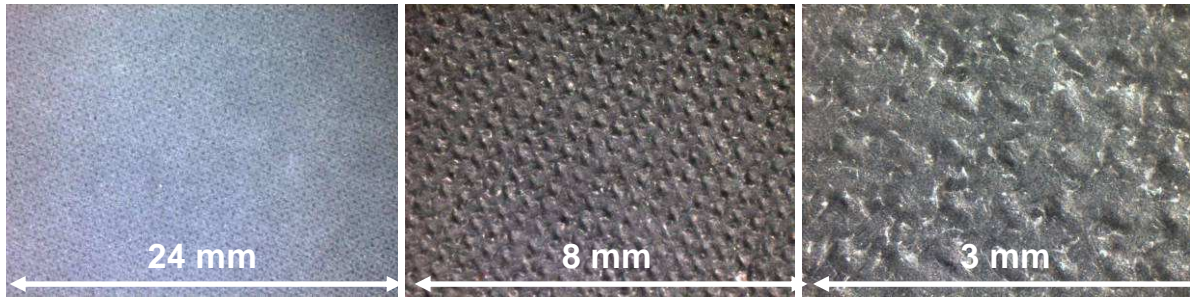


Figure III- 23: Microscopic images with grazing incidence light on the film surface.

The surface roughness of this film was determined by Perten measurements. The mean value of Ra was 3.41 μm .

To limit these defects, the method was adapted:

- The suspension concentration was increased from 0.2% to 0.5% in order to reduce the MFC flocculation and the aggregate formation.
- The woven metal clothes were replaced by cover papers (calendered papers) to reduce the roughness of the films.

Thereby, the suspension at 0.5% was stirred and filtered on a nitrocellulose ester membrane (pore size 0.65 μm) covering the metallic sieve. After filtration, the gel cake was peeled off from the membrane and stacked between two cover papers and two carrier boards. Films were dried in a sheet dryer at 93°C and under vacuum for 10 min (Figure III- 24).

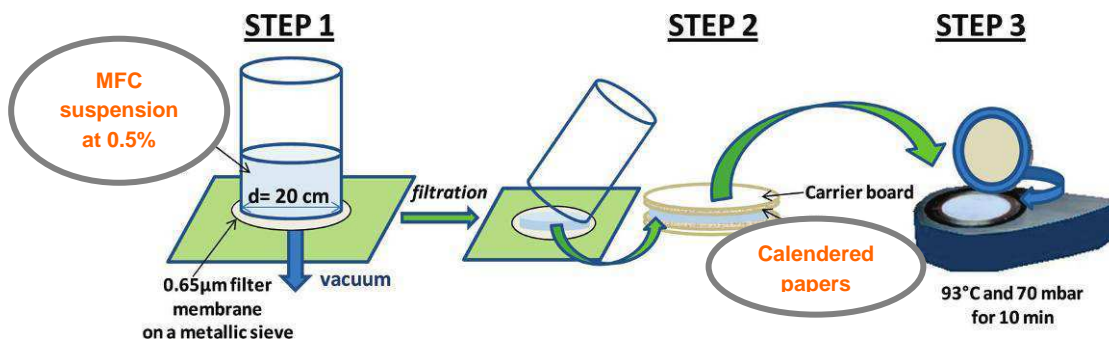


Figure III- 24: Method of film production by semi-automatic sheet former.

Flat and homogeneous films of 30 g/m^2 were thus produced by this technique as observed in Figure III-25.

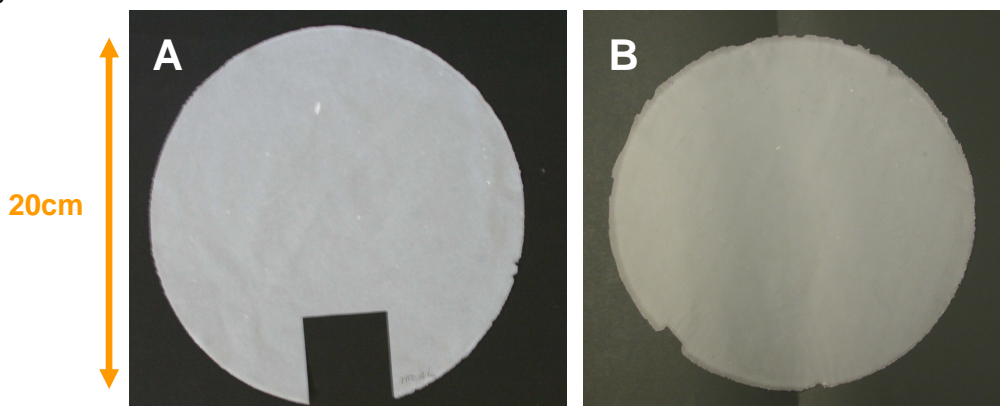


Figure III-25: MFC films obtained by Handsheet method from MFC-Arbo (A) and MFC-E-MG (B).

The improvement of the film surface quality was checked by microscope visualisation in Figure III-26. The adapted method strongly reduced the roughness and improved the smoothness of films.

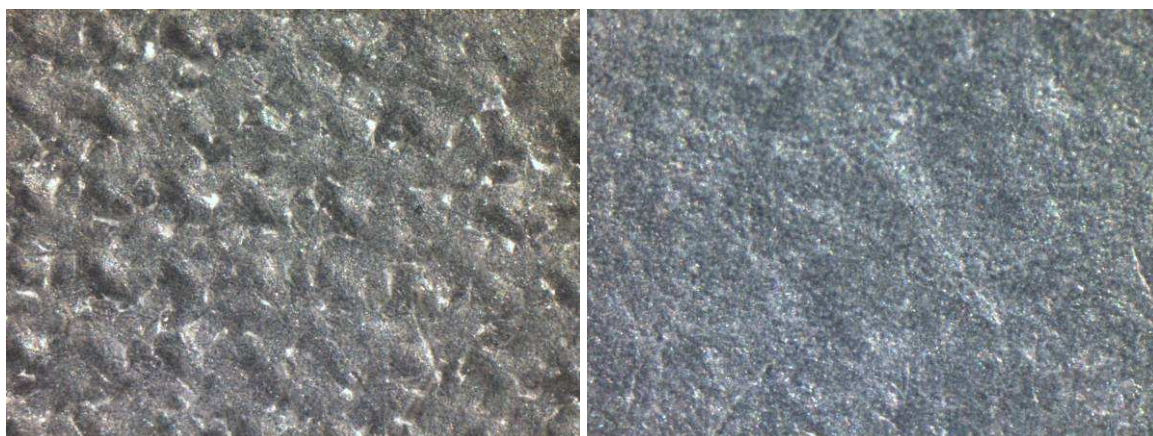


Figure III-26: Films surface obtained by the first (left) and the second (right) handsheet method from MFC-E-MG.

III.3.1.3. - Comparison between the two techniques

From the process point of view, these two techniques showed advantages and drawbacks. Table III-2 summarizes the parameters used for each technique. Casting/evaporation is easy to carry out and achievable without any specific device. However, the drying time is long and it is not obvious to obtain film with homogeneous thickness. Moreover, the free drying generally gives a wrinkling effect to the MFC film. The advantages of the handsheet method are its fastness and the smoothness of the films. Indeed, the drying under constraint allowed the formation of flat film. The impact of this drying condition on final properties might be determined.

	Casting/evaporation	Handsheet
Means	Petri dishes	Semi automatic sheet former
Preparation time	73 h	1-2 h
Solids	1%	0.5%
Drying temperature	23°C	93°C
Drying atmosphere	50% RH	0% RH
Drying time	72 h	10 min
Drying under restraint	No	Yes
Film diameter	13.5 cm	20 cm
Visual aspect	Shrinkage	Flat

Table III-2: Parameters of film production techniques.

The film properties were characterized according to the degree of fibrillation and the technique of production, using mainly MFC suspensions produced at lab scale. The structure of films was firstly analysed by microscopy, porosity and XRD measurements. Secondly, the mechanical and barrier properties were determined for each kind of suspension.

III.3.2. - Properties of enzymatic MFC films: Influence of the fibrillation and process

III.3.2.1. - Physical properties and morphology of MFC films

III.3.2.1.1. - SEM-FEG images

The fibril network obtained after the film formation was firstly observed by SEM-FEG microscopy. Here, the surface of the three films (MFC-Arbo cast film, MFC-E-MG cast film and MFC-E-MG handsheet film) showed their porosity and pores with more or less large sizes (Figure III-27). Commercial fine cellulose showed higher porosity compared to the MFC film as expected from the coarse dimensions of constituting fibrils. The magnification was lower for this sample.

Concerning the film process, the surface state of the film produced by the handsheet technique was different compared to cast films. A linting effect was observed, probably due to the process and most particularly the drying step. Indeed, films are peeled from savoyeux paper in the last step of the process leading to an eventual fluffing of the surface. The strong network formed by MFC after drying was observed on these images but also the porosity of the surface. The impact of porosity on the final film properties will be described in the following parts.

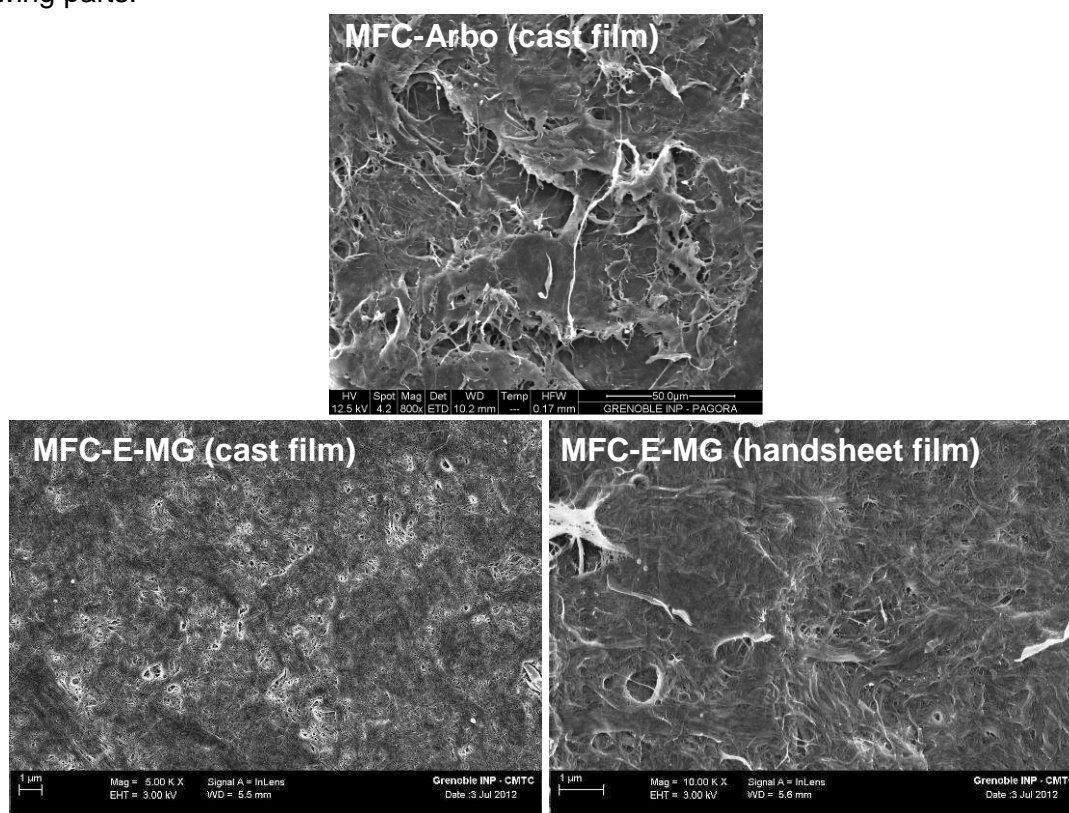


Figure III-27: Surface images of MFC films: MFC-Arbo cast film, MFC-E-MG cast film and MFC-E-MG handsheet film observed by SEM-FEG.

The film cross-sections were also observed in Figure III-28. As already described by Henriksson *et al.* [148] in the literature, films were organised in a layered and interlamellar structure. No obvious difference was observed between the two techniques of production as shown in Figure III-28. However, films prepared by the handsheet method seem to be more compact.

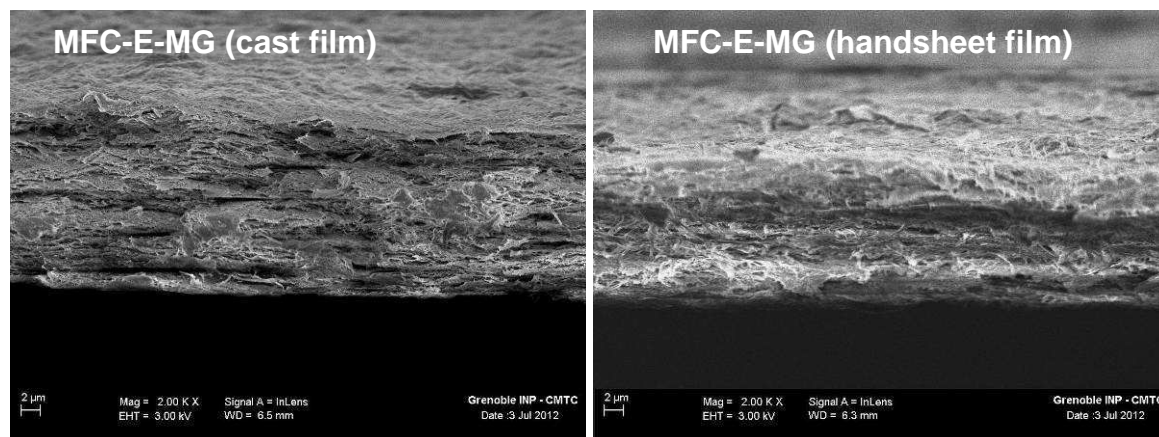


Figure III-28: Cross-section of MFC films: MFC-E-MG cast film and MFC-E-MG handsheet film observed by SEM-FEG.

III.3.2.1.2. - Film density

Figure III-29 presents the apparent density values (calculated from basis weight and thickness measurements) for all the films. The film network produced from MFC-Arbo was less dense than the other MFC films whatever the technique used. Indeed, the density of the films produced by the handsheet method was 1.16 g/cm^3 and 1.1 g/cm^3 for the MFC-E-MH and the MFC-E-MG films respectively and only 0.76 g/cm^3 for the MFC-Arbo films. In the case of cast films, the apparent density was lower with values of 0.67 , 0.97 and 1.04 g/cm^3 for MFC-Arbo, MFC-E-MH and MFC-E-MG respectively.

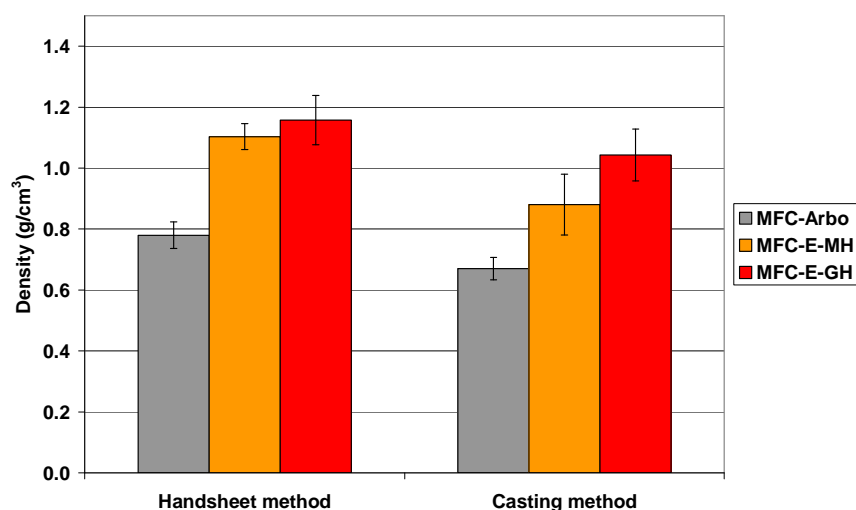


Figure III-29: Apparent density of MFC films produced by casting and handsheet method.

The density is linked to several parameters: the packing of fibrils, the number of bonds and contact points between fibrils and the residual water in films. The thinnest elements in MFC suspensions possessed a higher specific area promoting the formation of interfibrillar bonds. Thus, the film density increased with the degree of fibrillation. The handsheet method showed denser films compared to casting/evaporation films due to the vacuum filtration and the drying under constraint.

III.3.2.1.3. - Determination of the roughness by topography

The roughness of the films was determined by topography measurements after metallization. The roughness of films impacts their optical properties. Table III-3 reports the results obtained for each film.

Fibres were detected for the MFC-Arbo and the roughness was evaluated to be 2.5 μm . Enzymatic MFC sources produced films with lower roughness about 0.7 μm and 1 μm for cast and handsheet films, respectively. Therefore, the casting evaporation technique formed the smoothest films. This is probably ascribed to the different substrates used for film formation in each case.

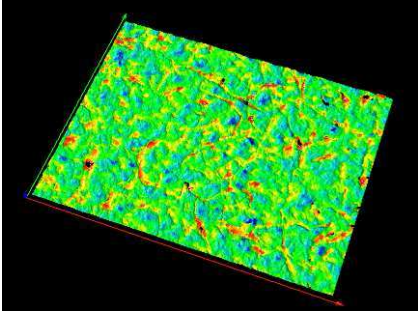
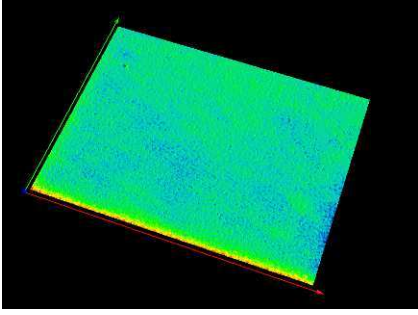
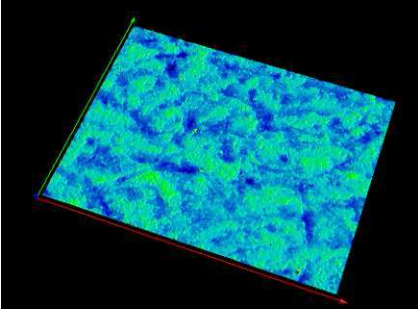
	3D Images of top side	Roughness (Ra) of top side
MFC-Arbo cast film		$2.41 \pm 0.02 \mu\text{m}$
MFC-E-MG cast film		$0.70 \pm 0.02 \mu\text{m}$
MFC-E-MG Handsheet		$1.02 \pm 0.05 \mu\text{m}$

Table III-3: Roughness measurements by topography.

These results were completed by Perten measurements carried out on the both sides of films. The mean values of Ra, described in Table III-4, are in agreement with values obtained by topography. The surface of films produced by casting/evaporation was lower compared to films produced by the Handsheet method.

	Top side	Reverse side
MFC-Arbo cast film	2.8 (\pm 0.3)	0.9 (\pm 0.1)
MFC-E-MG cast film	0.7 (\pm 0.1)	1.0 (\pm 0.1)
MFC-E-MG handsheet	1.2 (\pm 0.1)	1.2 (\pm 0.2)

Table III-4: Roughness measurements by perten

III.3.2.1.4. - Mercury porosimetry

To complete the structural analysis of MFC films, the pore size distribution was determined using mercury porosimetry. The measurement of the paper porosity by mercury porosimetry was demonstrated by Silvy *et al.* [149]. They defined two ranges of porosity in paper: the surface porosity (in the range of 10-100 μm) and the internal porosity (with pores from 0.1 to 10 μm). This technique was here used for the MFC films and showed interesting results. Mercury porosimetry is more generally used with heavy and dense materials such as clays for example. The preparation of samples was less obvious with paper or MFC films. Indeed, it was necessary to roll the sample on itself in a snail form to compact the samples.

Two replicates of MFC-E-MG samples were first analysed in order to check the measurement quality on this kind of material. Results are summarized in the Table III-5.

	MFC-E-MG cast film A	MFC-E-MG cast film B	Mean	SD
Apparent density (ISO)	1.04	1.04		
Bulk density	1.02	0.97	0.99	0.04
Skeletal density	1.48	1.41	1.45	0.05
Total porosity (%)	31	31	31	0
Surface porosity (%)	25	22	23.5	2.1
Surface pore size (μm)	3.8	3.9	3.85	0.07
Internal porosity (%)	6	9	7.5	2.1
Internal pore size (μm)	0.021/0.010	0.029/0.020		

Table III-5: Mercury porometry measurements on two films of MFC-E-MG.

The values were very closed for the two replicated except for the internal pore size. The pore size was very low closed to the detection limit of this measurement explaining the difference observed between the two samples.

MFC-Arbo and MFC-E-MG films were also analysed and the Figure III-30 shows the results obtained for each type of MFC films.

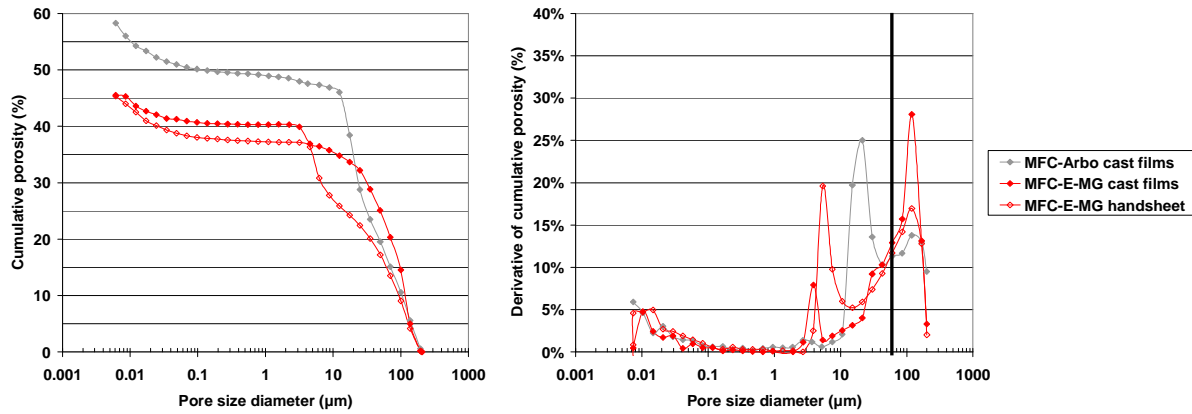


Figure III-30: Mercury porosimetry measurements.

Here, the presence of peaks around 150 μm on the derivative curve is representative of the filling of wraps and does not correspond to the real porosity of the samples. These first points were thus removed for the result analysis.

The pore size distribution is presented in Figure III-31 after the calculation. The surface porosity and the internal porosity were represented by the two peaks. The internal porosity was very low for each sample between 7 and 30 nm. This explains the high transmittance values for these materials.

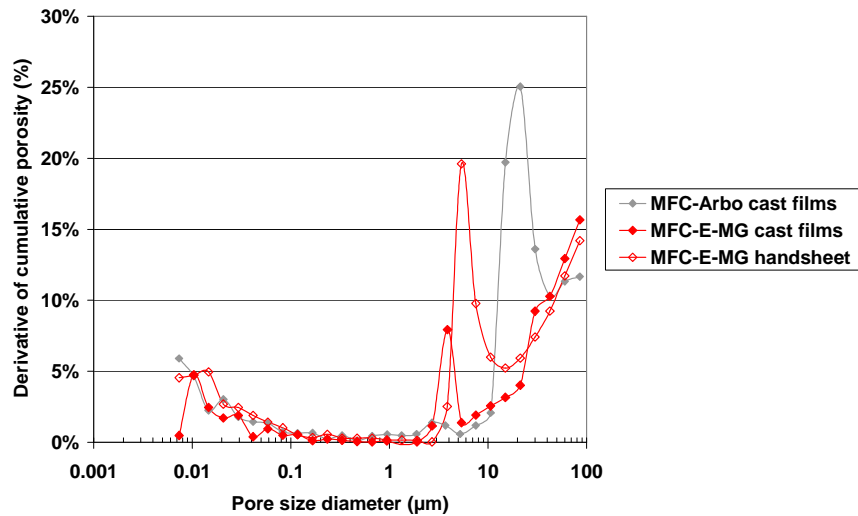


Figure III-31: Derivative of cumulative porosity of MFC films.

The porosity data for MFC films are summarized in Table III-6.

	MFC-Arbo cast film	MFC-E-MG cast film A	MFC-E-MG handsheet
Apparent density (ISO)	0.67	1.04	1.16
Bulk density	0.75	1.02	1.03
Skeletal density	1.44	1.48	1.62
Total porosity (%)	47	31	36
Surface porosity (%)	36	25	28
Surface pore size (μm)	21.2	3.5	5.3
Internal porosity (%)	11	6	8
Internal pore size (μm)	0.021/0.007	0.021/0.010	0.029/0.015

Table III-6: Density and porosity of MFC films.

The bulk density and thus the total porosity, obtained by the mercury porosimetry are of the same order of magnitude as the ones determined from the apparent density (ISO method). As observed from SEM micrographs, films produced from the biggest fibrils (MFC-Arbo) have the higher porosity reaching 47%. This also corresponds to the largest pore size with a surface porosity of 25 μm . Films prepared with the thinnest elements have a more compact structure and thus a lower porosity around 31%. By comparison, paper produced from softwood bisulphite pulp has a porosity of 67% after a low refining (a °SR of 15) and of 48% after a high refining (a °SR of 77) [149]. The surface porosity was also reduced to 3.5 μm . Concerning the film production method, it seems that the film porosity is higher with a value of 36% when the handsheet method was used. The film density was in the same range of cast films contrary to the value determined from the thickness. The size of pores at the surface was around 6.5 μm . This result is in agreement with previous MEB-FEG images of the film surface and the roughness results. Once again, this could be due to the film peeling from the calendered paper in the last step of the manufacturing process.

These results were higher compared to the results obtained by Henriksson *et al.* [76]. The MFC films porosities were between 20 and 28% depending on the degree of polymerization. The drying under 10 kPa applied pressure used for the film formation could be one of the reasons for this discrepancy.

The mercury porosity measurements gave interesting information concerning the structure of MFC films. The fibrillation of fibres led to more compact materials compared to paper. However, in spite of the strong ability of MFC to form a network, MFC films kept an important porosity compared to polymer materials. The low pore size (in the range of nm) explained the good transmittance values of MFC films and their low permeability reported in literature [91, 92].

III.3.2.1.5. - Bendtsen permeability

Firstly, the air permeability was evaluated using Bendtsen measurements. Each sample had a low air permeability in ambient conditions (23°C-50% RH) with values lower than $10^{-2} \text{ cm}^3/\text{m}^2 \cdot \text{Pa} \cdot \text{s}$, the detection limit of the device.

III.3.2.1.6. - XRD diffraction: Determination of the crystallinity index

The density and the structural organization of the fibrils have a strong impact on the final properties of the films. Nevertheless, the film properties depend also on the crystallinity index of the material. Indeed, it is believed that the highest crystallinity leads to the highest tensile strength of fibres and thereby improves mechanical properties of the corresponding nanocomposites [150]. Moreover, the crystalline part impacts the barrier properties because it is considered to be impermeable [151]. X-ray diffraction measurements were carried out on films using two modes: the reflection mode and the transmission mode. Two kinds of films were compared (casting and handsheet method) to check the influence of the drying step on the crystallinity index (Figure III-32).

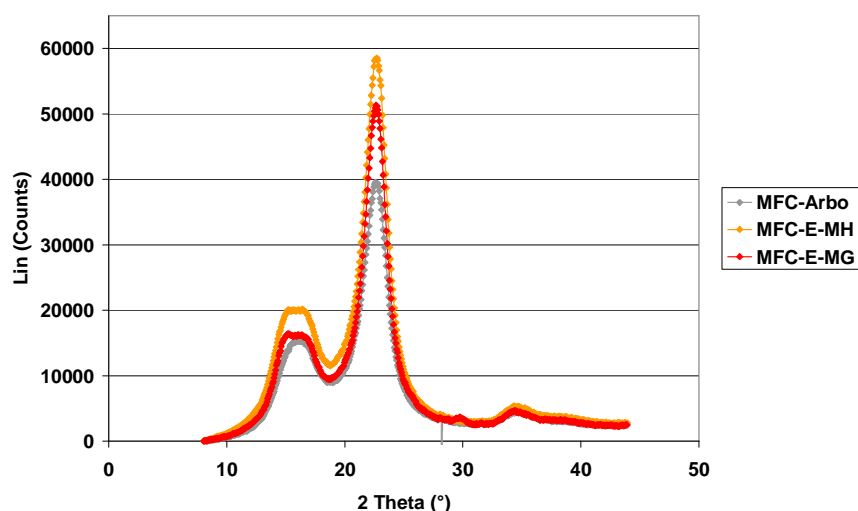


Figure III-32: X-ray diffraction patterns of MFC cast films.

The results were very similar for all the samples and it was not possible to observe any significant difference between the mechanical treatments used. Siró *et al.* [114] indicated also that there was no significant change in the crystallinity as a result of increasing homogenization.

The cellulose I β was identified on this spectra. The crystallinity index, summarized in Table III-7, was evaluated for each film using the Segal method [152]:

$$I_c = 1 - I_1/I_2 \quad (\text{Eq. 15})$$

with I_1 = Intensity at the minimum $2\theta=18^\circ$ corresponding to the amorphous domain and I_2 = Intensity for $2\theta=22.5^\circ$ corresponding to the crystalline region.

Films	Crystallinity index
MFC-Arbo cast film	71.5
MFC-Arbo handsheet	72.0
MFC-E-MH cast film	75.2
MFC-E-MH handsheet	75.8
MFC-E-MG cast film	76.3
MFC-E-MG handsheet	75.5

Table III-7: Calculated crystallinity index of each MFC film.

No significant difference was observed between the two kinds of films (obtained by casting/evaporation or by handsheet method). The difference observed between the films was thus not due to a difference in crystallinity ratio. The values 71% and 75% were in agreement with values reported in literature for the MFC. Alemdar and Sain [150] obtained MFC with a crystallinity degree of 70% for wheat straw source and 78% for soy hull source. However, Moon *et al.* [153] showed that MFC from wood and plant fibres had a crystallinity of 51-69% compared to 43-65% for the initial source.

The Segal method is very fast to use but remains a qualitative method and is limited to precisely determine the crystallinity [154].

A second X-ray experiment was carried out in transmission mode to observe the possible orientation of fibrils in films. Only MFC-E-MG films were tested here. In this mode, the symmetric and asymmetric crystalline plans were detected. The two diffractograms obtained by this method were different although the film was exactly the same. An isotropic material always reflected in the same way whatever the diffusion angle. Therefore an orientation was well revealed here. Figure III-33 compares the two diffractograms (symmetric and asymmetric). The difference in signal intensity was clear, most particularly for the diffraction angle around 35°. The orientation could be more or less accentuated according to the film formation but this cannot be quantified by this measurement.

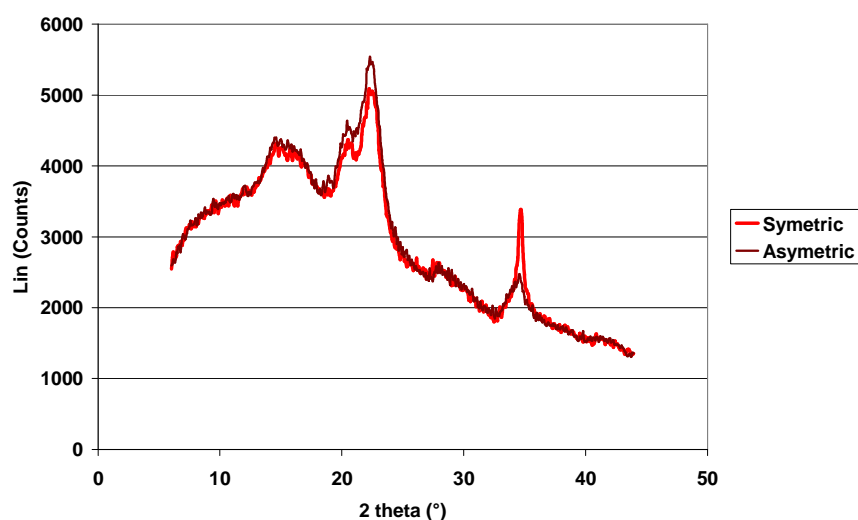


Figure III-33: X-ray diffraction patterns of MFC-E-MG film measured in symmetric and asymmetric mode.

XRD measurements allowed determining the crystallinity index of MFC films. No significant difference was observed here meaning that the difference of film properties were mainly due to the film organisation.

III.3.2.2. - Measurement of transparency

Pictures of MFC films (see Figure III-20, Figure III-25) showed the difference in transparency according to the source. This was quantified by three measurements: the total transmittance, the transmission haze and the clarity values. Obtained values are summarized in Table III-8. The transmittance allowed quantifying the light which passes through the sample. This value depends on the material and its homogeneity. Here again, the most fibrillated samples

offered the highest transmittance values. However, the haze values were very high explaining that the films were highly translucent but not totally transparent. Thus, on the contrary, the clarity values were very low. Moreover, the global transparency was generally higher for films produced by casting-evaporation compared to the handsheet method. Two reasons could explain this result. First, the content in thin elements was probably higher after casting-evaporation because no material loss is possible contrary to what occurs with the filtration technique. The second reason is the higher roughness and porosity of films produced by the handsheet method. This explanation is in agreement with the porosity results described previously.

	MFC-Arbo		MFC-E-MH		MFC-E-MG	
	Cast	Handsheet	Cast	Handsheet	Cast	Handsheet
Transmittance	81.4 (0.9)	69.6 (0.8)	83.1 (0.8)	83.4 (0.5)	91.3 (0.4)	85.2 (0.6)
Haze	97.0 (0.0)	97.2 (0.1)	97.5 (0.2)	98.1 (1.3)	90.0 (0.7)	95.5 (0.2)
Clarity	5.2 (0.0)	5.3 (0.1)	5.1 (0.1)	4.6 (0.1)	7.1 (0.4)	6.1 (0.1)

Table III-8: Transparency measurements of MFC films.

Standard deviations are indicated into brackets.

This first part described the physical properties of films and firstly showed the strong difference between the MFC-Arbo and MFC-E-MH films. Indeed, the film produced from the commercial source showed low density, high porosity and low transparency. The film quality was largely improved when using the thinner elements produced at lab scale. Concerning the technique of film formation, the handsheet method produced films with higher surface roughness. The impact of the physical properties of films was observed on the resulting mechanical and barrier properties of films in the next parts.

III.3.2.3. - Mechanical properties of MFC films

III.3.2.3.1. - Tensile tests

Regarding the source, the Young's modulus values were significantly higher for the films obtained from the microfibrillated cellulose compared to the commercial source MFC-Arbo (Figure III-34). The ability of thin MFC to form a dense structure with high number of interfibrillar bonds led to stiffer materials. The density of films and the element size being very similar for the MFC-E-MH and MFC-E-MG, their Young's modulus values were also in the same range.

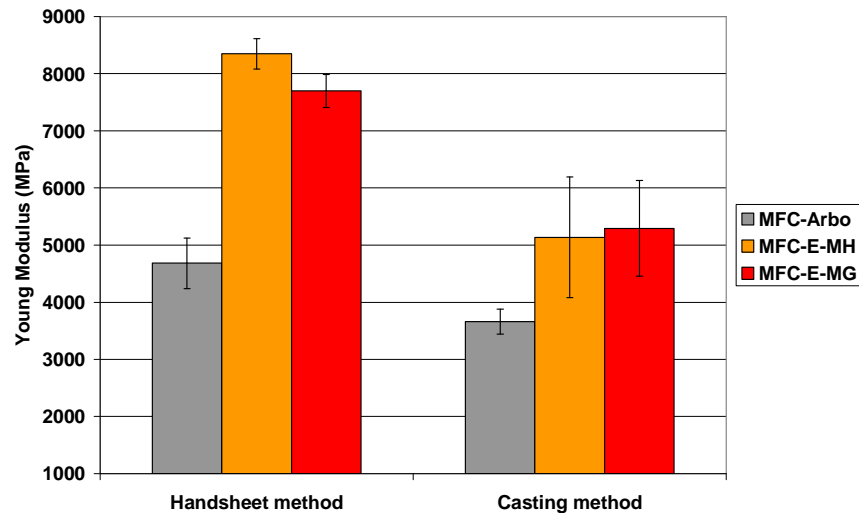


Figure III-34: Young's modulus values of MFC films.

The Young's modulus values of films produced by the handsheet method were greater than those of cast films. The apparent density of these films showed more compact films, which was not the case when considering the mercury porosimetry results.

However, the difference in density was probably not the only reason for this improvement. Indeed, Figure III-35 reports the specific Young's modulus values obtained by dividing the experimental data by the density of MFC films. The values were always slightly higher for the films produced by the handsheet method compared to casting/evaporation.

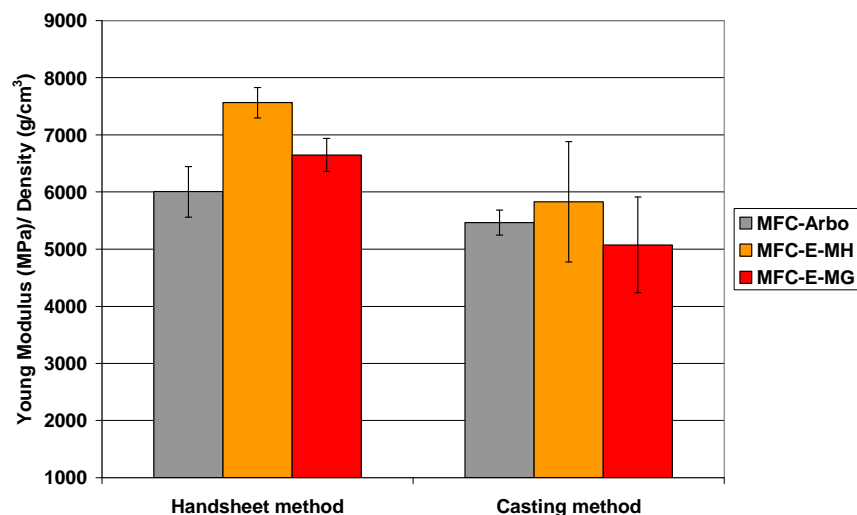


Figure III-35: Specific Young modulus values of MFC films.

The drying method could be a reason for this result. Indeed, the drying conditions were very different for the two techniques: the handsheet method used a fast vacuum drying at 93°C for 10 min compared to the slow drying in ambient conditions for the casting/evaporation technique.

Several phenomena could thus be envisaged. Firstly, the effect of the rate of drying on the degree of hornification studied by Brancato et al. [155]. The comparison between the drying of fibres in ambient air, on a hot plate, and in a microwave oven showed that the drying at a faster rate increased the degree of hornification. The hornification phenomenon is a

rearrangement of cellulose molecules in fibrils and interfibril aggregation upon drying. This leads to a slight increase of the degree of crystallinity of cellulose. However, no significant difference was observed in our case from X-ray diffraction measurements.

A second possibility, described by Sehaqui *et al.* [93], is the increase of the fibril orientation in the plane by drying under constraint. Our results are in agreement with those obtained by Sehaqui *et al.* [93] for films quite twice as thick as. Their cast films presented a Young's modulus of 10.3 GPa which is smaller than the 13.4 GPa obtained for films produced by the handsheet method. The values obtained here were much lower compared to the literature values. The thinness of our films led to brittle films, weakened by the jaws during the measurement. Thicker films should be analysed to check the Young's modulus value.

The third possible explanation is that the drying conditions also influence the shrinkage of the fibres. More shrinkage giving higher strain at break was observed. Drying under constraint decreased the shrinkage, formed less extensible paper and increased the bonding strength [156]. The increase of bonding strength leads to an increase of the Young's modulus.

The tensile strength values were also determined during these tensile tests and are described in Figure III-36. Once again, the tensile properties of commercial fine cellulose (MFC-Arbo) were largely lower compared to the MFC produced at lab scale. As observed previously with Young's modulus values, the handsheet method formed films with higher strength compared to the casting/evaporation method.

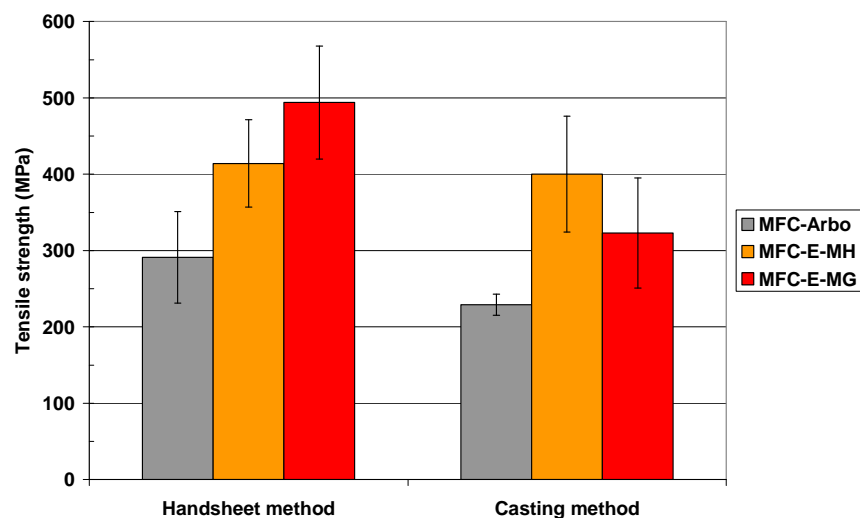


Figure III-36: Tensile strength values of MFC films.

The elongation at break values were very dependent on the technique used as observed in the Figure III-37. Indeed, the elongation at break of cast films was twice as high as the one of handsheet films. The results clearly indicated the influence of drying under constraint on the shrinkage and the extensive properties of films.

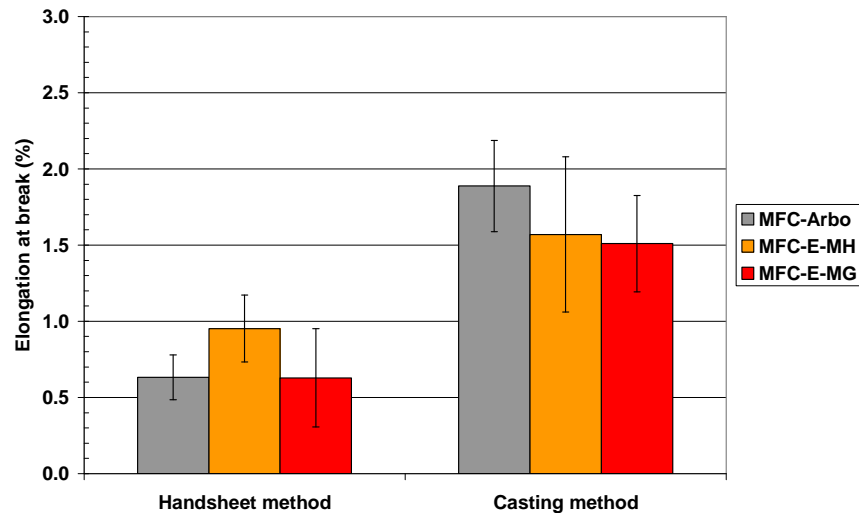


Figure III-37: Elongation at break (%) of MFC films.

III.3.2.3.2. - Burst index

In the paper industries, other measurements are commonly used to evaluate the mechanical properties of paper such as the burst and the tear index. Firstly, Figure III-38 shows the results concerning the burst index of MFC films produced by the two methods. For films prepared by the handsheet method, the values were 3 or 4 times higher with the use of more fibrillated sample. Once again, the higher number of interfibrillar bonds and contact points between fibrils leads to a higher strength. Nevertheless, this time cast films showed the highest values. Burst index depends on the number of inter-fibrils bonds and on the entanglement. The number of bonds between fibrils was probably higher after a slow and free drying compared to a fast drying. Moreover, if the handsheet films display a preferential orientation as described by Sehaqui *et al.* [93], the burst resistance could be lowered.

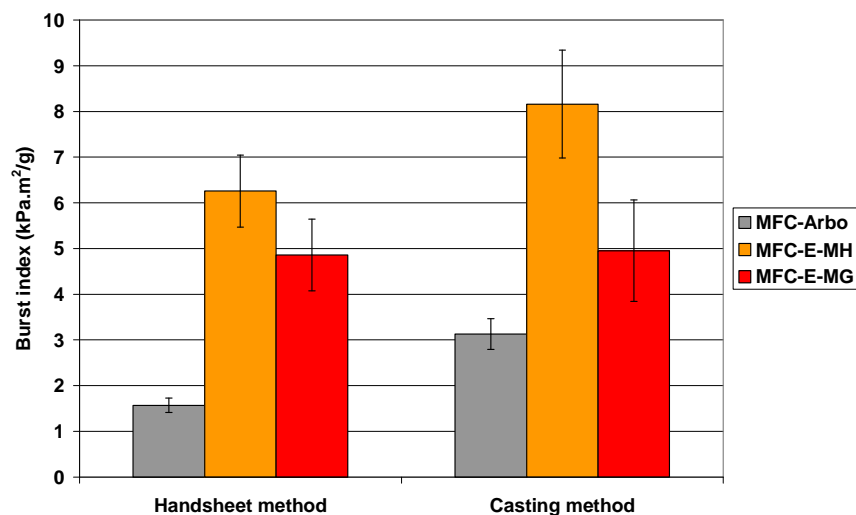


Figure III-38: Burst index of MFC films.

III.3.2.3.3. - Tear resistance

Tear resistance is an important property in the applications and more particularly for the processability of sheets under strain. Figure III-39 shows the results obtained for MFC films

produced by the two methods. The length of the fibrils is an important factor influencing the tear properties. Indeed, entanglements occur more easily with long fibres, thereby giving the tear resistance of the material. MFC-Arbo had a length of 500 μm , which is much higher than the length of other MFC estimated at 1-3 μm . This explained the better tear resistance of MFC-Arbo films. However, the aspect ratio should be taken into account assessing the possibility of entanglements. Once again the casting method offered results showing a higher entanglement of fibrils thanks to a long drying.

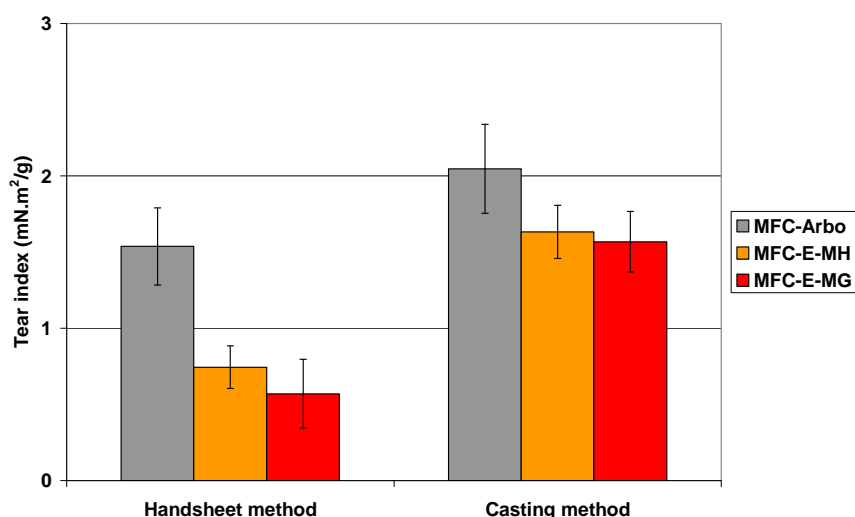


Figure III-39: Tear index properties for MFC films.

It is worth noting that the tear index of MFC films was very low compared to standard paper and this can lead to limitations for the use of MFC films. It could be interesting to study solutions to improve this property. To date, no paper reports this kind of results in literature.

III.3.2.3.4. - Conclusion

Tensile test results showed high Young's modulus values for the films produced with the thinnest elements. However, the values were low compared to the literature values. As described in the literature review, the method of film production determined the density of films linked to final mechanical properties. In this present work, the influence of drying conditions was observed on the final tensile properties of films. Several possible explanations were thus established. The tearing and bursting properties were generally not studied in the literature. However, they both are essential properties for packaging applications. Thus, the low tear index observed for MFC films could be a drawback for their use in such applications.

III.3.2.4. - Barrier properties of MFC films

MFC is promising for the development of barrier materials. The ability of MFC to entangle and to form a network offer good barrier properties. The fibrillation influence on the film barrier properties has been here studied according to the production method.

III.3.2.4.1. - Grease resistance

The grease resistance was determined using a Cobb measurement with peanut oil during 24h. The value was around 1 g/m^2 . Greaseproof paper corresponds to dense and well

bonded paper. To create this kind of paper, a high degree of beating is necessary. The high density and the small number of large surface pores give the grease resistance properties [157]. The MFC films thus showed the conditions required to develop a good grease resistance material.

III.3.2.4.2. - Water resistance

The water absorption as well as the swelling of MFC films was determined to evaluate the water resistance of the latter. For this, Cobb measurements were carried out with thickness measurement before and after the exposure to water. Cobb 60 index values, shown in Figure III-40, were not valid in our case according to the standard because some water passed through the films during the measurement. However, this could give an indication of the water resistance.

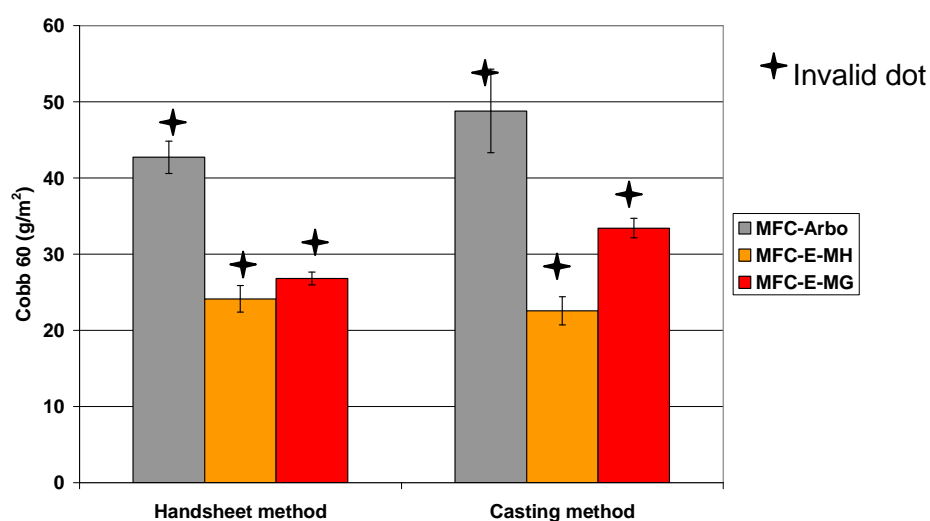


Figure III-40: Cobb 60s index of MFC films (Area 10 cm²).

MFC produced at lab scale were less sensitive to water compared to MFC-Arbo. The strong interactions between fibrils reduced the number of accessible OH groups at the surface. Conversely, MFC films strongly swelled in the presence of water compared to commercial MFC. The structure was very sensitive to water and thin elements swelled more easily than big elements (Figure III-41). This swelling effect generally leads to the network being loosened reducing barrier properties.

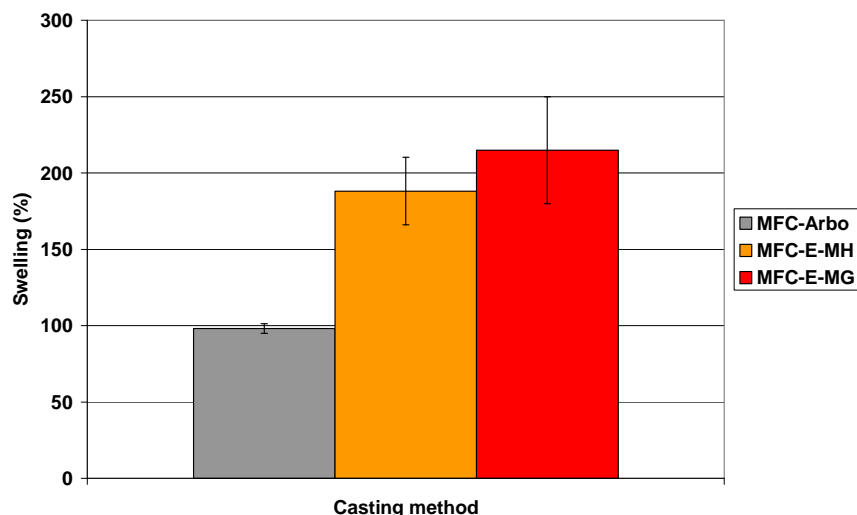


Figure III-41: Water swelling of MFC films.

For the use of MFC films in barrier materials, it will be necessary to improve the resistance to water. Indeed, the total immersion of films in water under moderate stirring lead to fast disaggregation of films (<1min).

III.3.2.4.3. - Water vapour transmission rate (23°C-50% RH)

Figure III-42 shows the results concerning the water vapour transmission rate (WVTR) of MFC films produced by the two methods at 23°C-50% RH.

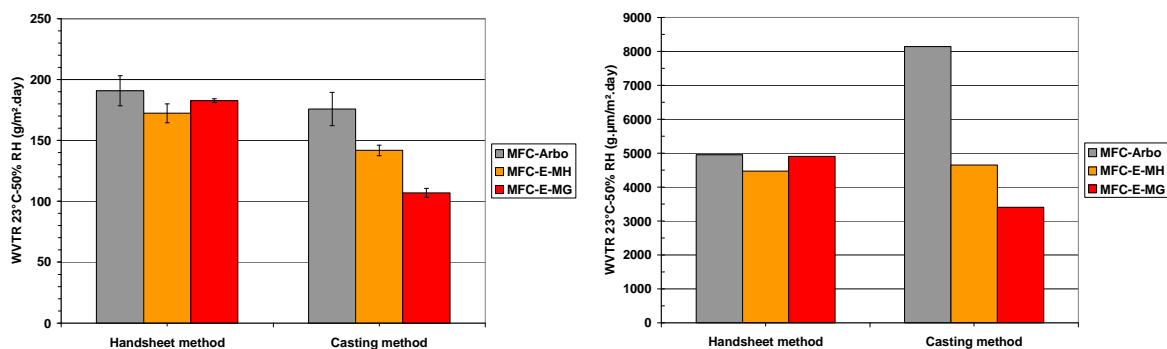


Figure III-42: Water vapour transmission rates values of MFC films at 23°C-50% RH.

The water vapour transmission rate values obtained at 23°C-50% RH were quite high with the lowest value of 100 g/m².day corresponding to 3400 g.μm/m².day for MFC-E-MG cast films. By comparison, the value for a PVOH film is around 30 g.μm/m².day. The water vapour permeability results from two main factors:

- The diffusivity which depends on the porosity and the tortuosity of the material.
- The water vapour solubility depending on the water affinity of the material.

Cellulosic materials are highly sensitive to water, the water affinity is very high and the water sorption at the fibre surface is very important. Okubayashi *et al.* [158] studied the water sorption on staple lyocell and cotton fibres. Water molecules directly adsorbed on the hydroxyl groups of external surface, amorphous regions, inner surface of voids and crystallites (Figure III-43).

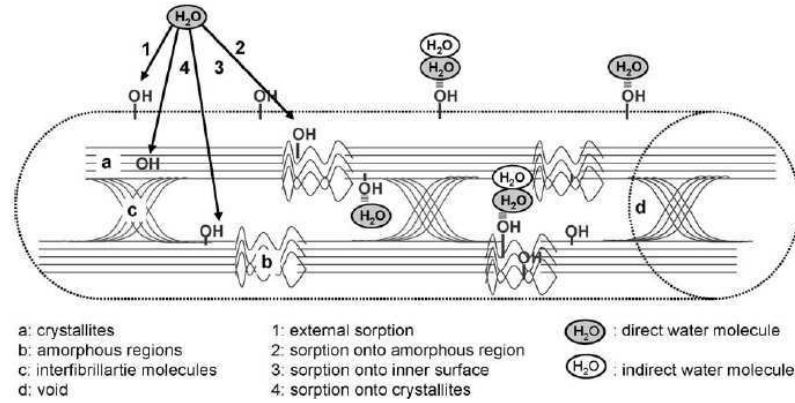


Figure III-43: A schematic diagram of direct and indirect sorption onto external surface (1), amorphous regions (2), inner surface of voids (3) and crystallites (4) [158].

In Figure III-42, WVTR values of MFC films obtained by the handsheet method were higher than those observed for cast films except for MFC-Arbo. The reason could be the higher porosity of these films because MFC-E-MG handsheet films showed 36% of porosity compared to 31% for the cast film.

In the case of cast films, a trend was well observed according to the degree of fibrillation. The WVTR values decreased with the increase of the degree of fibrillation.

The sorption measurements showed the same evolution for each sample. The sorption and desorption curves are described Figure III-44 for relative humidity between 40% and 85%. The quantity of water at the equilibrium was different according to the thinness of elements. Indeed, the increase of the degree of fibrillation, by increasing the specific surface area, increased the water sorption. A paper made from spruce/pine pulp was used as reference here and clearly showed the influence of fibrillation on the water sorption.

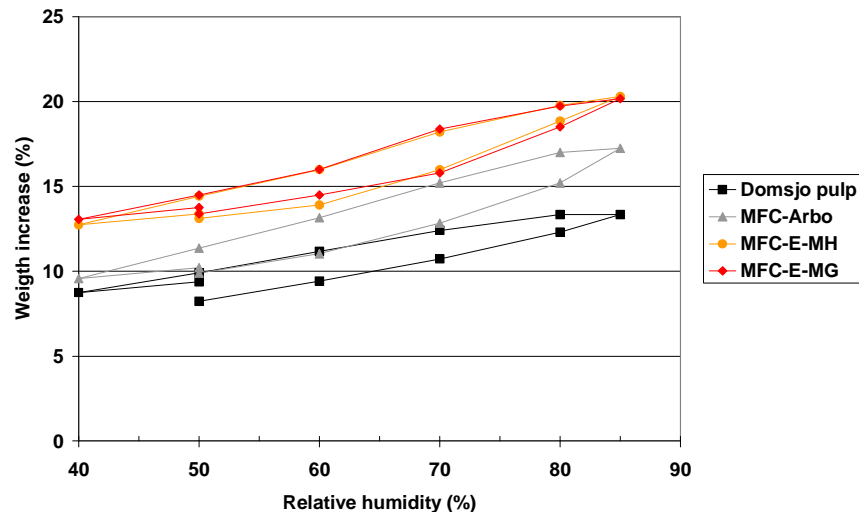


Figure III-44: Sorption and desorption measurements for MFC cast films.

Although the water affinity was higher for the MFC-E-MH and MFC-E-MG films, their WVTR (23°C-50% RH) values were the lowest ones. Therefore the difference of permeability was mainly due to the film porosity. MFC-Arbo cast films had the highest porosity leading to the highest diffusivity and high WVTR values. The homogeneous MFC-E-MG formed a closer network leading to the lowest diffusivity and thus showed the best value of WVTR.

The WVTR strongly depends on the porosity of the network. A homogeneous MFC suspension and the thinnest fibrils gave the tightest network and thus the best results.

However, the porosity and water affinity of cellulose did not allow to obtain sufficient water vapour barrier materials for self-standing MFC films. This conclusion was also made recently by Rodionova *et al.* [159]. The WVTR (23°C-50% RH) of MFC films, produced by filtration through a paper filter, was of 170 g/m².day for a thickness of 28 µm corresponding to 4760 g.µm/m².day. This moisture barrier is not sufficient for an application in food packaging and has to be improved. This study showed the effect of hornification on the barrier properties of films. Indeed, the drying strategies showed a clear influence on the hornification leading to morphological changes. Spence *et al.* [18] also obtained a value of 21500 g.µm/m².day.

Several additives were tested to improve this value. Indeed starch, calcium carbonate and kaolin clay were added in wet-end leading to the permeability reduction with 10% of calcium carbonate. Subsequently, the MFC films were coated by beeswax, paraffin or starch, the best value was obtained using 10 g/m² of beeswax.

The water vapour transmission values obtained in this work were in agreement with the few results reported in literature (Table III-9).

References	WVTR (g.µm/m ² .day)
Present work	3400
[159]	4760
[18]	21500

Table III-9: Summary of WVTR of MFC films (23°C-50% RH) reported in literature.

III.3.2.4.4. - Oxygen transmission rate (23°C-0% RH)

To preserve food from oxidation phenomena, packaging materials limit the oxygen transport through the film. The oxygen transmission rate (OTR) measurements were carried out at 23°C-0% RH. The results are described in Figure III-45 and in Table III-10.

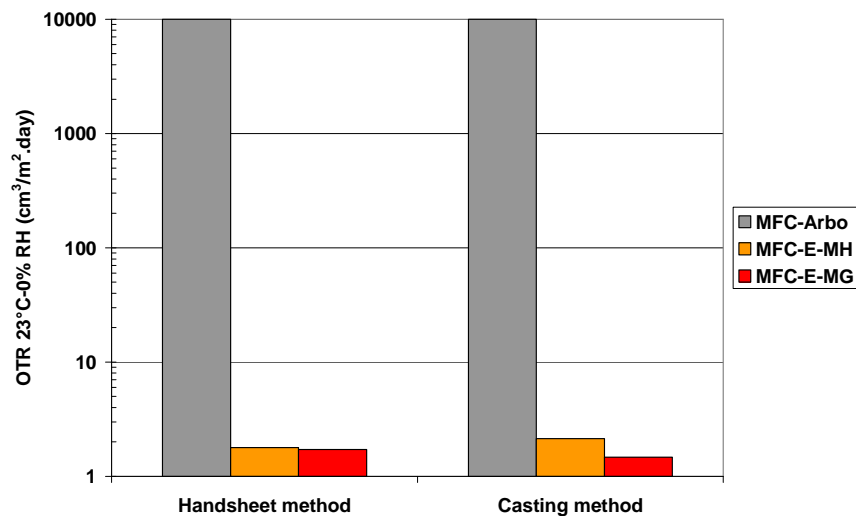


Figure III-45: Oxygen transmission rate of MFC films.

In dry conditions, strong entanglements between fibrils allowed to obtain promising values. Indeed, the OTR value around $2 \text{ cm}^3/\text{m}^2.\text{day}$ was in the same range as the one obtained for PVOH films which are well-known for their excellent oxygen barrier properties. The influence of the element size was once again observed with a strong difference between OTR values of MFC-Arbo films and MFC-E-MG films. All values are summarized in Table III-10.

	MFC-Arbo		MFC-E-MH		MFC-E-MG	
	Hand-sheet	Cast	Hand-sheet	Cast	Hand-sheet	Cast
OTR 23°C-0% RH ($\text{cm}^3/\text{m}^2.\text{day}$)	>10000	>10000	1.8	2.1	1.7	1.4
Oxygen permeability 23°C-0% RH ($\text{cm}^3.\mu\text{m}/\text{m}^2.\text{day}.\text{bar}$)	>400000	>460000	53	64	44	44

Table III-10: Oxygen transmission rate and permeability of MFC films.

Table III-11 summarized some literature results. Our results were of the same order of magnitude as the values obtained by Rodionova *et al.* [159]. However, a high dispersion of the results is found in the literature. Once again, film properties depend strongly on the source, on the methods to produce the MFC and on the methods used for the film production.

References	Pulp pre-treatment	Thickness (μm)	Oxygen permeability 23°C-0% RH ($\text{cm}^3.\mu\text{m}/\text{m}^2.\text{day}.\text{bar}$)
Present work	Enzymatic	30	44
[92]	Mechanical	22	357
[159]	Mechanical	22	54
[91]	Carboxymethylation	5	0.06

Table III-11: Comparison of oxygen permeability of MFC-E film with literature values.

III.3.2.5. - Conclusion

Two methods of the film production were employed and compared: casting/evaporation and handsheet method. The handsheet method was firstly adapted to improve the film quality. Films were very different according to the process: casting/evaporation produced films with the highest transparency while the handsheet technique allowed obtaining flat and homogeneous films in thickness in a shorter time. Film properties depended on the MFC source and production process. Indeed, films produced from the most fibrillated MFC gave the best values in mechanical and barrier properties. The drying condition also seemed to influence the MFC network properties. Except for the tensile properties, the properties of films were better for the films produced by casting/evaporation. Finally, the high strength of the films showed the reinforcement potential of these materials. Oxygen barrier permeability as well as their ability to form a tight network demonstrated the possibility to use them in order to develop barrier layers. However, the porosity and the water sensitivity of the films

limit their water vapour permeability. Solutions must be found to improve these properties for the use of MFC in packaging applications.

III.3.3. - Influence of the TEMPO pretreatment on MFC film properties

Properties of TEMPO MFC films were compared with those of enzymatic MFC films in order to assess the impact of the modification induced by the chemical treatment. Here films were only prepared by the casting method because the high water retention of oxidized MFC led to long filtration time.

As previously seen in the morphological characterisation section, the TEMPO MFC suspension was more homogeneous in size compared to the enzymatic pretreatment. The fibril length was also lower after this pretreatment leading to lower aspect ratio.

The first important difference was the aspect of films. Films prepared from TEMPO MFC presented a very high transparency, high brightness but also higher brittleness compared to enzymatic MFC films [Figure III-46].



Figure III-46: Visual aspect of TEMPO MFC film. Compared with enzymatic?

III.3.3.1. - SEM-FEG images

The high transparency of TEMPO MFC films as well as resulted from the thinness of fibrils and from their highly closed surface, as observed in Figure III-47. Contrary to the MFC films previously observed, the porosity of the surface was very low and no large pores were detected.

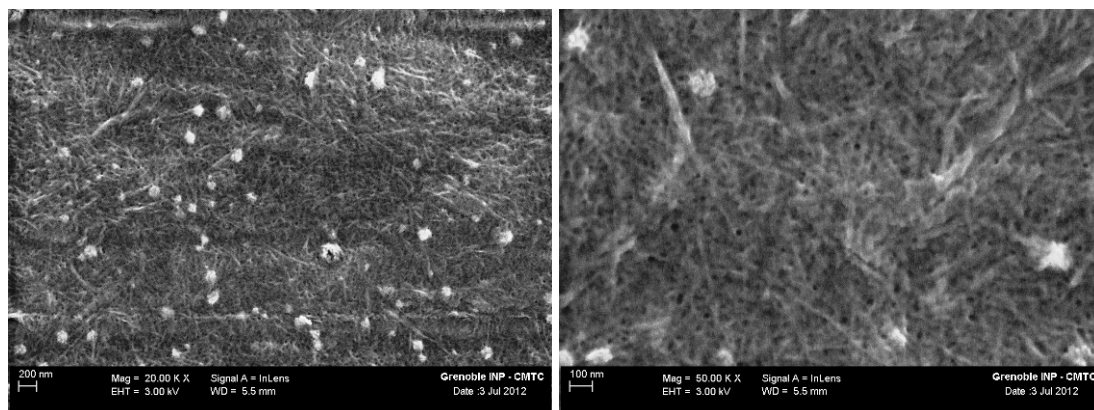


Figure III-47: SEM-FEG photos of oxidized MFC film surface.

The white dots, observed at the surface, were due to chemical residues resulting from the TEMPO reaction. Indeed, a MEB Micro X analysis was carried out at the surface of the film produced with MFC obtained by Tempo and enzymatic pretreatment. Figure III-48, the element composition of TEMPO film showed a high concentration of sodium, used for the TEMPO reaction [160].

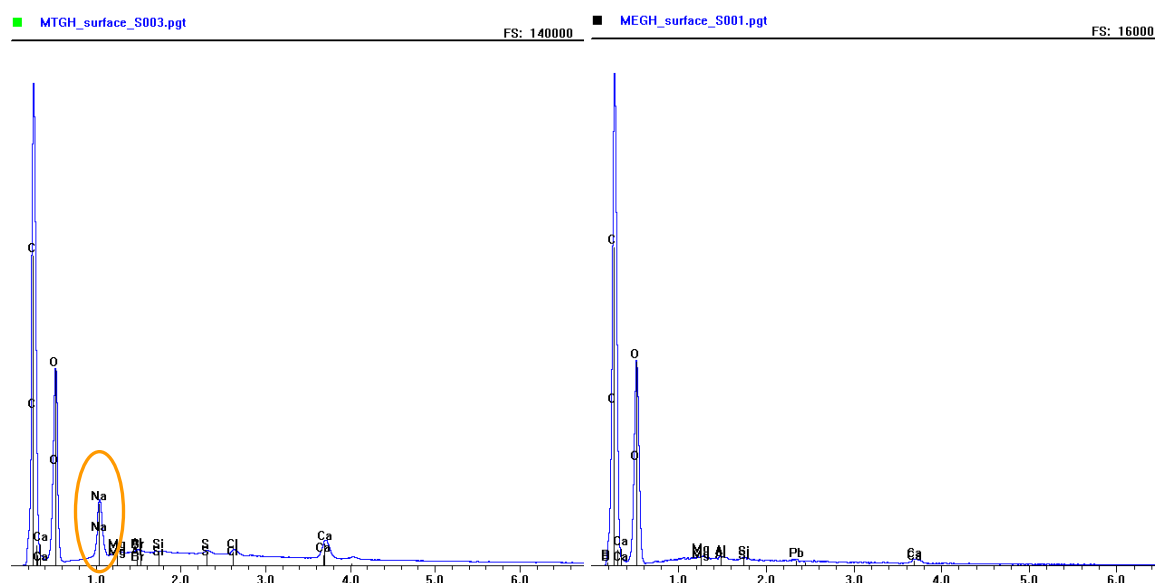


Figure III-48: MEB Micro X analysis of TEMPO MFC films (left) and enzymatic MFC films (right).

III.3.3.2. - Roughness measurement by topography

The smoothness of films was investigated with topography images of the film surface (Figure III-49). Here the image reached the limit of the device with the interference strips emergence. The roughness was estimated to be 0.15 μm . This low value was confirmed by perten measurement with a mean value Ra of 0.30 μm .

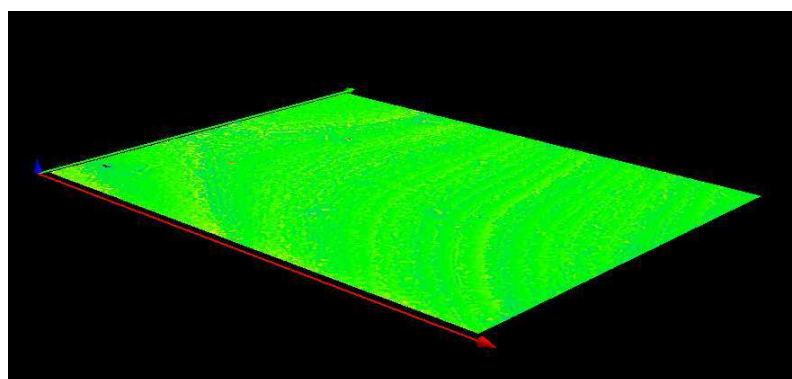


Figure III-49: Topography image of the TEMPO MFC film surface.

III.3.3.3. - Mercury porosimetry

TEMPO oxidized MFC formed more compact films than enzymatic MFC. The apparent density reached 1.25 g/cm^3 . The mercury porosimetry confirmed the lower void fraction in the film with a total porosity of 27% (Figure III-50).

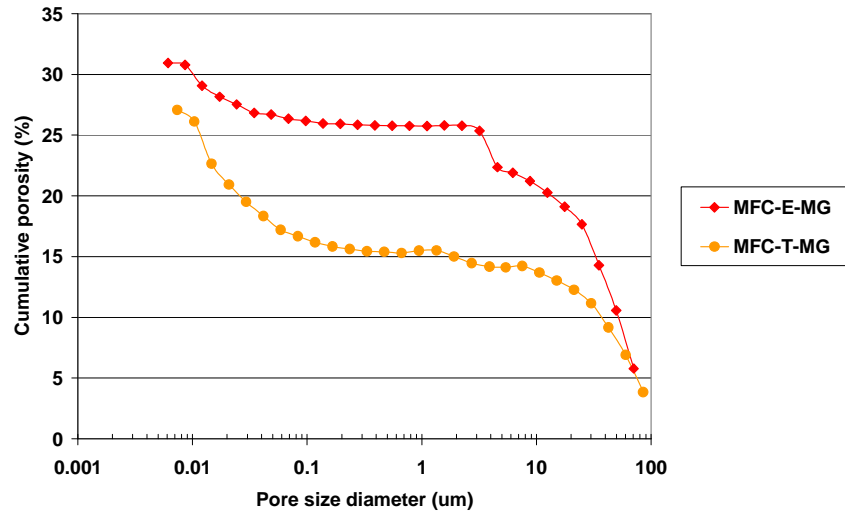


Figure III-50: Mercury porosimetry measurements of MFC films: Cumulative porosity.

Results of size distribution showed that the surface porosity was very low with a pore size of 1.5 μm . This is in agreement with SEM-FEG images from which a very closed surface was observed. The size of internal pores was of the same order of magnitude as for the other films but the percentage was more important in this case. The comparison of pore size distribution between the two kinds of MFC films is visualized in Figure III-51.

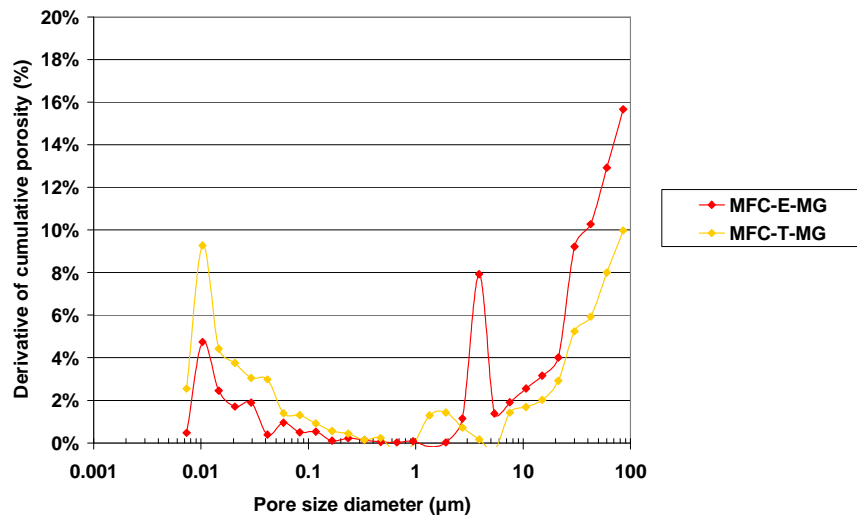


Figure III-51: Mercury porosimetry measurements of MFC films:
Derivative of cumulative porosity.

The density and porosity data are reported in Table III-12 for the TEMPO oxidized MFC and enzymatic MFC films. For the TEMPO oxidized MFC films, a difference was observed between the density determined from the basis weight and the thickness and the one measured by mercury porosimetry. It is worth noticing that the porosity values were calculated after deduction of interstrip points. This calculation method only gives an approximate value. However, the comparison between samples was quite possible and the pore size was accurate.

	Enzymatic pretreatment	TEMPO pretreatment
Bulk density (ISO)	1.04	1.25
Bulk density	1.02	1.13
Skeletal density	1.48	1.55
Total porosity (%)	31	27
Surface porosity (%)	25	15
Surface pore size (μm)	3.5	1.6
Internal porosity (%)	6	12
Internal pore size (μm)	0.021/0.010	0.041/0.010

Table III-12: Density and porosity for MFC films according to the pretreatment.

Fukuzumi *et al.* [98] determined a very low porosity for TEMPO MFC films by positron annihilation lifetime spectroscopy. Indeed, a constant pore size of 0.47 nm was revealed from the film surface to the interior. This value was extremely low compared to values obtained by mercury porosimetry. But, the pore size of 10 nm corresponds to the detection limit of the measurements. It was thus impossible to check the presence of smaller pore in the film. However, the pore size detected was in agreement with MEB-FEG and topography visualisation.

III.3.3.4. - Properties of TEMPO oxidized MFC films

Film properties were determined and the results were compared for both kinds of microfibrillated cellulose in Table III-13.

	Enzymatic pretreatment	TEMPO pretreatment
Density (g/cm^3)	1.02	1.2
Transmittance	91.3 (± 0.4)	91.2 (± 0.3)
Haze	90.0 (± 0.7)	34.9 (± 1.7)
Clarity	7.1 (± 0.4)	73.1 (± 5.7)
Young's modulus (Gpa)	5.3 (± 0.9)	8.6 (± 1.2)
Tensile strength (MPa)	323 (± 72)	384 (± 90)
Elongation at break (%)	1.5 (± 0.3)	0.4 (± 0.06)
Cobb index 60s (g/m^2)	33 (± 1.0)	157 (± 2)
WVTR 23°C-50% RH ($\text{g}/\text{m}^2\cdot\text{day}$)	107 (± 4.0)	144 (± 4)
Water vapour permeability 23°C-50% RH ($\text{g}\cdot\mu\text{m}/\text{m}^2\cdot\text{day}$)	3400	3744
OTR 23°C-0% RH ($\text{cm}^3/\text{m}^2\cdot\text{day}$)	1.4 (± 0.3)	1.3 (± 0.3)
Oxygen permeability 23°C-0% RH ($\text{cm}^3\cdot\mu\text{m}/\text{m}^2\cdot\text{day}$)	44	36

Table III-13: Comparison of enzymatic and TEMPO MFC film properties. Standard deviation is indicated in brackets.

Firstly, TEMPO MFC formed a denser film with a density of 1.2 (g/cm^3). TEMPO MFC suspensions had thinner elements favouring a more compact arrangement of the fibrils in the film.

The mechanical properties of TEMPO MFC were improved with a Young's modulus value of 8.6 GPa compared to enzymatic MFC films. This result was in agreement with the literature. Indeed, Fukuzumi *et al.* [71] reported a Young's modulus value of 6.9 (± 1.4) GPa for a 20 μm -thick film made from TEMPO-oxidized softwood cellulose. However, TEMPO MFC films were less flexible with an elongation at break three times lower compared to enzymatic MFC films. Concerning the water absorption capacity determined by Cobb measurement, TEMPO MFC films had lower properties with a value almost five times higher than for enzymatic MFC films. The carboxyl groups give a higher surface charge to fibrils which increased the hydrophilic character of the films. This is one of the drawbacks of the use of TEMPO MFC in the film productions.

The hydrophilic character was confirmed by the film water sorption results Figure III-52. The sorption and desorption curves exactly showed the same trends for both curves. However, the percentage of absorbed water is higher for a given relative humidity level than for TEMPO MFC films.

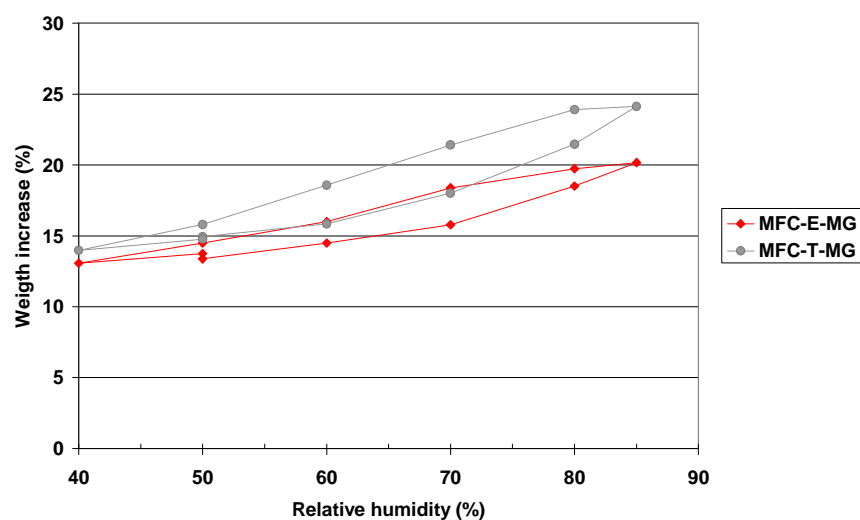


Figure III-52: Sorption measurement for MFC films according to the pretreatment.

This higher hydrophilicity was probably the reason for the higher water vapour transmission rate observed for TEMPO MFC films. Indeed, the high density of TEMPO MFC films might improve the barrier properties and decrease the permeability. This was the case for the oxygen transmission rate measurement in dry conditions where the value was lower than the one observed for the enzymatic MFC films. A comparison with results obtained in literature is observed in Table III-14. Rodionova *et al.* [73] showed the influence of carboxyl content on the oxygen permeability. An important difference was observed with values decreasing from 1293 to 4 $\text{cm}^3 \cdot \mu\text{m}/(\text{m}^2 \cdot \text{day} \cdot \text{bar})$ for a carboxyl content of 0.3 and 1 mmol/g, respectively. TEMPO MFC films obtained in this study had a higher oxygen permeability. However, in our study the measurements were carried out for self-standing MFC films and not for MFC films casted on PET film as in this earlier study.

References	Carboxyl content (mmol/g)	Thickness (μm)	Oxygen permeability 23°C-0% RH ($\text{cm}^3 \cdot \mu\text{m}/\text{m}^2 \cdot \text{day} \cdot \text{bar}$)
Present work	1.1	26	36
[98]	1.4	1 (casted on PET)	0.08
[73]	0.3-1	5 (casted on 50 μm PET)	1293 - 4
[72]	1.7	1 (casted on PET)	0.17

Table III-14: Comparison of oxygen permeability value (23°C-0% RH) with literature values.

III.3.3.5. - Conclusion

This part of the study demonstrated the influence of pulp pretreatment on the final film properties. The use of TEMPO-oxidized MFC showed many advantages such as: the decrease of the number of passes through the homogenizer, reducing energy costs, the production of homogeneous suspensions, the preparation of more compact films and the production of highly transparent films. But some drawbacks were also observed such as: the use of chemicals for the production, lower tensile properties and a highly hydrophilic character.

III.3.4. - Conclusion

Two methods were firstly selected to develop MFC films: casting/evaporation and handsheet method. The handsheet method seemed to be more appropriate for the development of films on a large scale. However, the influence of drying on the network formation should be studied more in detail. The properties of MFC films, obtained here, showed a high Young's modulus value but the tear index must be improved for the use of this kind of film for packaging applications. Concerning the barrier properties, the WVTR was not sufficient and a solution should be proposed to improve these values. The oxygen permeability of films in dry conditions was promising compared to those of common packaging materials described in the literature (Figure III-53).

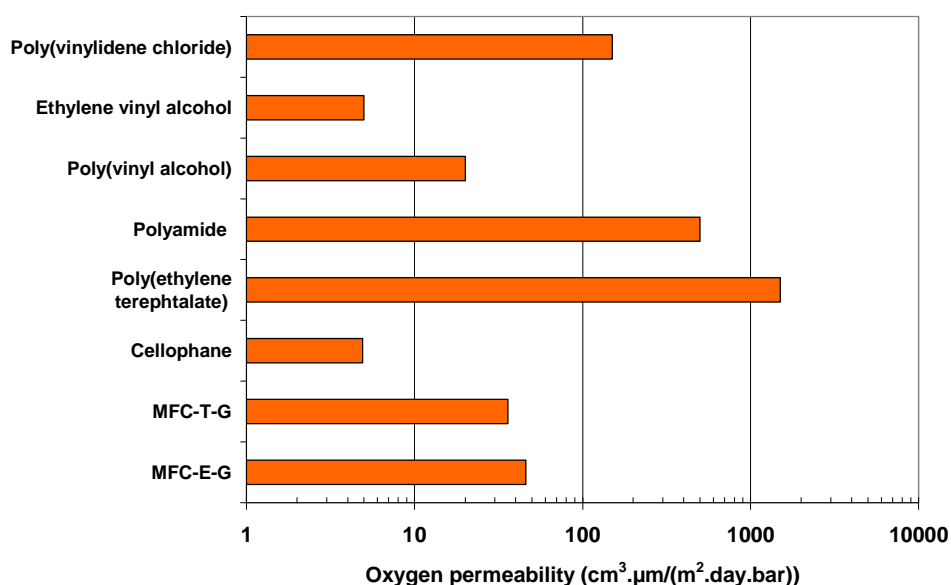


Figure III-53: Oxygen permeability in dry condition of several packaging materials.

For example, the value for MFC films was of the same order of magnitude as for a PVOH film, described as an excellent barrier film. The influence of the pretreatment on film properties was clearly defined that's why it is important to define a common nomenclature for these materials and to differentiate the MFC according to the process used.

To conclude, the development of MFC films was successful in this study. In the future, work must focus on the improvement of water sensitivity and the increase of the MFC packing should be interesting to study.

III.4. - Addition of sorbitol in MFC films

The results presented in this part are only preliminary results and a deeper investigation should be implemented.

Sorbitol is a polyol found in several fruits like apple or synthesised by hydrogenation of glucose. It is currently used in association with starch playing a plasticizer role. In our study, it was added to MFC to improve its film forming properties. Two effects were reported, firstly an improvement of the flexibility of MFC films and secondly an improvement of their barrier properties.

The porosity of MFC remained a drawback for their barrier properties and most particularly for the water vapour transmission rates. The introduction of additives could fill the voids and decrease the permeability like observed in Table III-15. Indeed, the WVTR at 23°C-50% RH was decreased from 107 to 34 g/m².day. The OTR 23°C-0% RH showed similar values with and without sorbitol.

	MFC films	MFC + 20 pph sorbitol films
WVTR 23°C-50% RH (g/m ² .day)	107 (4)	34 (3)
OTR 23°C-0% RH (cm ³ /m ² .day)	1.4 (0.3)	1.3 (0.3)
Cobb index 60s (g/m ²)	33 (4)	62 (12)
Swelling (%)	47	110

Table III-15: Properties of MFC films in presence or not of sorbitol.

However, the presence of sorbitol in the film increased the water sensitivity. Indeed the Cobb index 60s of MFC/sorbitol films, measuring the water adsorption of films, was twice as high as MFC films without sorbitol. This could be explained by both the hydrophilic nature of the polyol and the limitation of interfibrillar bonds.

These results showed that solution could be found to improve the water vapour permeability of MFC films. Indeed, the addition of sorbitol allowed to reduce the WVTR values but increase the water sensitivity of films. Others strategies to improve the MFC film properties, could be envisage such as the use of modified MFC, the addition of cross linkers or the grafting by chromatogeny of the film surface.

III.5. - Conclusion

Several kinds of microfibrillated cellulose (MFC) suspensions were firstly characterised in this chapter. Their properties were compared according to the treatment used and to the production scale.

MFC produced by the disintegration of cellulose corresponds to very thin elements with a diameter of 10-30 nm and a length of 1-3 μm . The MFC morphology and their aspect ratio depend on the process used; the fibril length was for example shorter after the TEMPO-mediated oxidation pretreatment. MFC suspensions have a gel-like behaviour for low solid content (2%). Indeed, the high aspect ratio coupled with high specific surface area of MFC leads to strong interactions and entanglements. Moreover, it is worth noticing that the drying of MFC led to irreversible aggregation, impossible to redisperse. This material has thus two major drawbacks for their use on a large scale: their low solid content and their viscosity.

Subsequently, the development of films was carried out using two methods. The fast Handsheet method produced flatter and more homogeneous films compared to the casting/evaporation technique. However, the drying step seems to have an impact on the network formation and thus on films properties. Except for the Young's modulus, the mechanical and barrier properties of cast films were higher than that of handsheet films. The handsheet method using the sheet former is a more industrially viable method to produce films on a large scale. However, the effect of drying must be largely studied to control the hornification phenomenon.

The use of TEMPO pretreatment allowed to reduce the number of passes in the homogenizer. However, the surface modification with the presence of carboxyl groups leads to more hydrophilic properties.

The last part of this chapter concerned the use of sorbitol to improve the MFC films properties. Strong reduction of WVTR at 23°C-50% RH was observed although the water sensitivity remained high.

IV - Development of MFC based nanocomposites

IV.1. - Introduction

A composite material results from the combination of two or more materials. Most composites consist of two main constituents: a continuous matrix material and a dispersed reinforcing phase or filler. The filler mainly consists of fibres from various origins such as glass, carbon, or natural fibres (flax, hemp...). More recently, the introduction of nanoparticles in a matrix has attracted the interest of many researchers. Indeed, these materials offer unique mechanical, electrical, optical and thermal properties with low loading requirements [161].

In chapter 3, the advantages of microfibrillated cellulose (MFC) materials but also their drawbacks have been outlined. The low concentration and the high viscosity of MFC aqueous suspensions should be considered for the processing of composites. Indeed, strong inter-particle interactions occurring during drying limit the possibility to work with dry powder. As a consequence a hydrophilic and water-soluble matrix was used in order to process the composite films from a water medium. It allowed to keep the good dispersion level of MFC in aqueous medium. Starch and PVOH were thus selected, starch for its natural origin and the PVOH for its good barrier properties. The introduction of MFC in such matrices has already showed some reinforcement potential in the literature [53, 124, 125, 133,]. However, its influence on barrier properties was not studied in detail.

The present chapter aims at investigating the combination of MFC with either starch or PVOH matrices in order to obtain improved materials suitable for packaging. In order to determine the best conditions for the manufacture of composites, a preliminary study was conducted. The mechanical and barrier properties of starch/MFC composites were then discussed as well as the influence of the addition of sorbitol. A similar approach was conducted for PVOH/MFC composites. A comparison between both composite systems was carried out in the last part.

IV.2. - Manufacture protocol of MFC composites

In this chapter, the influence of MFC addition on matrix properties was only studied for one MFC source. This MFC source corresponded to an enzymatic pretreated pulp homogenized in a Masuko grinder (MFC-E-MG) (Figure IV-1).



Figure IV-1: Photos of MFC-E-MG suspension at 2 wt%.

Few solutions could be envisaged for the production of composite films. The casting/evaporation technique was thus used for the development of MFC films. A study was firstly conducted to determine the proper casting/evaporation conditions for the development of matrix/MFC composite films.

Casting/evaporation being a slow process, the mixture have to be stable over time to develop final homogeneous composites. The density of starch was considered equivalent to the one of amylopectin, i.e. 1.26 g/cm³ [96] because waxy maize starch consists of 98 wt% amylopectin. The density of poly(vinyl alcohol) is 1.24 g/cm³ [162]. The density and viscosity of starch or PVOH solutions at low concentration between 1 and 5 wt% at room temperature are reported in Table IV-1.

Solution concentration	Starch		PVOH	
	Density (g/cm ³)	Viscosity (mPa.s)	Density (g/cm ³)	Viscosity (mPa.s)
1 wt%	1.001		1.003	
3 wt%	1.006	< 10	1.005	< 10
5 wt%	1.024		1.021	

Table IV-1: Density and viscosity of starch and PVOH solutions at room temperature.

The density of cellulose is considered to be 1.5 g/cm³. The Stokes law is generally used to determine the sedimentation rate of spherical particles. The formula (1) defines the sedimentation rate v (m/s) according to the particle size and the fluid viscosity:

$$v = \frac{2r^2 g \Delta(\rho)}{9\eta} \quad (\text{Eq. 16})$$

where r is the radius of the sphere, $\Delta(\rho)$ is the difference in density, η is the viscosity of the solution.

In this case, the formula is not valid because MFC is made of particles that are not spherical; they have high aspect ratio and interact with the water by swelling. The real diameter of MFC as well as its real density in suspension are unknown due to their flexibility and swelling in water medium. In order to determine the sedimentation rate, visual examination was thus

carried out according to the concentration of the mixture and stirring time. The mixture concentration is directly linked to the viscosity of the suspension. The influence of stirring time could increase the filler/matrix interactions and limit the sedimentation. Three concentrations were selected, namely 1%, 3% and 5% which corresponded to the limit of the good spreading of the suspension. The stirring times ranged between 1 hour and 24 hours. After mixing, the PVOH/MFC suspensions were poured into test tubes and the sedimentation was observed every hours.

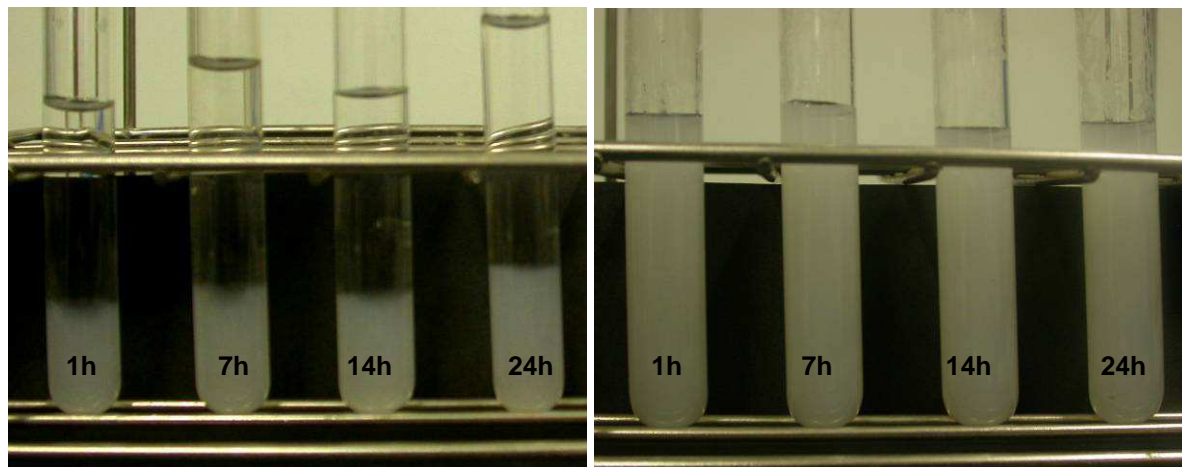


Figure IV-2: PVOH/MFC (90/10) suspension at 1 wt% (left) and at 5 wt% (right) after different stirring times and 1h of rest.

Figure IV-2 (left) shows photos of tubes filled with PVOH/MFC (90/10) with a total concentration of 1%. The observation showed that whatever the stirring time ranging between 1h and 24h, particle settling always took place and this phenomenon appeared just after stopping the stirring. After 1 h of rest, the sedimentation phenomenon was clearly observed.

Conversely, no phase separation was observed for the suspensions concentrated at 5% regardless the stirring time (Figure IV-2 (right)). These experiments showed that the stirring time has a weak influence on the sedimentation rate compared to the concentration (related to the medium viscosity). For the intermediate concentration (3%), the sedimentation phenomenon also appeared although the sedimentation rate was slower than for suspensions at 1%. This means that a concentration gradient was formed in composite when using low concentration suspensions. Figure IV-3 compares the sedimentation level of PVOH/MFC (90/10) suspensions after 24h of stirring and 24h of rest. Thus for this PVOH/MFC ratio, it is necessary to use a total concentration of 5% to form a homogeneous composite by casting/evaporation.

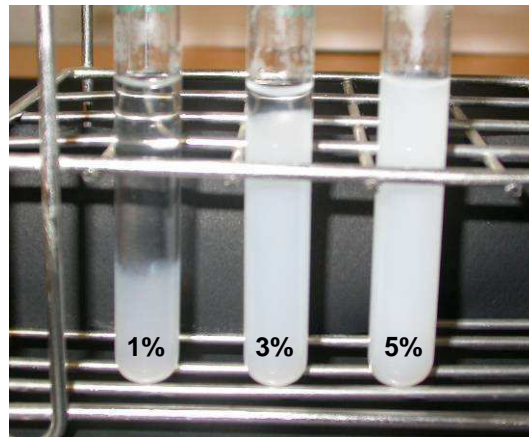


Figure IV-3: PVOH/MFC suspensions at 1 wt%, 3 wt% & 5 wt% after 24h stirring and 24h of rest.

This test was also carried out with starch/MFC suspensions for the concentration of 5 wt% (Figure IV-4). Whatever the stirring time, no sedimentation was observed for the starch/MFC mixture. The same behaviour was observed for PVOH and starch solutions because the density and viscosity of these solutions were very similar.

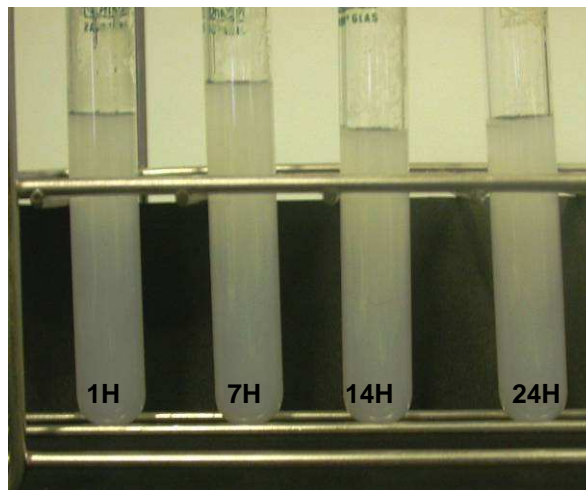


Figure IV-4: Starch/MFC (90/10) suspension at 5 wt% after different stirring times and 1h of rest.

According to these results, the casting/evaporation procedure was defined as described in Figure IV-5:

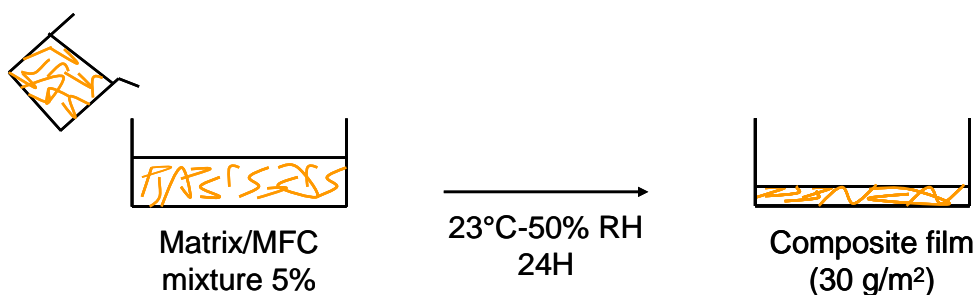


Figure IV-5: Method for composite production.

The concentration of 5 wt% was used for MFC contents lower than 30 wt%. Indeed the concentration was adapted for higher MFC contents in order to obtain good spreading of the suspension in the mould and thus films with homogeneous thickness.

IV.3. - Influence of MFC addition on the starch matrix properties

IV.3.1. - Introduction

Starch is a widely available polymer source, extracted from renewable materials and largely studied as a potential substitute of petroleum plastics. Additive-free starch films (without plasticizers) are very brittle and difficult to handle. However, the introduction of plasticizers has a negative effect on the barrier properties of starch films [120]. The processing of composites based on starch was extensively studied these last years. The introduction of fillers such as nanoclays is a possible solution to confer barrier properties to starch films. The compatibility between starch and nanoclays is not always optimal and the use of additives (cationic starch for example) is required to obtain good exfoliation of nanoclays in starch. MFC displays a good compatibility with starch thanks to the hydrophilic character of both materials. These interactions should thus lead to the improvement of starch properties.

The starch chosen in this study was a modified starch with hydrophobic groups, developed by Cargill to reduce its water sensitivity. Moreover, the solution obtained from this starch had a low viscosity.

First, MFC was added in unplasticized starch and its influence was studied for ratios ranging from 0% to 100%. The structure of composites was analysed by microscopic observation. The mechanical properties as well as the barrier properties were evaluated according to the MFC content. The effect of the addition of sorbitol in the starch/MFC composites was investigated in a second step.

IV.3.2. - Structure of starch/MFC composites

The structure of the composite determines the end properties of the material. The homogeneity of the filler distribution and dispersion in the matrix is an essential criterion to produce composites with optimized properties. A schematic representation of the degree of dispersion and distribution of particles in a polymer matrix is given in Figure IV-6.

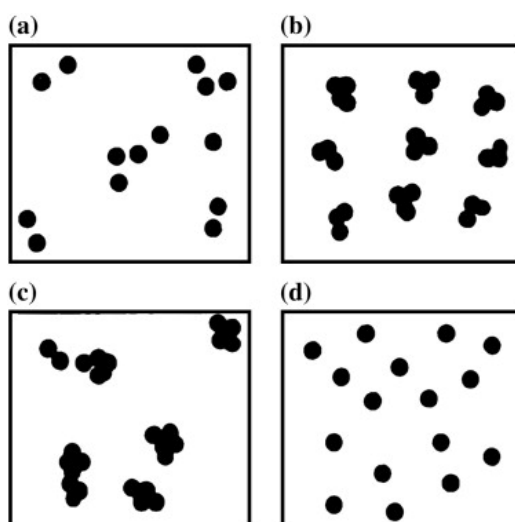


Figure IV-6: Concept of dispersion and distribution of particles in composites: (a) good dispersion poor distribution, (b) poor dispersion good distribution, (c) poor dispersion and distribution, (d) good dispersion and distribution [163].

Moreover, the improvement of mechanical and barrier properties could result from several phenomena:

- An increase of the starch crystallinity. Indeed, MFC filler could act as nucleating agent for the polymeric matrix and favour the crystallisation of starch films.
- Strong interactions between MFC and the starch matrix.

IV.3.2.1. - Visual aspect

The influence of MFC addition on the visual aspect of starch films was firstly investigated. Figure IV-7 shows photos of unplasticized starch films filled with three different MFC contents (10 wt%, 30 wt% and 50 wt%). Starch films were very brittle, very difficult to handle and to characterize. The introduction of MFC clearly improved the film quality and most particularly their handiness. Films containing MFC seemed more ductile than unfilled starch films. However, the transparency slightly decreased with the presence of MFC in starch films. The values of transparency measurement are detailed in Table IV-2. The transmittance values were similar whatever the MFC content in starch matrix. However, the Haze value increased strongly with the MFC introduction explaining the decrease of film transparency. Moreover, the haze increased with the increase of MFC content.

MFC content (%)	Transmittance	Haze	Clarity
0	91.7 (± 2.3)	1.7 (± 0.5)	85.3 (± 0.3)
5	92.5 (± 0.2)	62.2 (± 2.8)	9.9 (± 1.6)
10	92.5 (± 0.2)	71.3 (± 2.8)	9.9 (± 0.6)
30	93.1 (± 0.2)	77.2 (± 2.0)	9.7 (± 0.5)
50	93.1 (± 0.2)	83.2 (± 1.5)	9.2 (± 0.6)
75	92.8 (± 0.3)	75.9 (± 2.5)	9.4 (± 0.4)

Table IV-2: Transparency measurements of MFC films according to the MFC content in starch matrix.

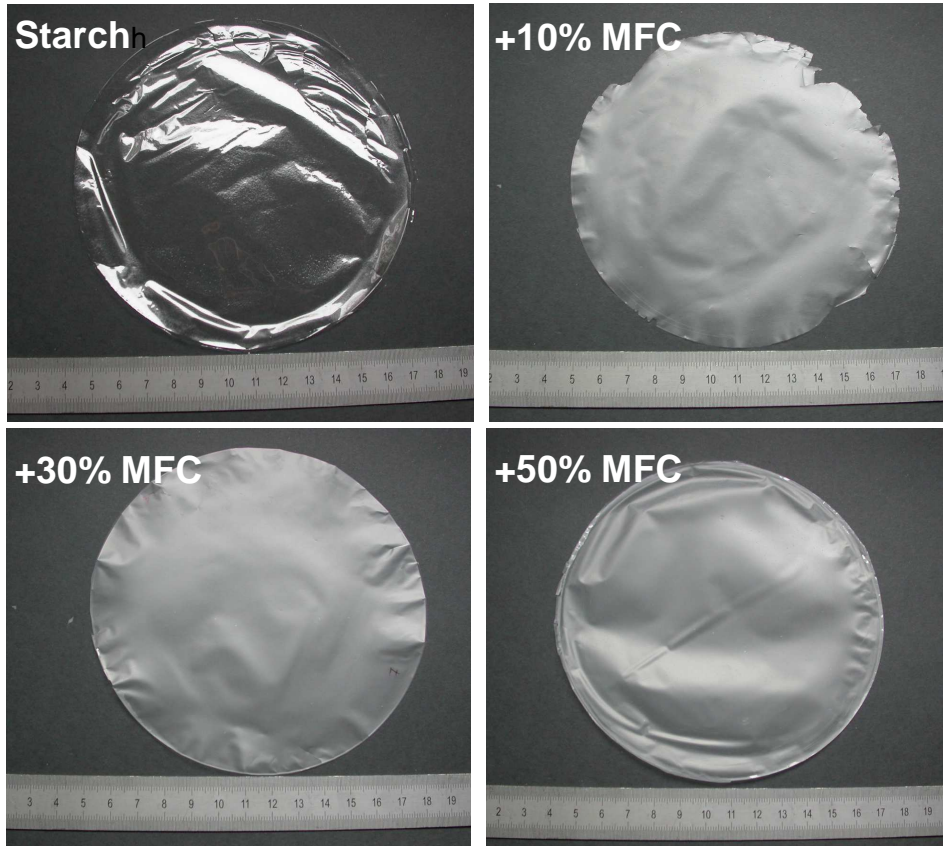


Figure IV-7: Pictures of starch/MFC films for several MFC contents.

IV.3.2.2. - Thickness and density of films

The thickness and apparent density (ρ_e) of films were determined for the films conditioned at 23°C-50% RH. These values were compared with theoretical densities (ρ_t) calculated from a rule of mixture involving starch and cellulose densities, i.e. 1.26 and 1.5 g/cm³, respectively. The void content (V) in percent was thus determined from these values using the formula:

$$V = \frac{\rho_t - \rho_e}{\rho_t} * 100 \text{ (Eq. 17)}$$

The results obtained with films conditioned at 23°C-50% RH are summarized in Table IV-3.

MFC content (wt %)	Film thickness (μm)	Experimental density (g/cm ³)	Theoretical density (g/cm ³)	Void content (%)
0	28.4 (± 3.4)	1.18 (± 0.12)	1.26	6
5	23.4 (± 1.1)	1.23 (± 0.05)	1.27	3.3
10	28.2 (± 2.1)	1.14 (± 0.07)	1.28	11.2
30	27.7 (± 2.6)	1.21 (± 0.07)	1.33	9.5
50	31.6 (± 1.9)	1.12 (± 0.07)	1.38	18.8
75	28.4 (± 3.2)	1.12 (± 0.14)	1.44	22.2
100	31.8 (± 2.5)	1.04 (± 0.09)	1.5	30.7

Table IV-3: Film thickness, theoretical and experimental density and void content of composite films according to the MFC content.

These results showed that the void content continually increased according to the MFC content.

IV.3.2.3. - Polarized light microscopy

Starch and cellulose have similar chemical compositions which restricted the composite characterization. Polarized light microscopy is a method used to check the homogeneity of composites and observe the presence of MFC within the starch matrix. Indeed, highly crystalline and birefringent cellulose nanocrystals can rotate light and thus appear bright when observed between crossed polarizers [135]. The crystalline part of MFC should thus be visible under polarized light.

Unfilled starch film was firstly analysed in transmission by light polarized microscopy. No bright points were observed at the film surface (Figure IV-8). This suggested that the starch film was amorphous or poorly crystallized.

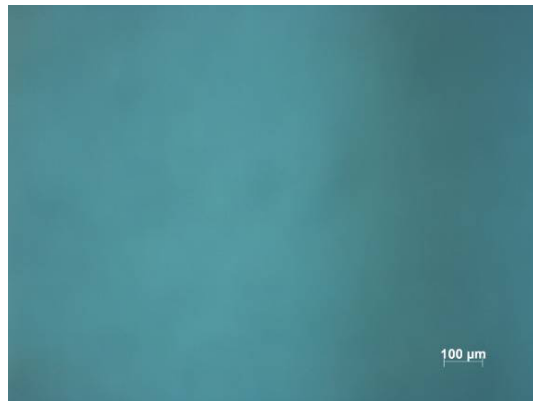


Figure IV-8: Polarized light microscopy image of a starch film.

Composite films with 5 wt% and 10 wt% MFC were secondly analysed and presented in Figure IV-9. This time, bright points appeared and were found to be homogeneously dispersed over the surface.

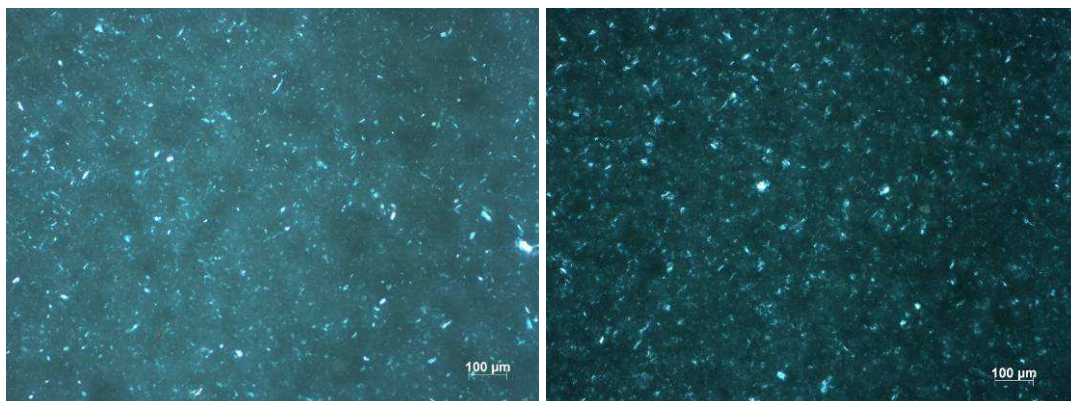


Figure IV-9: Polarized light microscopy images of starch/MFC films with a ratio of 95/5 (left), 90/10(right).

This proved the good distribution level of MFC in starch films. However, the size of these points was quite high (around 10 μm) and revealed that MFC was not totally individualized in the matrix but under the form of small aggregates. Therefore, the distribution of MFC in

starch was good but the dispersion seemed low. This corresponded to the case b in Figure IV-6.

Therefore, the polarized light microscopy revealed the crystalline part of MFC and gave a good visualization of the composite homogeneity. No similar results were reported in literature with MFC. However, this technique was also used by Vigneshwaran *et al.* [164] to determine the efficiency of Gum arabic for cellulose nanocrystal distribution in starch film. The distribution of whiskers firstly was very poor like observed in Figure IV-10a. The Gum arabic addition improved the whisker distribution and optical photos were similar to those obtained in this work in Figure IV-10b.

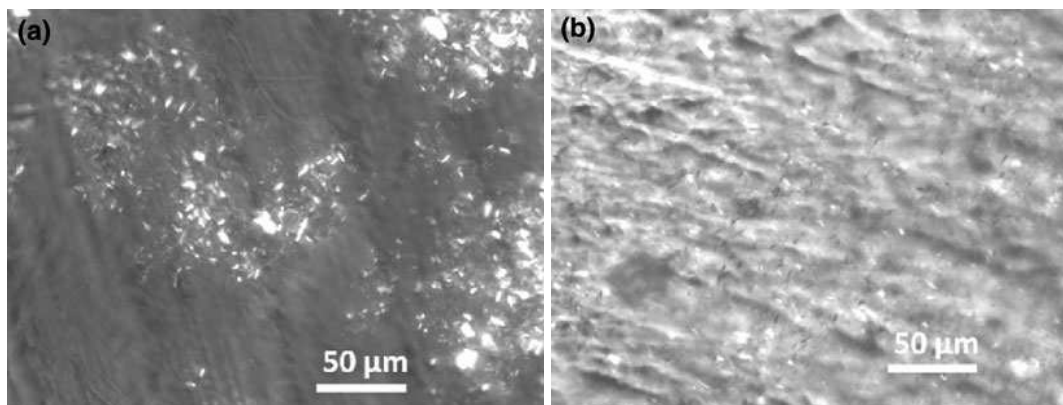


Figure IV-10: Polarized optical micrographs of starch nanocellulose film (a) and starch nanocellulose (dispersed by Gum arabic) films (b) [164].

Thus, the distribution of MFC was good in the nanocomposites but the dispersion could probably be improved by the use of additives.

IV.3.2.4. - SEM-FEG

The MFC distribution seemed homogeneous according to polarized light images. Subsequently, SEM-FEG observation was carried out to study the structure and the homogeneity in the cross section of starch/MFC composite films. The cross section of starch films was compared with the one of starch/MFC composites (Figure IV-11). Starch films were very smooth compared to the structured section of starch/MFC films. No phase separation was observed and this proved the good general settling of MFC in the matrix.

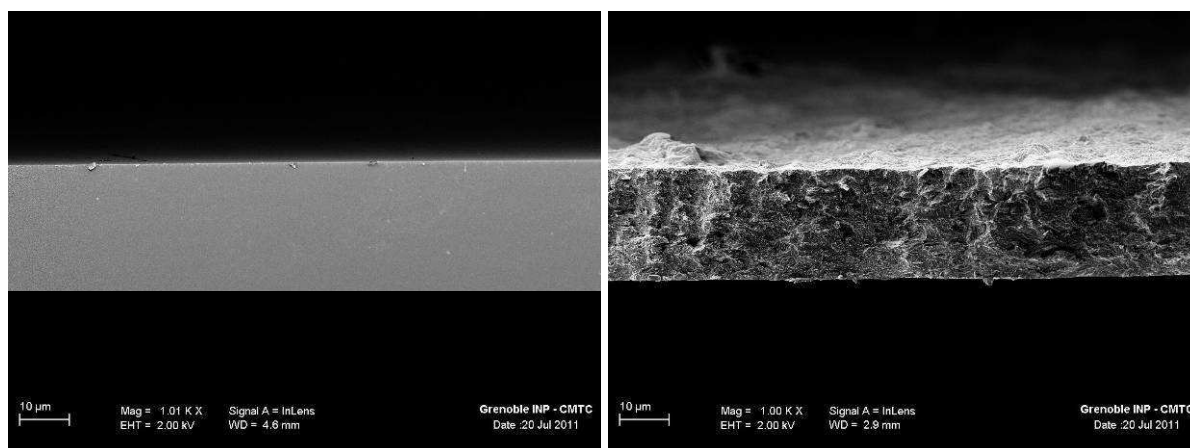


Figure IV-11: SEM-FEG of cross-section of starch (left) and starch/MFC (70/30) (right) films.

A lamellar organisation was observed in Figure IV-12. As Svagan *et al.* [96], the fractured surface showed a fibrous lamellar structure. The large presence of voids inside the composite also appeared in this micrograph. This is in agreement with the density value showing a void percentage of 10% for the starch/MFC (70/30) composites.

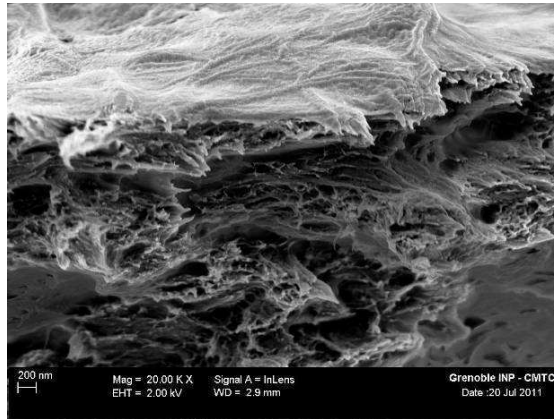


Figure IV-12: SEM-FEG images of starch/MFC (70/30) film at higher magnification.

The film surface images also were very different depending on the presence or the absence of MFC (Figure IV-13). The surface observed corresponded to the top surface that is to say the opposite side to the side in contact with the mould. The fibril network was clearly observed on the film surface with a random orientation of fibrils. The presence of MFC at the surface increased the roughness of starch films and this explained the decrease of their transparency after MFC addition observed visually on composite films. The surface seemed to be quite close which is a positive aspect for the development of barrier properties. However, some larger elements were visible at the surface; these aggregates could affect the mechanical properties of composites.

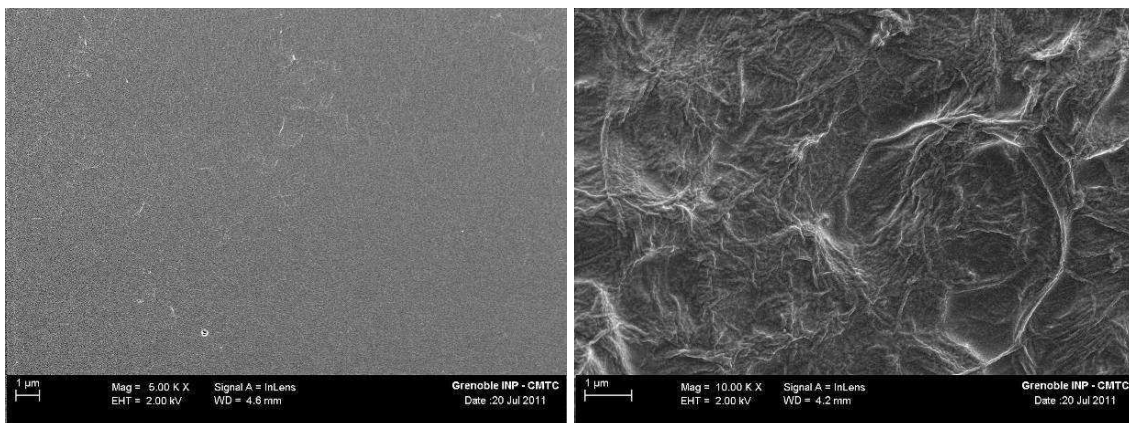


Figure IV-13: SEM-FEG images of the top surface of unfilled starch (left) and starch/MFC (70/30) (right) films.

The microscopic observations demonstrated the satisfactory distribution of MFC within the starch film. This homogeneous morphology is a key factor for reinforcing conditions.

IV.3.3. - Mechanical properties of starch/MFC composites

The influence of MFC on the mechanical properties of the starch matrix was studied by tensile tests. Figure IV-14 shows the evolution of the Young's modulus value according to the

MFC content. The reinforcement effect was clearly observed with an increase of the Young's modulus as a function of the MFC content. It increased from 1284 to 2137 MPa with the addition of 10 wt% MFC and to 3874 MPa with 30 wt%. From 50 wt% of MFC, the Young's modulus value levels off and starch/MFC composites display the same stiffness as pure MFC film.

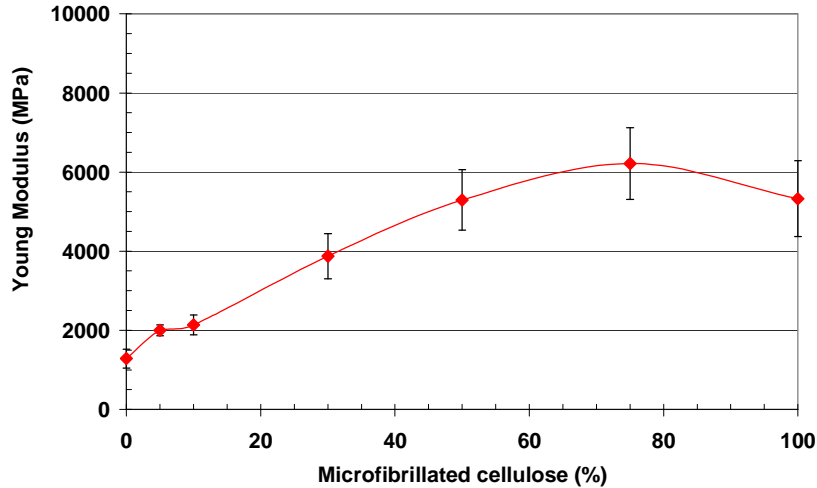


Figure IV-14: Young's modulus of starch/MFC films.

Figure IV-15 shows the evolution of the tensile strength value according to the MFC content and the same trend was observed confirming once again the reinforcing capability of MFC for the starch matrix.

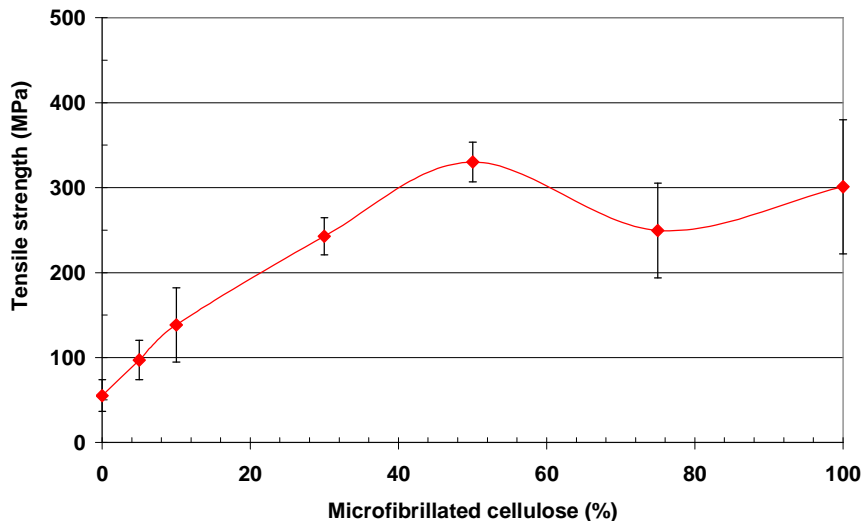


Figure IV-15: Tensile strength of starch/MFC films.

An improvement of the elongation at break was also observed as shown in Figure IV-16. The value increased for the low MFC contents (5 wt% and 10 wt%) and reached a maximum value of 1.2%. However, the elongation at break remained very low for these materials that were very brittle.

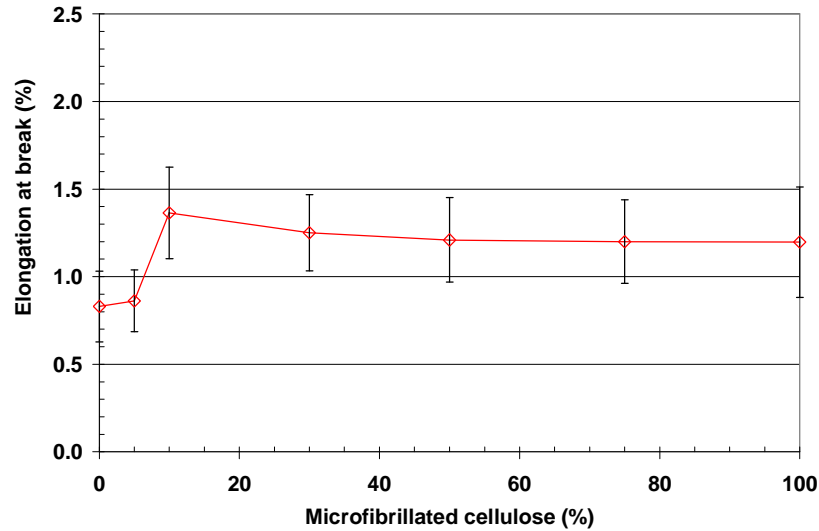


Figure IV-16: Elongation at break of starch/MFC films.

Therefore, the addition of MFC improved the rigidity of starch films as well as its ductility. As observed previously from microscopic investigation, MFC was well distributed within the matrix and the composites were thus homogeneous. This favoured the observation of good mechanical properties. Moreover, the reinforcement effect should be partly due to the formation of a MFC network and to favourable interactions between MFC and matrix favouring the matrix/filler stress transfer through the interface. This explained the highest Young's modulus value for the starch/MFC (25/75) film compared to the MFC film. Other studies in literature [96,127] also reported the effect of the addition of MFC produced by enzymatic pretreatment followed by mechanical shearing in amylopectin films. Similar reinforcing effect was observed with a strong improvement of the Young's modulus with the MFC content (Figure IV-17). Compared to literature values, the Young's modulus values obtained in the present study are lower but the strength values are higher.

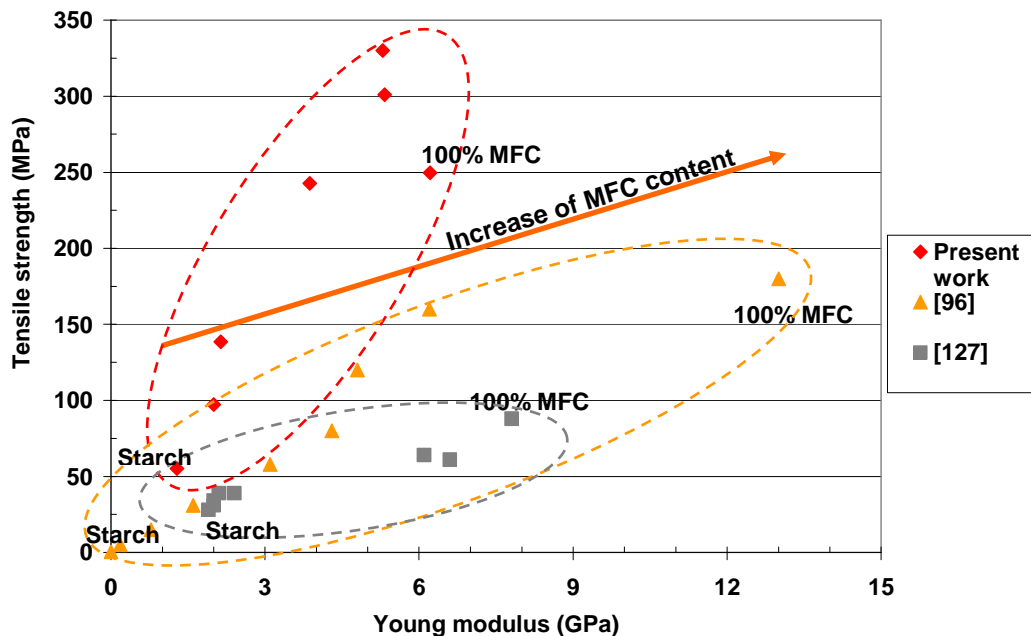


Figure IV-17: Comparison of the mechanical properties of starch/MFC films with literature values.

Mechanical properties of MFC composites were analysed according to the MFC content. An improvement of mechanical properties was observed for the Young's modulus as well as the tensile strength values. This reinforcement effect of MFC was also reported in literature but the final values depend on the initial matrix and on the MFC used.

IV.3.4. - Barrier properties of starch/MFC composites

Starch material generally displays good grease and oxygen barrier properties in the dry state. Indeed, the water sensitive character of starch negatively impacts the barrier properties. Moreover, the presence of plasticizer in starch film improves the ductility but decreases the barrier properties. Indeed, the plasticizer increases the chain mobility reducing the glass transition temperature and increasing the permeability. The problem with starch based membrane is to find the proper balance between good barrier properties and mechanical performances [120]. Here, MFC played two roles:

- A role of plasticizer with the improvement of ductility,
- A role of filler with the increase of tortuosity in order to enhance the barrier properties of starch films.

IV.3.4.1. - Water vapour transmission rate

The water vapour transmission rates of composites (conditioned at 23°C-50% RH) were measured to study the influence of MFC addition on barrier properties. A decrease of water vapour permeability was observed according to the MFC addition as shown in Figure IV-18. The lower value reached 110 g/m².day for a MFC concentration of 50 wt%. This value corresponded also to the value obtained for the MFC film. This showed that the resulting network obtained from 50% in MFC was the same as in pure MFC films.

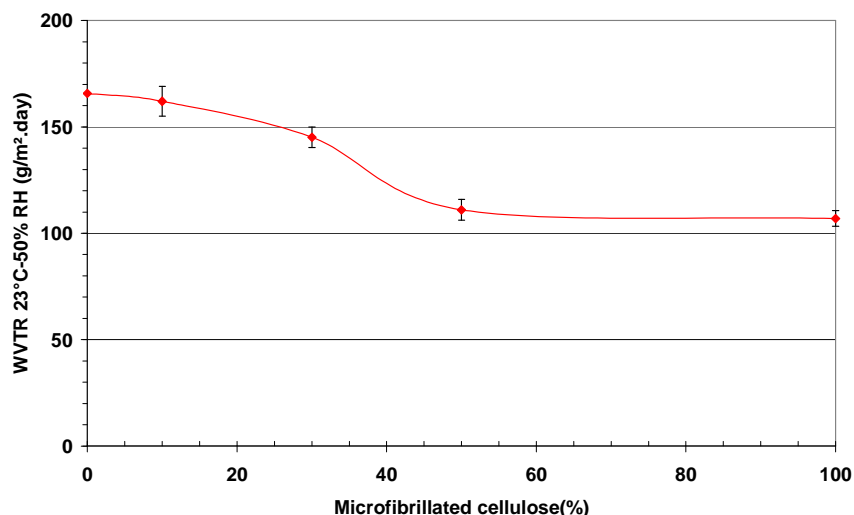


Figure IV-18: WVTR of starch/MFC films at 23°C-50% RH.

Several reasons could explain this improvement of WVTR values. First, MFC with its crystalline domains increased the global crystallinity of the material and then the tortuosity limiting the diffusion phenomenon. The gas molecule diffusivity of MFC film was described by Belbekhouche *et al.* [113]. Figure IV-19 schematically shows the increase of molecule pathway in the MFC network. SEM-FEG images showed the fibril network within the matrix which reduced the molecule diffusion.

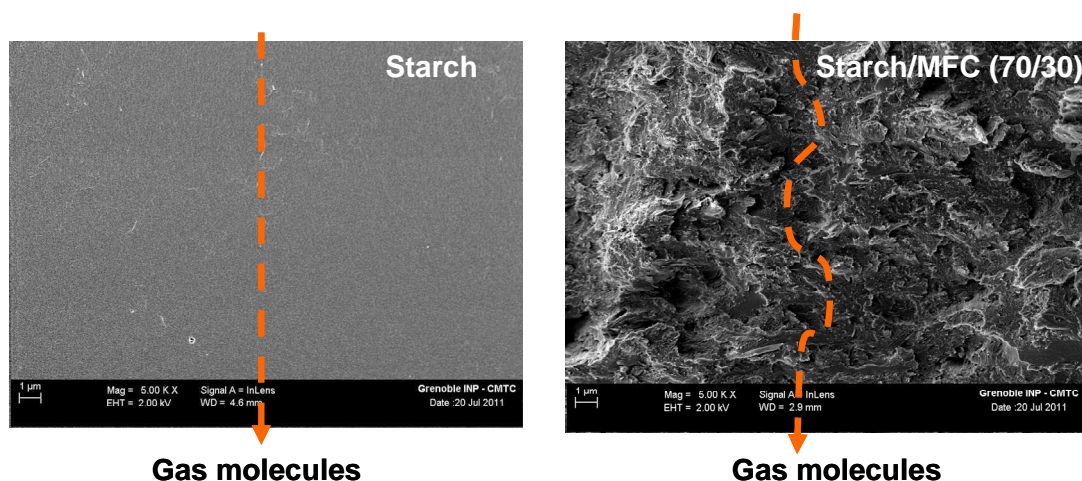


Figure IV-19: Schematic representation of the gas molecule diffusivity in starch and starch/MFC (70/30) films.

Secondly, the improvement in barrier properties could result from the decrease of the water solubility of composite films. The influence of MFC addition on the water solubility was studied by water sorption measurements. The water content of films conditioned at 23°C-50% RH was firstly determined by TGA analysis (Figure IV-20). Starch film had an initial water content of 12% at equilibrium. The introduction of MFC decreased this value to 7% for a MFC content of 50%.

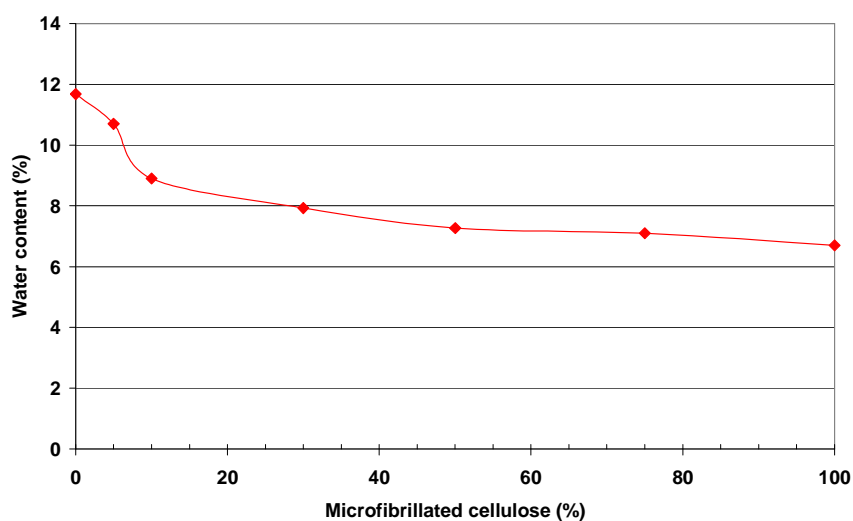


Figure IV-20: Water content in starch/MFC films conditioned at 23°C-50% RH.

Moreover, Figure IV-21 shows the water sorption and desorption of starch/MFC films according to relative humidity for several MFC concentrations (0, 10 and 100 wt%). Once again, the water sorption was linked to the MFC concentration. The sorption of starch decreased with the MFC introduction. Moreover, after desorption the structure found again its initial state.

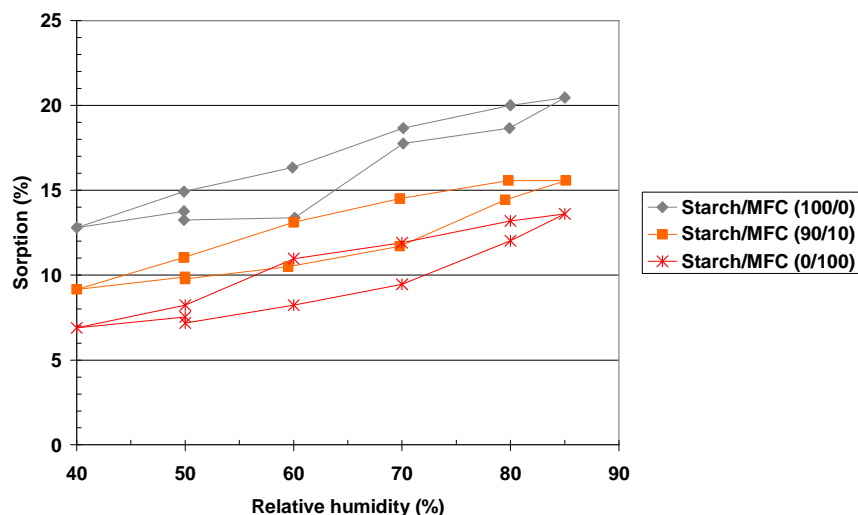


Figure IV-21: Water sorption of starch/MFC films.

These results demonstrated that the presence of MFC decreased the water sorption of starch films. This conclusion was also reported by Svagan *et al.* [126]. One of the reasons is that cellulose nanofibers are less hygroscopic than starch. Indeed, cellulose has a higher degree of molecular order and a higher crystallinity. This reduced water sorption could be also related to strong interactions between MFC and starch matrix decreasing the starch chain mobility and then swelling.

IV.3.4.2. - Oxygen permeability

The oxygen permeability of starch/MFC composites was determined for the films with the 50% MFC content. Indeed, the films with lower MFC content were too brittle for the measurements. The oxygen permeance of starch/MFC (50/50) films was $5 \text{ cm}^3/\text{m}^2 \cdot \text{day} \cdot \text{bar}$ for a $25 \text{ }\mu\text{m}$ thick film corresponding to an oxygen permeability value of $125 \text{ cm}^3 \cdot \mu\text{m}/\text{m}^2 \cdot \text{day} \cdot \text{bar}$ at 23°C -0% RH. Plackett *et al.* [127] obtained better value for the same starch/MFC (50/50) film with an oxygen permeability of $20 \text{ cm}^3 \cdot \mu\text{m}/\text{m}^2 \cdot \text{day} \cdot \text{bar}$ at 23°C -50% RH. The starch/MFC (50/50) value was high compared to the oxygen permeability of PVOH or cellophane, viz. 20 and $41 \text{ cm}^3 \cdot \mu\text{m}/\text{m}^2 \cdot \text{day} \cdot \text{bar}$, respectively, but in the same magnitude range as polyamide [21,107]. All of these results are summarized in Table IV-4.

	Oxygen permeability ($\text{cm}^3 \cdot \mu\text{m}/\text{m}^2 \cdot \text{day} \cdot \text{bar}$)	Conditions
Starch/MFC (50/50)		
Present work	125	23°C -0% RH
[127]	20	23°C -50% RH
PVOH [21]	20	23°C -0% RH
Cellophane [107]	41	23°C -0% RH
Polyamide [21]	100-1000	23°C -0% RH

Table IV-4: Oxygen permeability of Starch/MFC (50/50), PVOH, Cellophane and polyamide films.

IV.3.5. - Influence of MFC addition on the structure of starch film

The characterisation of samples showed an improvement of mechanical and barrier properties. Three analyses were carried out to establish the influence of MFC on the structure of starch films. X ray diffraction (XRD) was firstly used to evaluate the crystallinity of composites and it was completed by DSC measurements. Finally, TGA experiments were carried out to determine the thermal stability of composites.

IV.3.5.1. - X-ray diffraction

XRD analysis was carried out on starch/MFC films (Figure IV-22).

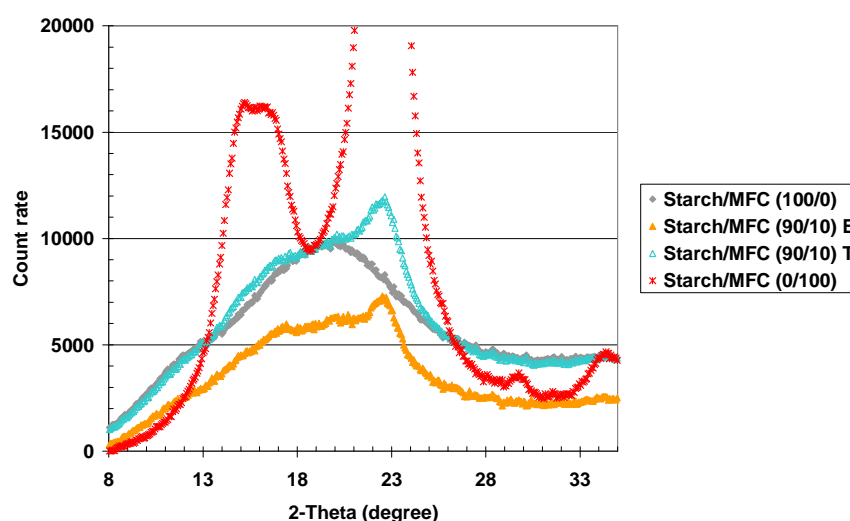


Figure IV-22: XRD analysis of starch/MFC films.

Starch and MFC films were firstly studied. The diffractogram of starch film in grey showed a broad hump and did not show any diffraction peak. This means that starch film is mainly an amorphous material. As observed in the first part on the characterisation of MFC film, microfibrillated cellulose films presented two main peaks around 16° and 23° corresponding to cellulose I β (red curve). The orange curve corresponds to the diffractogram of starch/MFC (90/10) film. These experimental data were compared with the theoretical curve in blue determined by a rule of mixture. No significant difference was observed between the theoretical and experimental curves. The impact of MFC on the crystallinity of starch was thus not revealed by this technique. Svagan *et al.* [96] obtained the same results and reported that no data supported the crystalline order or transcrystallinity order in the matrix.

IV.3.5.2. - DSC measurements

XRD experiments were completed by DSC analysis. The DSC measurements on starch materials are difficult to analyse because the crystallinity of starch is linked to the humidity in the material.

The DSC measurements showed an endothermic peak for each starch/MFC composite samples (Figure IV-23). However, this peak seemed to correspond to the water evaporation and not to a melting endotherm. This result is in agreement with XRD experiments that did not show any diffraction peaks related to starch in films.

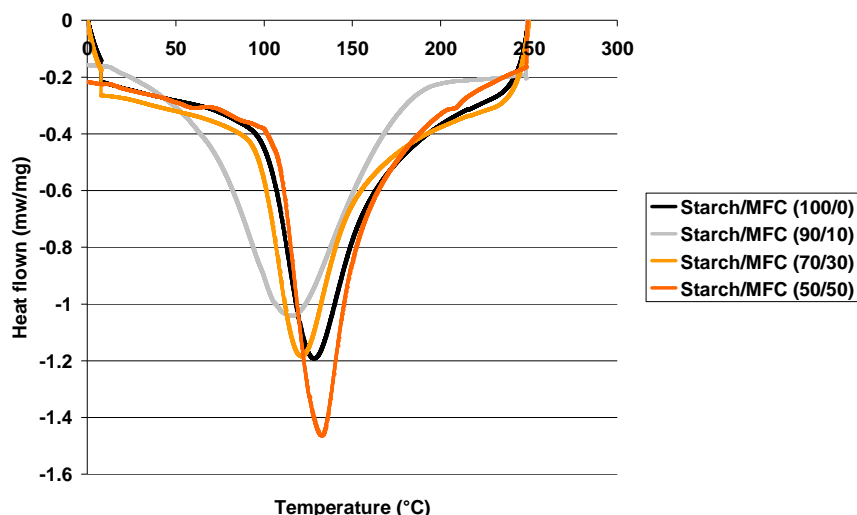


Figure IV-23: DSC analysis of starch/MFC films.

These analyses showed that the starch matrix was amorphous and that the MFC addition had no effect on the crystallisation of the matrix. Therefore, the improvement of mechanical and barrier properties was not due to the increase of crystalline order of starch.

IV.3.5.3. - TGA experiments

TGA experiments were carried out to study the influence of MFC on the thermal stability of starch. Two data were obtained from TGA measurements: the mass loss of the samples and the heat flow as a function of temperature.

The evolution of the sample weight as a function of temperature was firstly investigated and shown in Figure IV-24. An initial weight loss of the samples occurred around 100°C. This corresponded to the water evaporation.

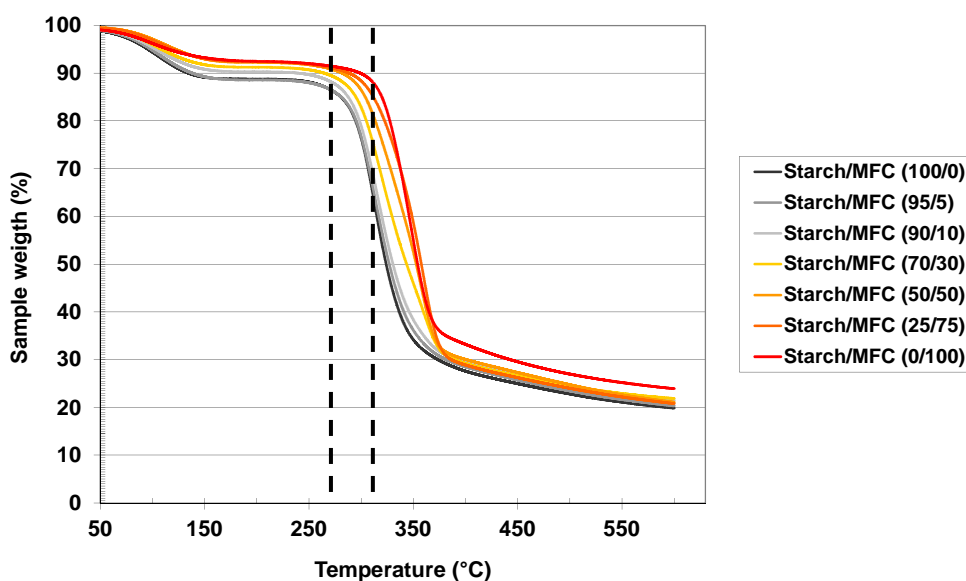


Figure IV-24: TGA of starch/MFC films.

A second weight loss for the samples was observed from 275°C with the degradation of the samples. An increase by 45°C of the degradation temperature of starch films was observed

according to the MFC content. This confirmed the presence of strong interactions between starch and MFC.

The heat flow, Figure IV-25, showed an endothermic peak in this temperature range which confirmed the results previously obtained from DSC analysis.

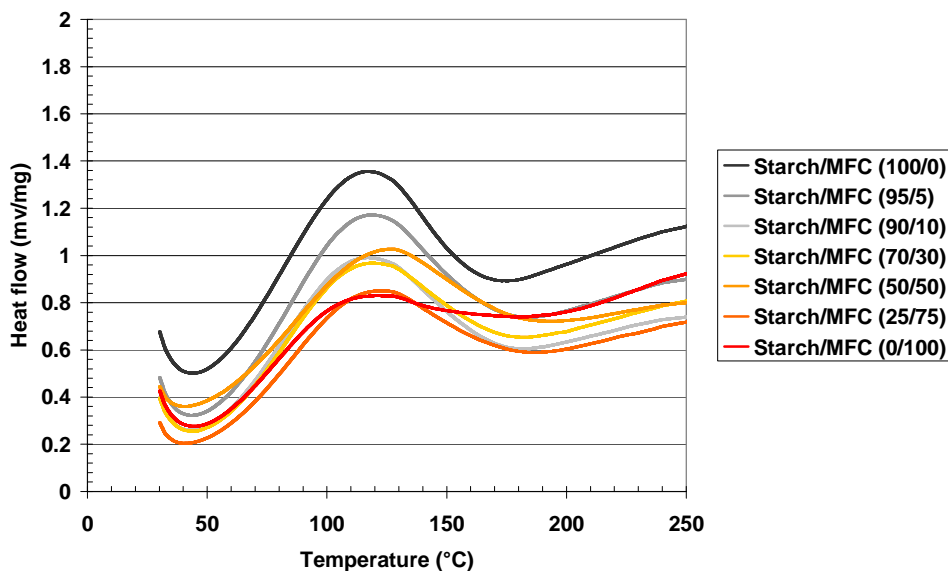


Figure IV-25: Heat flow measurement determined from TGA experiments.

To conclude this part on the structural investigation of nanocomposites, the addition of MFC did not show any significant effect on the crystallinity of the starch matrix. However, TGA confirmed the presence of strong interactions between starch and MFC. These interactions allowed the improvement of starch properties with an increase of its mechanical properties and a reduction of its water vapour permeability. The addition of plasticizer was tested to observe its influence on the composite properties.

IV.3.6. - Study of the influence of sorbitol addition

Starches are continuously studied to compete with and replace synthetic polymer for different applications [118]. However, as observed in the first part, starch films are very brittle. To reduce this brittleness, starch are currently associated to plasticizers such as glycerol, poly(ethylene glycol), or sorbitol for example. The improvement of the film quality leads to the enhancement of the barrier properties but the addition of plasticizer reduces the barrier properties. This part investigates the influence of the addition of sorbitol (S) on the composite film properties. Sorbitol was mainly chosen for its natural origin. Indeed, sorbitol is extracted during the conversion of corn wheat and potato into starch (Figure IV-26).

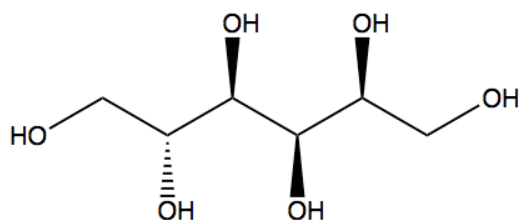


Figure IV-26: Sorbitol molecule.

Only one sorbitol content was tested in this study. The ratio was fixed at 20 wt% in order to avoid the degradation of barrier properties [165]. A new series of composites was thus produced following the same procedure but using starch/sorbitol as matrix. Starch was firstly solubilised at 95°C and the plasticizer was added after cooling to 60°C. Once again, MFC suspensions were added to starch/sorbitol mixture with a ratio ranging from 0% to 100% according to starch/sorbitol.

The mechanical and barrier properties of starch/S/MFC composites were evaluated and compared with the previous results.

IV.3.6.1. - Structure of starch/S/MFC films

IV.3.6.1.1. - Visual aspect

The sorbitol content (20% wt) was not high enough to form a good plasticized starch film. Indeed, cracks appeared in starch films after water evaporation (Figure III-54). A good film formation was nevertheless observed after the addition of MFC, as shown from the visual aspect of the starch/S/MFC composite (54/16/30) in Figure III-54. Compared to sorbitol-free starch, composite films were more flexible.



Figure III-54: Films of 30g/m² of starch/sorbitol (80/20) (left) and starch/S/MFC (56/14/30) (right).

A previous study by Vigié *et al.* [166] showed the possibility to process starch films with 20 wt% sorbitol. Another investigation, reported by Gaudin *et al.* [167], showed that the plasticisation of starch and its classical improvement effect of ductility were only possible for higher plasticizer contents. With sorbitol, the increase of elongation started from a content of 27%. For low sorbitol contents, the plasticizer does not play its role and this phenomenon was called antiplasticization. The consequences of this effect were described in the literature

[168]. Here, the combination of MFC and sorbitol were studied to improve the mechanical and barrier properties of the starch matrix.

IV.3.6.1.2. - Thickness and density

The apparent density was determined for each starch/S/MFC composite conditioned at 23°C-50% RH (Table IV-5).

Compared to starch/MFC films, the void content was slightly reduced. However, these values were only qualitative due to the variation of the film thickness which strongly influenced on the final values.

MFC content (wt%)	Film thickness (μm)	Calculated density (g/cm^3)	Theoretical density (g/cm^3)	Void content (%)
5	27.9 (± 1.8)	1.24 (± 0.06)	1.32	5.9
10	28.4 (± 1.1)	1.22 (± 0.05)	1.33	8.8
30	30.2 (± 1.9)	1.17 (± 0.03)	1.37	14.3
50	29.7 (± 2.2)	1.18 (± 0.07)	1.40	15.9
75	33.1 (± 3.4)	1.12 (± 0.05)	1.45	22.9

Table IV-5: Film thickness, theoretical and experimental density and void content of composite films according to the MFC content.

IV.3.6.1.3. - SEM-FEG

The introduction of sorbitol in composite films was expected to modify their structure. The cross section of plasticized starch/S/MFC (56/14/30) films was observed by SEM-FEG microscopy in Figure IV-27. The appearance of the structure was more closed and the lamellar structure was no more distinguished. The voids seemed to be filled by the sorbitol molecules.

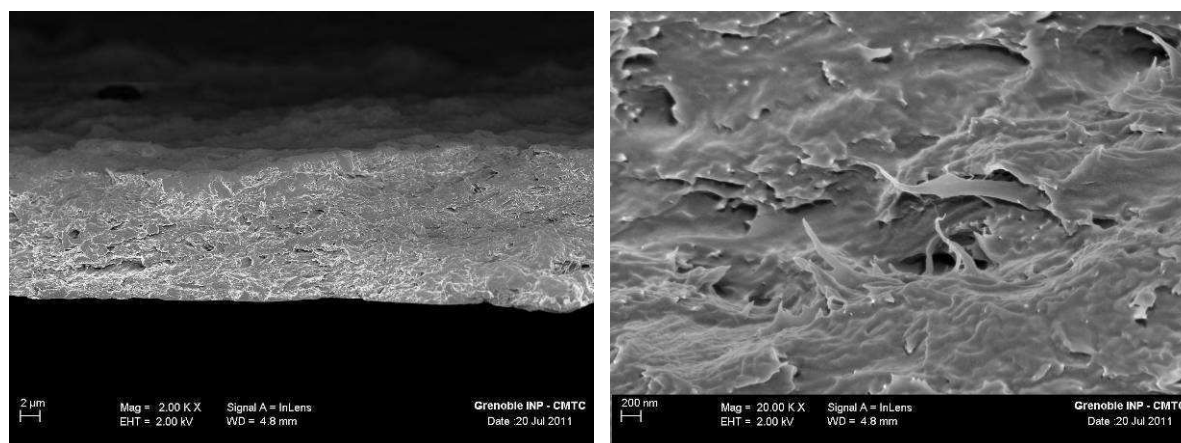


Figure IV-27: SEM-FEG images of the cross-section of plasticized starch/S/MFC (56/14/30) films.

IV.3.6.2. - Mechanical properties

IV.3.6.2.1. - Tensile properties

The evolution of the Young's modulus value of composites as a function of MFC content is

shown in Figure IV-28 for both two kinds of matrix, i.e. sorbitol-free starch and starch/sorbitol (80/20).

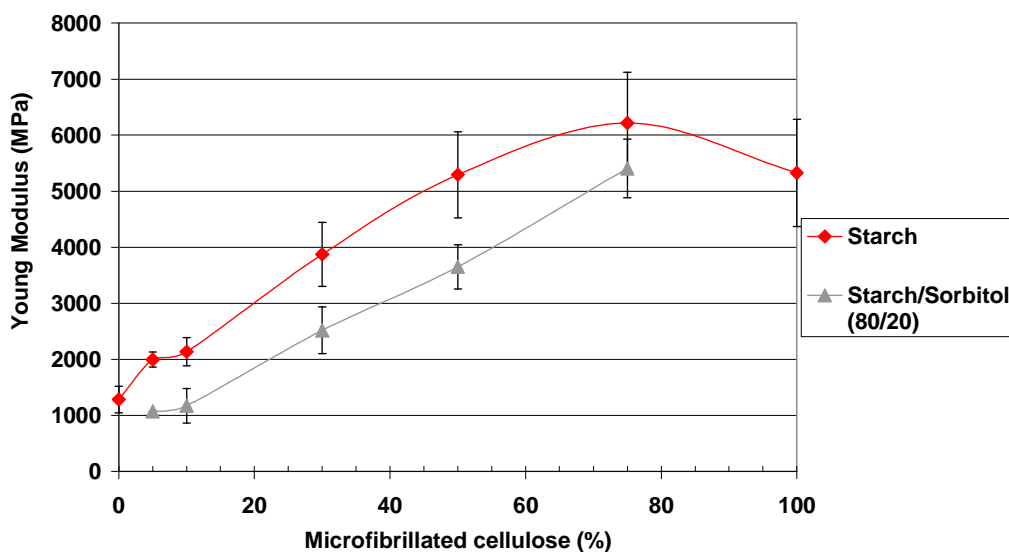


Figure IV-28: Young's modulus of starch/MFC and starch/S/MFC composites.

The addition of sorbitol decreased the Young's modulus of composite films compared to sorbitol-free starch films as expected. However, the introduction of MFC had once again a reinforcement effect because the Young's modulus values increased when increasing the MFC content. The stiffness of starch films was thus decreased in presence of sorbitol but the starch/MFC interactions seemed to be unaffected leading to good mechanical properties of composite systems.

The same trend was also observed for the tensile strength values (Figure IV-29). As reported by several researchers, the increase in polyol concentration in starch leads to the decrease of the glass transition and the tensile strength [169]. Indeed, the plasticizer reduces the intermolecular forces in starch films increasing the mobility of polymer chains and the flexibility of films.

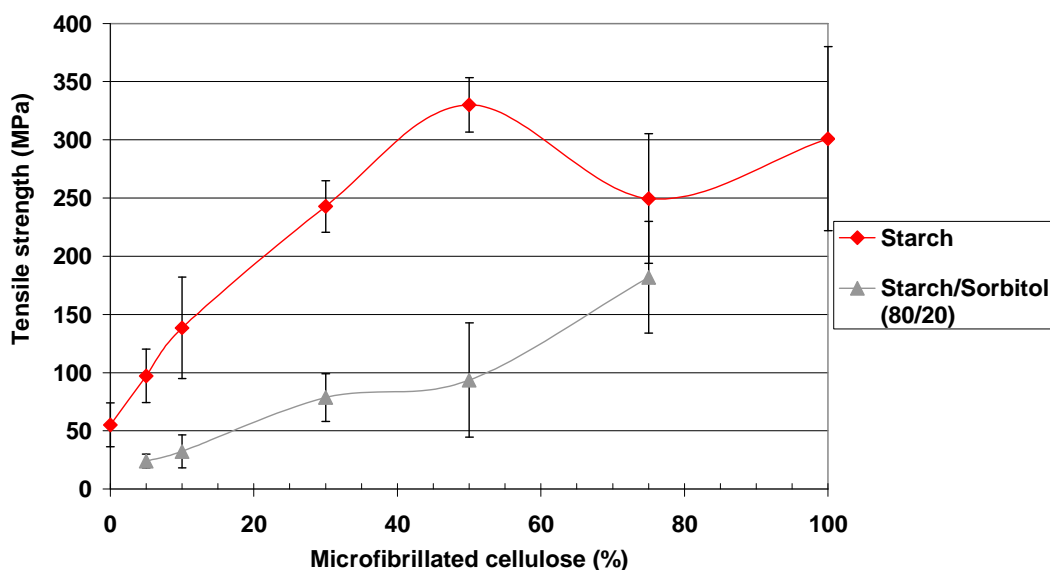


Figure IV-29: Tensile strength of starch/MFC and starch/S/MFC composites.

Figure IV-30 shows the evolution of the elongation at break for composite films as a function of MFC content. Surprisingly, the introduction of plasticizer did not enhance the ductility of the films. Indeed, the values were lower for plasticized matrix based composites than for unplasticized starch systems.

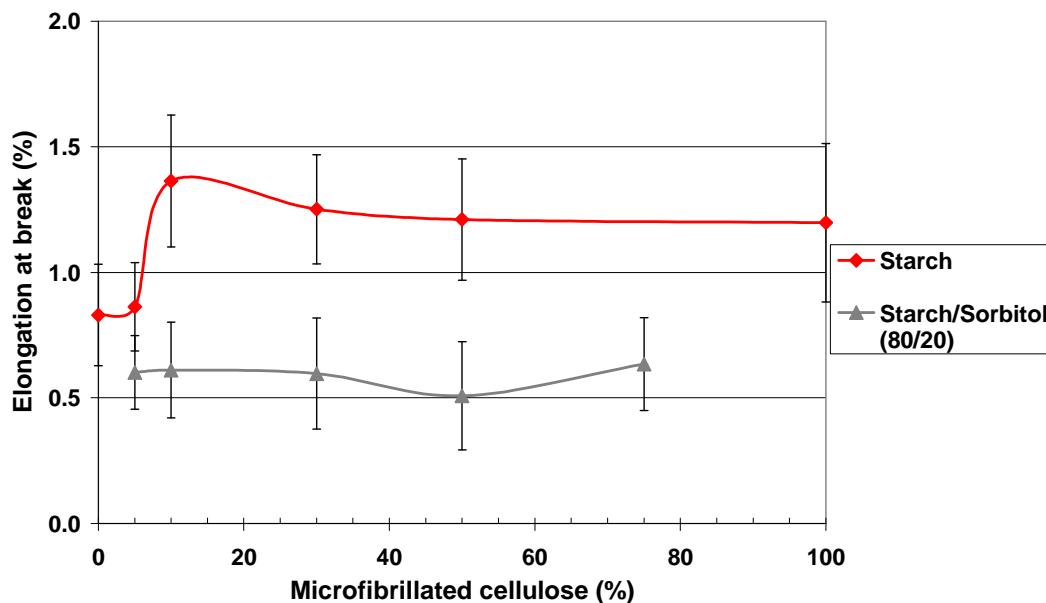


Figure IV-30: Elongation at break for starch/MFC and starch/S/MFC composites.

Therefore, the investigation of the mechanical properties of plasticized starch films showed that the sorbitol did not play the role of classical plasticizer in this case. This behaviour was similar to the antiplasticization phenomenon. This result is in agreement with Gaudin *et al.* [167] who found an antiplasticization phenomenon for sorbitol contents lower than 27%.

The antiplasticization could be due to strong interactions occurring between the polymer and the plasticizer inducing a “cross-linking” effect at low concentrations in addition to possible crystallisation [170].

IV.3.6.2.2. - TGA analysis

TGA measurements were carried out in order to determine the influence of MFC on the thermal degradation of plasticized starch. shows that the thermal degradation was the same for the starch/sorbitol film and sorbitol-free starch film. Moreover, the addition of MFC increases slightly the degradation temperature of plasticized starch. This confirmed that favourable interactions between MFC and starch still exist in presence of sorbitol.

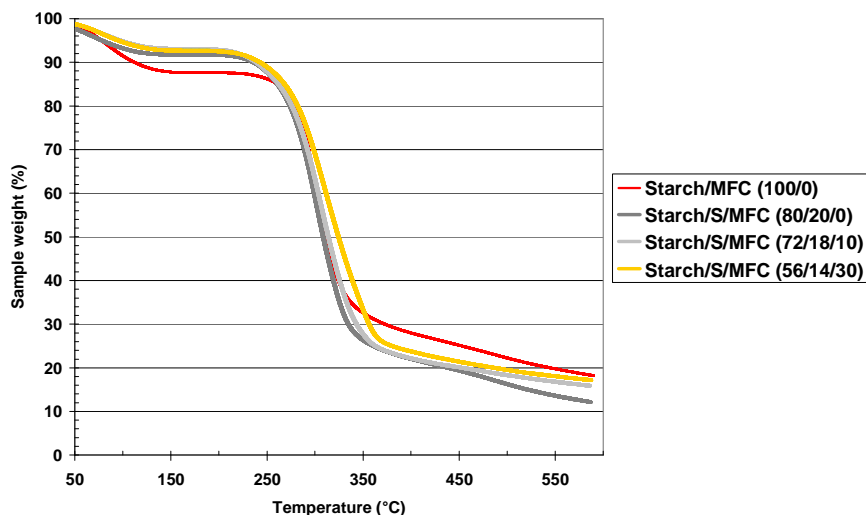


Figure IV-31: TGA thermograms of starch/sorbitol (80/20) and starch/S/MFC composite films.

IV.3.6.2.3. - Conclusion

The addition of sorbitol decreased the mechanical properties of starch film but once again the addition of MFC improved the mechanical strength of plasticized starch. Moreover, the elongation at break of composite films was also reduced indicating that the sorbitol content was insufficient to plasticize the matrix.

IV.3.6.3. - Barrier properties

The barrier properties of starch/S/MFC composites were evaluated according to the MFC content except for the neat matrix (sample without MFC). The MFC/S/MFC (80/20/0) was effectively too brittle to measure its WVTR by the dish method. The evolution of the water vapour transmission rate (WVTR) value at 23°C-50% RH as a function of MFC content is plotted in Figure IV-32. The introduction of sorbitol had a very positive effect on barrier properties: the WVTR value was 8 times lower for the starch/S/MFC (72/18/10) compared to the sorbitol-free composite. This improvement could be the consequence of the antiplasticization effect and interactions between starch and sorbitol. Gaudin *et al.* [167] observed a decrease of the oxygen permeability of starch film by addition of low sorbitol quantities. The diffusion decreased thanks to hydrogen interactions between starch and sorbitol. Indeed, these interactions reduced the molecular motion needed for the oxygen diffusion.

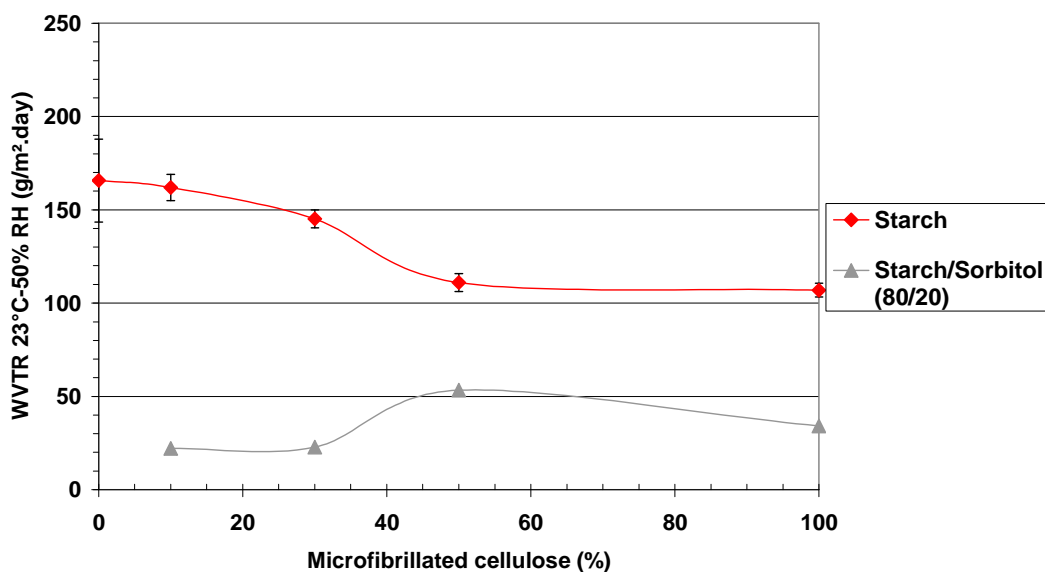


Figure IV-32: Effect of sorbitol and MFC addition in composites on WVTR measurements.

However, the addition of MFC had no significant influence on the water vapour permeability of plasticized starch matrix. The value reached 20 g/m².day for the MFC contents lower than 50% and increased to 50 g/m².day for higher MFC contents. Plackett *et al.* [127] also observed this trend for the oxygen permeability of composites. The addition of glycerol counteracted the positive influence of MFC in terms of improvement of barrier properties.

The water content of plasticized composites was also determined by TGA for films conditioned at 23°C-50% RH (Figure IV-33). The water content was strongly decreased with the addition of sorbitol with a value of 11.8% and 6.8% for starch and plasticized starch, respectively. Most probably, sorbitol molecules replaced the water in films. Moreover, the obtained values were almost the same for all films regardless the MFC content.

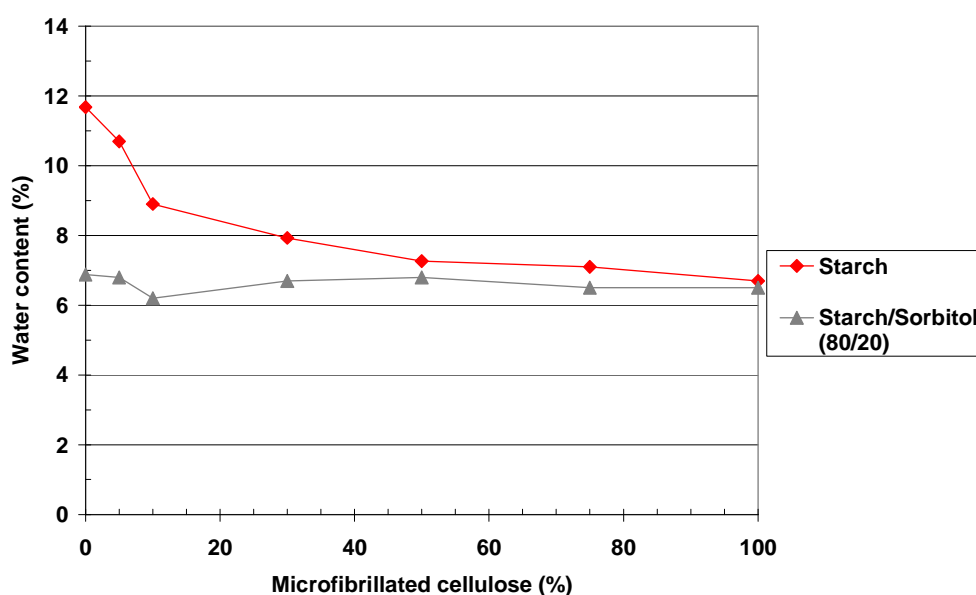


Figure IV-33: Water content in starch/MFC and starch/S/MFC films conditioned at 23-50% RH.

This trend was confirmed by the sorption measurements as shown in Figure IV-34. Indeed, there was no strong difference between the sorption curves associated with the different MFC contents.

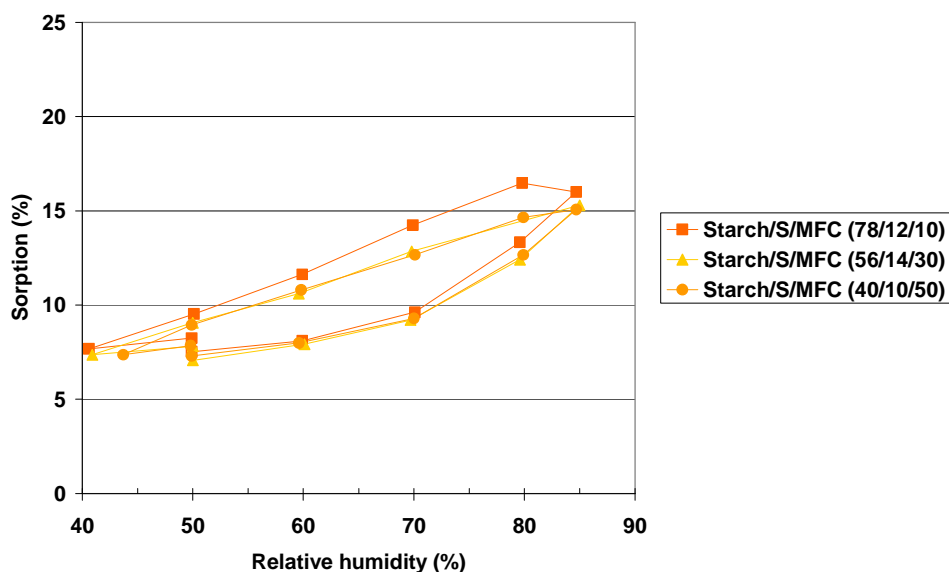


Figure IV-34: Water sorption desorption of starch/S/MFC films.

Thus, the presence of sorbitol in composite films decreased the water vapour permeability of starch probably thanks to the filling of voids by sorbitol molecule which decreased the diffusion of water molecules. These results also showed that the presence of water in films mainly influenced the water vapour transmission rate values. The effect of MFC on the barrier properties was no significant for unplasticized starch. However, for the chosen sorbitol content (20 wt%), starch/plasticizer system did not form film without MFC. Thus the addition of sorbitol allowed improving the water vapour permeability of starch and MFC gave the film forming ability.

IV.3.7. - Conclusion

The development of starch/MFC composites was successful. The introduction of MFC improved the mechanical properties and decreased the water vapour permeability. Moreover, the oxygen permeability showed an acceptable value. The addition of sorbitol was a first step to improve the composite film properties. Indeed at low concentration, the presence of sorbitol did not affect the starch/MFC interactions. The reinforcement potential of MFC was thus preserved and the water vapour barrier properties were improved.

Currently, the performance of this composite remains too low for barrier material applications. The water sensitivity and their high water vapour permeability are the main limitations of these materials.

IV.4. - Influence of MFC addition on the PVOH matrix properties

IV.4.1. - Introduction

The starch/MFC composite materials have barrier properties that are not sufficient to develop a biosourced packaging material. Another polymeric matrix, poly(vinyl alcohol) (PVOH) was

thus selected. This third part discusses the results obtained for PVOH/MFC composite films. PVOH is a partly biodegradable polymer and is already known for its excellent barrier properties. The addition of MFC in PVOH could act on several aspects such as the reinforcement effect, the improvement to the water sensitivity or the increase of the biodegradability.

Therefore, composites were developed and their mechanical and barrier properties were assessed for MFC contents ranging from 0 wt% to 75 wt%. In this study, the PVOH used had a degree of hydrolysis of 98.4% (+/- 0.4%) and a molecular weight of 27000 g/mol [162]. This high degree of hydrolysis meaning a high density of hydroxyl groups, was chosen to favour the compatibility and the interactions with MFC.

Once again, the composites were produced using the casting/evaporation technique detailed previously. PVOH was firstly heated at 95°C in water to ensure its solubilisation before the addition of MFC.

IV.4.2. - Structure of PVOH/MFC composites

IV.4.2.1. - Visual aspect

The PVOH/MFC composite films, observed in Figure IV-35, were produced by casting/evaporation. Films seemed homogeneous with no apparent flocculation but a decrease of the transparency was firstly visually observed for films containing MFC. This could result from the presence of MFC aggregates in films. Indeed, Lu *et al.* [133] reported that the transparency of the resulting films confirms the homogeneous dispersion of MFC in PVOH.

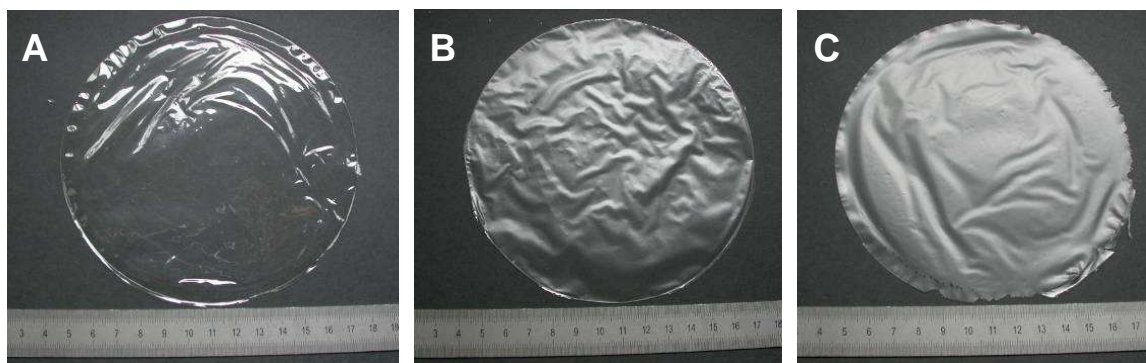


Figure IV-35: Photos of pure PVOH film (A), PVOH/MFC composite films with 10% MFC (B) and 30% MFC (C).

Secondly, these observations were confirmed by the transparency measurements (*cf.* Table IV-6). The total transmittance of light was quite the same for all composite films whatever the MFC content. However, the haze values increased with the increase of MFC content leading to the lower transparency after MFC addition.

MFC content (%)	Transmittance	Haze	Clarity
0	92.9 (± 0.2)	4.2 (± 0.8)	85.3 (± 0.3)
5	92.8 (± 0.1)	63.7 (± 1.9)	12.2 (± 0.3)
10	93.1 (± 0.1)	75.9 (± 0.8)	11.1 (± 0.2)
30	93.6 (± 0.0)	81.4 (± 0.2)	9.4 (± 0.1)
50	93.2 (± 0.1)	83.4 (± 0.3)	9.3 (± 0.1)
75	91.9 (± 0.6)	82.0 (± 0.6)	9.4 (± 0.2)

Table IV-6: Transparency measurements of PVOH/MFC composites.

IV.4.2.2. - Thickness and density of films

Table IV-7 summarizes the values of apparent density, theoretical density and void content for each PVOH/MFC film according to the MFC content.

PVOH films showed a density close to the theoretical density demonstrating the good film formation and the production of dense PVOH films. The introduction of MFC increased the void content of final composites. For MFC contents of 5 and 10% wt, the void content remained very low.

MFC content (wt %)	Film thickness	Calculated density	Theoretical density	Void content (%)
0	25.0 (± 2.2)	1.20 (± 0.08)	1.24	3.2
5	27.0 (± 1.1)	1.18 (± 0.05)	1.25	5.8
10	26.2 (± 1.3)	1.21 (± 0.06)	1.27	4.4
15	27.8 (± 1.3)	1.10 (± 0.04)	1.28	14.0
30	33.7 (± 1.2)	0.96 (± 0.05)	1.32	27.1
50	31.2 (± 3.4)	1.04 (± 0.01)	1.37	19.7
75	28.8 (± 0.8)	1.25 (± 0.03)	1.44	12.9
100	31.8 (± 2.4)	1.04 (± 0.09)	1.5	30.7

Table IV-7: Film thickness, theoretical and experimental density and void content of composite films according to the MFC content.

The increase of MFC content in PVOH matrix led to the increase of film porosity. The barrier properties were measured to confirm if this porosity impacts or not on the properties of PVOH/MFC films.

IV.4.2.3. - SEM-FEG images

A good dispersion level of the filler in the matrix is a key parameter to achieve effective reinforcement. Here, only SEM-FEG observations were done to investigate the homogeneity of composites. Indeed, PVOH is a semicrystalline polymer and its crystallites are revealed under polarized light microscope. Thus, it was impossible to detect and differentiate the microfibrils by the polarized light microscope technique.

The SEM-FEG images of the cross-section of PVOH and PVOH/MFC films are presented in Figure IV-36.

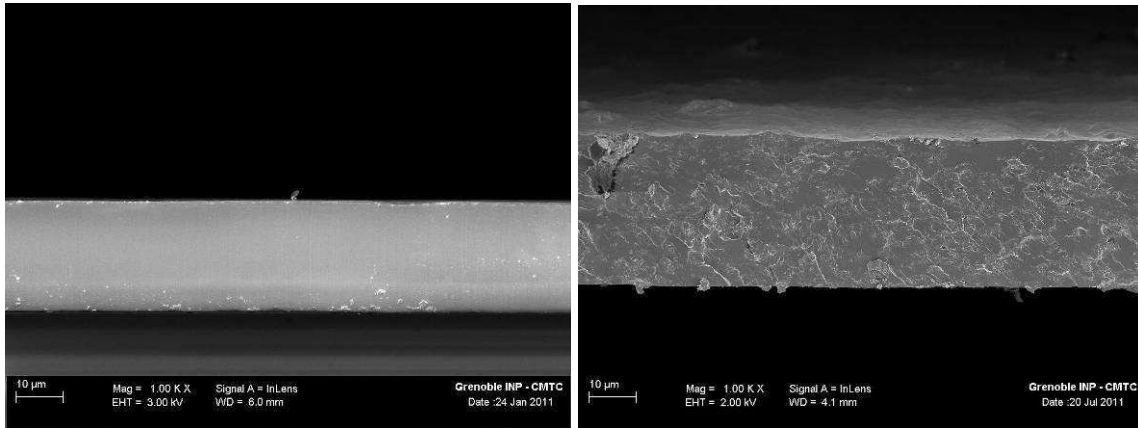


Figure IV-36: SEM-FEG images of the cross section PVOH film (left) and PVOH/MFC (95/5) film (right).

The PVOH film was a very dense and smooth material. This confirmed the density values reported previously. For the PVOH/MFC composites, it was very difficult to detect MFC in the matrix. Indeed, the microfibrils were probably well embedded in the PVOH matrix. The observed white dots may correspond to the thin microfibrils. Their repartition was homogeneous in the material thickness. The global distribution of MFC was homogeneous but the size of these white dots suggests the presence of fibril aggregates.

The PVOH/MFC (95/5) composites appeared compact for this MFC content because no voids were detected on the micrograph.

IV.4.3. - Mechanical properties of PVOH/MFC composites

Tensile tests were carried out for PVOH/MFC composite films to evaluate the effect of MFC on the mechanical properties of PVOH matrix. The combination of MFC with PVOH improved the mechanical properties of this matrix as confirmed by the evolution of the Young's modulus value in Figure IV-37. Indeed, it increased continuously according to the MFC content. Composites were stiffer with values reaching 2500 MPa and 3300 MPa with 10 wt% and 30 wt% of MFC, respectively, compared to the pure PVOH film value of 1800 MPa.

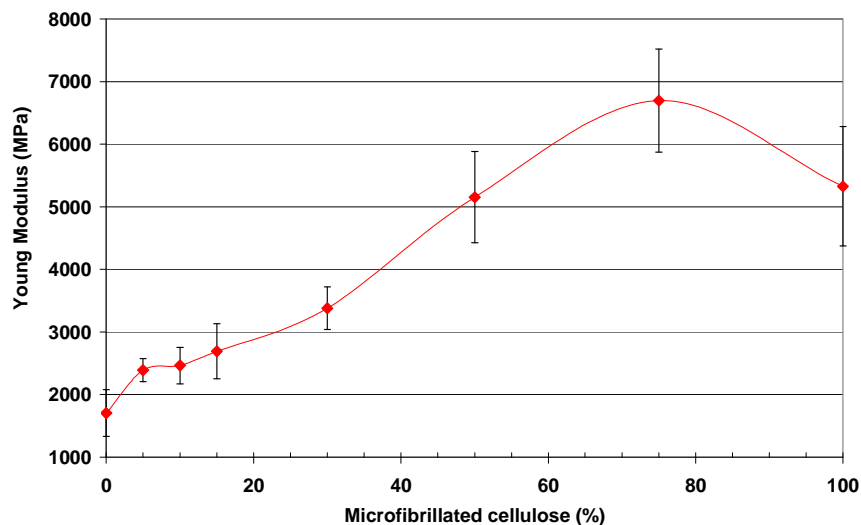


Figure IV-37: Young's modulus of PVOH/NFC films.

The addition of MFC also improved the tensile strength value of the PVOH matrix but only for the lowest contents below 15 wt% (Figure IV-38). For the highest MFC contents, between 30 wt% and 75 wt%, the tensile strength was lower although the standard deviation was very high.

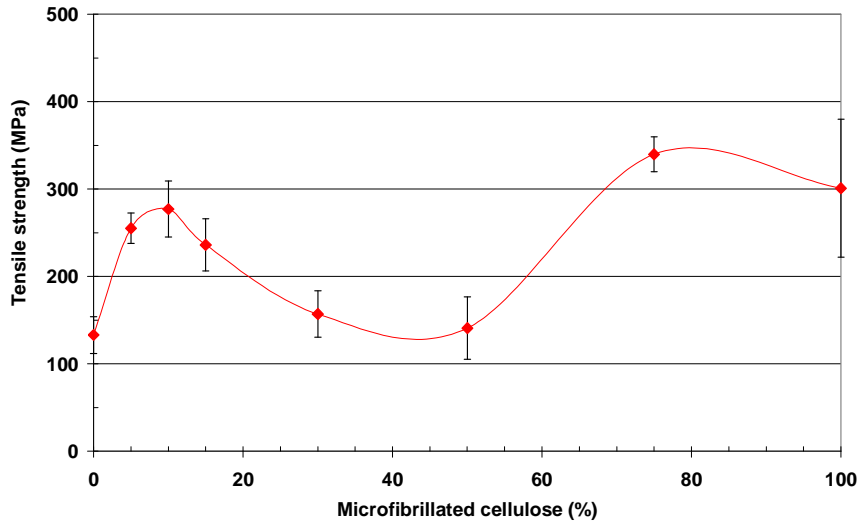


Figure IV-38: Tensile strength of PVOH/MFC films.

Several explanations of this result were possible. MFC aggregation within the matrix was possible leading to the decrease of PVOH/MFC interactions and to the decrease of the film cohesion. This was observed with the high void content values for high MFC contents. Another potential explanation is the production method. Indeed, to reach a correct spreading, the PVOH/MFC mixture for the ratios (70/30) and (50/50) was diluted to 3% compared to 5% for the lowest MFC ratios. This dilution could have an impact on the material formation and its structure. Complementary works could be interesting to perform to determine the real impact of the dilution on the final material structure.

The value of the elongation at break confirmed this trend with a slight improvement after the addition of MFC up to 15% and a reduction for the highest MFC contents (Figure IV-39).

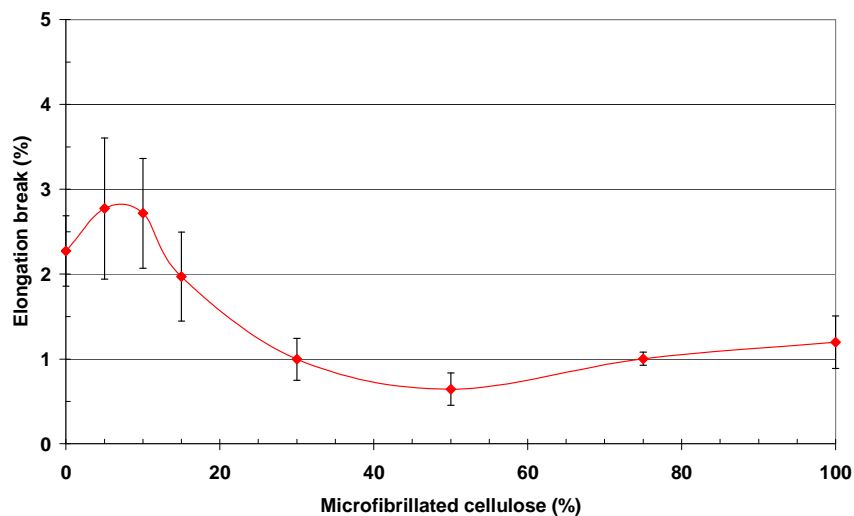


Figure IV-39: Elongation at break of PVOH/MFC films.

The addition of MFC in the PVOH matrix had a positive effect with good reinforcement potential.

In the literature, the reinforcement potential of MFC in PVOH matrix was also reported for a broad MFC content range. The graph, shown in Figure IV-40, summarizes the reported strength and Young's modulus values which are compared with the values obtained in this study. As observed at the bottom of this graph, the mechanical properties of pure PVOH films generally were quite low. In this present work, the PVOH selected showed higher tensile strength compared to PVOH films reported in literature. This explained the high tensile strength of PVOH/MFC composites in this study compared to other reports.

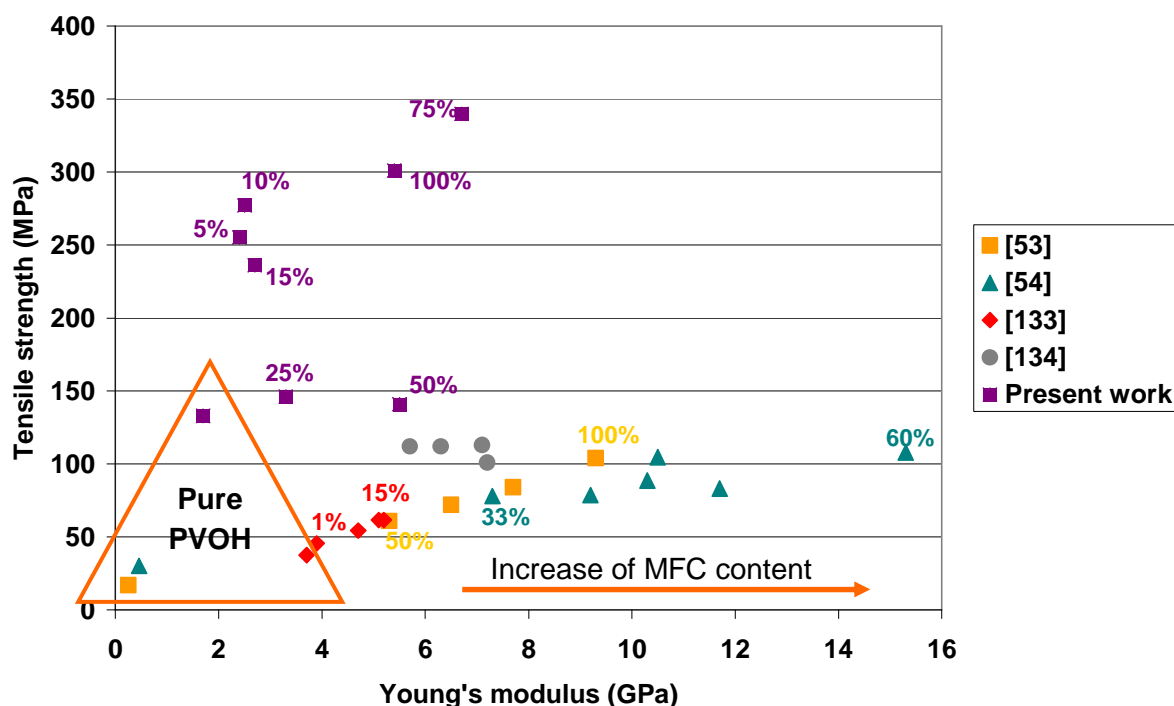


Figure IV-40: Comparison between the mechanical properties reported in the literature for PVOH/MFC composites and our results.

Therefore, the mechanical properties of PVOH/MFC composite films showed a good improvement of the stiffness of the material with MFC addition for the lowest MFC contents. From 30 wt% MFC, a probable aggregation decreased the tensile strength of the material. PVOH is a hydrophilic polymer which should allow good interactions with MFC. However, the properties of these polymers generally depend on the relative humidity. Tensile tests were carried out for the composite samples in tropical conditions at 38°C and 90% RH. The Young's modulus value is shown for composites conditioned at 23°C-50% RH and 38°C-90% RH in Figure IV-41.

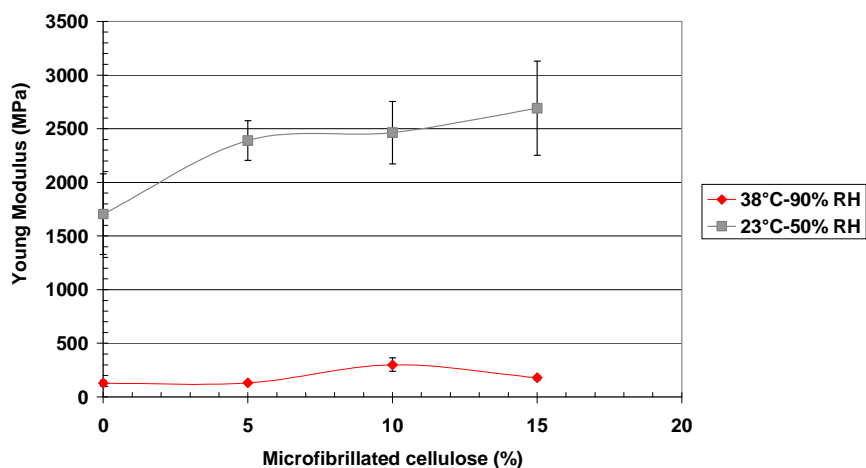


Figure IV-41: Young's modulus of PVOH/MFC composites films at 23°C-50% RH and 38°C- 90% RH.

Under highly moist atmosphere, the mechanical properties were strongly modified with a significant decrease of the Young's modulus from 2500 MPa to 300 MPa for the composite PVOH/MFC (90/10). The addition of MFC increased the Young's modulus although the reinforcement effect was also lower at 38°C-90% RH compared to 23°C-50% RH.

This trend was also observed, Figure IV-42, for the tensile strength values. Once again, the increase of relative humidity decreased the tensile properties. However, the tensile strength values were higher, with a slight increase from 275 to 300 MPa for the composite PVOH/MFC (90/10).

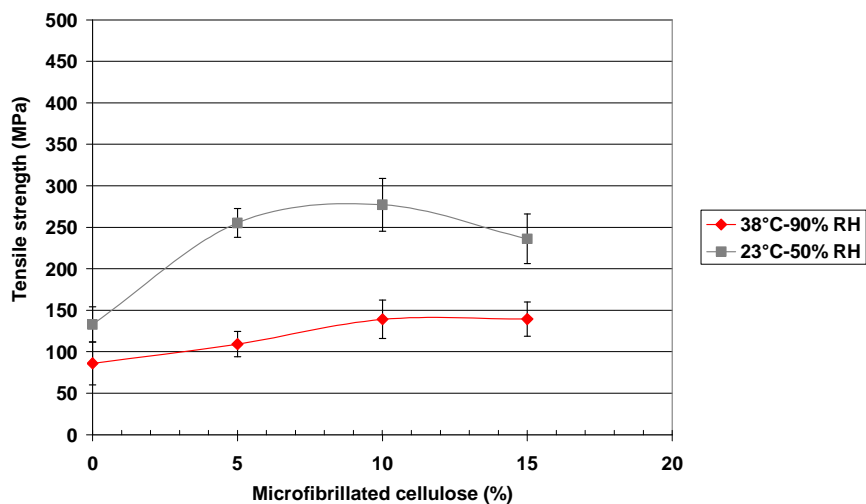


Figure IV-42: Tensile strength of PVOH/MFC composites films at 23°C-50% RH and 38°C- 90% RH.

At last, the elongation at break values demonstrated the good ductibility of materials under these humidity conditions (Figure IV-43). Indeed, the elongation of composite films during the tensile tests were strongly increased compared to measurements carried out in ambient conditions. However, the introduction of MFC strongly decreased the elongation at break value showing thus the decrease of PVOH chain mobility in presence of MFC. This result could be due to favourable interactions between PVOH and MFC.

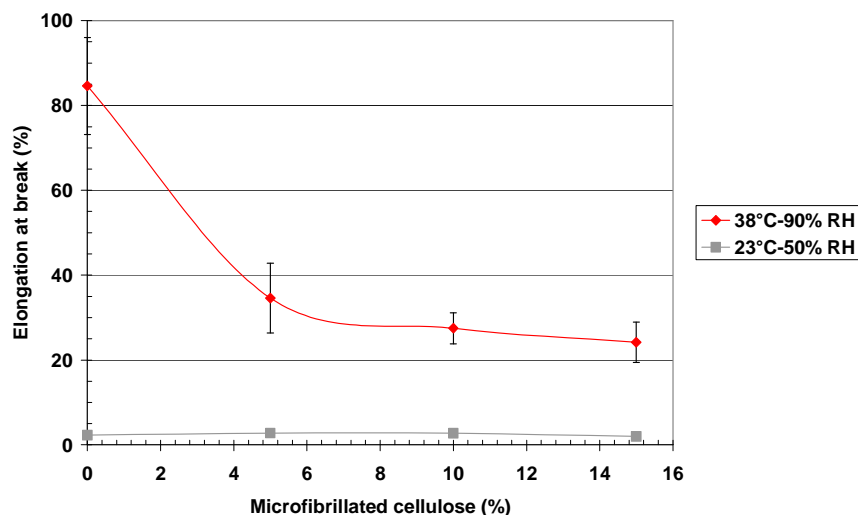


Figure IV-43: Elongation at break of PVOH/MFC films at 23°C-50% RH and 38°C- 90% RH.

Thus, PVOH/MFC materials were more elastic under high relative humidity. Indeed, water molecules play the role of plasticizer for PVOH chains. Roohani *et al.* [130] studied the evolution of the glass transition temperature for films of copolymer of poly(vinyl alcohol) and poly(vinyl acetate) for several relative humidity conditions. The study showed that the glass transition temperature was lower than ambient temperature at 98% RH. This explains the low Young's modulus value obtained at high relative humidity.

The reinforcement potential of MFC was less significant in this case: the value was unmodified after addition of 5% MFC. The formation of an aqueous or highly moist interface decreasing the filler/matrix interactions was suggested by Roohani *et al.* [130]. In this work, the elongation at break being lower in presence of MFC, it could be supposed that the PVOH/MFC interactions also took place under high moisture atmosphere.

IV.4.4. - Barrier properties of PVOH/MFC composites

Even if the reinforcement potential of MFC in PVOH matrix has been extensively reported, few studies described the barrier properties of PVOH/MFC composites.

IV.4.4.1. - Water vapour transmission rate at 23°C-50% RH

The water vapour transmission rate values at 23°C-50% RH for PVOH/MFC composites were determined according to the dish method (standard ISO 2528). The values for composite films of 30 g/m² were very low, as observed in Figure IV-44. For MFC content lower than 25%, values were below 1g/m².day corresponding to the lower limit detection of the dish standard.

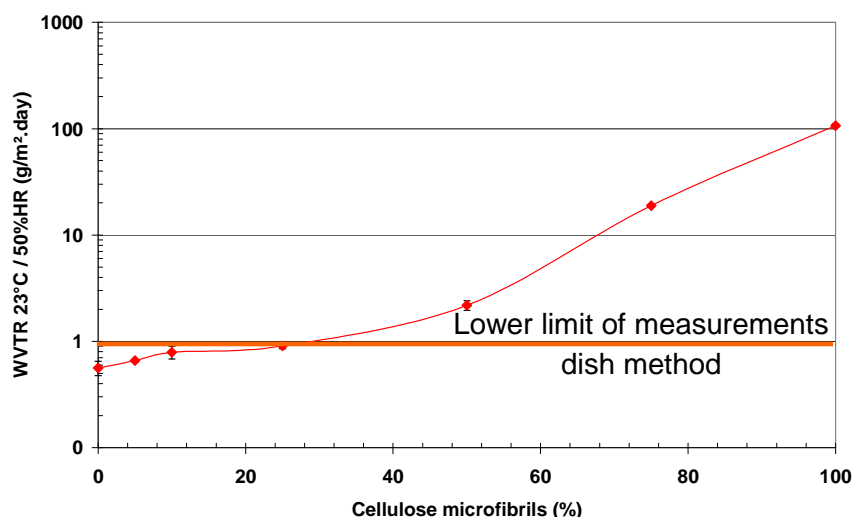


Figure IV-44: WVTR at 23°C-50% RH of PVOH/MFC films.

Therefore, the PVOH matrix kept its good barrier properties after MFC addition for the lowest MFC contents. The interactions between PVOH and MFC allowed to obtain very cohesive films and to keep their excellent water vapour permeability at 23°C-50% RH. From 50% MFC, the barrier properties of the films were strongly altered, probably due to the presence of aggregates for these high MFC contents. These results are in agreement with the mechanical results.

IV.4.4.2. - Water vapour transmission rate at 38°C-90% RH

The moisture sensitivity of PVOH films is one of their drawbacks for the use of this polymer. Indeed, at high humidity level the water vapour permeability of films is strongly increased. As described previously, water molecules plasticized the PVOH film leading to an increase of chain mobility. A second series of WVTR measurements was thus carried out in tropical conditions in order to determine the effect of MFC in these high moisture conditions (Figure IV-45).

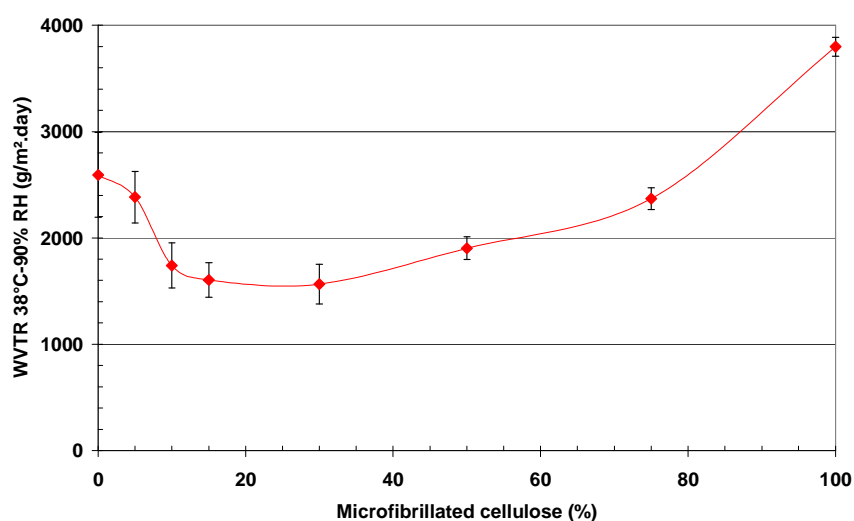


Figure IV-45: WVTR at 38°C-90% RH of PVOH/MFC films.

Under such high moisture conditions, the WVTR value of PVOH film reached 2750 g/m².day, well above 1 g/m².day observed in ambient condition. However, the curve showed an

important decrease of water permeability values with the introduction of MFC up to a ratio of 25% (Figure IV-45). Once again, a degradation of the barrier properties was observed for the highest MFC contents.

This improvement of moisture permeability observed for the low MFC contents could be ascribed to several phenomena. A first explanation is the decrease of available OH interfacial groups involved in H-bonding with cellulose because of favourable matrix-filler interactions, hence decreasing the water sensitivity of PVOH. The second phenomenon is the decrease of interfacial chain mobility induced by PVOH/MFC interactions. The result is in agreement with the elongation at break values previously observed for composite films, proving a decrease of the chain mobility in presence of MFC.

IV.4.4.3. - Water sorption of PVOH/MFC films

TGA experiments were firstly used to determine the water content of PVOH/MFC films conditioned at 23°C-50% RH. The moisture content was lower for films containing MFC, as indicated in Figure IV-46. Moreover, the moisture level was the same regardless the MFC content in composite films.

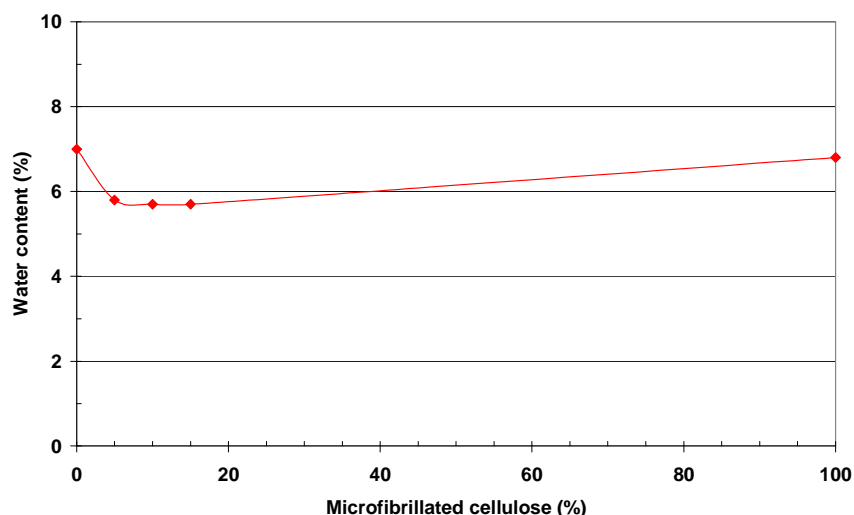


Figure IV-46: Water content in PVOH/MFC films conditioned at 23°C/50%RH.

Subsequently, the sorption was determined according to the different moisture levels. The same trend was observed and the water content was found to decrease by adding MFC as shown in Figure IV-47. As observed from mechanical properties, the presence of MFC in film decreased the PVOH chain mobility thanks to favourable interfacial interactions.

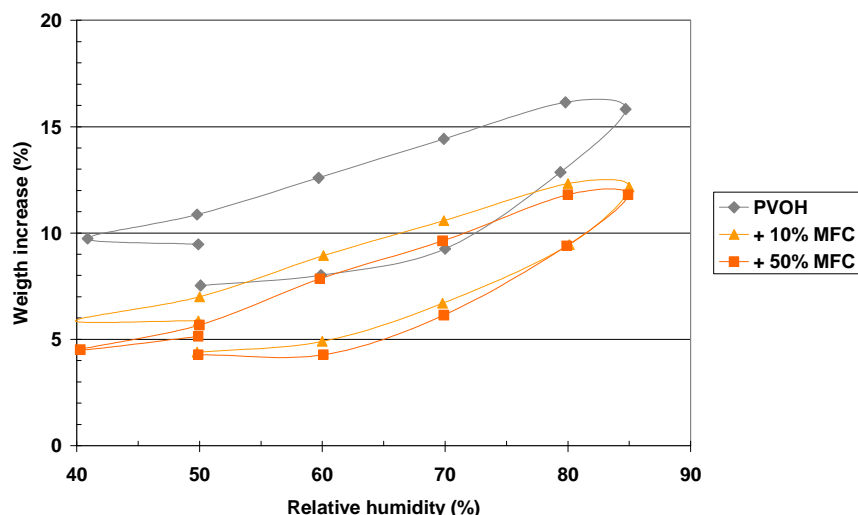


Figure IV-47: Water sorption of PVOH/MFC films for different relative humidity conditions.

IV.4.4.4. - Oxygen transmission rate at 23°C-0% RH

The oxygen transmission rate (OTR) at 23°C-0% RH was measured for the films with the lowest MFC content which showed the best results for water vapour permeability. The results showed no significant difference between samples (Table IV-8). Whatever the MFC content, the OTR values were very low with values smaller than or equal to $35 \text{ cm}^3 \cdot \mu\text{m} / \text{m}^2 \cdot \text{day} \cdot \text{bar}$.

	PVOH		PVOH/MFC (95/5)		PVOH/MFC (90/10)	
	Test 1	Test 2	Test 1	Test 2	Test 1	Test 2
OTR ($\text{cm}^3 / \text{m}^2 \cdot \text{day}$)	1.1	0.75	1.1	0.6	1.3	0.7
Oxygen Permeability ($\text{cm}^3 \cdot \mu\text{m} / \text{m}^2 \cdot \text{day} \cdot \text{bar}$)	27.5	18.75	29.7	16.2	35.1	18.9

Table IV-8: Oxygen permeability of PVOH/MFC films at 23°C-0% RH.

These values are in agreement with the literature values which define the oxygen permeability in dry conditions of PVOH film at $20 \text{ cm}^3 \cdot \mu\text{m} / \text{m}^2 \cdot \text{day} \cdot \text{bar}$. The low permeability of composite films confirmed the good cohesion and strong interactions between PVOH and MFC.

IV.4.5. - Thermal behaviour of PVOH/NFC composites

IV.4.5.1. - Differential scanning calorimetry

DSC measurements were carried out to determine the influence of MFC addition on the degree of crystallinity of the PVOH matrix (Figure IV-48). Measurements were carried out on films stored at 23°C-50% RH.

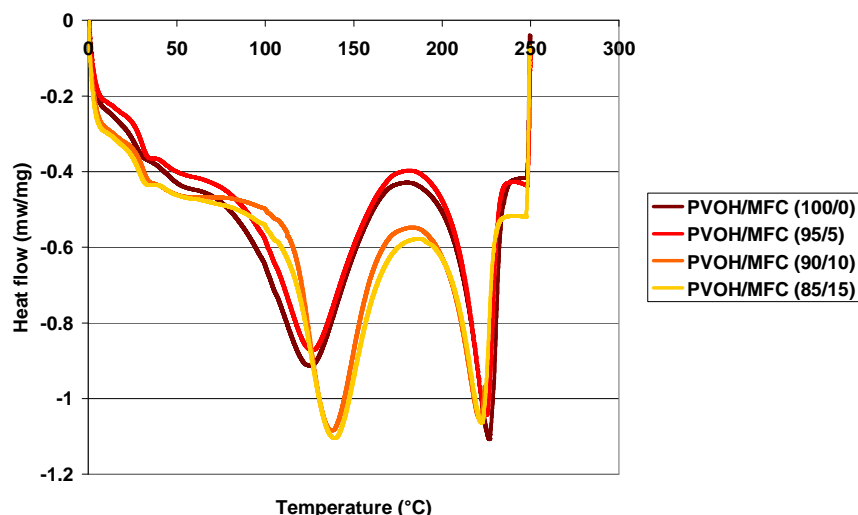


Figure IV-48: DSC analysis of PVOH/MFC films conditioned at 23°C-50% RH.

DSC analyses were carried out for the most homogeneous composite films corresponding to MFC contents lower than 15%. Two main peaks were observed on the DSC thermograms, the first one corresponding to the evaporation of moisture contained in films and the second one to the melting of PVOH crystalline domains.

All results are summarized in Table IV-9. The glass transition temperature slightly increased according to the MFC content. This could be ascribed to the strong interactions between PVOH and cellulosic filler. This is in agreement with the results obtained from tensile tests. However, this evolution is very low and within the experimental error.

	T _g (°C)	T _m (°C)	ΔH _m (J/g)	X ^c	X ^p
PVOH	15.7	226	77	0.47	0.47
+ 5% MFC	16.0	224	63	0.39	0.41
+ 10% MFC	16.6	222	54	0.33	0.37
+ 15% MFC	17.0	222	53	0.33	0.39

Where $X^c = \Delta H_m / \Delta H_m^\circ$ with $\Delta H_m^\circ = 161.6$ J/g corresponding to the heat of fusion for 100% crystalline PVOH; $X^p = X^c / w$ with w being the weight fraction of polymeric matrix in the composite.

Table IV-9: DSC measurements of PVOH/MFC films.

The crystallinity of PVOH matrix was also slightly influenced by the MFC addition. Indeed, both the melting temperature and the degree of crystallinity of the matrix decreased with MFC addition. Indeed, the PVOH/MFC interactions restricted the ability of PVOH chains to form crystalline regions. The PVOH crystallite growth was thus lowered in presence of MFC. Hrabalova *et al.* [171] reported the same observations after MFC addition in PVOH matrix. The decrease of the melting temperature was explained by the restriction of spherulite growth or crystalline imperfection. The authors suggested a second explanation of this result: in some composite systems, especially in well miscible system, the decrease of the melting temperature confirms specific interactions between the blended components [130].

These results were comparable to those reported by Lu *et al.* [133] in Table IV-10. In this study, the addition of MFC only had a slight influence on the thermal properties of PVOH films. For low MFC contents (1 wt%, 5 wt%) an increase of the polymer crystallinity was

observed and conversely a decrease was observed for higher MFC contents (10 wt%, 15 wt%).

	Tg (°C)	Xc (%)	Tm (°C)
PVOH	69.9	55.5	221.1
1 wt% MFC	71.2	57.1	220.9
5 wt% MFC	69.3	59.1	222.1
10 wt% MFC	70.5	52.2	219.6
15 wt% MFC	70.8	51.4	217.7

Table IV-10: Glass transition temperature, degree of crystallinity and melting temperature literature values for PVOH/MFC films [133].

IV.4.5.2. - Thermogravimetric analysis (TGA)

TGA experiments were performed to determine the degradation temperature according to the MFC content.

Figure IV-49 shows the weight loss of samples as a function of the temperature. The degradation of PVOH and PVOH/MFC films occurred in two steps: the first one for temperatures around 275°C and the second one around 450°C. A shift towards higher values of the degradation temperature was observed with the addition of MFC. Once again, this proved the presence of favourable PVOH/MFC interactions.

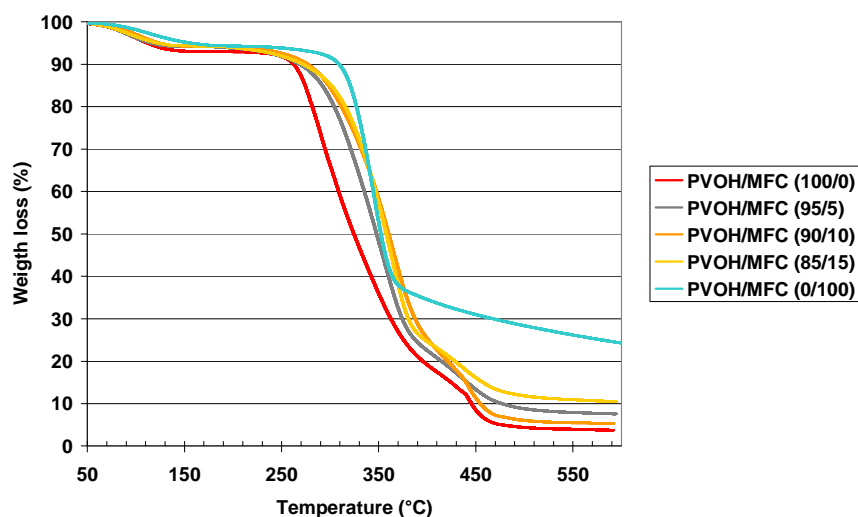


Figure IV-49: TGA experiments for PVOH/MFC films.

IV.4.6. - Effect of thermal treatment on the PVOH/MFC films

PVOH/MFC composite films seemed very promising for the development of new packaging materials. However, as already observed for the WVTR at 38°C-90% RH these materials are water sensitive. For example, the Cobb measurements were impossible because films were destroyed by water during the 60s of the measurement. To limit this phenomenon, a thermal treatment could be a simple solution.

IV.4.6.1. - DSC analysis

A proper heat treatment can enhance the crystallinity of PVOH films without materially affecting the T_m or the T_g values of the polymer [172]. In order to check this, DSC analysis was carried out on films treated for 5 min at three different temperatures, namely 120°C, 140°C and 160°C (Figure IV-50). The curves showed differences in the heat of fusion and thus in crystallinity according to the heat treatment. Indeed, the crystallinity increased from 39% to 46% after the heat treatment at 160°C.

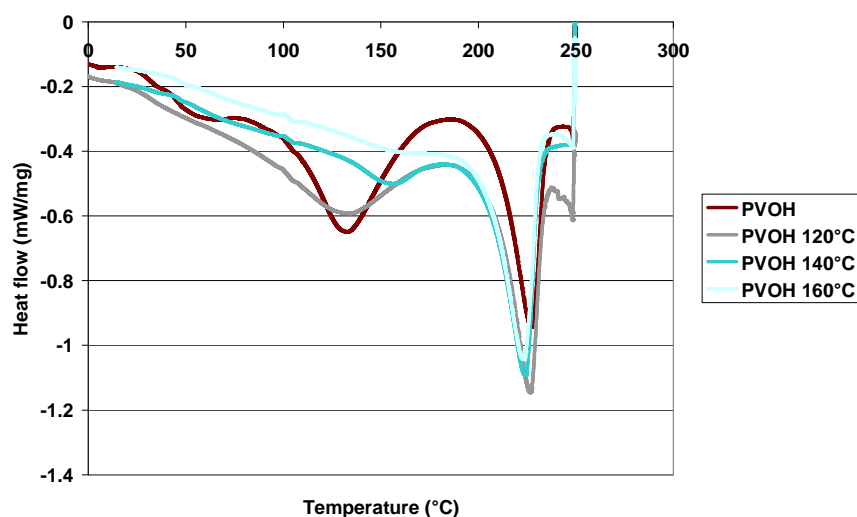


Figure IV-50: DSC thermograms for PVOH films conditioned at 23°C-50% RH according to the thermal treatment.

IV.4.6.2. - Water solubility

According to DSC analysis, PVOH and PVOH/MFC films were heat-treated at 160°C during 60s to avoid film degradation and high brittleness. The influence of heat treatment was only tested on the water sensitivity of films. For this, films were immersed in water during one hour under stirring. After filtration and drying overnight the weight of the residue was determined and compared to the initial weight.

This corresponds to the “water solubility” of films which values are collected in Table IV-11.

	% solubilised PVOH material	
	Without treatment	Treatment at 160°C
PVOH	92%	7%
PVOH/MFC (90/10)	90%	7%
PVOH/MFC (75/25)	89%	12%

Table IV-11: Percentage of solubilised PVOH material after immersion in water for 1 hour.

These results mainly showed the efficiency of the thermal treatment to reduce the water sensitivity of films. Indeed, the “water solubility” decreased from 92% to 7% after a treatment at 160°C. Once again, the introduction of 10% MFC within the matrix preserved the properties of PVOH film. However, the film cohesion decreased for the highest MFC contents (25%) and a degradation of the properties was observed.

IV.4.7. - Conclusion

PVOH/MFC composites displayed very interesting materials. Indeed, the addition of MFC improved the performances of PVOH films. A first positive effect was demonstrated with a good reinforcement ability of MFC in PVOH matrix. Moreover, it was shown that MFC improved the barrier properties of the polymer. Although the MFC addition had no influence on water vapour permeability under ambient conditions, its effect was clearly observed in tropical conditions with a significant decrease of water vapour permeability. These improvements were mainly due to strong interactions between PVOH and the cellulosic filler. The presence of hydroxyl groups in both materials allowed developing hydrogen interactions leading to a close network. The oxygen permeability remained excellent after the MFC addition.

Thus the addition of low MFC content (< 15 wt%) in PVOH matrix offered a material with improved properties compared to neat PVOH films.

Once again, the most important limitation of these products is their water sensitivity. A preliminary study showed that a thermal treatment is a first way to decrease this water sensitivity.

IV.5. - Comparison of the properties of starch/MFC and PVOH/MFC nanocomposite properties

The required properties to develop packaging materials are very high and difficult to reach. However, packaging manufacturers and consumers seek for biodegradable and recyclable materials. Here, two model systems were investigated from microfibrillated cellulose and two matrices, namely starch and PVOH.

Starch based materials are environmentally friendly systems because they combined two materials derived from renewable resource and have a high biodegradability. However, the barrier performance of starch/MFC system was too low for a possible use in packaging. The development of new formulations must be conducted for this system.

PVOH is a good film forming polymer and its barrier properties are better those of starch. The addition of MFC allowed improving again the properties of the polymer, mainly the mechanical properties and the water sensitivity.

Table IV-12 summarizes and compares the final properties obtained for the best starch and PVOH systems reinforced with MFC.

	Starch	Starch/MFC (50/50)	Starch/S/MFC (56/14/30)	PVOH	PVOH/MFC (95/5)
Young's modulus (MPa)	1200	5300	3900	1800	2400
WVP (g.µm/m ² .day)	4920	3410	600	17	18.9
OP (cm ³ .µm/m ² .day.bar)	-	125	49	18.8	16.2

Table IV-12: Summary of properties obtained for the best starch/MFC and PVOH/MFC films.

The barrier propertie level of packaging firstly depends on the final packed product. The second aspect is naturally the cost of the layer. This economic aspect directly impacts the material choice for an industrial. Although the starch/MFC system showed the lower barrier properties, the starch price is very low compared to PVOH. For this reason, it would be really

interesting to find means to improve this system thanks to plasticizers or cross linking agent for example.

PVOH/MFC composites showed an interesting efficiency barrier system. However, for the moment it is difficult to report the link performance/cost because the MFC cost was not evaluated on an industrial scale.

IV.6. - Conclusion

This study allowed the development of composite films using two different matrices and evaluating the influence of MFC on their mechanical and barrier properties. A protocol was firstly established to manufacture composites from PVOH or starch matrices. MFC content varied from 5 wt% to 75 wt% in composite in order to find the optimal system with the best properties. The results showed that the MFC addition improved the final properties of both matrices. A reinforcement effect as well as an enhancement of thermal properties was clearly demonstrated. Regarding the barrier properties, the introduction of MFC reduced the WVTR value of starch under ambient condition and the one of PVOH in tropical conditions. Structural analysis allowed also understanding the impact of MFC addition on the structure of the matrices. The influence of sorbitol on the properties of starch/MFC composites was studied. Their mechanical properties were degraded for a low sorbitol content with a reduction of tensile properties. However, the barrier properties were highly improved particularly with a reduction of WVTR at 23°C-50% RH and of OTR at 23°C-0% RH. These results could be explained by an antiplasticization effect. This work should be completed with several sorbitol contents and other types of plasticizers.

For the moment, the results obtained with the PVOH system are more promising for the development of packaging materials. The addition of MFC showed several advantages such as mechanical reinforcement and a reduction of water vapour permeability. However, possible improvements could be made out on the MFC dispersion with additives, on their water resistance with the possible addition of cross-linker or the impregnation of films.

The chapter allowed to understand the layer formation and to select the best formulations for coating process. PVOH/MFC was thus selected to develop paper & board packaging at larger scale.

The coating colour formulation as well as the properties obtained with coated paper & board is described in the last part of this report related to the development of new barrier paper & board materials using microfibrillated cellulose.

V - Development of barrier packaging board based on MFC

V.1. - Introduction

There is a growing interest for the development of biosourced materials combining low environmental impact and high barrier properties in order to minimize the use of petroleum based polymers. Currently, few technically and economically competitive solutions are available. The aim of this study was thus to develop a new packaging material using microfibrillated cellulose. The packaging materials were elaborated from a base board for its good mechanical properties, its biodegradability and its recycling ability as well as its folding resistance. Indeed, box boards have three main advantages: the protection, the converting ability and the print quality. The Table V-1 summarized characteristics influencing these properties and which might be preserved after coating process.

Protection	Converting	Printing
Mechanical properties (Bursting, Tearing) Rigidity Surface cohesion in Z	Basis weight Rigidity Cohesion Dimensional stability Glueing	Smoothness Whiteness Ink absorption Brightness

Table V-1: Main characteristics of box board.

Therefore, a first barrier layer was deposited on the board surface by coating processes to provide the barrier properties to the final material. Effectively, MFC has a real potential for developing a barrier layer thanks to its ability to form a close network. However, the low solid content (2%) of the suspension as well as its high viscosity is the main drawback for its use in coating processes. To limit these problems, MFC was combined with a PVOH matrix to form a gas and grease barrier layer. Indeed, this system showed very good barrier properties in the previous chapter on nanocomposites. A second barrier layer, more particularly a water resistant layer was then applied on the top of the first layer to form a packaging material. This multilayer system is described in Figure V-1.

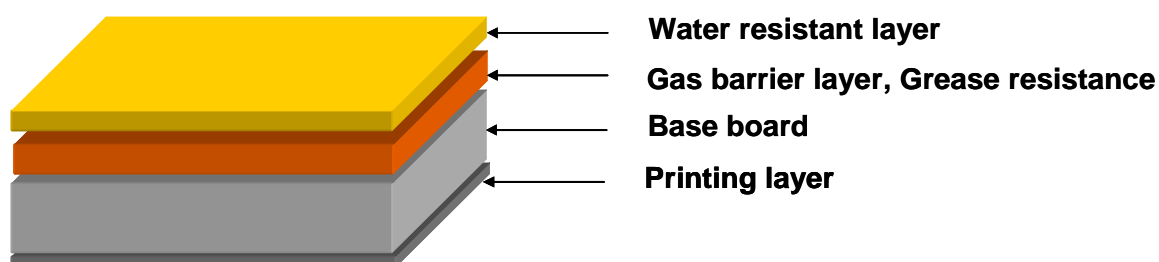


Figure V-1: Scheme of the barrier packaging board.

This chapter describes the development of packaging materials using MFC. The first two parts deal with the production of PVOH/MFC layer on the board surface from lab to pilot scale. The first section details the development of the formulation, the choice of the coating process and the first results obtained at lab scale. The second part expands on the transfer of the process to pilot scale and the properties of the obtained coated board. The last part presents the final demonstrator with the additional top coating layer and its barrier properties.

Moreover, an overview of the biodegradability and converting aspects concludes this chapter. The choice of MFC grades used in this chapter was carried out in the framework of the SUNPAP project and according to the available quantity.

V.2. - Optimisation of the formulation and coating parameters at lab scale

V.2.1. - Introduction

The first step in this work was the adaptation of PVOH/MFC cast films to the coating process in order to deposit a PVOH/MFC layer onto the board surface. These lab trials were carried out using MFC-E-MG (Enzymatic pre-treatment and Masuko grinder treatment).

V.2.2. - Matrix selection

The chapter 4 showed that the barrier properties of films were more efficient for PVOH/MFC composites compared to starch/MFC composites. The main properties are summarized in the Table IV-12: Summary of properties obtained for the best starch/MFC and PVOH/MFC films. Table IV-12. According to these results, the matrix chosen in this study was poly(vinyl alcohol) (PVOH).

	Starch	Starch/MFC (50/50)	Starch/S/MFC (56/14/30)	PVOH	PVOH/MFC (95/5)
Young's modulus (MPa)	1200	5300	3900	1800	2400
WVP (g.µm/m ² .day)	4920	3410	600	17	18.9
OP (cm ³ .µm/m ² .day.bar)	-	125	49	18.8	16.2

Table IV-12: Summary of properties obtained for starch/MFC and PVOH/MFC composites.

For these coating trials, the PVOH grade was unchanged with a degree of hydrolysis of 98% in order to guarantee good barrier properties.

V.2.3. - Preparation of coating colours

V.2.3.1. - Influence of MFC addition on the coating colour solids

PVOH granules were totally dissolved in water under stirring at 95°C for one hour. The polarity of PVOH building blocks induced association phenomena. According to the PVOH supplier [162], its viscosity solution rose very quickly when increasing the polymer concentration that should be limited to 25% to have an acceptable processability (Figure V-2).

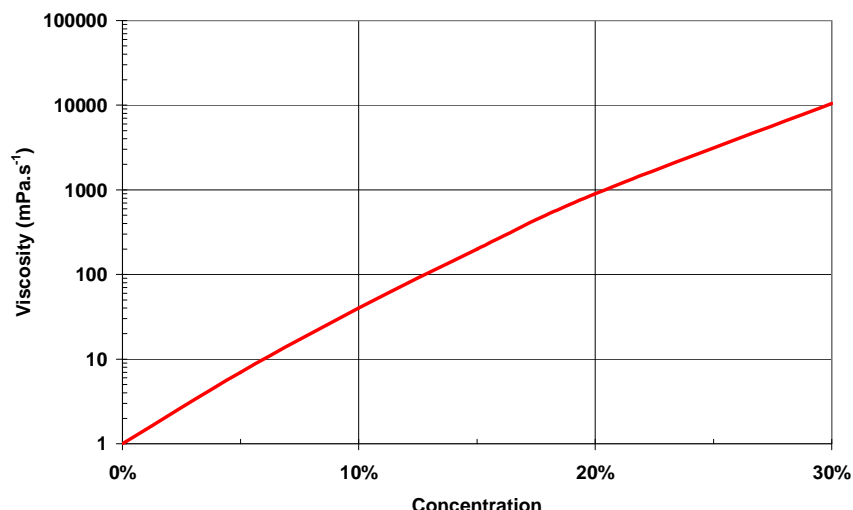


Figure V-2: Viscosity of PVOH solutions at 20°C according to the concentration [162].

After the preparation of the PVOH solution, the addition of the MFC suspension with 2% solids led to a significant decrease of the solid content depending on the MFC content. This is represented by the grey curve in Figure V-3. In red, the evolution of the viscosity was also reported according to the MFC content. The MFC content was expressed as the percentage of MFC in the solid nanocomposite films. The curve is divided into two parts: at low MFC contents (up to 10 wt%) a decrease of the viscosity is observed due to the dilution of the formulation. For higher MFC contents the viscosity leveled off.

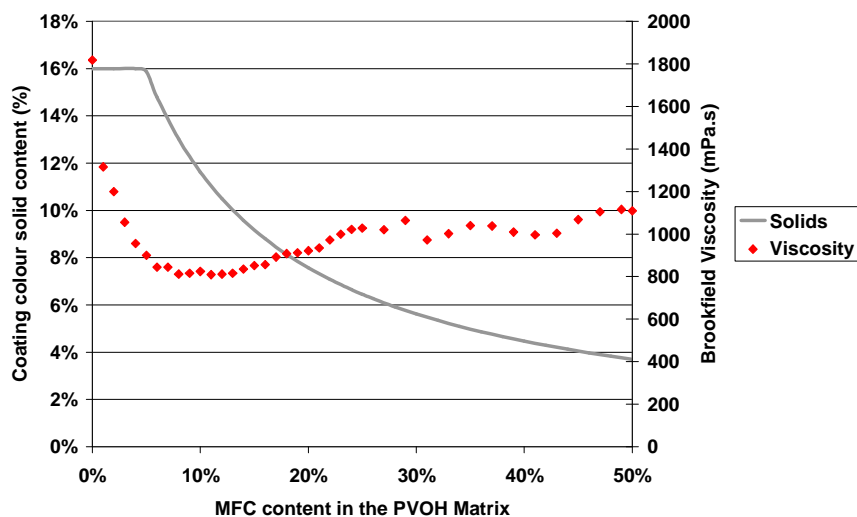


Figure V-3: Solid content and viscosity of coating colours according to the MFC content.

The solid content of the coating colour is an important parameter for the coating process. Indeed, a formulation with a low solid content deposits a low coat weight and the number of passes must be adapted according to the concentration as observed in Figure V-4. These values corresponded to a coat weight of 8 g/m².

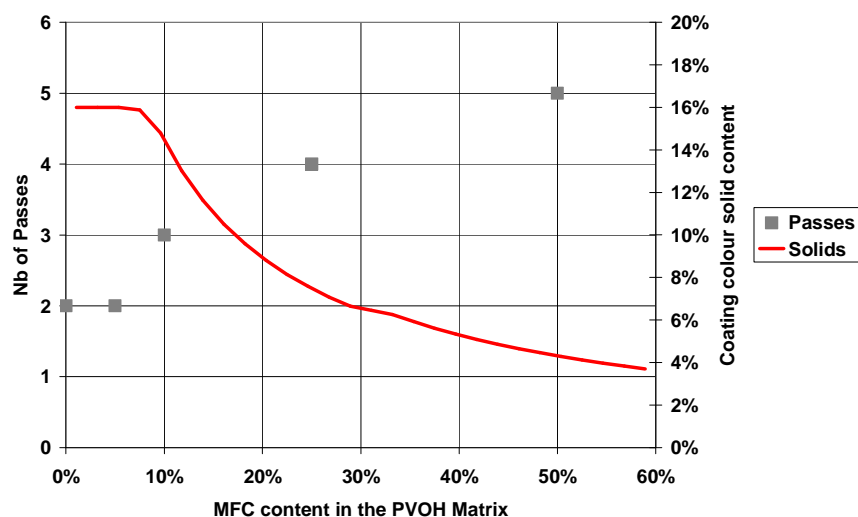


Figure V-4: Number of passes according to the solid content to get a dry coat weight of 8 g/m^2 .

However, the increase of the number of passes leads to an important increase of the production cost and to the degradation of the base substrate. Moreover, low solid contents increase the quantity of water to evaporate and thus the drying energy cost or the difficulties to dry on pilot machine.

Thus, the concentration strongly impacts the coating process and it is necessary to work with a formulation having a concentration as high as possible.

In our case, it was impossible to increase the concentration of the initial PVOH solution. Three strategies were thus imagined and studied:

- Increase of the concentration of MFC suspension with centrifugation process
- Increase of the concentration of MFC suspension with dialysis process
- Increase of the solid content of the mixture by directly solubilizing PVOH in MFC suspensions

V.2.3.2. - Methods tested to increase the concentration of MFC based coating colour

V.2.3.2.1. - Increase of MFC concentration by centrifugation

Centrifugation is a rapid method to remove water from a suspension. Indeed, the centrifuge force applied to the suspension induces the formation of a two phases system with water at the upper side of the suspension. After centrifugation, water was easily extracted and the concentration of the MFC suspension increased. The MFC suspension was introduced in centrifuge tubs with a solid content of 1.85% and was centrifuged for 6 cycles of 15 min each (cf. Figure V-5). The maximum MFC concentration obtained by this technique reached 6.3%. Indeed, no phase separation was obtained with additional cycles.

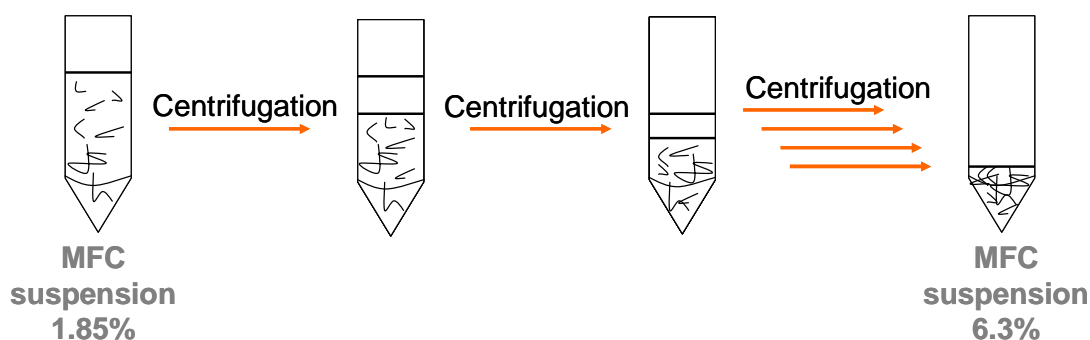


Figure V-5: Increase of MFC concentration by centrifugation.

The visual aspect of MFC concentrated to 6.3% is observed in Figure V-6



Figure V-6: Photos of MFC suspension at 6.3% after centrifugations.

This increase of the solid content naturally led to the increase of the viscosity. As observed in Figure V-7, the viscosity increased 10 times although the increase in concentration only was of 3.4 times.

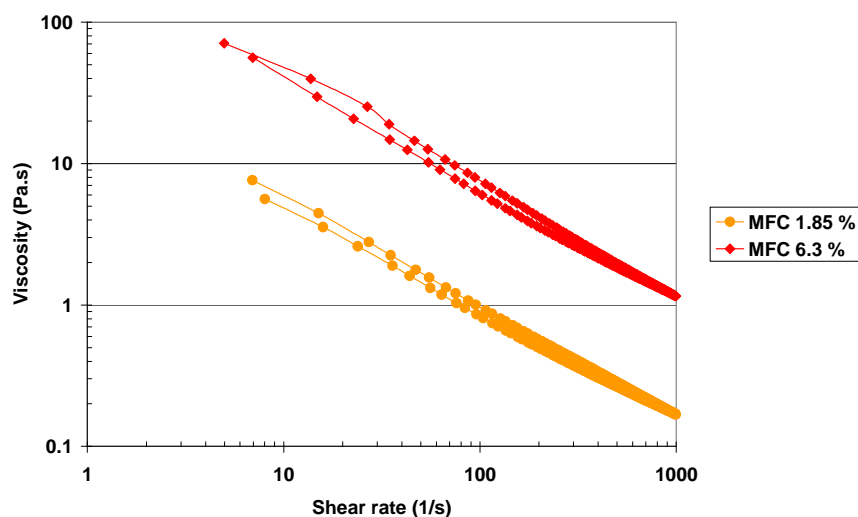


Figure V-7: Viscosity of MFC suspension before and after centrifugation.

This 6.3% MFC suspension was then mixed with a PVOH solution to check the dispersion ability of this very viscous material. The final mixture was very homogeneous showing the possible dispersion of concentrated MFC suspensions after centrifugation.

V.2.3.2.2. - Increase of MFC concentration by inverted dialysis

Inverted dialysis is the second method used to increase the concentration of MFC suspension. The principle, described in Figure V-8, was firstly to introduce the MFC suspension in a membrane having a molecular weight cut off (MWCO) of 12000-14000 g/mol. This system was then immersed in a polyethylene glycol (PEG) aqueous solution at 15%. PEG used had a molecular weight of 100000 g/mol in order to prevent its diffusion inside the membrane. Only water can enter and go outside the membrane. A strong concentration gradient between both sides of the membrane led to the water migration outside the membrane in order to reach a concentration balance.

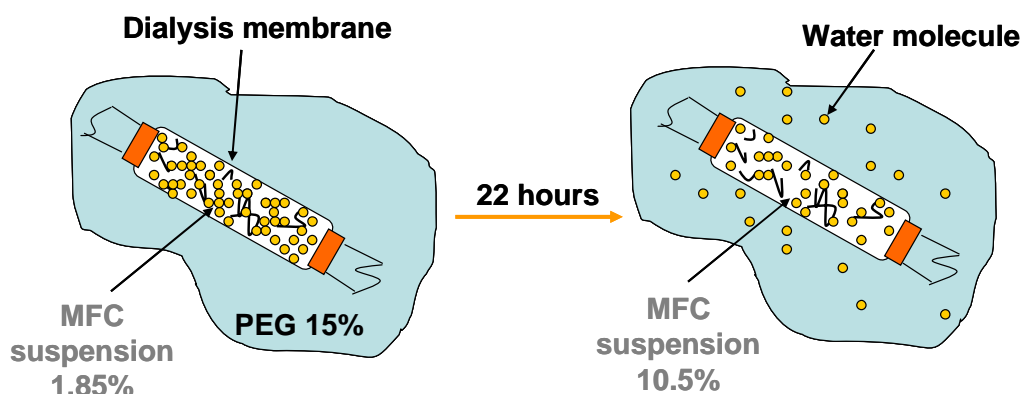


Figure V-8: Concentration of MFC suspension by inverted dialysis.

The concentration of the MFC suspension increased from 1.85% to 10.5% with this technique and the visual aspect of the suspension is seen in Figure V-9.



Figure V-9: Visual aspect of MFC concentrated at 10.5 wt% by inverted dialysis.

However, tests showed that the dispersion of this highly concentrated MFC suspension in the PVOH matrix was difficult and inhomogeneous. Indeed, after a long stirring with high shear forces, residual aggregates were always visualized in PVOH/MFC solutions.

V.2.3.2.3. - Direct solubilization of PVOH in MFC suspension

The third and last technique used to increase the solid content of the coating colour consisted in adding the PVOH powder directly in the MFC suspension (cf. Figure V-10).

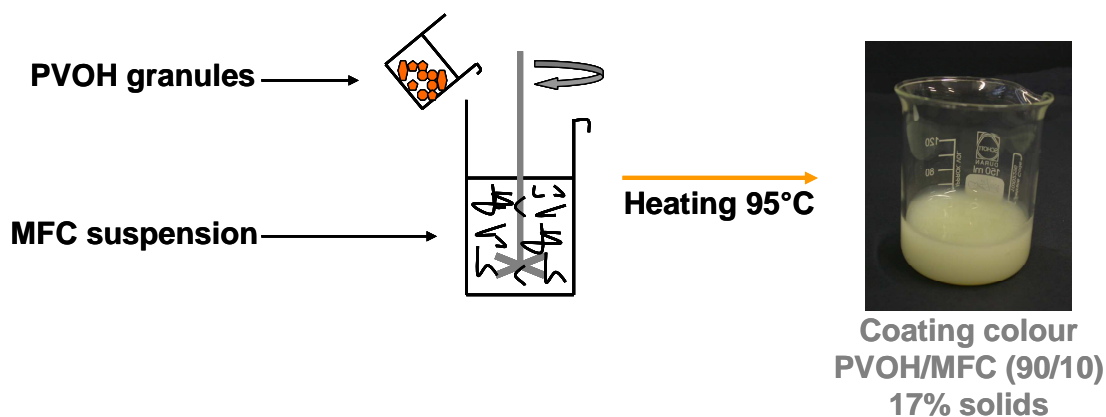


Figure V-10: Solubilization of PVOH in MFC suspension.

The solubilization of PVOH was carried out in the MFC suspension at 95°C under stirring for 1 hour. For a 90/10 wt%/wt% PVOH/MFC ratio, the solid content of the mixture reached 17%. This technique was very fast and allowed to obtain directly a homogeneous coating colour.

This technique was thus chosen and used to perform the following coating trials. Indeed, the preparation method was very fast in only one step and provided a homogeneous suspension. This was not the case for the centrifugation and dialysis, which were more difficult to apply on large quantities with a longer process and dispersion problems in the case of dialysis. Moreover, the influence of the temperature (95°C) on the MFC properties was determined in order to validate the choice of this technique. For this, a MFC suspension was stirred and heated at 95°C for 1 hour in the same conditions as for the solubilization of PVOH. Its viscosity value was compared with the one of the initial MFC suspension in Figure V-11. No significant difference was observed between both curves meaning that the network of the MFC was not impacted by the heating at 95°C.

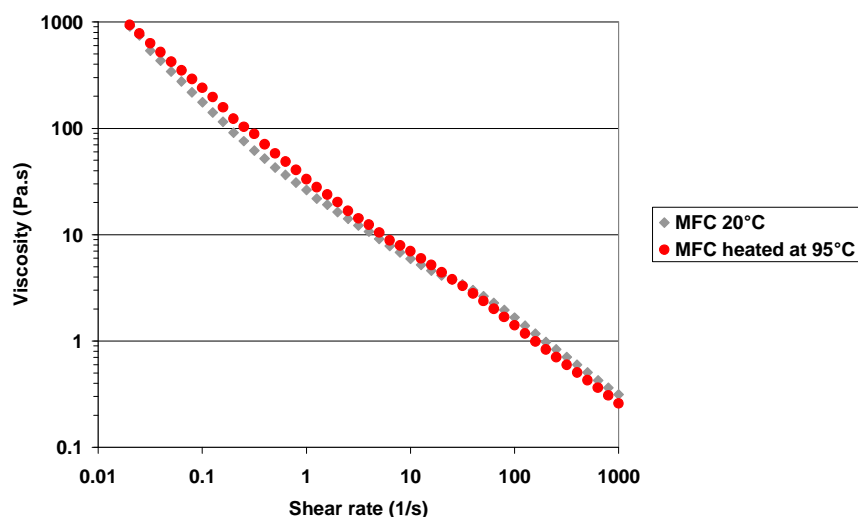


Figure V-11: Viscosities of MFC before and after heating at 95°C during 1 hour.

Moreover, films made from MFC before and after heat treatment were produced and characterized. Mechanical properties of these films, observed in Table V-2, did not show significant differences between the two kinds of films.

	Young's modulus (MPa)	Tensile strength (MPa)	Burst index (kPa.m ² /g)	Tear index (mN.m ² /g)
MFC before heating	5780 (± 720)	323 (± 72)	3.52 (± 0.51)	1.42 (± 0.14)
MFC after heating 95°C 1 hour	6199 (± 494)	388 (± 37)	3.84 (± 0.82)	1.32 (± 0.15)

Table V-2: Mechanical properties of MFC cast films produced from MFC before and after heating at 95°C during 1 hour.

V.2.3.3. - Preparation of PVOH/MFC coating colour

The influence of the MFC addition in PVOH coating colour was carried out for three ratios: 5%, 10% and 15%. As described previously, the solubilization of PVOH was carried out directly in the MFC suspension at concentrations described in Table V-3. Finally, a dilution was carried to reach a final solid content of 15% for each PVOH/MFC mixture.

MFC content (% wt)	Mixture concentration during the solubilization (% wt)
5	20
10	17
15	15

Table V-3: Concentration of mixture according to the MFC content during the preparation of coating colours.

V.2.4. - Viscosity measurement and choice of the coating technology

The viscosity and the rheological behaviour of coating colours are important factors which influence the choice of the coating process. The Brookfield viscosity was determined at 100 rpm for each suspension with a concentration of 15% and at 20°C. Values are reported in Table V-4.

Coating colour	T (°C)	Spindle	Brookfield viscosity (mPa.s)
PVOH	20.2	3	218
PVOH/MFC (95/5)	20.5	4	876
PVOH/MFC (90/10)	20.1	4	1340
PVOH/MFC (85/15)	19.8	5	2280

Table V-4: Brookfield viscosity of coating colours according to the MFC ratio.

The range of viscosity observed for the PVOH/MFC suspensions was compared with the advised viscosity of each coating technology. Here, the viscosity corresponds to usual Brookfield viscosity values and did not considered the shear thinning behaviour of PVOH/MFC mixtures. The PVOH/MFC suspensions had high viscosity especially for 15% MFC. Thus, the most appropriate coating process was the rod and blade coating as observed Figure V-12. This process also was one of the most currently used to develop barrier layers.

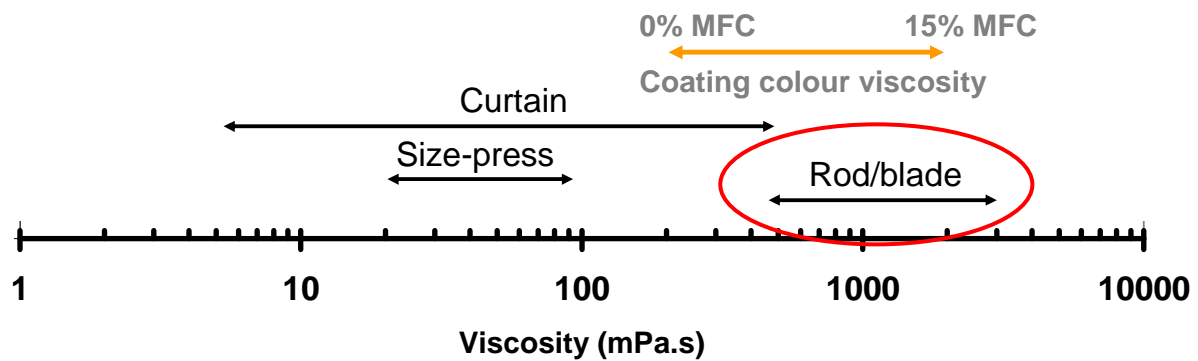


Figure V-12: Coating colour viscosity according to the coating technology [25].

First, coated board samples were thus produced with a laboratory rod coater.

V.2.5. - Production of coated board samples using rod meyer coating

Coated board samples were produced at lab scale to study the influence of PVOH/MFC addition on the final properties of coated board. Coating colours with several MFC ratios ranging from 0% to 15% were deposited on the uncoated bleached kraftboard 223 g/m² dry (from Stora Enso) surface using lab rod coater.

Figure V-13 shows the principle of the rod coating system. The coating colour was deposited on the board surface and spread with the wire wound rod. Figure V-14 describes the structure of the rod with wire coils. The amount of material and thus the coat weight deposited can be adjusted according to the size (width) of the wound. Two other parameters had an influence on the final coat weight: the spreading speed adjusted by the speed of the moving board and the load applied to the rod by weights. Drying was carried out by an infrared dryer system during 3 minutes.

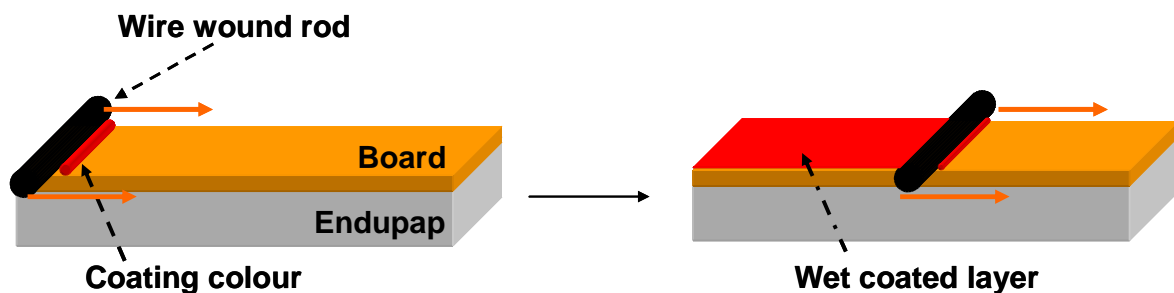


Figure V-13: Scheme of principle of the lab rod coating system.

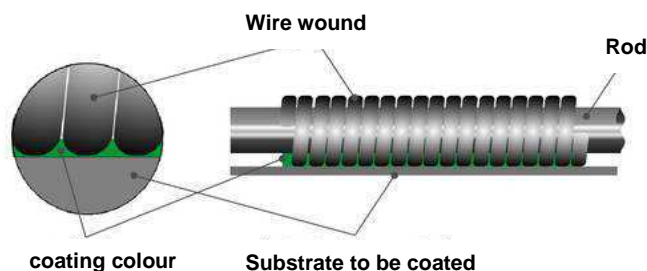


Figure V-14: Scheme of the wire wound rod [173].

A homogeneous and sufficient coverage of the substrate is necessary for the development of barrier properties. According to the kind of substrate, its roughness and its absorption capacity, the required level of the coat weight is different to reach the same level of properties.

Stinga [129] showed in their study that the minimum coat weight to obtain a good coverage with PVOH (Mowiol 4_98) on an uncoated board was between 9 and 15 g/m². From a coating colour concentration of 15%, two passes were necessary to reach this value.

Ten A4 sheets were produced for each formulation after two passes in the rod coater and an infra-red drying.

V.2.6. - Characterisation of PVOH/MFC coated boards

V.2.6.1. - Observation of the surface by SEM

SEM images were firstly performed to check the adequate coverage of the surface with 10 g/m² coating. Indeed, a good coverage is required to develop a barrier layer. The fibres and the porosity of initial board were clearly observed in Figure V-15 (left). Except a small hole, probably due to a blistering effect, the coverage of the surface by PVOH/MFC (95/5) layer was very good, reducing completely the permeability of the base board.

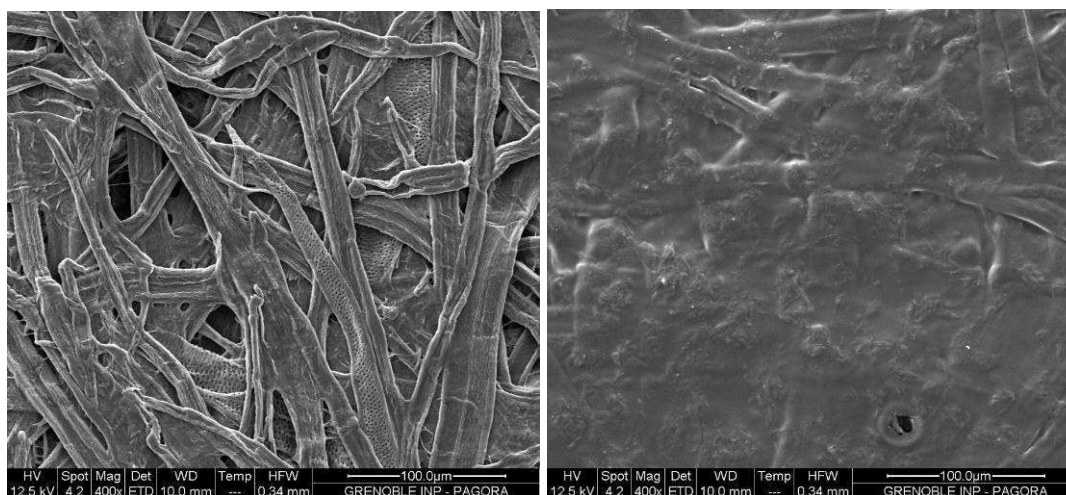


Figure V-15: SEM-FEG images of board before and after coating.

V.2.6.2. - Properties of coated board samples

V.2.6.2.1. - Thickness and coat weight

Table V-5 summarized the basis weight and the thickness of coated samples produced at lab scale. The basis weight deviation of the base board reduced the precision of the calculated coat weight. The layer deposited at the board surface reached between 7.4 and 10 g/m².

	Coated board		Coating layer	
	Basis weight (g/m ²)	Thickness (μm)	Basis weight (g/m ²)	Thickness (μm)
Base board	219.0 (3.4)	324.7 (4.4)		
PVOH	227.7 (1.4)	330.3 (4.0)	8.7	5.6
MFC 5%	228.0 (1.0)	328.4 (3.9)	9.0	3.7
MFC 10%	229.4 (1.2)	327.7 (3.9)	10.4	3
MFC 15%	226.4 (1.4)	332.9 (3.1)	7.4	8.2

Table V-5: Basis weight and thickness of coated board and coating layer.

The determination of the thickness by the deduction of the base board thickness from the coated board thickness gave very low values. This showed that the uncoated board had high roughness and that the coating colour closed the surface as observed Figure V-16. Once again, this justified the need to have a minimum coat weight quite high to close the surface of the uncoated board.



Figure V-16: Effect of the roughness of the uncoated board on the final thickness.

V.2.6.2.2. - Mechanical properties

The objective of this study mainly was to bring barrier properties to board. However, it is important to check that the process used for this don't degrade the mechanical properties. Indeed, the mechanical properties of board are needed to transport products in the best conditions. Therefore, mechanical properties of coated samples were systematically analysed in parallel to barrier properties.

Results regarding the mechanical properties (Figure V-17) showed that the coating slightly increased the Young's modulus of the board. However, the results were roughly similar regardless the MFC ratio. The breaking length of coated boards also was in the same range as the one of the base board.

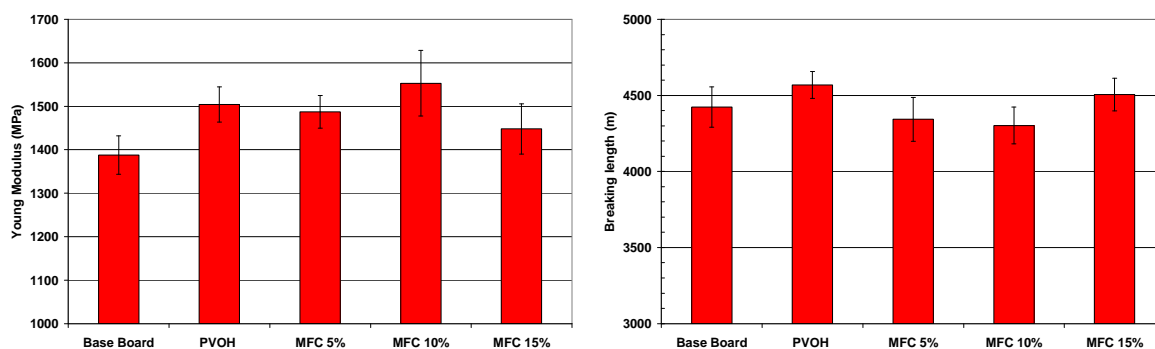


Figure V-17: Mechanical properties of coated boards.

The results of tear and burst index are described in Figure V-18. The coating led to a decrease of the tear index and an increase of the burst index values. The swelling of the board during the coating trials could reduce the bonding forces between fibres and explain this first trend. On the contrary, the PVOH/MFC surface coating increased the adhesion between fibres and improved the burst of the board.

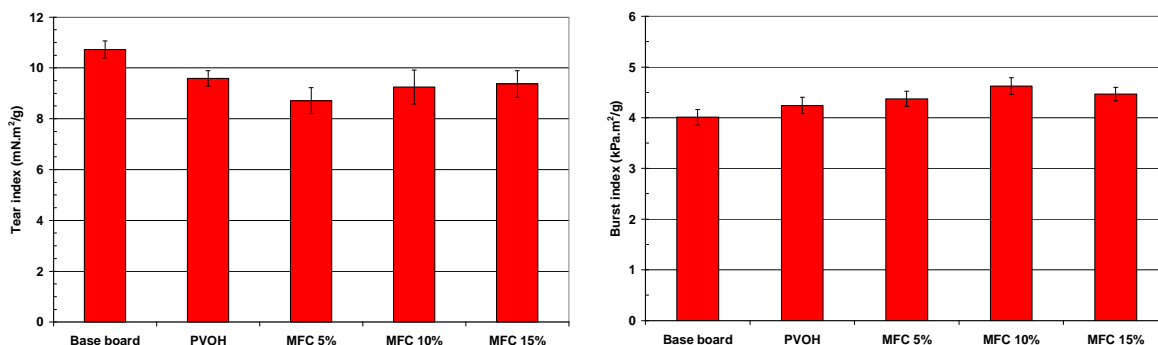


Figure V-18: Tear and burst index of coated boards.

Thus, the layer deposited did not have a major influence on mechanical properties. Interestingly no degradation was observed despite the two rod coater passes with a coating colour with a 15% solid content.

V.2.6.2.3. - Barrier properties

Bendtsen air permeability measurements showed that the coating layer strongly improved the air permeability of the board (Figure V-19). The initial value of 6 cm³/m².Pa.s was decreased to 0.2 cm³/m².Pa.s. This value corresponds to the lower detection limit of the device and all coated samples reached this limit value. Thus this measurement only gave an overview of the coating efficiency but did not allow to conclude which of the samples gives the best properties.

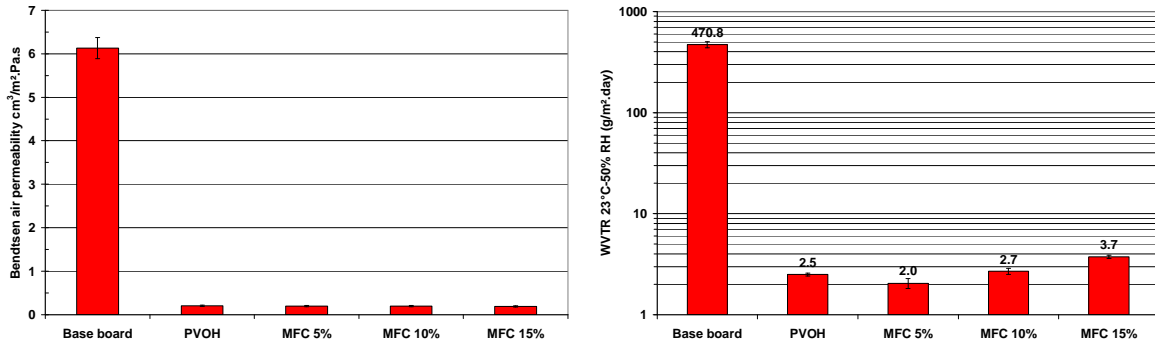


Figure V-19: Bendtsen air permeability and WVTR (23°C-50% RH) values of coated board.

Water vapour transmission rate measurements at 23°C-50% RH also presented good enhancement after coating. Indeed, the PVOH/MFC coating offered interesting values from 2 to 4 g/m².day corresponding to a transmission rate reduction by a factor 100 (Figure V-19). Samples containing 5% showed the best results.

The oxygen transmission rate (OTR) was also determined at 23°C-0% RH and showed significant differences between the samples (Figure V-20). Once again, the coating improved the barrier properties of board with a strong reduction of OTR values: whereas the OTR of base board exceeded the maximum detection of our device (10 000 cm³/m².day), the value obtained for PVOH coating was 2500 cm³/m².day. Then the addition of 5% MFC even decreased the OTR of PVOH coated board reaching a value of 340 cm³/m².day. However, a degradation was observed with higher MFC addition rates. This lack of improvement could be due to the presence of some pinholes in the layer.

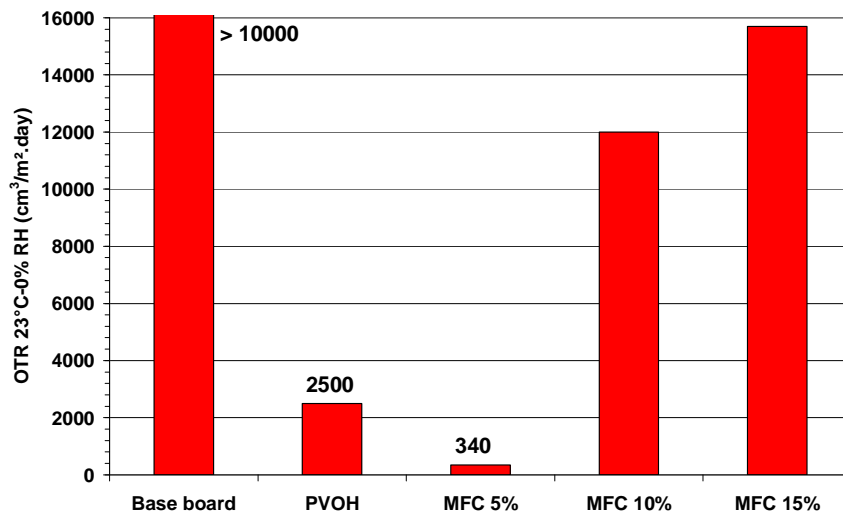


Figure V-20: Oxygen transmission rate at 23°C-0% RH.

These OTR measurements thus confirmed the WVTR results and showed interesting barrier properties for 5% MFC content.

V.2.7. - Comparison with PVOH/MFC composite results

The results obtained for coated layers were compared to the results obtained previously with PVOH/MFC composite films. The permeance equation for multilayer materials is described by Rogers [174]:

$$1/Q_{tot} = L_{tot}/P_{tot} = L_1/P_1 + L_2/P_2 + \dots L_n/P_n \quad (\text{Eq. 18})$$

where Q_{tot} = Transmission rate of the multilayer; P_{tot} = permeance of the coated film; L_{tot} = total thickness of the coated samples; P_1, P_2, P_n = permeance of the n single layers; L_1, L_2, L_n = thickness of the n single layers. Figure V-21 gives a schematic representation of the permeance in multilayer materials.

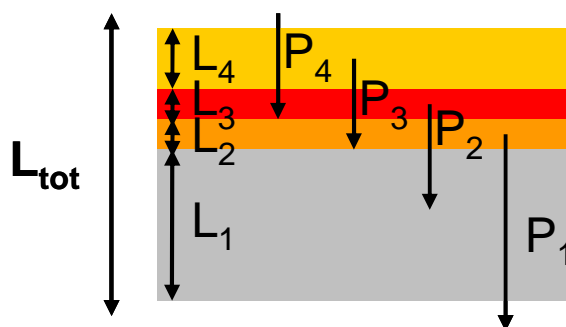


Figure V-21: Schematic representation of the permeance in multilayer materials.

The water vapour and oxygen transmission rates of films and coated layers are compared in Table V-6.

		Thickness (μm)	WVTR 23°C-50% RH ($\text{g}/\text{m}^2\cdot\text{day}$)	OTR 23°C-0% RH ($\text{cm}^3/\text{m}^2\cdot\text{day}$)
PVOH	Film	25	0.6	0.8
	Coated layer	5.6	2.5	2500
PVOH/MFC 5%	Film	27.0	0.7	0.6
	Coated layer	3.7	2	340
PVOH/MFC 10%	Film	26.2	0.8	0.7
	Coated layer	3	2.7	12000

Table V-6: Comparison between barrier properties of PVOH/MFC films and PVOH/MFC coated layer.

The permeance of the base board was very high compared to the barrier layer. Thus, the total permeance of the coated board was mainly due to the permeance of the barrier layer. The experimental thickness of the coated layer was probably underestimated here. However regarding the WVTR at 23°C-50% RH, similar values were obtained for 1 μm cast films and 1 μm coated layer. Therefore, model films gave an overview of the final product developed by coating. But it is not sufficient. Indeed, the OTR values showed important differences between films and coated layers. The drying of cast films was carried out in ambient conditions whereas an infra-red system was employed for coated layers. The drying influences the layer surface quality with the eventual formation of pinholes due to blistering effects. The low OTR of the coated layer compared to model films could be induced by some defects at the layer surface. At last, the absorption ability of the board and its roughness also

influenced on the final layer thickness and thus impacted the barrier properties of the coated layer.

This comparison showed that the preparation of model films is a good way to test the efficiency of formulations and evaluate the properties of future layers deposited by coating processes. However, the final properties of coating layers differed according to the substrate and to the drying quality.

V.2.8. - Conclusion

The possibility to use MFC in a coating process was demonstrated during these first lab trials. For this, the method of preparation was adapted with the solubilization of PVOH directly in the MFC suspension to reach the highest possible solid content. Coated samples were produced at lab scale with a good coverage without strips. Regarding the properties of coated boards, the improvement of water vapour permeability and oxygen permeability was clear after coating and the addition of 5% MFC showed a positive effect on the PVOH layer. Moreover, the mechanical properties were preserved after coating. However, the OTR values were low compared to values obtained with model films. The use of more closed boards and a better drying control are possibilities to improve the final properties.

The concept was thus tested at pilot scale in order to confirm or not the interest of MFC use to develop barrier coating layer.

V.3. - Development of PVOH/MFC barrier layer from lab to pilot scale

V.3.1. - Introduction

This part addresses the development of a PVOH/MFC barrier layer at pilot scale. This layer corresponding to the pre-coat (Figure V-22) was applied to bring a gas and grease barrier layer to the board. The up-scaling and the runnability of trials were firstly detailed and the results of coated board sample characterisations were then analysed. Three kinds of MFC/NFC were tested during these pilot trials. The formulation giving the best results was then selected for the production of the final packaging material.

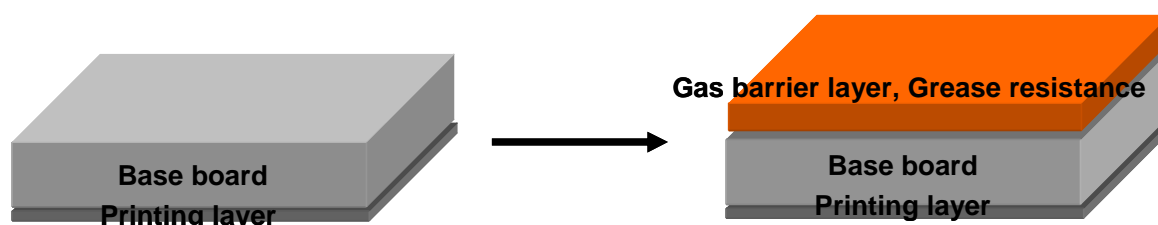


Figure V-22: Production of final barrier packaging board: Gas barrier layer.

V.3.2. - Formulation of the grease/O₂ barrier layer

Three types of MFC produced at pilot scale were introduced in the PVOH solution (Mowiol 4-98): MFC-E-GH, MFC-T-GH and MFC-T-CR. Figure V-23 shows the TEM images of each type of microfibrillated cellulose.

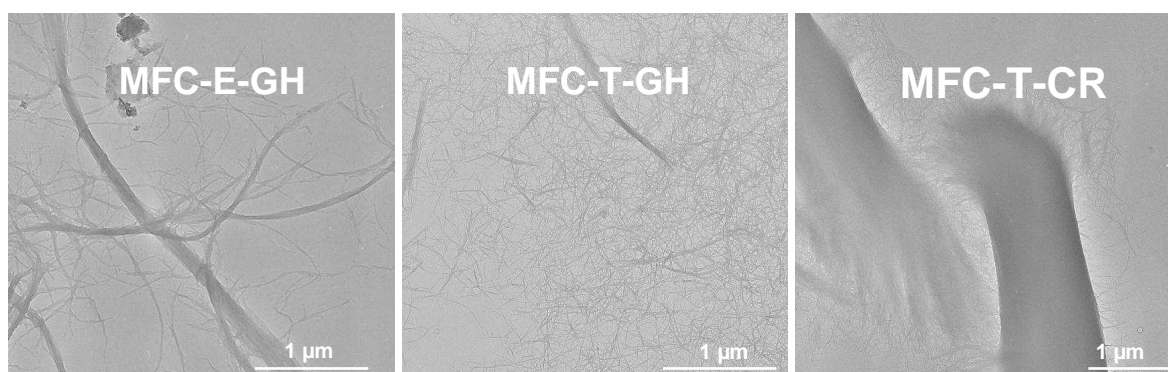


Figure V-23: TEM images of MFC produced at pilot scale.

According to the results obtained previously at lab scale, only two MFC contents were selected, namely 5 pph (≈ 5 wt%) and 10 pph (≈ 9 wt%). Figure V-24 summarizes the formulations tested at pilot scale.

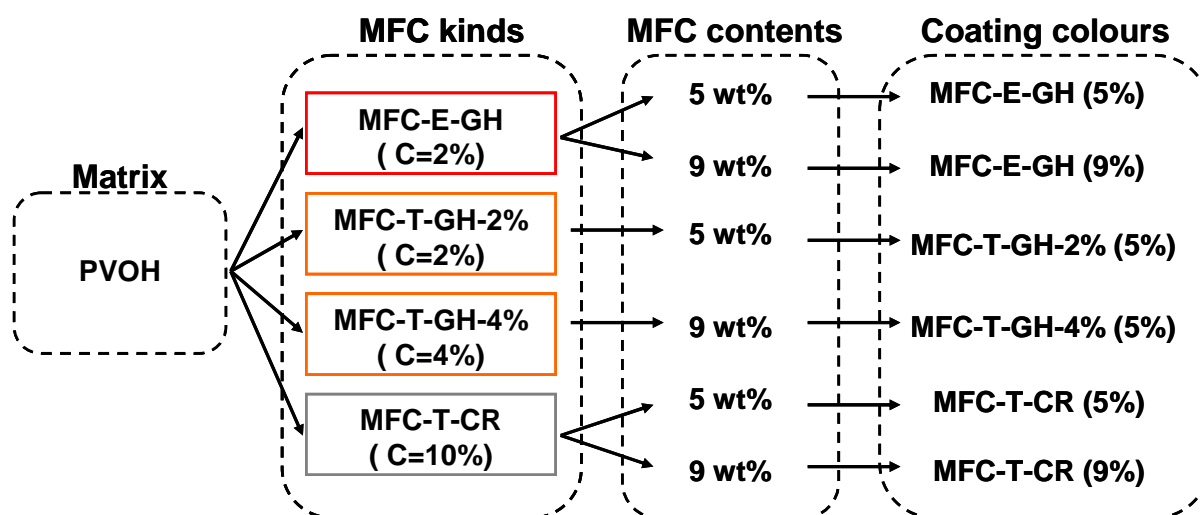


Figure V-24: Formulations of the barrier layer tested at pilot scale.

Moreover, two strategies were employed for the preparation of the formulation in relation to the MFC concentration:

- PVOH was directly solubilized in the MFC suspension for MFC contents lower than 2%.
- For higher solid contents of MFC suspensions (4% and 10%), PVOH was first solubilized and then mixed with the MFC suspension.

V.3.3. - Runnability

The pilot trials are a first and important step in the up-scaling stage; they allowed to confirm the feasibility of formulations at larger scale and to maintain or the not the lab results.

V.3.3.1. - Parameters to control

The transfer from lab to pilot scale requires the control of a higher number of parameters as described in Table V-7. Indeed, the preparation of coating colour involving the direct solubilization of PVOH in the MFC suspension was optimised at lab scale using a 1L quantity with a water bath. The preparation in larger quantity using the direct steam injection was thus a step to validate.

Moreover, the possibilities in terms of viscosity and drying are reduced at pilot scale compared to lab scale. On the pilot coater, the viscosity has to be adapted according to the pumping and coating system. The coat weight and the drying were also determined according to the machine speed. To succeed the pilot trials, all these parameters have to be controlled and adapted in consequence.

	Lab scale	Pilot scale
Solubilization of PVOH in MFC suspension	Water bath	Direct steam injection
Rheology of coating colour	Broad viscosity range	Viscosity adapted to the equipment (pumping, coating system)
Coat weight	Several passes possible	Machine speed, Blade parameters
Drying	Infra-red system Long drying time possible	Electric Infra-red system + forced hot air Time set by the machine speed

Table V-7: Parameters to be monitored at pilot scale.

V.3.3.2. - Rheological behaviour of PVOH/MFC coating colours

Rheological properties of PVOH/MFC mixtures were studied to check the application possibilities. As shown in Figure V-25, the coating colours displayed a shear thinning behaviour, i.e. the viscosity decreased largely when the shear rate increased.

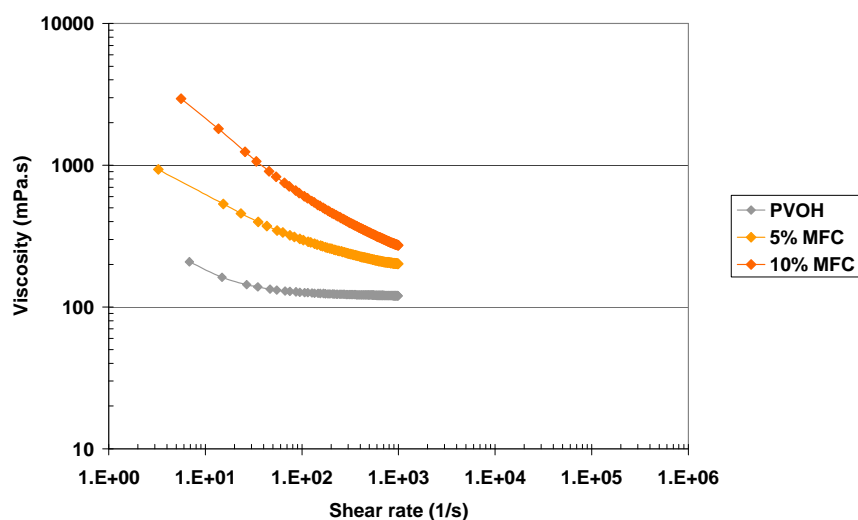


Figure V-25: Viscosity of PVOH and PVOH/MFC coating colours as a function of the shear rate.

Shear rates applied on coating colours during the different steps of the coating process are indicated on the graph. Pumping induces the lower shear rates between 1 and 100 1/s. In this shear rate range the viscosity was very high and this critical point has to be checked. The stirring, in the middle range of shear rates could benefit from the shear thinning

behaviour to facilitate the stirring step. The blade coating and the applicator roll both induce very high shear rates; the viscosity corresponding to these shear rates are acceptable.

V.3.3.3. - Brookfield viscosity of formulations

To limit the problems on the pilot machine, the Brookfield viscosity of each formulation was determined according to its concentration and adapted if necessary to reach the optimum conditions. The pumping system and the coating colour flow in the system were possible until the upper limit viscosity of 1200 mPa.s. A very low flow back was observed for highly viscous coating colour leading to the overflowing as observed in Figure V-26.



Figure V-26: Overflowing of coating colour.

Each formulation was diluted according to its viscosity in order to reach the limit value of 1200 mPa.s. However, the dilution involves a decrease of the coat weight deposited and an increase of the drying demand. In our case, the lower limit in solids had to be fixed at 14% in order to deposit a minimum coat weight of 10 g/m². The obtained results for each formulation are given in Figure V-27. With the limitations, two formulations were impossible to run. Indeed, it was impossible to reach 1200 mPa.s in viscosity for the formulations containing MFC-T-GH at 2% and 4% with a concentration of 14%.

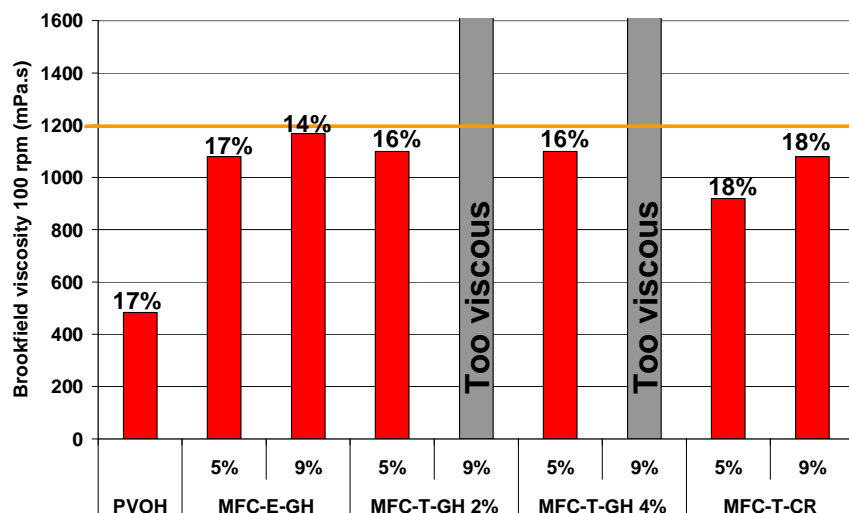


Figure V-27: Concentration and viscosity parameters for all PVOH/MFC formulations

Therefore, pilot trials were carried out using seven final formulations. For all coating colours, the preparation of 50L of coating colour by solubilization of PVOH in a MFC suspension was successful. Indeed, no aggregates were visually observed and the viscosity of the PVOH/MFC blend was closed to the values observed during the lab trials. The upscaling of this protocol was thus validated during these trials.

V.3.4. - Sample production

Coated board samples were prepared on CTP's pilot coater with a Soft-Tip blade equipment and a speed of 70 m/min. Indeed, the Soft-Tip equipment gave the best layer quality without stripes compared to the rod coating system.

Here, the blade scrapes the coating excess at the board surface as described in Figure V-28. The final coat weight was determined according to the length of the blade and the angle between the blade and the paper.



Figure V-28: Principle of the Bent blade [25] (left), photo of DUBLADE Soft-Tip [175].

The barrier layer was thus deposited at the surface of the Ensocoat board. This board was different from the one used for lab trials. This board already pre-coated, had a closed surface which decreased the adsorption of coating colour in board and allowed to obtain a better coating hold out and a more homogeneous layer favouring the barrier properties.

According to the runnability of the formulation, several samples were produced with one or two passes through the blade coater resulting in coat weight comprised between 10 and 20 g/m² (Figure V-29).

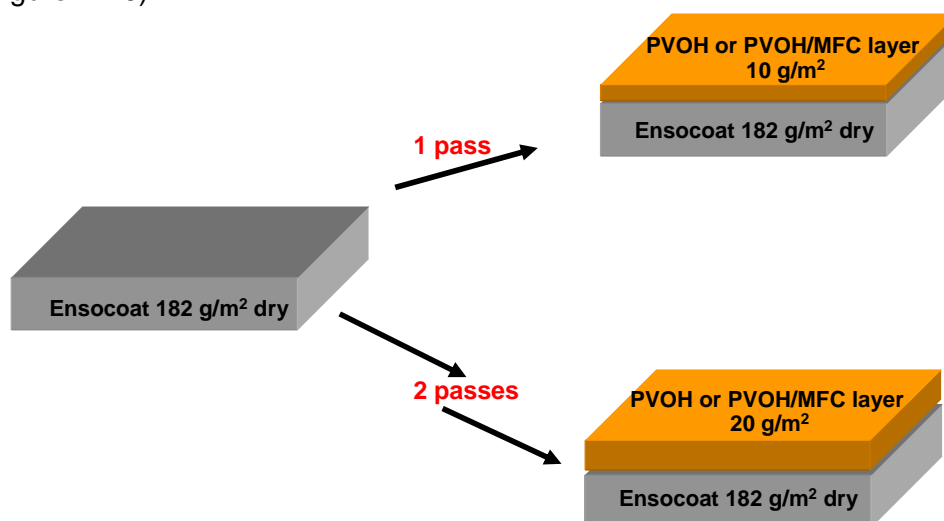


Figure V-29: Coating strategy.

At last, twelve different samples were produced and characterized. Table V-8 details the coating parameters for each sample.

Barrier layer composition			Coating parameters	
Matrix	Grade of MFC	MFC content (wt%)	Number of passes	Coat weight (g/m ²)
PVOH	Without MFC	0	1	10
	MFC-E-GH	5	1	10
			14	
		2	20	
		1	10	
	9	2	10	
		20		
	MFC-T-GH-4%	5	1	10
	MFC-T-GH-2%	5	1	10
	MFC-T-CR	5	1	10
14				
9	1	10		

Table V-8: Coated board samples produced at pilot scale.

Table V-8 gives the list of the coated samples produced and characterized. However, several trials, not indicated here, were done and did not offer good results. More particularly trials were carried out to produce boards with a higher PVOH coat weight. None of these trials were satisfactory because the deposition of two pure PVOH layers one on the other was impossible. Indeed, difficulties in drying the reels were observed leading to the total gluing of reels. On the contrary, a strong blistering phenomenon was obtained. More generally, the samples with a PVOH barrier layer were very difficult to produce. Indeed, PVOH is a good

film forming material and the appropriate drying strategy was very hard to find. The limit between the reel blocking and the blistering of the surface was effectively very narrow. However, this conclusion is really dependent on the coat weight deposited and on the drying potential of pilot coater.

V.3.5. - Characterisations of coated boards

V.3.5.1. - Thickness and basis weight

The basis weight and the thickness of coated boards are summarized in Table V-9. From this data, the basis weight and thickness of the coated layers were calculated by subtraction.

References	Coated board		Coated layer	
	Basis weight	Thickness	Basis weight	Thickness
Base board	182.0 (± 1.6)	209.3 (± 2.5)		
PVOH 10 g/m ²	191.6 (± 2.0)	224.1 (± 2.6)	9.6	14.8
MFC-E-GH (5%) 10 g/m ²	192.1 (± 1.1)	224.5 (± 1.6)	10.1	15.2
MFC-E-GH (9%) 10 g/m ²	190.5 (± 1.1)	222.7 (± 2.2)	8.5	13.4
MFC-E-GH (5%) 20 g/m ²	202.6 (± 1.5)	233.8 (± 1.4)	20.6	24.5
MFC-E-GH (9%) 20 g/m ²	199.2 (± 2.3)	230.4 (± 2.8)	17.2	21.1
MFC-T-GH-4% (5%) 10 g/m ²	192.5 (± 0.7)	227.2 (± 1.9)	10.5	17.9
MFC-T-GH-2% (5%) 10 g/m ²	192.5 (± 0.4)	231.0 (± 1.7)	10.5	21.7
MFC-T-CR (5%) 10 g/m ²	193.4 (± 0.4)	227.5 (± 2.1)	11.4	18.2
MFC-T-CR (9%) 10 g/m ²	192.5 (± 0.5)	230.7 (± 1.8)	10.5	21.4

Table V-9: Basis weight and thickness of coated boards.

The thickness of coated layers was quite high for this basis weight compared to the model films obtained in chapter 4. It is really difficult to know the exact thickness of the coated layer due to the influence of the substrate. Here, the high thickness could be due to the swelling of the board during the first pass in the blade coater. Swelling effect is described by a schematic representation in Figure V-30. The density of the layer seemed more important after two passes in the blade coater. Indeed, the swelling of board occurred only during the first pass when the coating colour is directly in contact with the substrate.

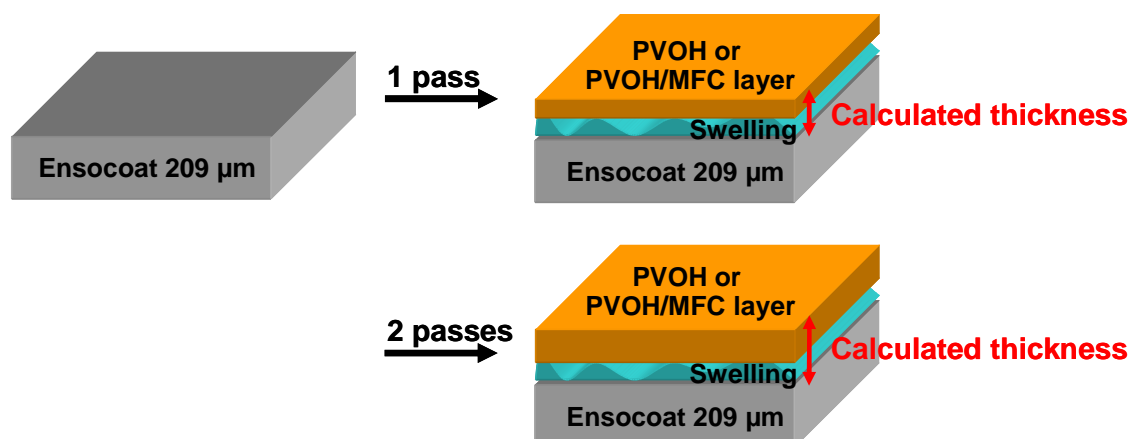


Figure V-30: Effect of board swelling on the final thickness of coated board.

V.3.5.2. - Surface observation

Barrier properties are depending on the layer quality. The surface of coated boards was thus observed in order to confirm the good coverage of the board.

V.3.5.2.1. - SEM images

The surface of coated samples was firstly observed using SEM and a backscattered electron (BSE) detector (Figure V-31). This detector gives images with an atomic number contrast. The light elements appear dark corresponding mainly to organic rich regions. On the contrary, heavy elements appear white corresponding mainly to inorganic area. Here the precoated layer of the base board, containing mineral charges, was well observed covering the fibre surface slightly observed in dark. The coverage by PVOH and PVOH/MFC layers was clearly observed on the other images. Indeed, the inorganic layer (white) disappeared under the organic layer (dark).

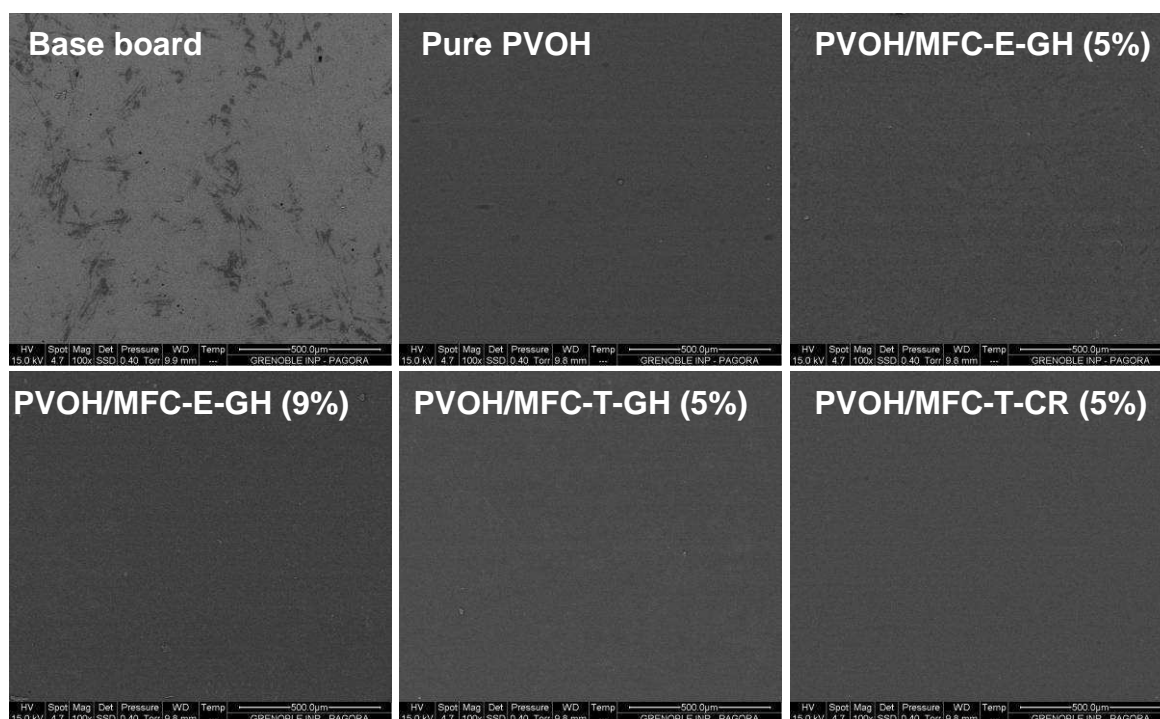


Figure V-31: SEM images with BSE detector of the base board and 10 g/m² coated samples.

Figure V-32 shows the surface topography with SEM observations with secondary electron (SE) detector. The surface aspect was different according to the presence or not of MFC. Indeed, the PVOH layer seemed very smooth compared to the PVOH/MFC layer where MFC could be slightly distinguished.

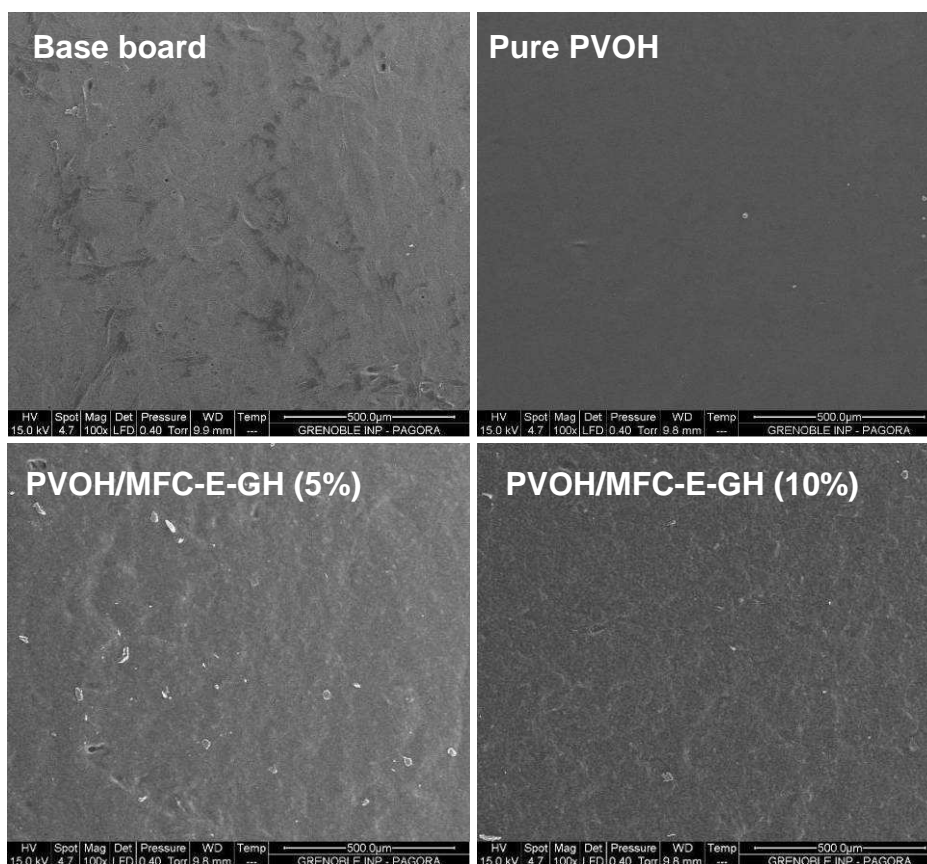


Figure V-32: SEM images with SE detector of the base board and 10 g/m² coated samples.

During the SEM observations, blistering phenomenon was also revealed on the PVOH layer (Figure V-33), an important defect which reduces the barrier properties. As soon as MFC was introduced into the PVOH, the blistering phenomenon was largely reduced showing that MFC improved the drying quality of the PVOH layer.

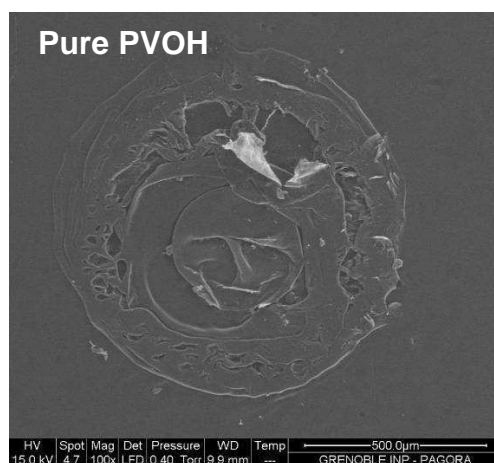


Figure V-33: Blistering phenomenon in PVOH layer.

The cross section of the coated board was also observed by SEM-FEG (Figure V-34). The coated layer observed on the base board was very dense and smooth. It was not possible to observe the presence of MFC which was totally embedded in the PVOH matrix.

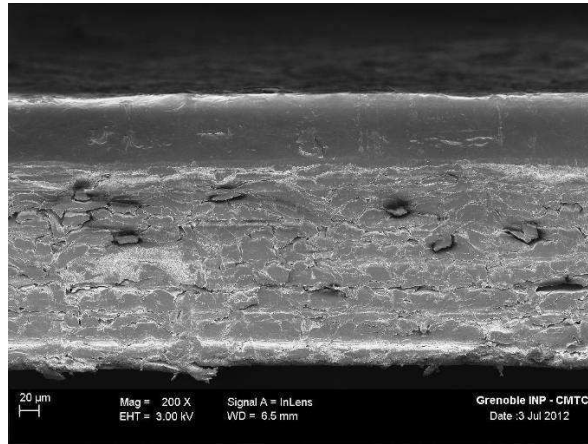


Figure V-34: SEM-FEG images of the coated board (PVOH/MFC-E-GH (5%)) cross section.

These observations firstly showed the good coverage of the base board with PVOH and PVOH/MFC layers. Moreover, the blistering effect occurring during the PVOH coating was revealed but this phenomenon was reduced in presence of MFC in the layer.

V.3.5.2.2. - AFM

In order to improve the understanding of the surface structure, the study of the surface topography and roughness was completed by AFM observations. This technique allowed obtaining a detailed description of the surface and to measure its roughness. The topography, the 3D images and the roughness (determined from this 3D view for an area of $100 \mu\text{m}^2$) of the coated board surfaces are shown in Table V-10 for layers of neat PVOH and with 5 wt% and 9 wt% of MFC. The PVOH layer was very smooth with a very low average surface roughness (R_a) of 0.7 nm compared to 40 nm for the layer containing 5 wt% MFC. The presence of MFC at the layer surface was well seen on these micrographs which leads to higher surface roughness. However, the surface roughness was not influenced by the MFC content. Moreover, the coating process did not lead to a possible orientation of the fibrils according to these images. Indeed, MFC seemed randomly oriented at the surface.

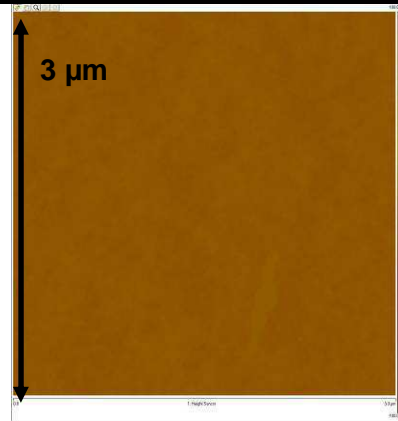
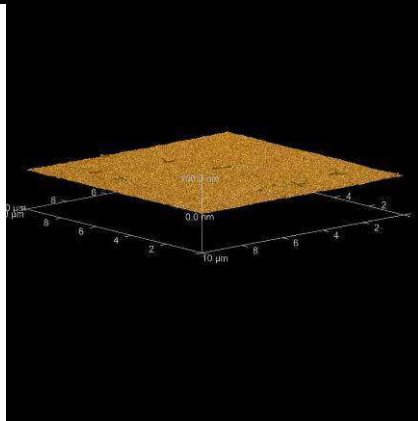
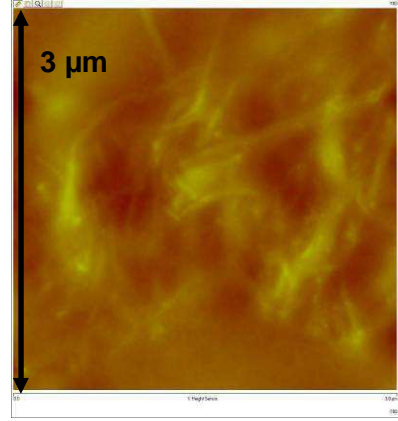
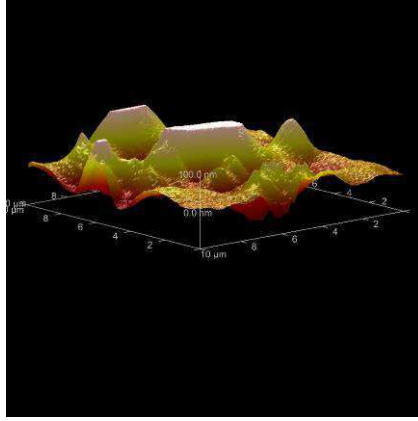
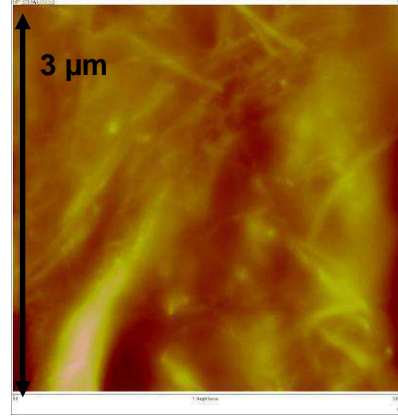
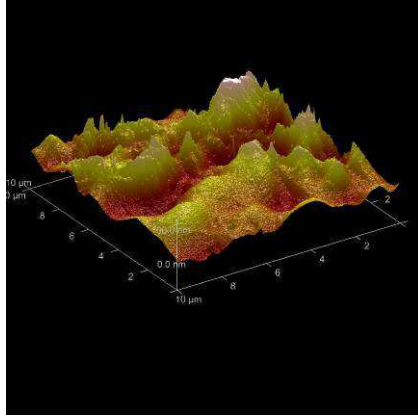
Reference	Topography	3D view	Roughness
PVOH layer on board			Ra= 0.70 nm Rq= 0.69 nm Rmax=25 nm
PVOH/MFC-E-GH (5%) layer on board			Ra= 40.1 nm Rq= 27.9 nm Rmax= 304 nm
PVOH/MFC-E-GH (10%) layer on board			Ra= 33.4 nm Rq= 26.3 nm Rmax= 267 nm

Table V-10: AFM images: Topography of PVOH and PVOH/MFC surface.

These images revealed the structure of PVOH/MFC layer surfaces. MFC was embedded in the matrix in the layer thickness but even appeared at the layer surface. This led to an increase of the roughness of the surface layer compared to neat PVOH. Thus, this explained thus the difference observed in glossy surface after MFC addition. Indeed, this difference in roughness had an impact on the glossy aspect.

V.3.5.3. - Mechanical properties

The impact of the coating process on the mechanical properties of the board was determined by tensile tests. A slight improvement of the Young's modulus of the base board can be observed with the addition of a PVOH layer (Figure V-35). This value was maintained with the MFC introduction whatever the kind of MFC used and the final coat weight.

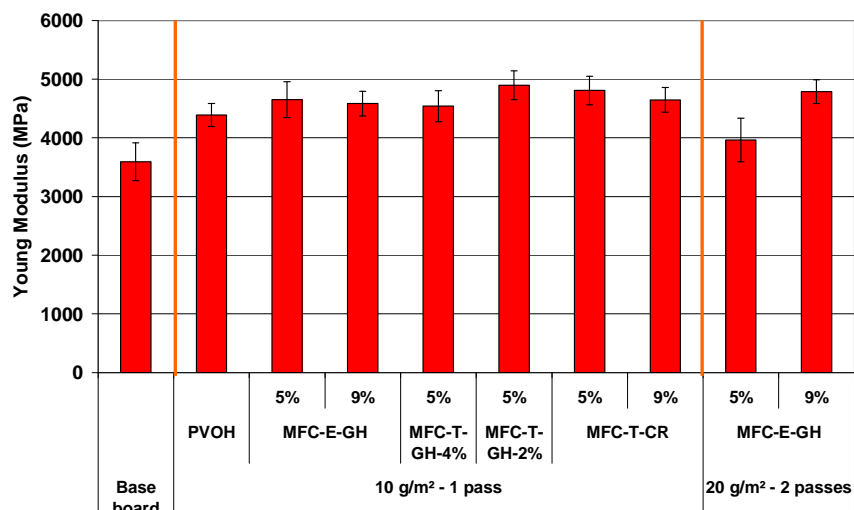


Figure V-35: Young's modulus of coated board samples.

The improvement of breaking length values of the boards was also observed after PVOH coating (Figure V-36). This time, the MFC addition slightly decreased the value compared to neat PVOH coated board but the values were always higher than for the uncoated board. No trend was observed according to the type or content of MFC.

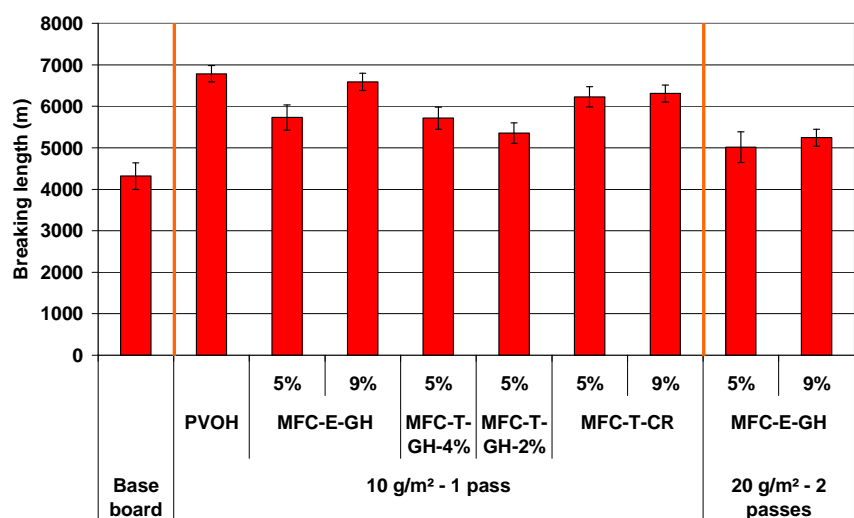


Figure V-36: Breaking length values of coated board samples.

As previously observed at lab scale, the deposition of the coating did not degrade the mechanical properties of the board. On the contrary, the tensile properties were slightly improved with coating although the MFC addition had no significant influence. Moreover, the increase of MFC content did not lead to higher improvement of mechanical properties.

V.3.5.4. - Barrier properties

Barrier properties of coated samples were studied covering several aspects such as:

- Grease resistance,
- Water resistance,
- Water vapour transmission rate for several humidity conditions,
- Oxygen transmission rate at 23°C-0% RH.

V.3.5.4.1. - Grease resistance

The grease resistance is an interesting characteristic for packaging applications because it is generally required to pack a broad range of food.

Here, the coating brought a very good grease barrier. Indeed, Cobb measurements were carried out after an exposure to coloured oil for 24 hours. The amount of absorbed oil after 24 hours was 212 g/m² for the base board. After PVOH/MFC coating, the value reached only 1-2 g/m² according to the MFC content and the type of MFC (Figure V-37).

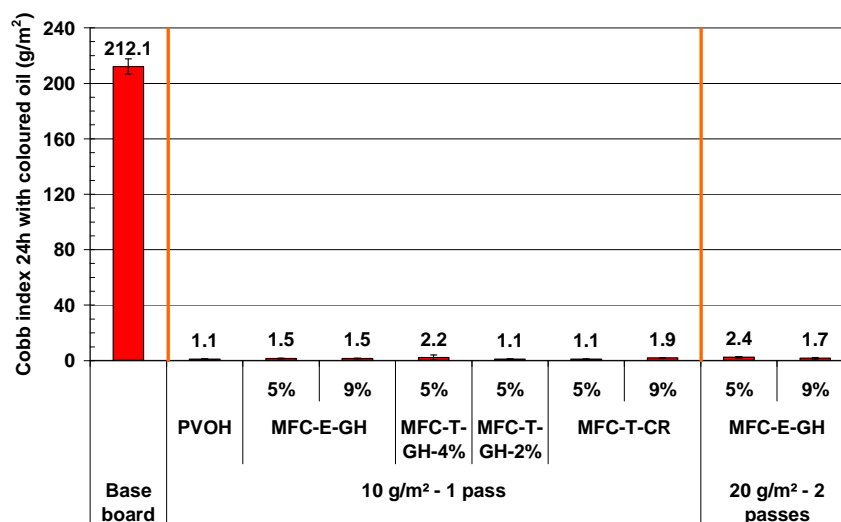


Figure V-37: Cobb index 24h with coloured oil for coated board samples.

The difference before and after coating was clearly visible on the pictures of the boards after the Cobb oil measurements (Figure V-38). Indeed, the base paper was totally red showing that the oil had largely penetrated inside the upper layer. On the contrary, all the barrier coated boards (PVOH/MFC 5% in this picture) remained white, meaning that they were highly resistant to grease.

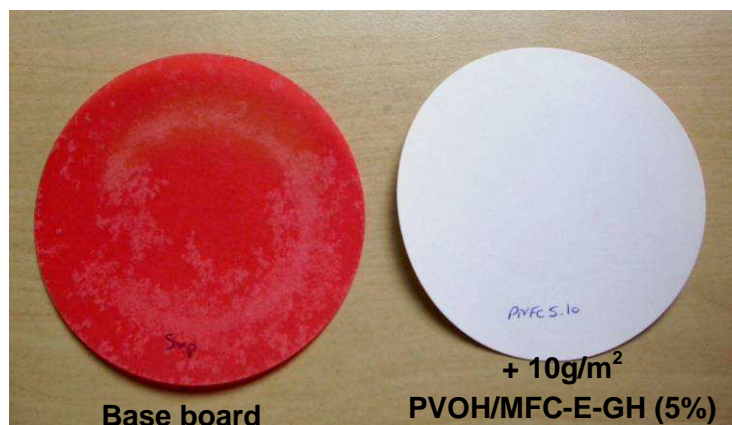


Figure V-38: Photos of board and coated board after Cobb measurements with oil.

PVOH was already known for its good grease barrier properties; here this property was preserved after the MFC addition.

V.3.5.4.2. - Cobb index 60s measurements

The water resistance of coated board samples was determined by specific Cobb60 index measurements. The solubility of the layer was taken into account in the calculation of the Cobb index. For this, the dry weight of the samples was determined before and after the Cobb measurements in order to quantify the layer weight dissolved during the measurement. This weight loss was then added to the water quantity absorbed during 60s. Figure V-39 and Figure V-40 give the results of solubility and specific Cobb index for each coated board sample.

Concerning the water solubility, the PVOH layer showed a high water sensitivity with 40% of the layer solubilised within one minute (Figure V-39). The introduction of MFC-E-GH greatly improved the water resistance of the layer. Indeed the dissolved part of PVOH/MFC layer was only 2%. However, the important standard deviation showed that the measurement was not accurate enough for very low values. The kind of MFC introduced in the layer had an influence on the layer solubility. Indeed, the use of TEMPO pretreated MFC had a lower impact on the reduction of PVOH layer solubility; 30% of the layer was always solubilised after 60s exposition to water.

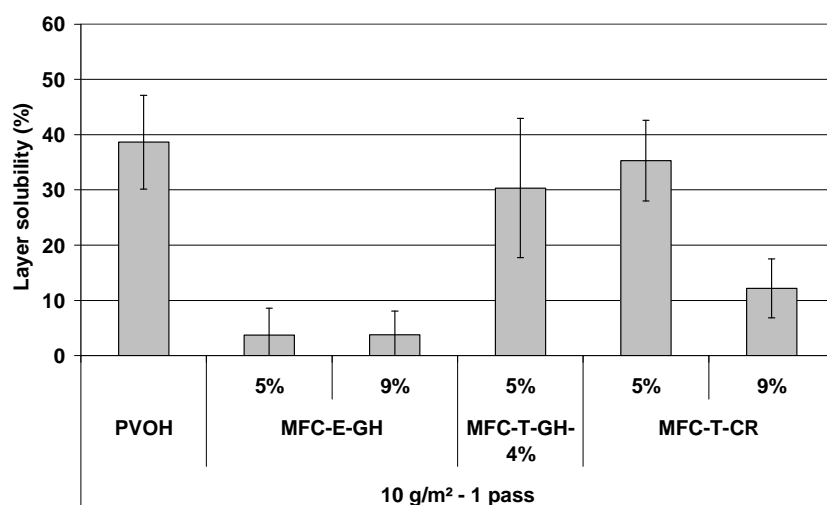


Figure V-39: Water solubility of the layer after contact with water for 60s.

Several reasons could explain these results. As observed in AFM images, MFC are present at the surface of the coating layer. The strong interactions between PVOH and MFC were demonstrated in Chapter 4. MFC could thus retain the PVOH on the layer. However, the retention seems to be different according to the type of MFC. Indeed, the impact of MFC-T-GH was lower than for MFC-E-GH. The hydrophilic character of TEMPO-oxidized MFC was probably the reason of this observation. Indeed, as previously observed in Chapter 3 dealing with MFC films and their properties, TEMPO MFC has a more important anionic charge at the fibre surface and this increase its hydrophilic character and water sensitivity. Moreover, the thinness of MFC-T-GH (observed in TEM images in the Introduction) could also reduce the retention ability of MFC for PVOH. Another possibility is that the surface charge of TEMPO MFC reduced the compatibility with no charged PVOH.

At last, it is needed also to consider an eventual influence of the drying on the final layer solubility. As detailed in the chapter 4, the heating of PVOH films at high temperature reduced their water solubility. During the pilot trials, it was difficult to control precisely the drying conditions; it is thus impossible to guarantee unchanged drying conditions for all coated samples.

The Cobb values showed a decrease of the water absorption from 20 g/m² to 5 g/m² with the use of 5% of MFC-E-GH (Figure V-40). However, the increase of the MFC content to 9% led to the increase of the Cobb value to 18 g/m². The film cohesion was possibly lower for this MFC content or there were MFC aggregates.

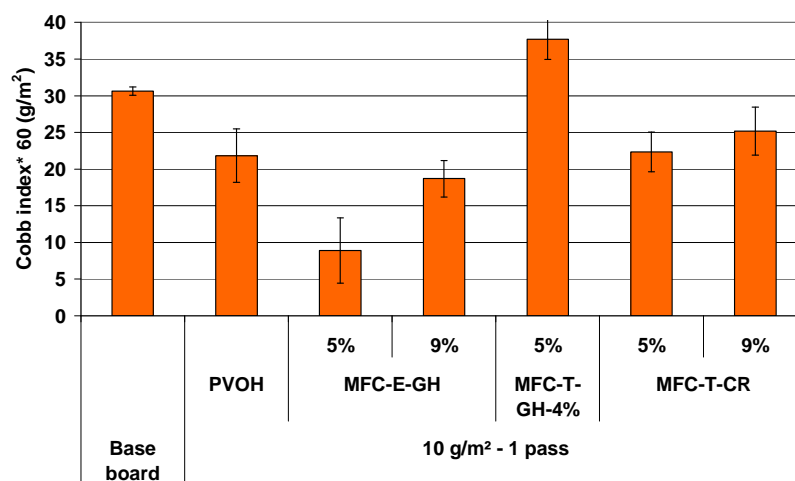


Figure V-40: Water resistance of coated board samples determined by Cobb index 60.

Following the same trend as the solubility, PVOH/TEMPO MFC layer showed the highest values. An important difference was observed between MFC-T-GH and MFC-T-CR. This was probably due to their difference in element size. Effectively, MFC-T-GH was very thin compared to the other and thus was also more sensitive to water. Indeed, the thinnest elements had also the highest specific area.

V.3.5.4.3. - Cobb index 300s measurements

When the measurement was performed for longer times (300s), the layer solubility was almost the same compared to 60s. No increase of the phenomenon was reported when increasing the water contact time (Figure V-41). This could mean that the interactions

between PVOH and cellulose were all the same strong and only the upper layer of PVOH layer can be dissolve in presence of water. Moreover, MFC has the same effect on the solubility of the PVOH layer.

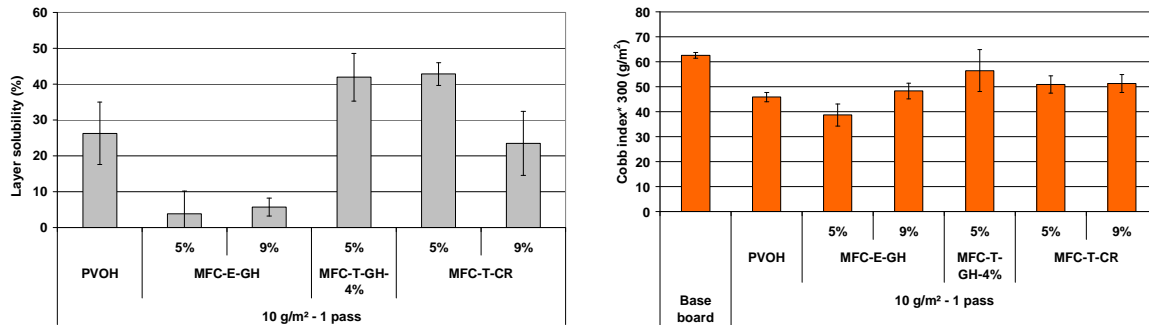


Figure V-41: Water resistance of coated board samples determined by Cobb index 300.

For this measurement time, the differences between samples were reduced and the Cobb index 300 values were closer. Although the difference in water resistance with and without MFC was largely lower, the best value was always obtained with 5% MFC.

This means that the water absorption rate of the PVOH/MFC layer was lower than the one of neat PVOH but the layer remains similarly water sensitive.

After these Cobb measurements, the layer removal was revealed by grease application. Indeed contrary to the layer, the board absorbed the grease. Photos in Figure V-42 show thus the impact of water on the layer. These results are in agreement with the solubility results.

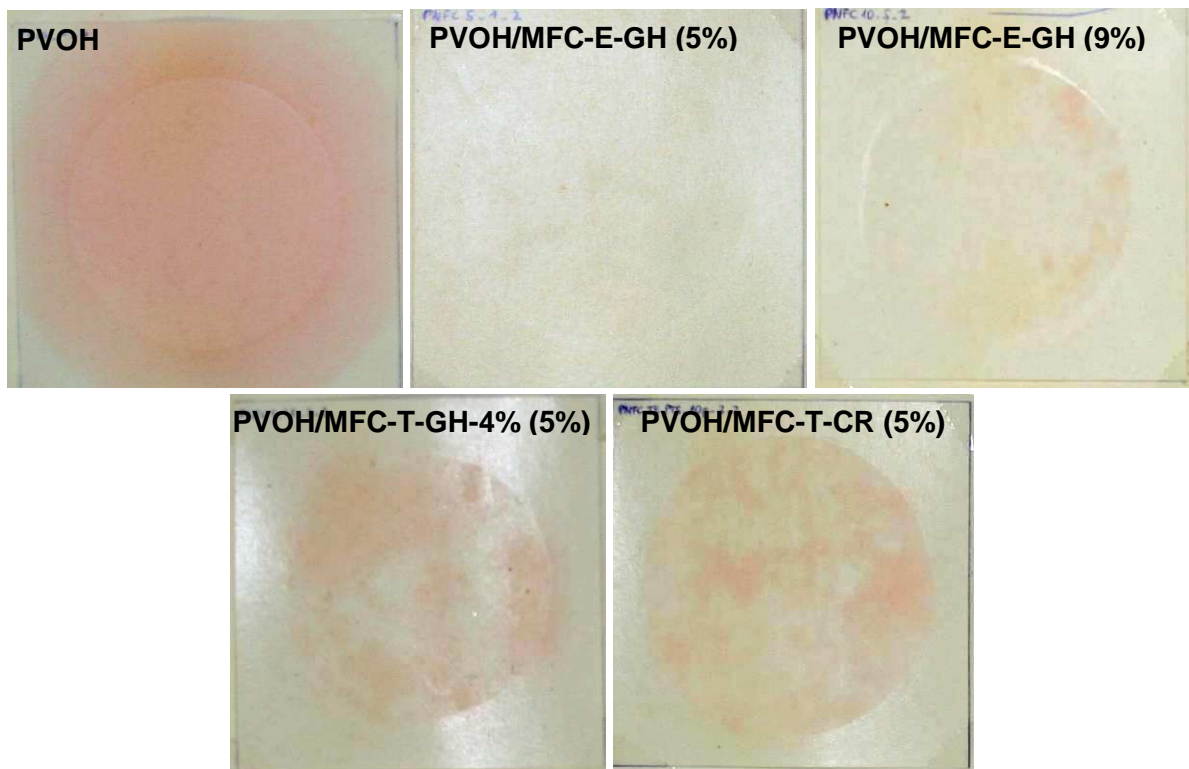


Figure V-42: Photos of coated boards after Cobb measurements and grease test.

To increase the contrast and to improve the visualisation, images editing was performed by coloration in black and white the pink and white area respectively (Figure V-43). The degradation of PVOH layer after Cobb measurement was thus clearly observed. The influence of MFC grade was also revealed; layers produced from TEMPO oxidized MFC were very affected compared to the layers with enzymatic pretreated MFC.

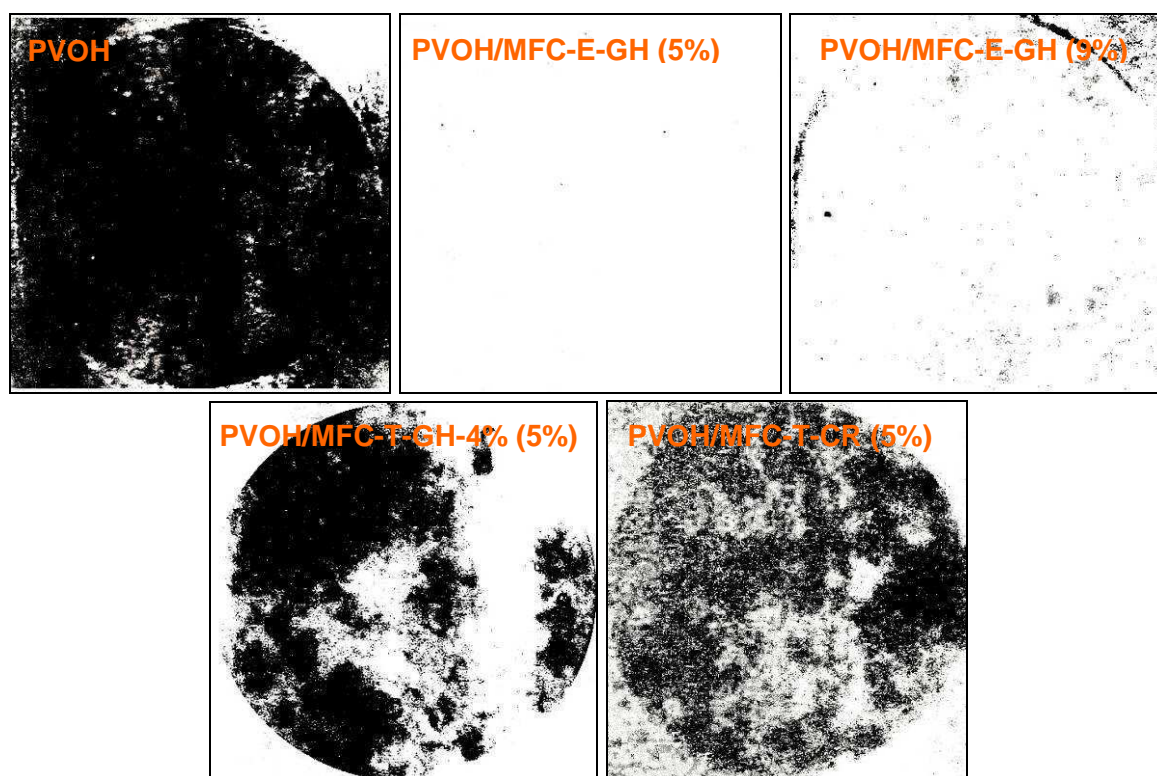


Figure V-43: Edited images of coated boards after Cobb measurements and grease test.

The addition of MFC-E-GH had a positive effect on the water resistance of the PVOH layer. An improvement of the layer adhesion could also be envisaged in presence of this MFC.

V.3.5.4.4. - Water vapour permeability

The water vapour transmission rate (WVTR) was studied under three conditions: 23°C-50% RH, 23°C-85% RH, and 38°C-90% RH in order to observe the influence of relative humidity on the barrier layer properties. The values of WVTR 23°C-50% RH are presented in Figure V-44 and Figure V-45. At ambient conditions, the WVTR obtained for a deposition of 10 g/m².day in one pass was around 2 g/m².day for neat PVOH or PVOH/MFC layer. Compared to the initial board value of 274 g/m².day, the improvement of barrier properties was obvious after coating.

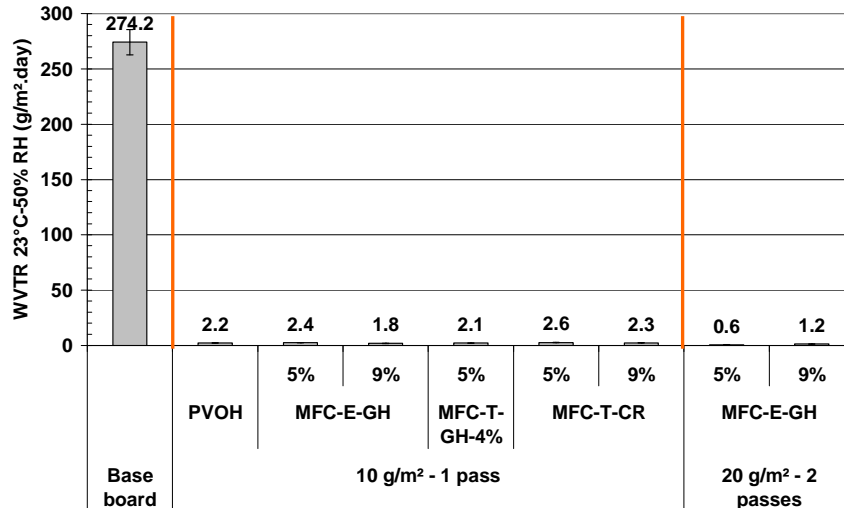


Figure V-44: WVTR at 23°C-50% RH for coated board samples.

The comparison of formulations was observed on the graph with smaller scale (Figure V-45). On this graph, no significant difference was observed according to the kind of MFC used and the MFC content. The increase of coat weight to 20 g/m² allowed decreasing the value to less than 1 g/m².day, the limit of the standard. This improvement was partially due to the masking of the defects of the 1st layer by the second layer.

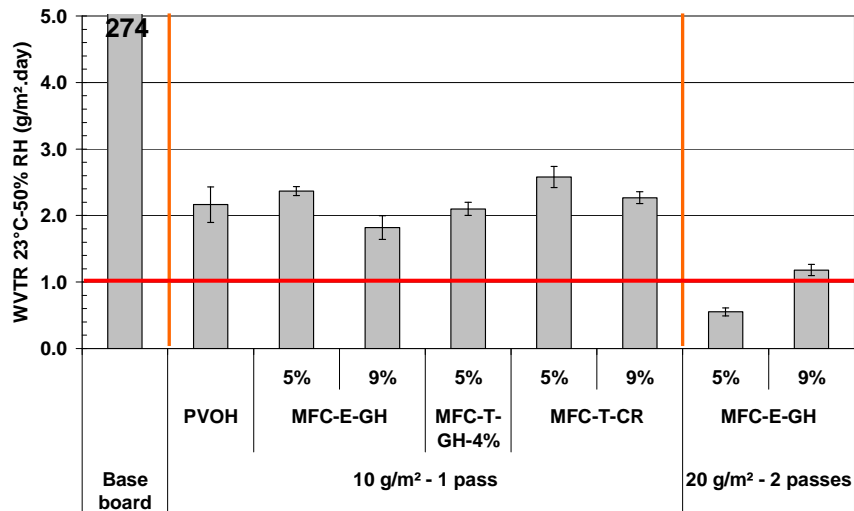


Figure V-45: WVTR at 23°C-50% RH of coated board samples (Zoom).

These results were compared with those obtained previously at lab scale (Figure V-46). Despite the fact that the substrates were initially different, results were very similar whatever the MFC content. The WVTR values of coated boards corresponded to the WVTR values of the PVOH or PVOH/MFC layers. This also confirmed the good coating quality obtained at pilot scale.

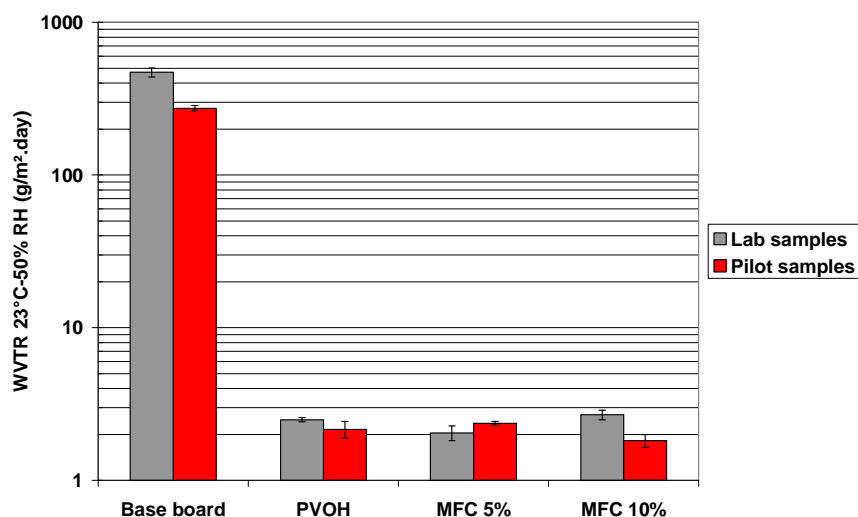


Figure V-46: Comparison of WVTR 23°C-50% RH of samples produced on a lab and on a pilot scale.

The influence of the relative humidity on the water vapour permeability was determined for three humidity levels: 23°C-50% RH, 23°C-85% RH, and 38°C-90% RH. Each condition corresponded to the water quantity in air according to the diagram of Mollier described in Table V-11.

Conditions	Water quantity in air (g/m ³)
23°C-50% RH	10
23°C-85% RH	17
38°C-90% RH	41

Table V-11: Water quantity in air for different relative humidities.

Figure V-47 clearly shows the loss of water vapour barrier properties with the increase of relative humidity. Here, the MFC addition did not have a significant effect on these properties contrary to the results obtained in Chapter 4 for nanocomposites. Here, the adhesion of the PVOH layer on board reduced the PVOH chain mobility and the impact of humidity on the layer properties. The impact of MFC addition, with hydrophilic character, also was lower in the coating case.

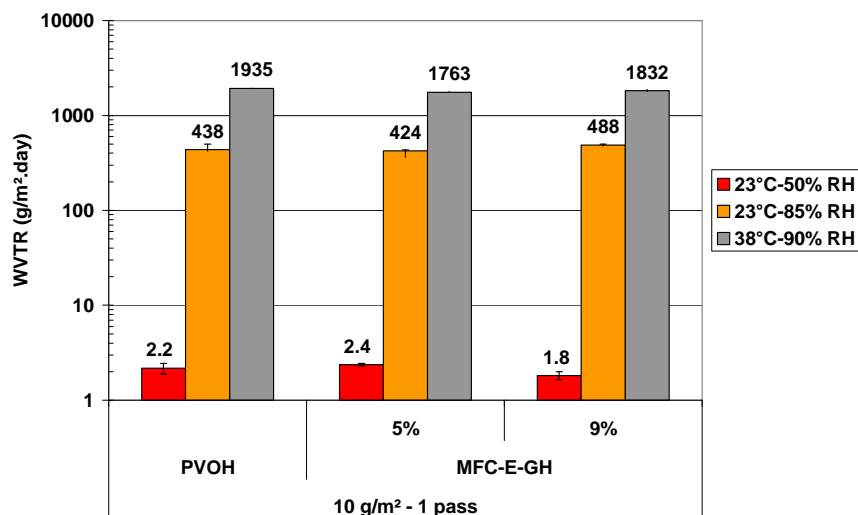


Figure V-47: Influence of the relative humidity on the WVTR of coated board samples.

.At 38°C-90% RH (Figure V-48), the three types of MFC gave WVTR values in the same range around 1800 g/m².day slightly below the value for neat PVOH (1935 g/m².day). The use of two passes and the deposition of 20 g/m² of PVOH + 5 wt% of MFC-E-GH allowed decreasing the WVTR down to 1200 – 1400 g/m².day. However, this decrease was not sufficient to justify the use of a layer twice as thick.

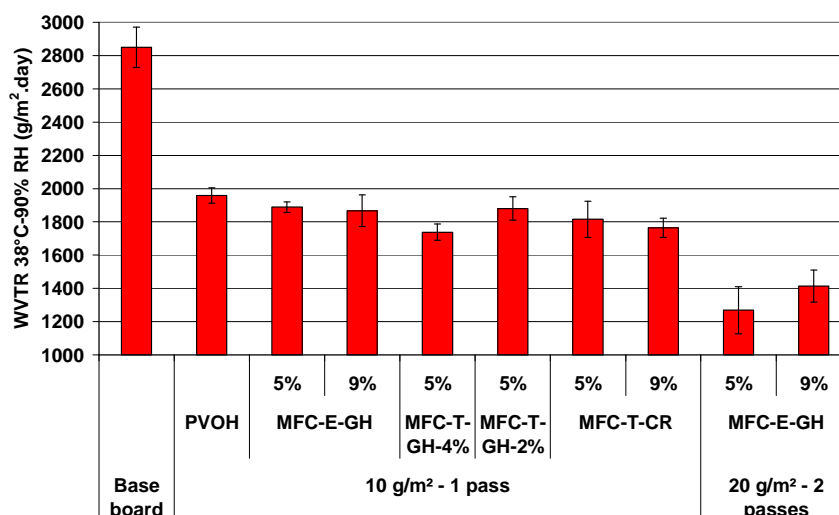


Figure V-48: WVTR at 38°C-90% RH of coated board samples.

As observed from the water resistance results, the PVOH/MFC layer was very sensitive to water and the barrier properties were degraded with the increase of relative humidity. The use of MFC did not modify significantly the water vapour barrier properties of PVOH. Indeed, the values remained very low in ambient conditions and a slight improvement was observed for the highest humidity level.

V.3.5.4.5. - Oxygen permeability (23°C-0% RH)

To complete the characterisation of barrier properties of coated samples, oxygen transmission rate measurements were carried out at 23°C-0% RH (Figure V-49). The results clearly showed the problem of blistering encountered with neat PVOH. Whereas PVOH is

known for being a very good oxygen barrier, the OTR values obtained for board coated with 10 g/m² of PVOH were very poor, above 600 cm³/m².day. OTR values were around 5-6 cm³/m².day.bar for MFC-E-GH and MFC-T-GH and around 9 cm³/m².day.bar for MFC-T-CR. These results showed the improvement of runnability and drying of the PVOH layer with the MFC addition, already observed from SEM images and during the pilot trials.

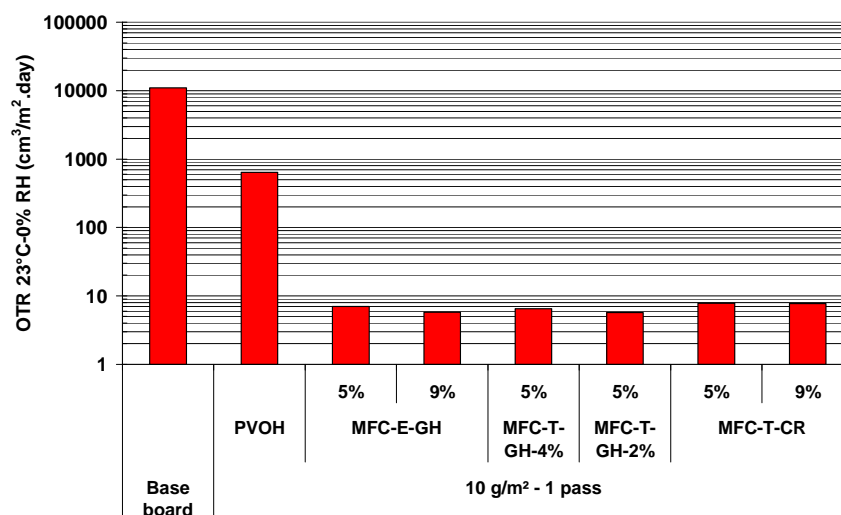


Figure V-49: OTR at 23°C-0% RH for coated board samples.

V.3.6. - Discussion

All the results demonstrated the beneficial effect of using MFC in terms of runnability and productivity. Indeed, MFC played a major role in the drying quality with the large reduction of blistering in PVOH layer after MFC addition. This led to the improvement of barrier properties directly linked to the layer quality. Moreover, MFC had strong interactions with PVOH allowing the development of a highly cohesive layer and the achievement of very promising barrier properties.

V.3.6.1. - Study of drying rate

In order to gain an understanding on the effect of MFC, the drying rate for each formulation was determined. Figure V-50 reveals a difference between the formulations of same solids with and without MFC. After MFC addition, the drying rate was higher compared to the drying rate of PVOH layer. Thus, It was to dry PVOH/MFC layer easier than neat PVOH layer. The water was evaporated faster probably thank to interfacial area between PVOH chain and MFC.

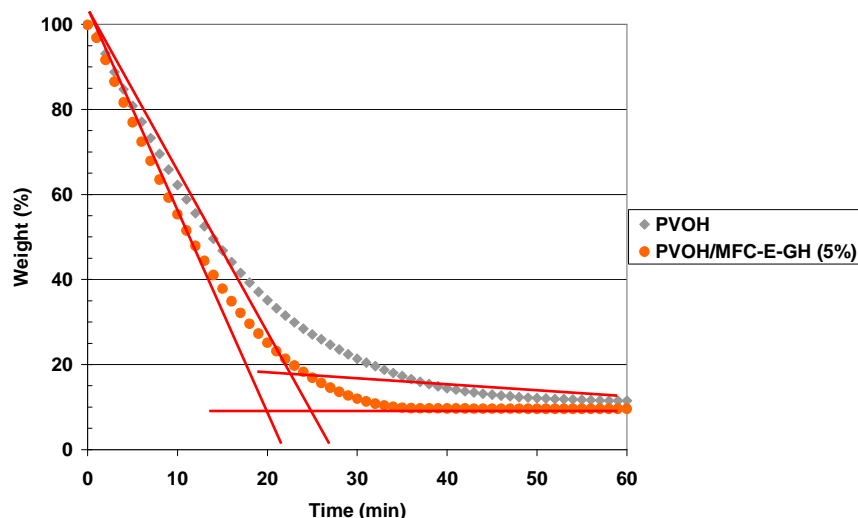


Figure V-50: Drying speed of PVOH and PVOH/MFC formulations.

This could explain the observation made during the pilot trials. Indeed, the blistering effect is mainly due to a drying in two steps (Figure V-51):

- Firstly the drying of the top layer catching the water molecule inside the layer.
- Secondly the drying of the bottom of the layer leading to the layer blistering to allow the water evaporation.

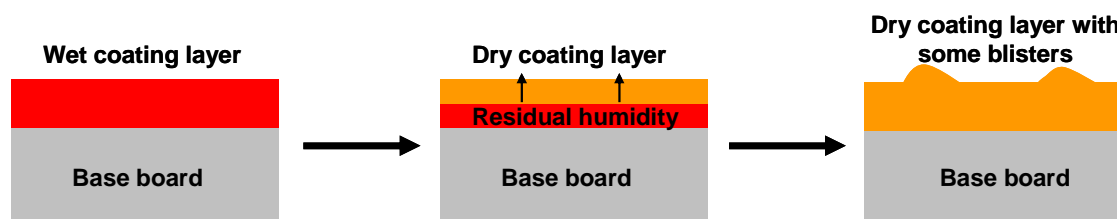


Figure V-51: Schematic representation of blistering effect.

This effect was not observed with MFC formulations which dried faster and more uniformly in the layer thickness.

V.3.6.2. - Influence of MFC on PVOH viscosity

The evolution of the viscosity according to the temperature could also give information on the interactions between macromolecules. Indeed the viscosity of PVOH aqueous solutions is linked to inter and intra hydrogen bonding between the PVOH chains and to PVOH-water hydrogen bonding [176]. In the PVOH/MFC mixture, the viscosity also depends on the PVOH/MFC hydrogen bonding. An increase of the temperature leads to the breaking of hydrogen bonds reducing the suspension viscosity.

Here, the viscosities of PVOH and PVOH/MFC formulations with a concentration of 15% were measured for different shear rates according to the temperature between 20°C and 80°C. The same trend was observed for each shear rate. Figure V-52 shows the results obtained for a shear rate of 800 s⁻¹. The influence of temperature on PVOH viscosity followed the same trend as the one described by the supplier (Figure V-53).

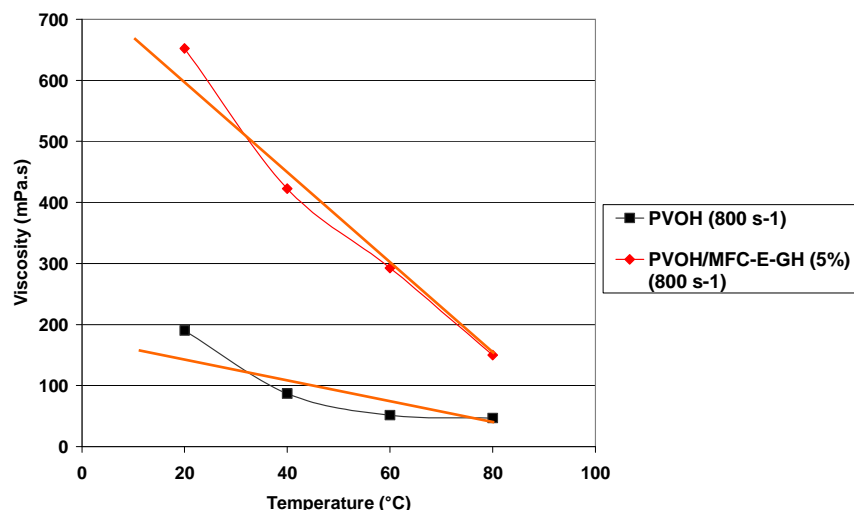


Figure V-52: Viscosity of PVOH and PVOH/MFC-E-GH (5%) suspensions at 15 wt% wt in solids for a shear rate of 800 s^{-1} according to the temperature.

The evolution of the viscosity as a function of temperature was different according to the presence or not of MFC. Indeed, the slope of the curve was largely higher in the case of PVOH/MFC 4.8% suspension (estimated at -8.3) compared to the PVOH suspension (estimated at -2.4). The result means that the hydrogen interactions between macromolecules and between macromolecules and water were lower in PVOH/MFC suspensions than those between PVOH chains.

Therefore, it could be deduced of the result that the water retention was lower in the PVOH/MFC formulation leading to an improved drying quality during the coating process.

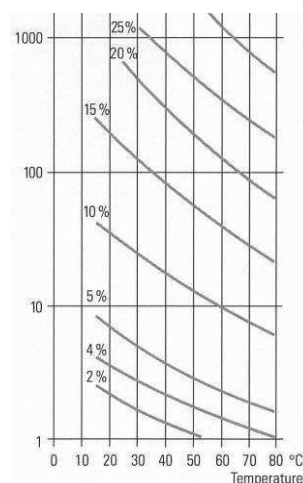


Figure V-53: Viscosity of Mowiol 4-98 according to the temperature and the solid content [162].

V.3.7. - Conclusion

These pilot trials studied the influence of several MFC grades on PVOH coated layer properties. Coated samples were thus produced from several formulations and with two MFC contents. The potential use of MFC in coating processes has thus been demonstrated at pilot scale. No similar results were reported before in literature. The first conclusion that can be

drawn from these trials is the improvement of the runnability and productivity with the introduction of MFC in the PVOH layer. Indeed, the blister number was reduced for the PVOH/MFC layer compared to pure PVOH layer. Regarding the MFC grades, the enzymatic MFC greatly improved the water resistance of PVOH compared to TEMPO treated MFC. Moreover, the use of 9% of MFC instead of 5% degraded the water resistance and did not improve significantly the WVTR and OTR.

At last, the improvement provided by a 20 g/m² layer compared to a 10 g/m² layer is not sufficient to justify the use of two times more product. Therefore, the barrier layer selected for the barrier packaging demonstrator was thus based on a 10 g/m² barrier layer of PVOH + 5% of MFC-E-GH.

V.4. - Production of barrier packaging materials using MFC at pilot scale

V.4.1. - Production of demonstrator with additional top coating layer

To protect the barrier layer, commercial latex was used to impart water and water vapour resistance. Commercial latex, defined as water barrier, was directly deposited onto the first barrier layer as a topcoat (Figure V-54). According to the results from the previous part, the barrier layer selected for the final demonstrator was the layer PVOH/MFC-E-GH (5%).

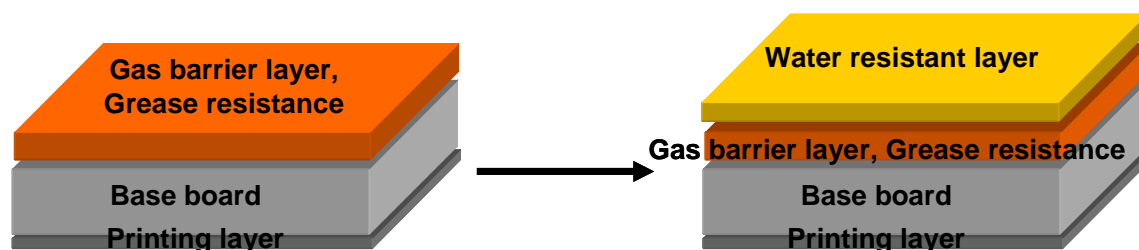


Figure V-54: Production of final packaging materials: Water resistant layer.

This part describes the production at pilot scale of the final packaging materials and their characteristics. Here, the results were compared before and after top coating.

Moreover, biodegradability results and converting ability is then detailed. At last, the performance of materials is compared with market products.

V.4.1.1. - Production of samples

The barrier latex was directly applied at 5-7 g/m² on the reels pre-coated with PVOH/MFC layer. Once again, these trials were carried out on the pilot coater with a SoftTip blade.

V.4.1.2. - Mechanical properties

Regarding the Young's modulus values of coated board, a slight improvement was observed for the base board value with the top coating layer (Figure V-55). Compared to this top coated base board, the values obtained for the barrier coated board were in the same range with or without the top coating layer.

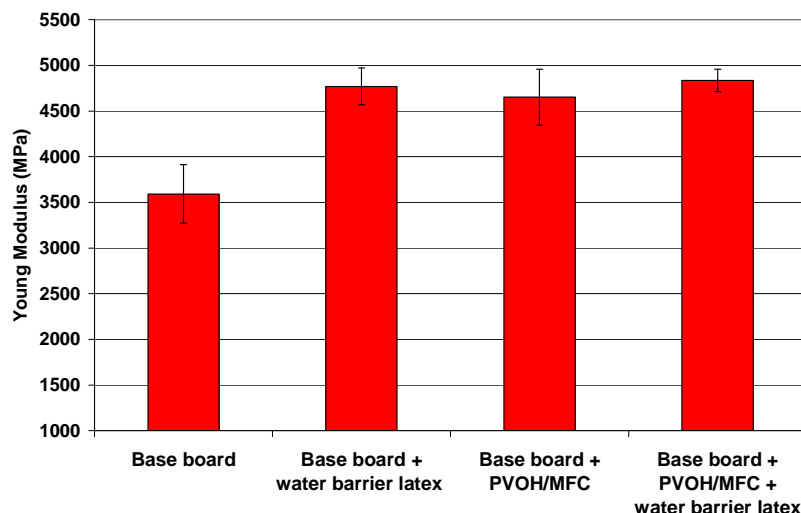


Figure V-55: Young's modulus of final packaging material.

V.4.1.3. - Barrier properties

V.4.1.3.1. - Water resistance

As expected, the barrier latex played perfectly its protection role: the water resistance was strongly improved with the top coating (Figure V-56). Indeed, the top coating applied onto the base board, without barrier layer, had a good Cobb index 60s value of 2 g/m². The value reached 1 g/m² for the board coated with both layers.

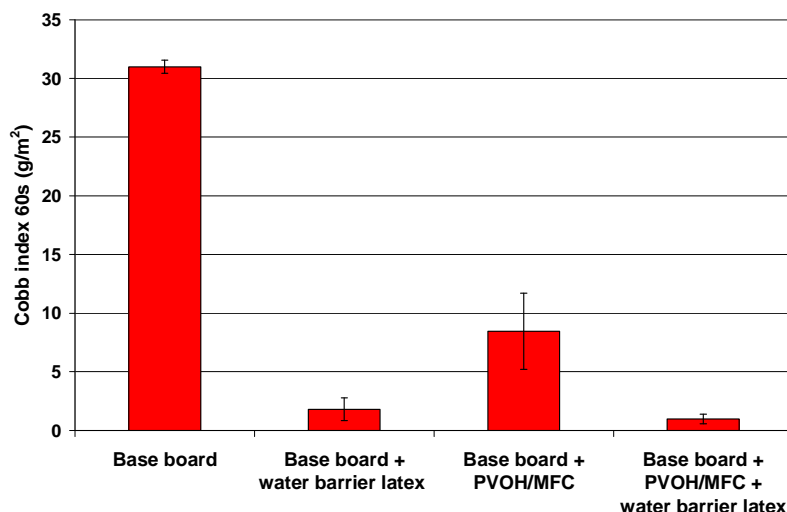


Figure V-56: Water resistance determined by Cobb index 60s measurements.

The reference for packaging applications is generally the Cobb index 1800s. In this case, the value reaches 2 g/m².

V.4.1.4. - Water vapour transmission rate

The top coating allowed also to reduce the WVTR of the base board and the barrier coated board as observed in Figure V-57. Indeed, this layer reduced the affinity of the substrate with water leading to the WVTR decrease.

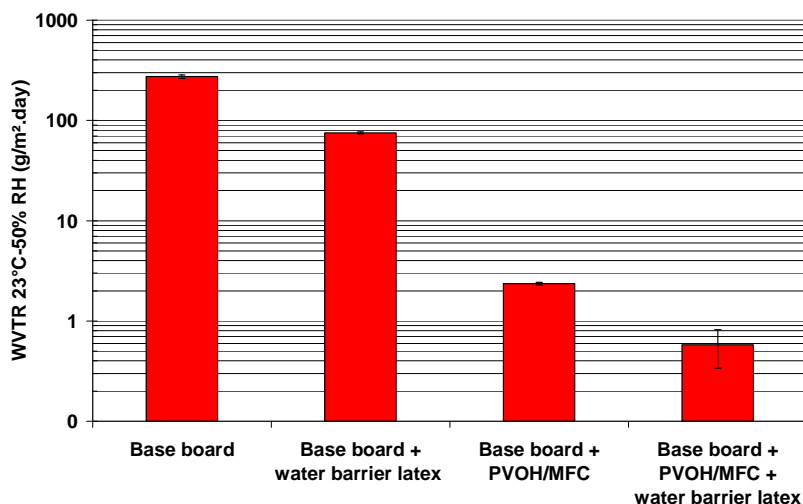


Figure V-57: WVTR 23°C-50% RH of the final packaging material.

Moreover, these results demonstrated the importance of the first gas barrier layer. Indeed, the best values were obtained for the demonstrator and the combination of two layers with a value of 0.5 g/m².day. After coating with barrier latex, the WVTR value of the base board was only of 70 g/m².day.

The same trend was observed as the water vapour permeability in tropical conditions (Figure V-58). Once again, the top coating largely reduced the value from 2600 g/m².day to 450 g/m².day, confirming the efficiency of this barrier latex as top coat to bring a water protection. The value of the final packaging material thus reached 250 g/m².day.

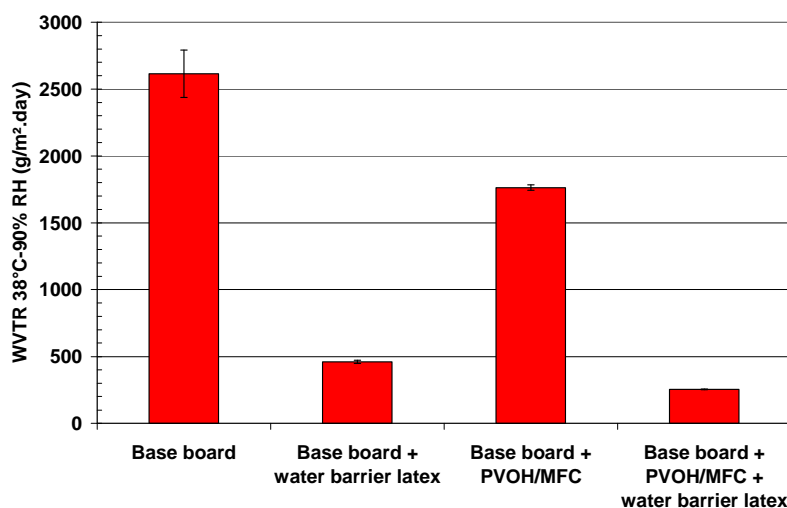


Figure V-58: WVTR 38°C-90% RH of the final packaging material.

V.4.1.5. - Oxygen transmission rate at 23°C-0% RH

The measurements of OTR represented in Figure V-59, showed once again that the single top coating layer did not improve the oxygen barrier of the base board. The barrier properties to O₂ are quite entirely brought by the barrier layer and slightly reinforced by the top coating layer. The best values were obtained for the 2 layer demonstrator (barrier + top coating layer) with an OTR around 5 cm³/m².day.bar at 23°C-0% RH.

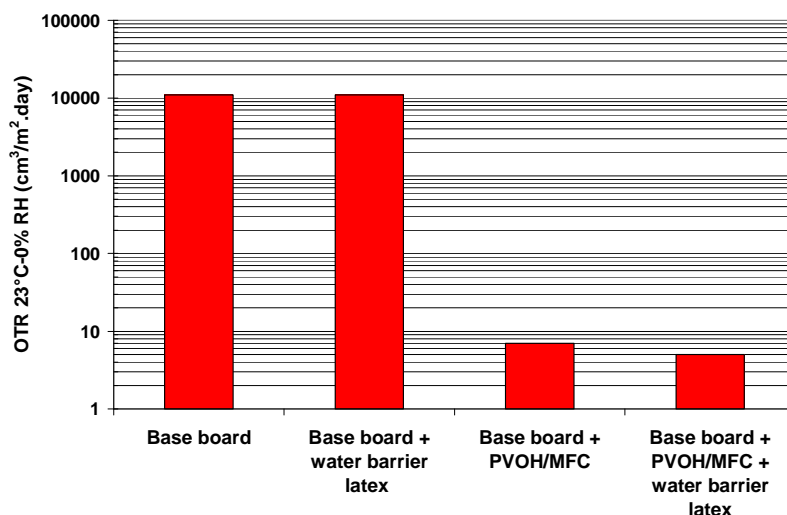


Figure V-59: OTR at 23°C-0% RH of the final packaging material.

V.5. - Comparison with other packaging materials

To complete this study, the properties of the demonstrator were compared with two kinds of materials:

- Firstly, materials developed using MFC and described in the literature
- Secondly, existing materials in the packaging market

V.5.1. - Comparison with the literature values

At the beginning of the PhD work, very few studies were reported on the development of barrier properties using MFC by coating processes. An interesting product was developed by Hult *et al.* [1]. Indeed the application of MFC and shellac by bar coater in one layer or multilayer system showed good properties with a WVTR at 25°C-50% RH of 6.54 g/m².day and an OTR at 25°C-50% RH of 4466 cm³/m².day from a base paper of 60 g/m², an MFC layer of 3 g/m² and a 10 g/m² top layer of shellac. It was difficult to make a real comparison but this gave an idea of results available in the literature for MFC barrier coating.

V.5.2. - Comparison with existing materials

Figure V-60 compares the barrier performances of the demonstrator with polymer films currently used in packaging applications.

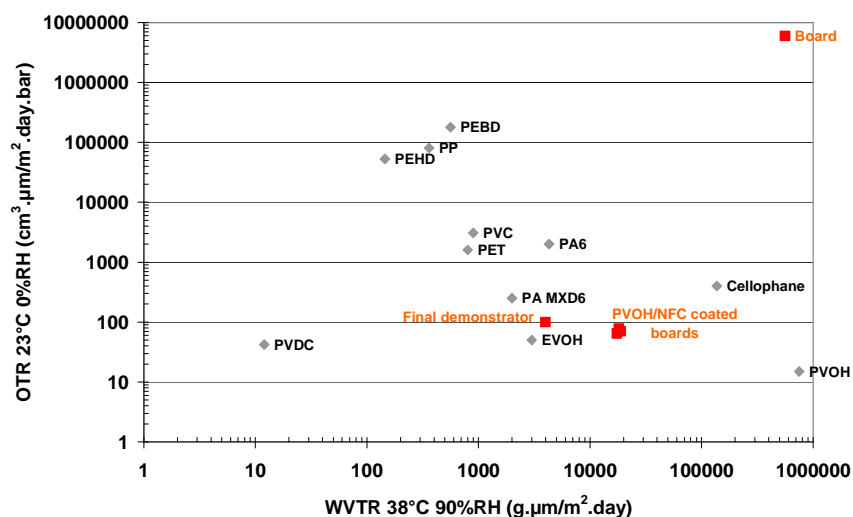


Figure V-60: Comparison of the barrier performances of the demonstrator with existing materials.

In terms of barrier properties, the final packaging materials had properties equivalent to those of EVOH or PA MXD6 films. The values were also better than cellophane for example.

V.6. - Converting

The ability to convert coated board into packages was checked as observed in Figure V-61.



Figure V-61: Production of boxes from coated board samples.

Coated board samples resisted well to groove and creasing allowing the production of boxes. However, grease tests after folding showed a degradation of the grease resistance probably due to the layer cracking during the converting. Further investigation should be carried out to decrease the brittleness of the layer and improve its creasing resistance. A solution could be the use of plasticizer although, as already described, it leads generally to the decrease of the barrier properties.

V.7. - Biodegradability

Biodegradability and compostability tests were carried out on intermediate and final packaging demonstrator. To complete the assessment, disintegration in composting process of paper boards was tested and the quality of the obtained final compost was checked as

well as the absence of any ecotoxicity effects with respect to seed germination and plant growth. The certification of compostability of packages and/or products in general is regulated by EN standard norms that list the specific requirements (EN 13432-2000 and EN 14995:2006)/1/2/. These tests were carried out in collaboration with Innovhub, one of the SUNPAP partners.

V.7.1. - Biodegradability of paper board samples

The board samples coated with PVOH/MFC coating were tested for biodegradability in compost. The results showed a fast biodegradation reaching 90% biodegradation within 50 days of test (Figure V-62).

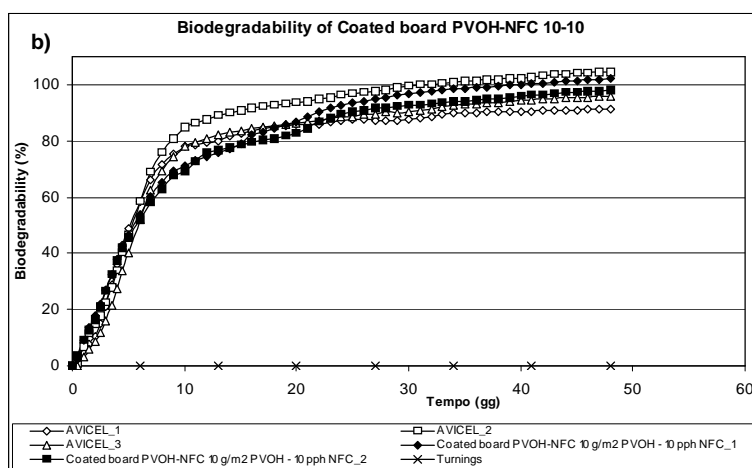


Figure V-62: Biodegradability of coated boards.

V.7.2. - Degradation tests in simulated composting conditions

Paper board samples were subjected to the disintegration test.

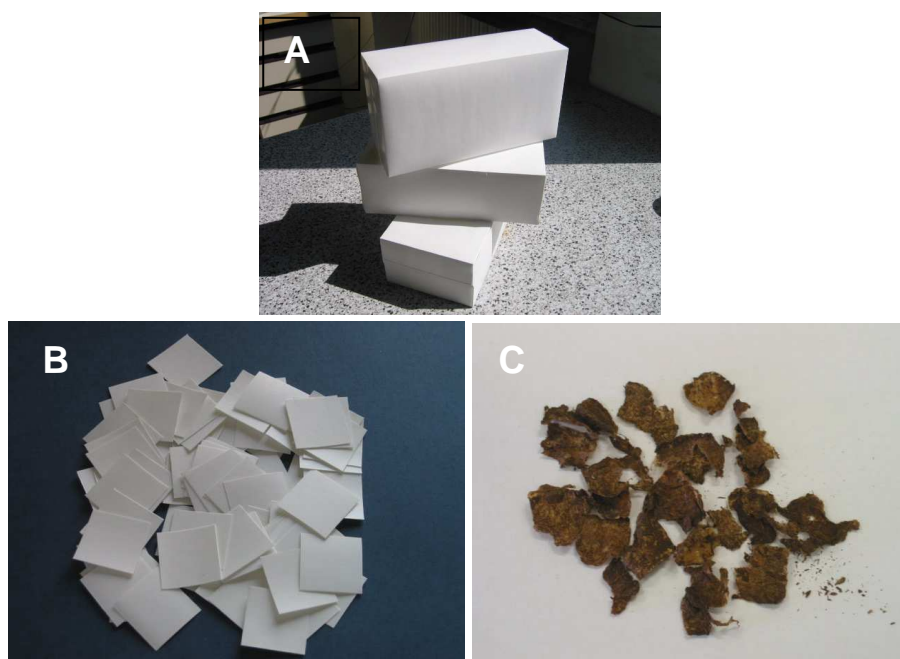


Figure V-63: Photos of board box samples (A) paper board before the test (B), residues after composting process (C).

As evidenced from the results reported in Table V-12, the only sample that was not completely degraded was the box board sample PVOH-MFC 10 g/m² PVOH -5 pph MFC, + commercial latex top coat of 5 g/m². The amount of the sample residues was very low (6 % of the initial weight), by hand and visual inspection the residues appeared as constituted by “plastic thin film” that could be ascribed to the commercial latex present on the overall board, or more likely, due to the very low number of piece residues, it could be due to the glued parts of the box.

	Initial sample weight (g)	Residual sample weight (g)	% degradation
Reference board	10.01	0	100
	10.03		
	10.02		
Coated board with 10 g/m ² of PVOH/MFC-E-GH (9%)	10.01	0	100
	10.08		
	10.09		
Board box with 10 g/m ² of PVOH/MFC-E-GH (5%) + water barrier layer	10.04	0.46	95
	10.06	0.52	95
	10.04	0.78	92

Table V-12: Degradation test results.

V.7.3. - Ecotoxicity effects of final compost

As reported in Table V-13, the board samples after disintegration did not affect the composting mixture. In fact, no toxic effect was detected with respect to seed germination and plant growth with the compost obtained in the presence of these samples.

Sample compost obtained in the presence of the specified samples.	25 % mixture of sample compost with test soil		50 % mixture of sample compost with test soil	
	% germination	% growth	% germination	% growth
Base board	96 (± 3)	95 (± 6)	89 (± 4)	92 (± 7)
Coated board with 10 g/m ² of PVOH	98 (± 4)	102 (± 7)	88 (± 4)	88 (± 6)
Coated board with 10 g/m ² of PVOH/MFC-E-GH (9%)	90 (± 5)	89 (± 3)	89 (± 6)	92 (± 4)
Board box with 10 g/m ² PVOH/MFC-E-GH (5%) + water barrier layer	92 (± 6)	91 (± 5)	87 (± 5)	93 (± 5)

Table V-13: Percentage germination and growth of compost obtained by the disintegration tests in the presence of the different board samples, the reported results are the average of ecotoxicity tests run in triplicate.

The biodegradability in compost of coated paper board samples containing MFC and PVOH in the coating colour was demonstrated to be similar to MFC-free coated paper board. The 90% degradation limit was reached quite fast, i.e. within 55 days testing, while the required time limit for biodegradability in compost is 90-180 days. The results of disintegration tests as

well as ecotoxicity tests confirmed that the analysed samples fulfilled the compostability requirements therefore they could be disposed in composting plant at their end of life.

V.7.4. - Conclusion

During this work, the possibility to use the MFC in coating process was determined at lab and pilot scale. Mechanical and barrier properties were evaluated for several PVOH/MFC coated board according to the MFC grade, the MFC content and the coat weight. The best PVOH/MFC layer was then selected to develop the final demonstrator. The final properties of the barrier board were thus determined as well as its converting ability and its biodegradability.

All the performed work allowed demonstrating, at pilot scale, the use of MFC in the development of a barrier layer packaging board. In the case of barrier layer, not any other study at pilot scale was currently referenced. Firstly, it was shown that runnability and productivity of the pilot coater were greatly improved with the introduction of MFC-E-GH in PVOH layers.

Moreover, the barrier packaging demonstrator was produced with good barrier properties, summarized in Table V-14:

Barrier properties	Demonstrator
Grease resistance (Oil Cobb index 24h)	2g/m ²
Water resistance (Cobb index 60s)	1 g/m ²
Water resistance (Cobb index 1800s)	2.5 g/m ²
WVTR @ 23°C-50% RH	0.5 g/m ² /day
WVTR @ 38°C-90% RH	250 g/m ² /day
Oxygen permeability @ 23°C-0%RH	6 cm ³ /m ² /day

Table V-14: Barrier properties of the demonstrator.

Lastly, the biodegradability and compostability tests were very positive and demonstrated the possibility to dispose these materials in composting plant at their end of life.

The negative point was the suggested loss of performance during the step of converting. Indeed, the grease resistance was lower after folding meaning a possible loss of barrier properties. Another measurement should be conducted to confirm this result.

V.8. - Conclusion

In this chapter, an example of industrial application based on the microfibrillated cellulose was studied. Indeed, the production of barrier packaging board with PVOH/MFC was carried out at lab and pilot scale. For this, coating colour preparation was adapted to reach the highest possible solid content and to guarantee acceptable drying conditions on a pilot coater. The solubilisation of PVOH at 95°C directly in MFC suspensions was selected allowing the preparation of homogeneous coating colours in only one step and the possible adaptation at large scale. Regarding the coating process, rod or blade systems were employed in order to deposit around 10 g/m² on the base board. In spite of quite high coating

colour viscosity, the PVOH/MFC suspension was successfully coated and the surface of coated board showed a homogeneous surface and a good coverage. However, the drying behaviour was different in presence or not of MFC. Problems of blistering were mainly observed with pure PVOH layer leading to some defects in the layer and a reduction of the barrier layer efficiency. This effect was reduced by the MFC introduction in PVOH layer which decreased probably the interactions between PVOH chains and water, increasing the drying rate. This result demonstrated the possibility of the use of MFC as drying agent. Moreover, the layer of PVOH/MFC showed a good barrier level with high grease resistance, low WVTR (23°C-50%RH) and low oxygen permeability (23°C-0% RH). However, the layer being water sensitive, a top layer was added to water protect the PVOH/MFC layer. A commercial barrier latex was thus deposited on the PVOH/MFC layer and showed a good water barrier efficiency.

This barrier material offers thus a new possibility to minimize the use of petroleum based polymer and to favour the use of renewable source.

General conclusion and perspectives

This work was achieved in the frame of the EU SUNPAP project (NMP4-LA-2008-228802). The general objective of this project was the scale up of nanoparticles in modern papermaking.

This PhD work aimed at proposing a new board based packaging material as an alternative to current products minimizing the use of petroleum based polymers thanks to the use of microfibrillated cellulose (MFC).

A state of the art allowed to identify the challenges to take up for the up-scaling the use of MFC in barrier coating. Some challenges are linked to the MFC intrinsic properties and their potential use for making materials and some others challenges are linked to industrialization of processes making real the manufacture and the use of MFC on full-scale existing machines.

Microfibrillated cellulose is a material of high interest, as illustrated by the number of studies growing every year. Indeed MFC combined both interesting properties (tensile strength, barrier to oxygen and grease) and renewable source. This materials has been known for more than 30 years, but its development was limited by the extremely high energy required for its production.

These last years, the interest in this material was renewed since the production of MFC has been improved with more efficient and less energy-consuming processes thanks to the use of either chemical or enzymatic pretreatments which make possible to produce various MFC grades from different sources. Nevertheless, due to the high aspect ratio of fibrils and to the MFC aggregation during the MFC drying, none measurement technique is available to determine the size distribution of fibrils in MFC. This makes difficult to characterise them and establish structure/properties laws.

The potential of MFC for the packaging development has been widely described when considering self standing MFC films, which showed generally good mechanical and barrier properties and high transparency. Some studies have also shown an interest for the use of MFC as reinforcement material in composites, but then the barrier properties were only seldomly detailed. Moreover, only very few studies reported the use of coating processes to apply either MFC or water based composites,. All these studies were achieved at laboratory scale and up today (2012), none product use MFC as key component of a material.

If most of the reported works were carried out at lab scale;it is because the production capacities of MFC were generally low with lab scale production. At the beginning of this project, the pilot building was reported by some research centers but the MFC production was not yet effective on a large scale. Moreover, the low solid contents and high viscosity of MFC suspensions are major drawbacks for their use at larger scale, in particular for coating processes. The introduction of MFC in matrices could be a solution to reduce these problems.

The thesis was divided into three main parts. Firstly, the study focussed on the characterisation of the MFC suspensions, on the manufacturing of MFC free films and on the determination of their properties. Secondly, the development of MFC based composites was studied as model films. The last part was devoted to the introduction of MFC in coating colours in order to develop a barrier layer at the board surface and to the demonstration at pilot scale of the industrial feasibility.

To study the influence of the fibrillation process on the intrinsic properties of MFC, several MFC suspensions of different grades were firstly characterized by combination of microscope techniques and viscosity measurements. The suspensions were more or less homogeneous according to the MFC production processes and seemed to be more homogeneous after the TEMPO pretreatment. The fibril size was estimated between 10-30 nm in width and 1-3 μm in length. However, microscope techniques were not sufficient to characterise completely the MFC suspensions and did not allow to measure the size distribution of MFC. Viscosity measurements gave complementary results with a qualitative indication on the degree of individualisation of MFC. A protocol, which was developed with a controlled shear stress rheometer, allowed to compare the different kinds of MFC suspensions. The viscosity of MFC suspensions appeared to be quite high for low solid contents (about 2%) but their highly pronounced shear thinning behaviour should improve their flow in high shear processes.

Two production methods of films, the casting/evaporation and the handsheet methods were developed and employed for this study. The size of fibrils as well as the homogeneity of suspension impacted directly the final properties of films: Films showed good tensile properties, interesting oxygen barrier and good transparency. However, the water vapour transmission rate and the water resistance of films were quite low and have to be improved to match requirements for packaging applications. Compared with enzymatic pretreatment, TEMPO MFC films showed higher transparency but lower tensile properties and more important water sensitivity attributed to the carboxylation of cellulose that brings a more hydrophilic behaviour. The first part of the study confirmed the interesting properties of MFC for the packaging applications; However, their low solid content reduces strongly the possibilities of use of MFC alone in coating processes. The introduction of MFC in water based matrices was thus envisaged to find a compromise between runnability and final properties.

The second part of this work dealt with the development of composite films using two matrices: a poly(vinyl alcohol) and a starch. The influence of MFC addition was assessed with respect to the mechanical and barrier properties of self standing films for MFC contents between 5 and 75 wt%. An improvement of final properties of the two kinds of matrix was observed with the reinforcement effect of MFC and the increase of the thermal degradation temperature of matrices. Structural analysis allowed to understand the impact of MFC addition on the structure of the matrices. The improvement was thus the effect of strong interactions between the MFC and matrix. The introduction of MFC also showed a reduction of WVTR value of starch film but the end performances were not sufficient for barrier applications. The sorbitol addition showed very positive results. Indeed, the barrier properties were highly improved with particularly a reduction of WVTR at 23°C-50% RH and of OTR at 23°C-0% RH. This was explained with an antiplasticization effect, observed at this sorbitol content reducing the tensile strength of starch. Nevertheless, the MFC introduction offered a good compromise thank to its reinforcement potential. Regarding the barrier properties of PVOH matrix, the MFC addition allowed to save low WVTR of the matrix under ambient conditions and to improve it in tropical conditions. At last, the heating treatment of PVOH/MFC films showed a very good influence on their water sensitivity with a strong reduction of film solubility when they were immersed in water. From these results, the best formulations were selected for the next step of the work that dealt with the use of coating processes to apply the water based composite onto a paperboard. The barrier properties

obtained with PVOH/MFC system are currently more promising compared to starch/MFC system for the development of packaging materials.

The potential of the use of MFC in coating process was firstly studied at lab scale. In order to guarantee the best coating quality, the higher coat weight and the minimum drying energy demand, an innovative strategy was carried out to obtain the coating colour with the highest possible solid content: The solubilisation of PVOH was carried out directly into the MFC suspensions. It was demonstrated that this strategy which allowed to get PVOH/MFC colours with a solid content reaching 15 wt%, didn't alter the material properties compared to a separate solubilization with a post mixing. Good gas barrier properties were obtained for the coated samples and more specifically for the PVOH/MFC layer with a MFC content of 5 wt%. These results were partially in agreement with the values obtained for PVOH/MFC films demonstrating a good transposition from model films to coated boards. However, it was underlined that both the board substrate and the drying of the coating layer played important roles on the final barrier properties. These results allowed to envisage the transfer of the PVOH/MFC formulations at larger (pilot) scale.

In the framework of the SUNPAP project, new means were developed to up-scale the MFC production capacities allowing to produce larger MFC quantities suitable for pilot coating trials. To develop a barrier board suitable for the market, a multilayer system was designed associating a base board and two barrier layers: the first one, a PVOH/MFC layer, offering grease resistance and oxygen barrier properties, the second one, a commercial barrier latex, giving a water resistant layer and water vapour barrier properties. The results of pilot trials showed that the runnability and the productivity of the coating pilot were greatly improved with the introduction of MFC in PVOH layers. Indeed, the increase of the drying rate in presence of MFC improved the drying of the coating and reduced the blistering phenomena observed on pure PVOH layers. This demonstrated the potential of MFC to be used as a drying additive.

Several coated samples were produced from several grades of MFC and two MFC contents. MFC enhanced the water resistance of PVOH layer revealing the high interactions between PVOH and MFC. The best properties, obtained with 10 g/m² layer of PVOH/MFC-E-GH 4.8 wt%, showed high grease resistance, low WVTR (0.5 g/m²/day at 23°C-50% RH) and a low oxygen permeability (6 cm³/m²/day at 23°C-0% RH). Commercial barrier latex was top coated on this layer to produce the final demonstrator. With a Cobb index 1800s value of 2.5 g/m², the top coating offered an efficient water protection. In partnership with Stora Enso, these trials were completed by the converting of coated samples into some folded boxes. But it seemed that the layer did not resist totally to the creasing and folding steps. Biodegradability and compostability tests, carried out by Innovhub, were very positive and demonstrated the possibility to dispose these materials in composting plant at their end of life.

Some perspectives could be envisaged to follow of this project.

The rheological characterisation of MFC suspensions showed a hysteresis loop attributed to the formation of structures under shear. Strain rheological characterizations could complete this study on the rheology of MFC suspensions. The implementation of techniques allowing the visualisation and the characterisation of these structures under flow should improved the understanding of phenomenon. The present work focus on the rheology of MFC suspensions "as produced" and a dedicated study coupling physical chemistry and rheology would be of

interest to understand the interactions between fibrils and between fibrils and solvent. This would permit to define ways to increase the MFC solids while keeping the viscosity as low as possible.

Concerning the use of MFC, this work improved the protocol to manufacture self-standing MFC films, in a shorter time, using a semi-automatic sheet former. The influence of drying and pressing on the final MFC film properties has not been studied in detail and it should be possible to better understand the film formation mechanisms and to get films with better properties. This would also pave the way to produce MFC reels on large production machines.

Some drawbacks were observed on the MFC films such as poor water resistance, moderate permeability to water vapour and transparency/tear strength. Complementary developments could be carried out with modified MFC or some additives such as nanofillers to improve the water resistance and the WVTR of the film. The transparency could be also improved by an eventual local water rewetting, a polishing or by impregnation. The tear resistance could be improved by the use of longer fibres or thanks to impregnation of other polymers.

Regarding the MFC based composites, the addition of MFC showed several advantages such as mechanical reinforcement and a reduction of water vapour permeability. However, several improvements could still be achieved: The MFC dispersion into the matrix could be improved using other starch or PVOH grades, more or less charged, or some dispersing agent. Nanoclays are recognized for their barrier improvement potential, so their use could be tested to reinforce the barrier properties of the matrix/MFC layer. Other kinds of plasticizer and different contents could be studied to avoid the antiplasticization effect and find a better compromise between mechanical and barrier properties. Several strategies could also be developed to improve the water resistance of the matrix/MFC layer with the possible addition of cross-linkers or the use of surface grafting such as chromatogeny.

In the particular case of PVOH/MFC films, complementary works should be achieved to better understand the PVOH/MFC interactions and the effect of heating treatment. Finally, the coating colour formulation could be improved according to the results obtained with MFC based composites and a more accurate focus should be put on understanding the mechanisms occurring during the drying of the coating layer.

For the first time, MFC were used in coating processes at pilot scale and demonstrated their potential for the production of barrier paperboards. However, the flexibility of the layer and its folding resistance should be improved to save their barrier efficiency after the converting of the coated board into boxes.

We hope that this work will be useful both to scientists to bring another brick in the wall of MFC material science and to industrialists to convince them of the potential of MFC either as a drying additive or as a useful component in barrier coating.

Literature cited

-
- [1] **Hult E.L.**, Iotti M., Lenes M., "Efficient approach to high barrier packaging using microfibrillar cellulose and shellac," *Cellulose* 17, no. 3 (2010): 575-586.
- [2] **Siró I.**, Plackett D., "Microfibrillated cellulose and new nanocomposite materials: a review," *Cellulose* 17, no 3 (2010): 459-494.
- [3] **Dufresne A.**, "Preparation of MFC", *In Nanocellulose : From nature to high performance tailored materials*, De Gruyter : New-York and Berlin, chap 2 (2012).
- [4] **Nieh W.**, Willis C., "Roadmap for the Development for International Standards for Nanocellulose", (June 2011). Available from TAPPI at www.tappi.org.roadmap standard.
- [5] **Turbak A.F.**, Snyder F.W., Sandberg K.R., "Microfibrillated cellulose, a new cellulose product: properties, uses and commercial potential", *Journal of Applied Polymer Science: Applied Polymer Symposia* 37 (1983):815-827.
- [6] **Coles R.**, *Food Packaging Technology*, R. Coles, D. McDowell, M.J. Kirwan eds., Blackwell publishing: Oxford (2003).
- [7] **Miller K. S.**, Krochta J. M., "Oxygen and aroma barrier properties of edible films: a review", *Trends in Food Science & Technology*. 8, no. 7 (1997): 228-237.
- [8] *Rapport d'activité 2010*, COFEPAC – Comité Français de l'emballage papier carton.
- [9] *Synthèse Emballages industriels, commerciaux and ménagers*, ADEME - Agence de l'environnement et de la maîtrise de l'énergie (2008).
- [10] *Europe Packaging Material Breakdown*, Global Packaging alliance. Online: <http://www.global-packaging-alliance.com> (June 2012).
- [11] **Petrie E.M.**, *Developments in Barrier Coatings for Paper and Board Packaging*, Pira International Ltd. :Leatherhed (2006).
- [12] European statistics 2007:
<http://epp.eurostat.ec.europa.eu/portal/page/portal/eurostat/home/> (June 2012)
- [13] "Packaging and packaging waste statistics in Europe 1998-2008. An analysis of official EU data by EUROPEAN", *The European organisation for packaging and the environment*, Perchards Ltd., St Albans, UK (2011)
- [14] **Girard F.**, "Transfert de matière à travers les matériaux d'emballage", *Formation Les matériaux barrière: Centre Technique du Papier*, Grenoble (2011)
- [15] **Jacques C.H.M.**, Hopfenberg H.B., Stannett V.T., "*The permeability of plastic films and coatings to gas, vapors, and liquids*", Plenum Publishing Corp: London (1974).
- [16] **Crank J.**, *The mathematics of diffusion*. 2nd ed.; Clarendon Press: Oxford (1975).
- [17] **Han J.H.**, Scanlon M.G., "Chapter 2 - Mass transfer of gas and solute through packaging materials", *Innovation in Food Packaging*, Han, J. H. ed., Elsevier Ltd.: Oxford (2005).
- [18] **Spence K.L.**, "Processing and Properties of Microfibrillated cellulose", PhDThesis, North Carolina State University (2011).
- [19] **Matthews G. P.**, Spearing M. C., "Measurement and Modelling of Diffusion, Porosity and Other Pore Level Characteristics of Sandstones", *Marine Petroleum Geology* 9, 146 (1992).

- [20] **Cooksey K.**, “Important factors for selecting food packaging materials based on permeability”, *Flexible packaging conference*, Burcharm International corp. (2004).
- [21] **Lange J.**, Wyser Y., “Recent Innovations in Barrier technologies for Plastic Packaging - a review”, *Packaging Technology and Science* 16, no. 4 (2003): 149-158.
- [22] *CEPI Annual Statistics 2011*, CEPI – Confederation of European Paper Industries (2012).
- [23] **Jenkins S.**, *The Future of Functionnal and Barrier Coatings for Paper and Board*, Pira International Ltd.: Leatherhed (2009).
- [24] **Twede D.**, Goddard R., *Packaging Materials*, Pira International Ltd. :Leatherhed (1998)
- [25] **Lyannaz L.**, Martinez P., *Formation Couchage des papiers – cartons: Centre Technique du Papier*, Grenoble (2011).
- [26] <http://packaging-technology.org/66-coating-equipment.html> (June 2012)
- [27] **Martinez P.**, “Etude expérimentale et simulation d’écoulements de fluides modèles et de dispersions pigmentaires dans une coucheuse rideau”, PhD Thesis, Université de Grenoble (2011)
- [28] **Petersen K.**, Nielsen P. V., Bertelsen G., Nilsson N. H., Mortensen G., “Potential of biobased materials for food packaging”, *Trends in food Science & Technology* 10 (1999): 52-68.
- [29] **Agoda-Tandjawa G.**, Durand S., Berot S., Blassel C., Gaillard C., Garnier C., Doublier J.L., “Rheological characterization of microfibrillated cellulose suspensions after freezing,” *Carbohydrate Polymers* 80, no. 3 (2010): 677-686.
- [30] **Da Silva Perez D.**, Tapin-Lingua S., Janodet A., Petit-Conil M., Dufresne A., “Nanofibres: Production of cellulose micro and nano-fibres: state of the art and first results”, *5th Intechfibres Research Forum: Centre technique du Papier*, Grenoble (2009).
- [31] **Huang C.L.**, Lindström H., Nakada R., Ralston J., “Cell wall structure and wood properties determined by acoustics-a selective review”, *European Journal of Wood and Wood Products* 61, no. 5 (2003): 321–335.
- [32] **Plomion C.**, Leprovost G. and Stokes A., “Wood formation in trees”, *Plant Physiology*, 127, (2001):1513-1523.
- [33] **Vallette P.**, Coudhens C., "Le bois, la pâte, le papier", 3^{ème} édition, *Centre Technique de l'industrie des Papiers, Cartons et Cellulose* (1992).
- [34] **Paralikar S.**, “Poly(vinyl alcohol)/Cellulose Nanocomposite Barrier Films”, PhD Thesis, Oregon state university (2006).
- [35] **Ashby M.F.**, “The CES EduPack Database of Natural and Man-made Materials”. Granta Design: Cambridge (2008).
- [36] **Azizi Samir A.S.**, Alloin F., Sanchez J.Y., Dufresne A., “Cellulose nanocrystals reinforced poly(oxyethylene)”, *Polymer* 45, no. 12 (2004): 4149-4157.

- [37] **Chen Y.**, Liu C., Chang P.R., Cao X., Andersson D.P., "Bionanocomposites based on pea starch and cellulose nanowhiskers hydrolyzed from pea hull fibre: Effect of hydrolysis time", *Carbohydrate Polymers* 76, no. 4 (2009): 607-615.
- [38] **Eichhorn S.J. et al.**, "Review: current international research into cellulose nanofibres and nanocomposites", *Journal of Materials Science* 45, no. 1 (2010): 1-33.
- [39] Nutrition Resources: Carbohydrates,
<http://nutrition.jbpub.com/resources/chemistryreview9.cfm>, Jones and Bartlett Publishers (june 2012).
- [40] **Dufresne A.**, Cavallé J.Y., Vignon M.R., "Mechanical Behavior of sheets prepared from sugar beet cellulose microfibrils", *Journal of Applied Polymer Science* 64, no. 6 (1997): 1185-1194.
- [41] **Pääkkö M. et al.**, "Enzymatic Hydrolysis Combined with mechanical shearing and high pressure homogenization for nanoscale cellulose fibrils and strong gels", *Biomacromolecules* 8, no. 6 (2007): 1934-1941.
- [42] **Henriksson M.**, Henriksson G., Berglund L.A., Lindstrom T., "An environmentally friendly method for enzyme-assisted preparation of microfibrillated cellulose nanofibers", *European Polymer Journal* 43, no. 8 (2007): 3434-3441.
- [43] **Saito T.**, Nishiyama Y., "Homogeneous suspensions of individualized microfibrils from TEMPO-catalyzed oxidation of native cellulose", *Biomacromolecules* 7, no. 6 (2006): 1687-1691.
- [44] **Janardhnan S.K.**, Sain M.M., "Isolation of cellulose microfibrils - An enzymatic approach", *BioResources* 1, no. 2 (2006): 176-188.
- [45] **Chakraborty A.**, Sain M., Kortschot M., "Cellulose microfibrils: A novel method of preparation using high shear refining and cryocrushing", *Holzforschung* 59, no. 1 (2005): 102-107.
- [46] **Abe K.**, Iwamoto S., Yano H., "Obtaining cellulose nanofibers with a uniform width of 15nm from wood", *Biomacromolecules* 8, no.10 (2007): 3276-3278.
- [47] **Syverud K.**, Chinga-Carrasco G., Toledo J., Toledo P.G., "A comparative study of Eucalyptus and Pinus radiata pulp fibres as raw materials for production of cellulose nanofibrils", *Carbohydrate Polymers* 84, no. 3 (2011): 1033-1038.
- [48] **Spence K.L.**, Venditti R.A., Habibi Y., Rojas O.J., Pawlak J.J., "The effect of chemical composition on microfibrillar cellulose films from wood pulps: mechanical processing and physical properties", *Bioresource Technology* 101, no. 15 (2010): 5961-5968.
- [49] **Dufresne A.**, Dupeyre D., Vignon M.R., "Cellulose microfibrils from potato tuber cells: Processing and characterization of starch-cellulose microfibril composites," *Journal of Applied Polymer Science* 76, no. 14 (2000): 2080-2092.
- [50] **Dinand E.**, Chanzy H., Vignon M.R., "Parenchyma cell cellulose from sugar beet pulp: preparation and properties", *Cellulose* 3, no.1 (1996):183-188.
- [51] **Dinand E.**, Chanzy H., Vignon M.R., "Suspensions of cellulose microfibrils from sugar beet pulp", *Food Hydrocolloids* 13, no.13 (1999):275-283.

- [52] **Azizi Samir A.S.**, Alloin F., Paillet M., Dufresne A., "Tangling effect in fibrillated cellulose reinforced nanocomposites", *Macromolecules* 37, no. 11 (2004): 4312-4316.
- [53] **Leitner L.**, Hinterstoisser B., Wastyn M., Keckes J., Gindl W., "Sugar beet cellulose nanofibril-reinforced composites," *Cellulose* 14, no. 5 (2007): 419-425.
- [54] **Bruce D.M.**, Hobson R.N., Farrent J.W., Hepworth D.G., "High-performance composites from low-cost plant primary cell walls", *Composites Part A: Applied Science and Manufacturing* 36, no. 11 (2005): 1486-1493.
- [55] **Malainine M.E.**, Mahrouz M., Dufresne A., "Thermoplastic nanocomposites based on cellulose microfibrils from opuntia ficus-indica parenchyma cell", *Composites Science and Technology* 65, no. 10 (2005): 1520-1526.
- [56] **Imai T.**, Putaux J.L., Sugiyama J., "Geometric phase analysis of lattice images from algal cellulose microfibrils", *Polymer* 44, (2003):1871-1879.
- [57] **Bhattacharya D.**, Germinario L.T., Winter W.T., "Isolation, preparation and characterization of cellulose microfibrils obtained from bagasse", *Carbohydrate Polymers* 73, (2008): 371-377.
- [58] **Siqueira G.**, Bras J., Dufresne A., "Cellulose Whiskers versus Microfibrils: Influence of the Nature of the Nanoparticle and its Surface Functionalization on the Thermal and Mechanical Properties of Nanocomposites", *Biomacromolecules* 10, no. 2 (2009): 425-432.
- [59] **Siqueira G.**, Tapin-Lingua S., Bras J., Da Silva Perez D., Dufresne A., "Morphological investigation of nanoparticles obtained from enzymatic and acid hydrolysis of sisal fibers", *Cellulose* 17, (2010a):1147-1158.
- [60] **Bendahou A.**, Kaddami H., Dufresne A., "Investigation on the effect of cellulosic nanoparticles morphology on the properties of natural rubber based nanocomposites", *European Polymer Journal* 46, (2010):609-620.
- [61] **Zuluaga R.**, Putaux J.L., Cruz J., Vélez J., Mondragón I., Gañán P., "Cellulose microfibrils from banana rachis: Effect of alkaline treatments on structural and morphological features", *Carbohydrate Polymers* 76, (2009): 51-59.
- [62] **Klemm D.**, Kramer F., Moritz S., Lindström T., Ankerfors M., Gray D., Dorris A., "Nanocelluloses: A New Family of Nature-Based Materials", *Angewandte Chemie International Edition* 50, no. 24 (2011): 5438–5466.
- [63] **Herrick F.W.**, Casebier R.L., Hamilton J.K., Sandberg K.R., "Microfibrillated cellulose: morphology and accessibility.", *Journal of Applied Polymer Science: Applied Polymer Symposia* 37 (1983):797-813.
- [64] **Nakagaito A.N.**, Yano H., "The effect of morphological changes from pulp fiber towards nano-scale fibrillated cellulose on the mechanical properties of high strength plant fiber based composites", *Applied Physics A* 78, no. 4 (2004): 547-552.
- [65] **Zimmermann T.**, Bordeanu N., Strub E., "Properties of nanofibrillated cellulose from different raw materials and its reinforcement potential", *Carbohydrate Polymers* 79, no. 4 (2010): 1086-1093.

- [66] **Boldizar A.**, Klason C., Kubat J., Naslund P., Saha P., "Prehydrolyzed cellulose as reinforcing filler for thermoplastics", *International Journal of Polymeric Materials* 11, no. 4 (1987): 229-262.
- [67] **Wågberg L.**, Decher G., Norgren M., Lindström T., Ankerfors M., Axnäs K., "The Build-Up of Polyelectrolyte Multilayers of Microfibrillated Cellulose and Cationic Polyelectrolytes," *Langmuir* 24, no. 3 (2008): 784-795.
- [68] **Wågberg L.**, Winter L., Ödberg L., Lindström T., "On the charge stoichiometry upon adsorption of a cationic polyelectrolyte on cellulosic materials", *Colloids and Surfaces* 27, no. 1-3 (1987): 163-173.
- [69] **Isogai A.**, Kato Y., "Preparation of Polyuronic Acid from Cellulose by TEMPO-mediated Oxidation", *Cellulose* 5, no. 3 (1998): 153-164.
- [70] **Saito T.**, Isogai A., "Introduction of aldehyde groups on surfaces of native cellulose fibers by TEMPO-mediated oxidation", *Colloids and Surfaces A: Physicochemical and Engineering Aspects* 289, no. 1-3 (2006): 219-225.
- [71] **Fukuzumi H.**, Saito T., Iwata T., Kumamoto Y., Isogai A., "Transparent and high gas barrier films of cellulose nanofibers prepared by Tempo-mediated Oxidation," *Biomacromolecules* 10, no. 1 (2009): 162-165.
- [72] **Fujisawa S.**, Okita Y., Fukuzumi H., Saito T., Isogai A., "Preparation and characterization of TEMPO-oxidized cellulose nanofibril films with free carboxyl groups", *Carbohydrate Polymers* 84, no. 1 (2011): 579-583.
- [73] **Rodionova G.**, Saito T., Lenes M., Eriksen Ø., Gregersen Ø., Fukuzumi H., Isogai A., "Mechanical and oxygen barrier properties of films prepared from fibrillated dispersions of TEMPO-oxidized Norway spruce and Eucalyptus pulps", *Cellulose* 19, no.3 (2012):705-711.
- [74] **Liu H.**, Fu S., Zhu J.Y., Li H., Zhan H., "Visualization of enzymatic hydrolysis of cellulose using AFM phase imaging", *Enzyme and Microbial Technology* 45, no. 4 (2009): 274-281.
- [75] **Zhang Y.H.P.**, Himmel M.E., Mielenz J.R., "Outlook for cellulase improvement: Screening and selection strategies", *Biotechnology Advances* 24, (2006): 452-481.
- [76] **Henriksson M.**, Berglund L.A, Isaksson P., Lindstrom T., Nishino T., "Cellulose nanopaper structures of high toughness", *Biomacromolecules* 9 (2008): 1579-1585.
- [77] **Ankerfors M.**, Lindstrom T., Henriksson G., "Method for the manufacture of microfibrillated cellulose", US Patent 2009/0221812.
- [78] **Andresen M.**, Johansson L.S., Tanem B.S., Stenius P., "Properties and characterization of hydrophobized microfibrillated cellulose", *Cellulose* 13, no. 6 (2006): 665-677.
- [79] GEA Niro Soavi, http://www.nirosoavi.com/literature/pdfs/GEA_Niro_Soavi_Profile.pdf (june 2012)
- [80] **Dalle P.**, Girard F., "Mechanical and barrier properties of films made of cellulose micro and nano fibrils", Centre Technique du Papier: Grenoble (2009).
- [81] **Taniguchi T.**, Okamura K., "New films produced from microfibrillated natural fibres", *Polymer International* 47, no. 3 (1998): 291-294.

-
- [82] Ultra-fine friction grinder “Supermasscolloider”, Masuko Sangyo Co. Ltd., <http://www.masuko.com/English/company/Introduction.html> (june 2012)
- [83] **Marx-Figini M.**, “Significance of the Intrinsic Viscosity Ratio of Unsubstituted and Nitrated Cellulose in Different Solvents”, *Die Angewandte Makromolekulare Chemie* 72, no. 1 (1978): 161–171.
- [84] <http://www.innventia.com/en/Our-Expertise/New-materials/Nanocellulose/> (June 2012)
- [85] **Pasbst W.**, “Fundamental considerations on suspension rheology”, *Ceramics – Silikaty* 48, no. 1 (2004): 6-13.
- [86] **Clarke B.**, “Rheology of coarse settling suspensions”, *Transactions of the Institution of Chemical Engineers* 45, no. 6 (1967): 251–256.
- [87] **Lowys M.P.**, Desbrières J., Rinaudo M., “Rheological characterization of cellulosic microfibril suspensions. Role of polymeric additives,” *Food Hydrocolloids* 15, no. 1 (2001): 25-32.
- [88] **Lasseuglette E.**, Roux D., Nishiyama Y.. “Rheological properties of microfibrillar suspension of TEMPO-oxidized pulp”, *Cellulose* 15, no. 3 (2008): 425-433.
- [89] **Iotti M.**, Gregersen Ø.W., Moe S., Lenes M., “Rheological studies of microfibrillar cellulose water dispersions”, *Journal of Polymers and the Environment* 19, no. 1 (2011): 137–145.
- [90] **Saarikoski E.**, Saarinen T., Salmela J., Seppälä J., “Flocculated flow of microfibrillated cellulose water suspensions: an imaging approach for characterisation of rheological behaviour” *Cellulose* 19, no. 3 (2012): 1–13.
- [91] **Aulin C.**, Gällstedt M., Lindström T., “Oxygen and oil barrier properties of microfibrillated cellulose films and coatings”, *Cellulose* 17, no. 3 (2010): 559-574.
- [92] **Syverud K.**, Stenius P., “Strength and barrier properties of MFC films”, *Cellulose* 16, no. 1 (2009): 75-85.
- [93] **Sehaqui H.**, Liu A., Zhou Q., Berglund L.A., “Fast preparation procedure for large, flat cellulose and cellulose/inorganic nanopaper structures”, *Biomacromolecules* 11, no. 9, (2010) p. 2195-2198.
- [94] **Nogi M.**, Iwamoto S., Nakagaito A.N., Yano H., “Optically Transparent Nanofiber Paper”, *Advanced Materials* 21, no. 16 (2009): 1595-1598.
- [95] **O’Sullivan A.**, “Cellulose: the structure slowly unravels”, *Cellulose* 4, no. 3 (1997): 173-207.
- [96] **Svagan A.J.**, Azizi Samir A.S., Berglund L., “Biomimetic polysaccharide nanocomposites of high cellulose content and high toughness”, *Biomacromolecules* 8, no. 8 (2007): 2556-2563.
- [97] **Missoum K.**, M. N. Belgacem, J. Bras, “AKD nano-emulsions: Innovative to increase the solid content of NFC suspensions”, *SUNPAP project – Final conference* (June 2012).

- [98] **Fukuzumi H.**, Saito T., Iwamoto S., Kumamoto Y., Ohdaira T., Suzuki R., Isogai A., "Pore Size Determination of TEMPO-Oxidized Cellulose Nanofibril Films by Positron Annihilation Lifetime Spectroscopy", *Biomacromolecules* 12, no. 11 (2011): 4057-4062.
- [99] **Yano H.**, Sugiyama J., Nakagaito A.N., Nogi M., Matsuura T., Hikita M., Handa K., "Optically Transparent Composites Reinforced with Networks of Bacterial Nanofibers", *Advanced Materials* 17, no. 2 (2005): 153–155.
- [100] **Chun S.J.**, Lee S.Y., Doh G.H., Lee S., Kim J.H., "Preparation of ultrastrength nanopapers using cellulose nanofibrils", *Journal of Industrial and Engineering Chemistry* 17, no. 3 (2011): 521-526.
- [101] **Hartman J.**, Albertsson A.C., Söderqvist Lindblad M., Sjöberg J., "Oxygen Barrier Materials from Renewable Sources: Material Properties of Softwood Hemicellulose-based Films", *Journal of Applied Polymer Science* 100, no. 4 (2006): 2985–2991.
- [102] **Hartman J.**, Albertsson A.C., Sjöberg J., "Surface- and bulk-modified galactoglucomannan hemicellulose films and film laminates for versatile oxygen barriers", *Biomacromolecules* 7, no. 6 (2006): 1983-1989.
- [103] **Sothornvit R.**, Krochta J.M., "Plasticizer effect on oxygen permeability of beta - lactoglobulin films", *Journal of Agricultural and Food Chemistry* 48, (2000):6298–6302.
- [104] **McHugh T.H.**, Krochta J.M., "Edible coatings films improve food quality", Technomic Publishing: Lancaster (1994).
- [105] **McHugh T.H.**, Krochta J.M., "Sorbitol- vs glycerol-plasticized whey protein edible films: integrated oxygen permeability and tensile property evaluation", *Journal of Agricultural and Food Chemistry* 42, (1994c):841–845.
- [106] **Rindlav-Westling A.**, Stading M., Hermansson A.M., Gatenholm P., "Structure, mechanical and barrier properties of amylose and amylopectin films", *Carbohydrate polymers* 36, (1998):217–224.
- [107] **Wu J.**, Yuan Q., "Gas permeability of a novel cellulose membrane", *Journal of Membrane Science* 204, no. 1 (2002):185–194.
- [108] **Newton K.G.**, Rigg W.J., "The Effect of Film Permeability on the Storage Life and Microbiology of Vacuum-packed Meat", *Journal of Applied Microbiology* 47, no. 3 (1979): 433–441.
- [109] **Butler B.I.**, Vergano P.J., Testin R.F., Bunn J.M., Wiles J.I., "Mechanical and Barrier Properties of Edible Chitosan Films as Affected by Composition and Storage", *Journal of Food Science* 61, no. 5 (1996): 953–956.
- [110] **Gröndahl M.**, Eriksson L., Gatenholm P., "Material Properties of Plasticized Hardwood Xylans for Potential Application as Oxygen Barrier Films", *Biomacromolecules* 5, no. 4 (2004): 1528-1535.
- [111] **Höije A.**, Sternemalm E., Heikkinen S., Tenkanen M., Gatenholm P., "Material properties of films from enzymatically tailored arabinoxylans", *Biomacromolecules* 9, no. 7 (2008):2042–2047.

- [112] **Minelli M.**, Baschetti M.G., Doghieri F., Ankerfors M., Lindström T., Siró I., Plackett D., "Investigation of mass transport properties of microfibrillated cellulose (MFC) films", *Journal of Membrane Science* 358, no. 1 (2010): 67–75.
- [113] **Belbekhouche S.**, Bras J., Siqueira G., Chappey C., Lebrun L., Khelifi B., Marais S., Dufresne A., "Water sorption behavior and gas barrier properties of cellulose whiskers and microfibrils films", *Carbohydrate Polymers* 83, no. 4 (2011): 1740–1748.
- [114] **Siró I.**, Plackett D., Hedenqvist M., Ankerfors M., Lindström T., "Highly Transparent Films from Carboxymethylated Microfibrillated Cellulose: The Effect of Multiple Homogenization Steps on Key Properties", *Journal of Applied Polymer Science* 119, no. 5 (2011): 2652–2660.
- [115] **Järnström L.**, Brossmer C., Nilsson P.O., Hansson P., Wiklander K., "Hydrophobically modified cationic starches for surface treatment" *TAPPI Coating Conference and Trade Fair*, (2000): 99-114
- [116] **Jansson A.**, Järnström L., "Barrier and mechanical properties of modified starches", *Cellulose* 12, no. 4 (2005): 423-433.
- [117] **Bertuzzi M.A.**, Armada M., Gottifredi J.C., "Physicochemical characterization of starch based films", *Journal of Food Engineering* 82, no. 1 (2007): 17-25.
- [118] **Chivrac F.**, Angellier-Coussy H., Guillard V., Pollet E., Averous L., "How does water diffuse in starch/montmorillonite nano-biocomposite materials?", *Carbohydrate polymers* 82, no. 1 (2010): 128-135.
- [119] **Gáspár M.**, Benko Zs., Dogossy G., Réczey K., Czigány T., "Reducing water absorption in compostable starch-based plastics", *Polymer Degradation and Stability* 90, no. 3 (2005): 563-569.
- [120] **Dole P.**, Joly C., Espuche E., Alric I., Gontard N., "Gas transport properties of starch based films", *Carbohydrate Polymers* 58, no. 3 (2004): 335-343.
- [121] **Sinha Ray S.**, Masami O., "New Polylactide/Layered Silicate Nanocomposites", *Macromolecular Materials and Engineering* 288, no. 12 (2003): 936-944.
- [122] **Chivrac F.**, "Nano-biocomposite: systèmes structures à base d'amidon et d'argiles", PhD Thesis, Université de Strasbourg (2009).
- [123] **Park H.M.**, Lee W.K., Park C.Y., Cho W.J., Ha C.S., "Environmentally friendly polymer hybrids Part I Mechanical, thermal, and barrier properties of thermoplastic starch/clay nanocomposites", *Journal of Materials Science* 38, no. 5 (2003): 909-915.
- [124] **Dufresne A.**, Vignon M.R., "Improvement of starch film performances using cellulose microfibrils", *Macromolecules* 31, no. 8 (1998): 2693-2696.
- [125] **Lopez-Rubio A.**, Lagaron J.M., Ankerfors M., Lindstrom T., Nordqvist D., Mattozi A., Hedenqvist M.S., "Enhanced film forming and film properties of amylopectin using microfibrillated cellulose", *Carbohydrate Polymers* 68, no.4 (2007): 718-727.
- [126] **Svagan A.J.**, Hedenqvist M.S., Berglund L., "Reduced water vapour sorption in cellulose nanocomposites with starch matrix", *Composites Science and Technology* 69, no.3-4 (2009): 500-506.

- [127] **Plackett D.**, Anturi H., Hedenqvist M., Ankerfors M., Gällstedt M., Lindström T., Siró I., “Physical properties and morphology of films prepared from microfibrillated cellulose and microfibrillated cellulose in combination with amylopectin”, *Journal of Applied Polymer Science* 117, no. 6 (2010): 3601–3609.
- [128] **Ramaraj B.**, “Crosslinked Poly(vinyl Alcohol) and Starch Composite Films. II. Physicomechanical, Thermal Properties and Swelling Studies”, *Journal of Applied Polymer Science* 103, no. 2 (2007): 909–916.
- [129] **Stinga C.**, “Utilisation de la chimie chromatogénie pour la conception et la réalisation de matériaux cellulosiques barrières à ‘eau, aux graisses et aux gaz”, PhD Thesis, Université Joseph Fourier Grenoble (2008)
- [130] **Roohani M.**, Habibi Y., Belgacem N.M., Ebrahim G., Karimi A.N., Dufresne A., “Cellulose whiskers reinforced polyvinyl alcohol copolymers nanocomposites”, *European Polymer Journal* 44 (2008): 2489-2498.
- [131] **Strawhecker K.E.**, Manias E., “Structure and Properties of Poly(vinyl alcohol)/Na⁺ Montmorillonite Nanocomposites”, *Chemistry of Materials* 12, no. 10 (2000): 2943-2949.
- [132] **Probst O.**, Moore E.M., Resasco D.E., Grady B.P., “Nucleation of polyvinyl alcohol crystallization by single-walled carbon nanotubes”, *Polymer* 45, no. 13 (2004): 4437–4443.
- [133] **Lu J.**, Wang T., Drzal L.T., “Preparation and properties of microfibrillated cellulose polyvinyl alcohol composite materials”, *Composites: Part A: applied science and manufacturing* 39 (2008): 738-746.
- [134] **Cheng Q.**, Wang S., Rials T.G., “Poly(vinyl alcohol) nanocomposites reinforced with cellulose fibrils isolated by high intensity ultrasonication”, *Composites Part A: Applied Science and Manufacturing* 40, no. 2 (2009): 218-224.
- [135] **Paralikar S.A.**, Simonsen J., Lombardi J., “Poly(vinyl alcohol)/cellulose nanocrystal barrier membranes”, *Journal of membrane science* 320, no.1-2 (2008): 248-258.
- [136] **Eriksen O.**, Syverud K., Gregersen O., “The use of microfibrillated cellulose produced from kraft pulp as strength enhancer in TMP paper”, *Nordic Pulp and Paper Research Journal* 23, no. 3 (2008): 299-304.
- [137] **Ahola S.**, Osterberg M., Laine J., “Cellulose nanofibrils-adsorption with poly(amidamine) epichlorohydrin studied by QCM-D and application as a paper strength additive”, *Cellulose* 15, no.2 (2008): 303-314.
- [138] **Mörseburg K.**, Chinga-Carrasco G., “Assessing the combined benefits of clay and nanofibrillated cellulose in layered TMP-based sheets”, *Cellulose* 16, no. 5 (2009): 795-806.
- [139] **Hamada H.**, Bousfield D.W., “Nano-fibrillated cellulose as a coating agent to improve print quality of synthetic fiber sheets”, *TAPPI 11th Advanced Coating Fundamentals Symposium* (October 2010).
- [140] **Meyer V.**, Tapin-Lingua S., Da Silva Perez D., Arndt T., Kautto J., “Technical opportunities and economic challenges to produce nanofibrillated cellulose in pilot scale: NFC delivery for applications in demonstration trials”, *SUNPAP project – Final conference* (June 2012).

- [141] **Weilbacher R.**, "Polyvinyl Alcohol:Structure and Applications", *Presentation of Kuraray product, Centre Technique du Papier*. Grenoble (Avril 2012).
- [142] **Sneck A.**, A. Tanaka, V. Meyer, J. Kretschmar, "Advanced characterization techniques to evaluate the structure of nanofibrillated cellulose", *SUNPAP project – Final conference* (June 2012).
- [143] **Goodyer S.**, "Rheological measurements for the coating industry", *Surface coatings International 2*, (2010).
- [144] **Berlioz S.**, "*Etude de l'estérification de la cellulose par une synthèse sans solvant. Application aux matériaux nanocomposites*", PhD Thesis, Université Joseph Fourier Grenoble (2007).
- [145] **Azizi Samir A.S.**, F. Alloin, A. Dufresne, "Review of Recent Research into Cellulosic Whiskers, Their Properties and Their Application in Nanocomposite Field", *Biomacromolecules* 6, no. 2 (2005): 612-626.
- [146] **Tatsumi D.**, Ishioka S. and Matsumoto T., "Effect of fiber concentration and axial ratio on the rheological properties of cellulose fiber suspensions", *Journal of the society of rheology* 30, no.1 (2002): 27-32.
- [147] **Hill R. J.**, "Elastic modulus of microfibrillar cellulose gels", *Biomacromolecules* 9, no.10 (2008): 2963–2966.
- [148] **Henriksson M.**, L. Berglund, "Structure and properties of cellulose nanocomposite films containing melanine formaldehyde", *Journal of Applied Polymer Science* 106 (2007): 2817-2824.
- [149] **Silvy J.**, C. Pannier, J. Veyre, *16th Eucepta Conference Proceedings*, Paris (1976).
- [150] **Alemdar A.**, M. Sain, "Isolation and characterization of nanofibers from agricultural residues – Wheat straw and soy hulls" *Bioresource Technology* 99, no. 6 (2008): 1664-1671.
- [151] **Lagaron J.M.**, R. Catal, R. Gavara, "Structural characteristics defining high barrier properties in polymeric materials", *Materials Science and Technology* 20, no. 1 (2004): 1-7.
- [152] **Segal L.**, J. J. Creely, A. E. Martin, C. M. Conrad, "An Empirical Method for Estimating the Degree of Crystallinity of Native Cellulose Using the X-Ray Diffractometer", *Textile Research Journal* 29, no. 10 (1959): 786-794.
- [153] **Moon R. J.**, Martini A., Nairn J., Simonsen J., et Youngblood J., "Cellulose nanomaterials review: structure, properties and nanocomposites", *Chemical Society reviews* 40, no. 7 (2011): 3941-3994.
- [154] **Thygesen A.**, Oddershede J., Lilholt H., Thomsen A. B., Ståhl K., "On the determination of crystallinity and cellulose content in plant fibres", *Cellulose* 12, no. 6 (2005): 563-576.
- [155] **Brancato A.**, F. L. Walsh, R. Sabo, S. Banerjee, "Effect of Recycling on the Properties of Paper Surfaces", *Industrial & Engineering Chemistry Research* 46, no. 26 (2007): 9103-9106.

- [156] **Pettersson G.**, Sjöberg J., Wågberg L., Höglund H., "Increased Joint-forming Ability of Ductile Kraft Pulp Fibres by Polyelectrolyte Multilayer treatment-Influence of Refining and Drying Strategies", *Nordic Pulp and Paper Research Journal* 22, no.2 (2007).
- [157] **Kjellgren H.**, M. Gällstedt, G. Engström, L. Järnström, "Barrier and surface properties of chitosan-coated greaseproof paper", *Carbohydrate polymers* 65, no. 4 (2006): 453–460.
- [158] **Okubayashi S.**, U. J. Griesser, T. Bechtold, "A kinetic study of moisture sorption and desorption on lyocell fibers", *Carbohydrate Polymers* 58, no. 3 (2004): 293-299.
- [159] **Rodionova G.**, Roudot S., Eriksen Ø, Männle F., Gregersen Ø, "The formation and characterization of sustainable layered films incorporating microfibrillated cellulose (MFC)", *BioResources* 7, no. 3 (2012): 3690-3700
- [160] **Saito T.**, Kimura S., Nishiyama Y., Isogai A., "Cellulose nanofibers Prepared by Tempo-Mediated Oxidation of native cellulose", *Biomacromolecules* 8 (2007): 2485-2491.
- [161] **Schmidt G.**, Malwitz M.M., "Properties of polymer–nanoparticle composites", *Current Opinion in Colloid & Interface Science* 8, no. 1 (2003): 103-108.
- [162] Mowiol Brochure, Clariant Gmbh Division CP (1999).
- [163] **Hedayati M.**, Salehi M., Bagheri R., Panjepour M., Maghzian A., "Ball milling preparation and characterization of poly (ether ether ketone)/surface modified silica nanocomposite", *Powder Technology* 207, no. 1-3 (2011): 296-303.
- [164] **Vigneshwaran N.**, Ammayappan L., Huang Q, "Effect of Gum arabic on distribution behavior of nanocellulose fillers in starch film", *Applied Nanoscience* (2011): 1–6.
- [165] **Guérin D.**, Bébien F., "Starch based barrier coating, example of a new European project "FlexpackRenew"", *8th Pagora days: Future of fibre based biomaterials for packaging ?*, Grenoble (2009).
- [166] **Viguié J.**, Molina-Boisseau S., Dufresne A., "Processing and Characterization of Waxy Maize Starch Films Plasticized by Sorbitol and Reinforced with Starch Nanocrystals", *Macromolecular Bioscience* 7, no. 11 (2007): 1206-1216.
- [167] **Gaudin S.**, Lourdin D., Le Botlan D., Ilari J., Colonna P., "Plasticisation and Mobility in Starch-Sorbitol Films", *Journal of Cereal Science* 29, no. 3 (1999): 273-284.
- [168] **Krogars K.**, "Aqueous-based amylose-rich maize starch solution and dispersion: a study on free films and coatings", PhD thesis, University of Helsinki (2003).
- [169] **Parra D.F.**, Tadini C.C., Ponce P., Lugão A.B., "Mechanical properties and water vapor transmission in some blends of cassava starch edible films", *Carbohydrate Polymers* 58, no. 4 (2004): 475-481.
- [170] **Lourdin D.**, Bizot H., Colonna P, ""Antiplasticization" in Starch-glycerol Films?", *Journal of Applied Polymer Science* 63, no. 8 (1997): 1047–1053.
- [171] **Hrabalova M.**, Schwanninger M., Wimmer R., Gregorova A., Zimmermann T., Mundigler N., "Fibrillation of flax and wheat straw cellulose effects on thermal, morphological and viscoelastic properties of poly(vinylalcohol)/fibre composites", *BioResources* 6, no. 2 (2011).

[172] **Hasimi A.**, Stavropoulou A., Papadokostaki K.G., Sanopoulou M., “Transport of water in polyvinyl alcohol films: Effect of thermal treatment and chemical crosslinking”, *European Polymer Journal* 44, no. 12 (2008): 4098-4107.

[173] <http://www.cmc.de/typo3temp/pics/87e77ae529.jpg>

[174] **Rogers C.E.**, “Permeation of gases and vapours in polymers”, *Polymer Permeability*, Comyn J., Elsevier Applied Science, London, (1985): 11–73.

[175] **Pesonen J.**, Bellmann G, Toivakka M., “The influence of coating color characteristics on board coating with a soft-tip blade”, 22nd PTS Streicherei-Symposium (Sept 2005).

[176] **Briscoe B.**, Luckham P., Zhu S., “The effects of hydrogen bonding upon the viscosity of aqueous poly(vinyl alcohol) solutions”, *Polymer* 41, no. 10 (2000): 3851-3860.

List of abbreviations

AFM	Atomic force microscope
CNC	Cellulose nanocrystals
CTP	Centre technique du Papier
DP	Degree of polymerization
DSC	Differential scanning calorimetry
MFC:	Microfibrillated cellulose
NFC:	Nanofibrillated cellulose
OTR:	Oxygen transmission rate
PEG	Poly(ethylene glycol)
PVOH	Poly(vinyl alcohol)
RH	Relative humidity
SEM	Scanning electron microscope
SEM-FEG	Field Emission Gun Scanning Electron Microscope
SR°	Schopper-Riegler degree
TEM	Transmission Electron Microscope
TGA	Thermal gravimetry analysis
SUNPAP	Scale-up of nanoparticles in modern papermaking
WVTR	Water Vapour Transmission rate
XRD	X-ray diffraction

Résumé étendu

Introduction

La fabrication des matériaux d'emballage est un secteur industriel majeur porteur d'innovations pour répondre aux attentes des donneurs d'ordres. Poussés par les évolutions réglementaires, sociétales, économiques et technologiques, les industriels demandent des matériaux toujours plus performants (résistance mécanique et propriétés barrières notamment), toujours plus légers, constitués de matériaux bio-sourcés avec un impact environnemental et un coût réduits. Dans le secteur des papiers et cartons d'emballage, les matériaux les plus performants sont généralement des combinaisons de plusieurs matériaux : papier/carton, film polymère pétrosourcé et éventuellement feuille d'aluminium. Cependant, ces matériaux dérivés du pétrole présentent plusieurs inconvénients tels que leur origine non renouvelable, leur coût directement indexé sur le prix du pétrole, leur faible recyclabilité et leur impact sur l'environnement. La prise de conscience de l'impact environnemental des emballages, perçue à travers des analyses du cycle de vie, poussent les industriels utilisateurs de ce type d'emballage à demander le remplacement des polymères pétrosourcés par des polymères biosourcés ne posant pas de problèmes de recyclage. De plus, l'utilisation de nanoparticules est une voie prometteuse pour développer des matériaux plus légers et plus performants. Parmi les nanomatériaux disponibles ou en cours de développement, les micro et nanofibrilles de cellulose semblent être les produits les plus intéressants car ils offrent les avantages naturels de la cellulose (ressource issue de la biomasse non compétitive avec l'agriculture vivrière, biodégradabilité), de surprenantes propriétés barrières (à l'huile et à l'oxygène) et de bonnes propriétés de résistance mécanique (résistance à la traction).

Les micro et nanofibrilles de cellulose (M-NFC) ont initialement été étudiées par Turback *et al.*¹ en 1983 et l'intérêt pour ces nanomatériaux s'est vraiment accentué depuis 2005 au regard du nombre de publications et de brevets réalisés sur le sujet donné en Figure 1.

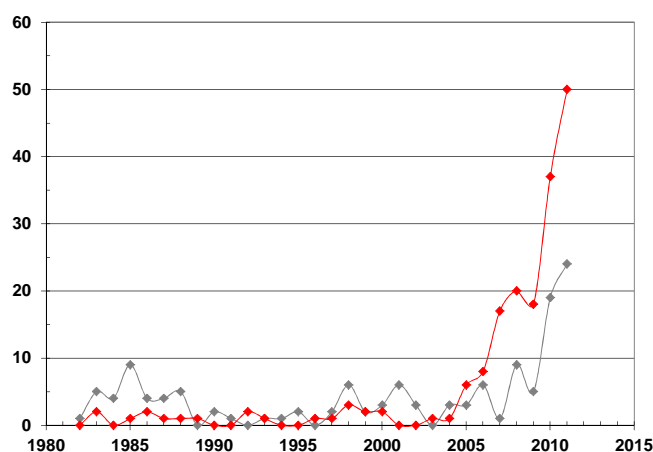


Figure 1: Nombre de brevets et d'articles contenant le terme « microfibrillated cellulose ».

La cellulose est un dérivé du bois ainsi que de diverses plantes annuelles, des algues ou encore de bactéries. Synthétisée à hauteur de 10^{11} tonnes par an, la cellulose est un matériau renouvelable et abondant. La structure du bois, représentée Figure 2 à différentes échelles, montre que celui-ci est constitué de fibres elle-même constituées d'un assemblage de microfibrilles de cellulose.

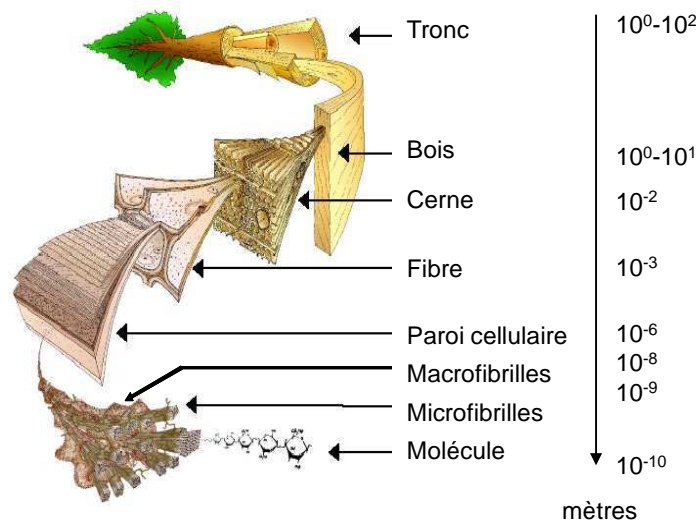


Figure 2 : Structure du bois².

Les microfibrilles de cellulose, appelées MFC, peuvent être extraites et isolées par des procédés de fibrillation correspondant à la délamination de la fibre. Turback *et al.*¹ et Herrick *et al.*³ ont initié la production de suspension de MFC en introduisant une suspension de fibres diluée dans un homogénéiseur sous une forte pression plusieurs fois de suite. Cependant ce procédé avait une forte demande énergétique. Afin de réduire les coûts de production, différentes techniques ont été développées en utilisant des prétraitements facilitant la fibrillation. Les trois principaux prétraitements sont :

- Le prétraitement mécanique permettant de diminuer la longueur de la fibre
- Le prétraitement enzymatique diminuant les interactions hydrogènes
- Le prétraitement chimique (hydrolyse acide, oxydation TEMPO, carboxyméthylation) qui réduit la longueur des chaînes, et/ou modifie la surface des fibres et/ou augmente l'espace interchaîne glucosidique.

Suite aux prétraitements, un traitement mécanique imposant un fort cisaillement est nécessaire pour défibriller la fibre et obtenir une suspension de MFC. Trois appareils sont principalement utilisés : l'homogénéiseur, le Masuko grinder et le microfluidizer décrit Figure 3.



Figure 3 : Description des appareils d'homogénéisation^{4,5,6}.

Les MFC ainsi produites ont un diamètre de 10-30 nm et une longueur d'environ 1-3 μm (cf. Figure 4). De plus, le procédé de fibrillation permet de conserver la partie cristalline tout comme la partie amorphe des microfibrilles.

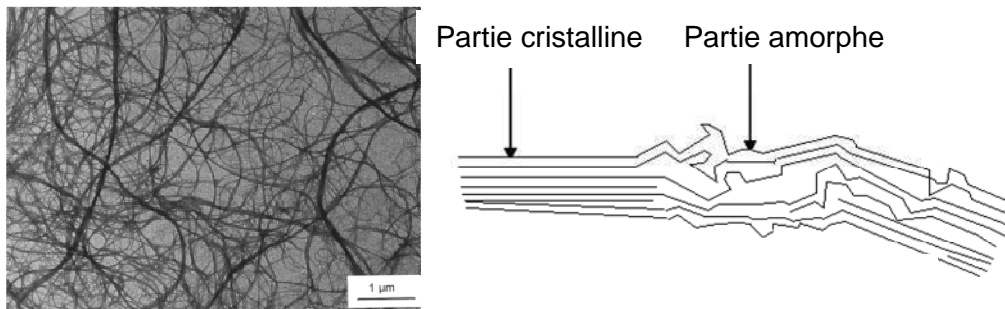


Figure 4 : Image MET de microfibrilles de cellulose².

Hormis leur caractère biosourcé, les MFC présentent de multiples avantages tels que leur faible densité, leur facteur de forme important, leur surface spécifique élevée et leur résistance mécanique. En effet, si on compare le module de Young spécifique des MFC avec ceux de divers matériaux, sa valeur est bien supérieure comme observé Figure 5.

Matériau	Module de Young (GPa)	Densité (g/cm ³)	Module spécifique (J/g)
Aluminium	69	2,7	26
Acier	200	7,8	26
Verre	69	2,5	28
Cellulose cristalline	139	1,5	92
Microfibrilles de cellulose	80-100	1,5	53-66

Figure 5 : Comparaison des propriétés mécaniques de divers matériaux^{7,8}.

De plus, il a été reporté dans la littérature que les MFC forment des films possédant des propriétés barrières prometteuses et supérieures à d'autres matériaux barrières (Figure 6).

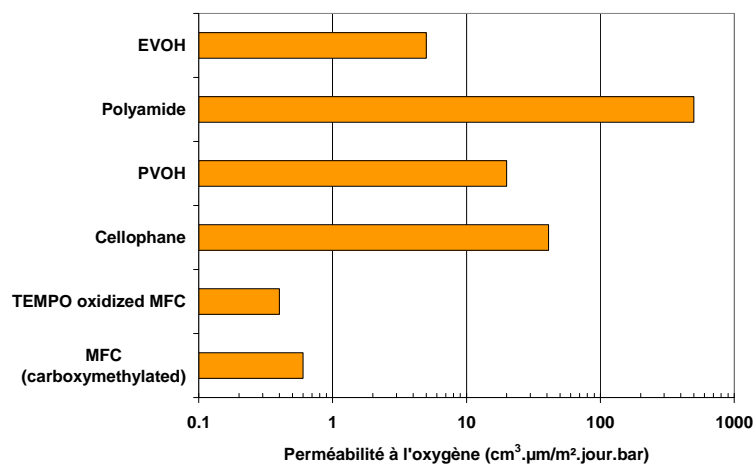


Figure 6 : Comparaison des perméabilités à l'oxygène de divers matériaux⁹.

L'objectif de cette thèse était ainsi de développer de nouveaux matériaux barrières à partir des microfibrilles de cellulose. Une partie des travaux a été réalisée dans le cadre d'un projet européen ayant pour principal objectif la mise à l'échelle industrielle de l'utilisation des MFC/NFC dans les procédés papetiers. L'étude est constituée de trois principales parties comme décrit Figure 7.



Figure 7: Organisation de l'étude.

Tout d'abord, l'étude s'est focalisée sur l'influence du degré de fibrillation sur les propriétés des suspensions de MFC et le développement de films 100% MFC. La seconde partie a été dédiée au développement de composites à partir de MFC et de deux matrices différentes l'amidon et l'alcool poly(vinyle) afin d'évaluer l'influence des MFC sur les propriétés mécaniques et barrières des deux matrices. Enfin, des formulations à base de MFC ont été établies dans une troisième partie permettant de reporter le potentiel des MFC pour produire des couches barrières à la surface d'un carton. Chacune de ces trois parties sera décrite de façon synthétique dans ce résumé étendu.

1. - Etude des suspensions et des films de MFC

Trois suspensions de MFC ont été étudiées afin d'établir l'influence du process sur les propriétés finales des suspensions et des films produits à partir de celles-ci. La caractérisation des MFC est difficile et il est actuellement impossible de déterminer la distribution de taille des éléments présents dans une suspension. En effet, les microfibrilles présentent un haut facteur de forme ne permettant pas d'évaluer le diamètre et la longueur des éléments aux mêmes échelles par microscopie. De plus, l'agrégation des MFC lors du séchage pour la préparation de l'échantillon rend difficile la visualisation de MFC individualisée. Ainsi, la combinaison de plusieurs techniques est nécessaire afin de caractériser et comparer plusieurs grades de MFC.

Les moyens de caractérisations mis en œuvre étaient premièrement la caractérisation microscopique et l'étude de la rhéologie des suspensions afin d'obtenir des indications sur la taille des éléments et le degré de fibrillation. Deuxièmement, des films produits par deux méthodes ont permis d'évaluer les propriétés intrinsèques des MFC.

1.1. - Matériels et méthodes

1.1.1. - Matériels

Trois types de MFC ont été étudiés dans cette étude. Les premières, nommées MFC-Arbo, correspondent à de la cellulose fine fournie par JRS et sont utilisées comme référence commerciale. Deux autres grades de MFC, MFC-E-MG et MFC-T-MG, produits à l'échelle laboratoire comme décrit Figure 8, ont été étudiés et comparés.

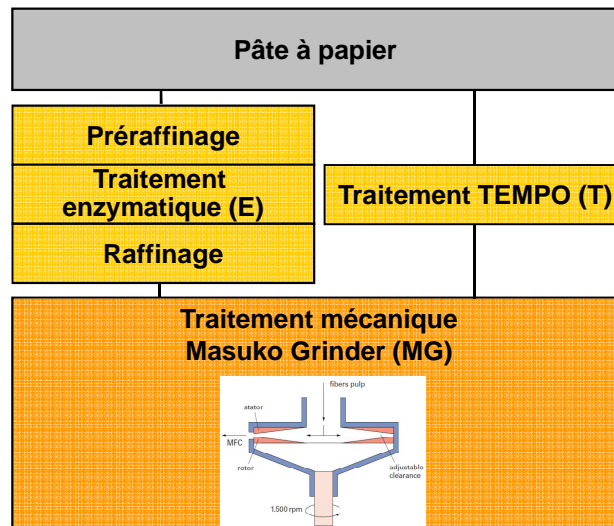


Figure 8 : Procédés de production des MFC-E-MG et MFC-T-MG.

Les trois grades de MFC ont ainsi une concentration et un aspect différent (cf. Figure 9). Les MFC-Arbo livrées à une concentration de 13% ont une apparence de pâte hyper raffinée. Les suspensions produites à l'échelle laboratoire, ont une concentration de 2% avec un comportement de type gel. La viscosité des suspensions est influencée par le prétraitement de la pâte avant fibrillation avec notamment une viscosité deux fois plus importante pour les MFC obtenues par traitement TEMPO.

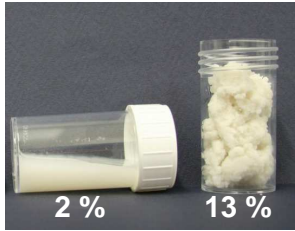
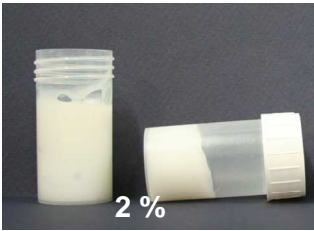
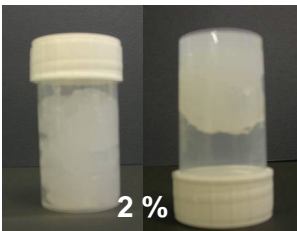
Référence commerciale	Production au laboratoire	
MFC-Arbo	MFC-E-MG	MFC-T-MG
		
$\eta = 3 \text{ Pa.s à } 1\text{s}^{-1}$	$\eta = 10 \text{ Pa.s à } 1\text{s}^{-1}$	$\eta = 20 \text{ Pa.s à } 1\text{s}^{-1}$

Figure 9 : Apparence des trois grades de MFC étudiés.

1.1.2. - Méthodes

Deux techniques ont été utilisées pour la production de films de MFC, la première est la coulée/évaporation et la seconde utilise une formette semi-automatique.

Tous les tests de caractérisation ont été réalisés sur les films après 24h de conditionnement à 23°C-50% HR.

Les films ont été soumis à des tests de traction en utilisant un Instron équipé d'une cellule de 500N. Les mesures sont réalisées selon la norme ISO 1924-2, à une vitesse de 10mm/min sur des échantillons de 15mm de large et 100 mm de long. Un minimum de 5 échantillons était testé par référence.

Les coefficients de transmission à la vapeur d'eau et à l'oxygène des films étaient déterminés suivant la norme ISO 2528 et la norme ISO 15105-2:2003 Annexe A respectivement.

1.2. - Résultats et discussion

1.2.1. - Morphologie des éléments

Les images de microscopie des trois grades de MFC, obtenues avec un microscope optique et un microscope électronique à balayage montrent des différences de taille des éléments (cf. Figure 10). En effet, les MFC-Arbo apparaissent avec des tailles d'éléments bien supérieures aux deux autres suspensions. Avec une production à l'échelle laboratoire, on observe au MEB l'obtention d'éléments fins, toutefois il est impossible d'en déterminer la longueur. D'autres techniques comme la rhéologie ont permis de confirmer que la taille des éléments de MFC-Arbo était supérieure à celle des MFC-E-MG elle même légèrement supérieure à MFC-T-MG.

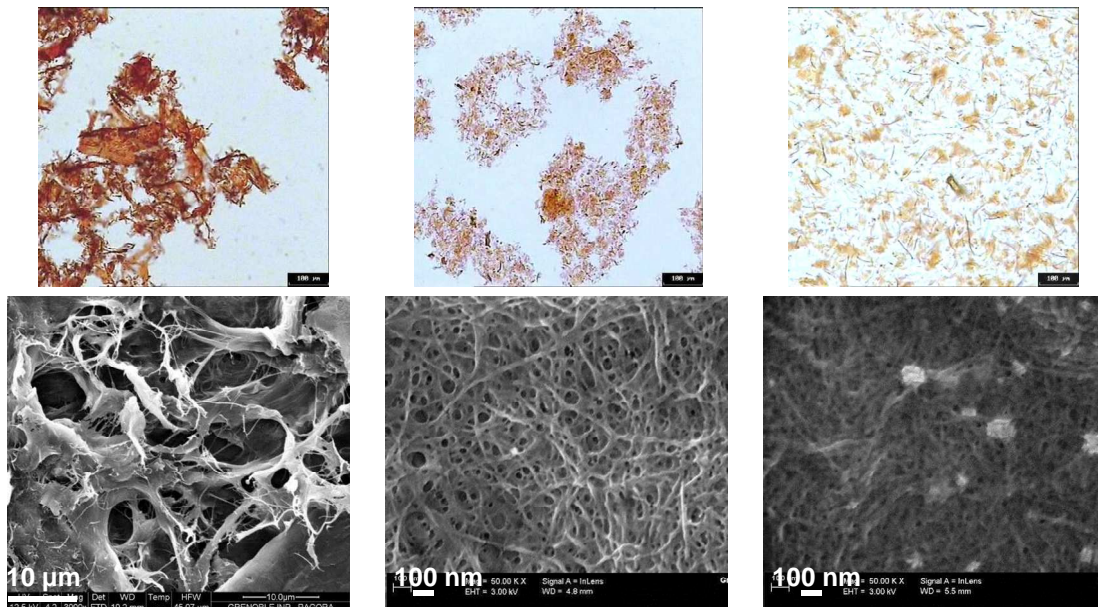


Figure 10 : Images microscopiques des trois grades de MFC.

1.2.2. - Propriétés des films de MFC produits par coulée/évaporation

1.2.2.1. - Apparence

L'apparence des films et leurs propriétés finales dépendent de la taille des éléments. En effet comme observé sur les photos Figure 11, la transparence des films augmente en fonction de la finesse des éléments.



Figure 11 : Apparences des films obtenues à partir de MFC-Arbo, MFC-E-MG, MFC-T-MG.

Ces observations sont confirmées par les valeurs de transmittance Figure 12. Ces différences peuvent être en partie dues à des différences de rugosité également observées. Enfin, la taille des éléments impacte directement sur la densité finale, en effet les éléments fins entraînent un compactage plus important avec un grand nombre d'interactions entre fibrilles.

	MFC-Arbo	MFC-E-MG	MFC-T-MG
Transmittance (%)	81	91	98
Rugosité (μm)	2.5	0.3	0.15
Densité (g/cm^3)	0.67	1.0	1.2

Figure 12: Propriétés des films de MFC produits à partir de MFC-Arbo, MFC-E-MG, MFC-T-MG.

1.2.2.2. - Résistance à la traction

Les propriétés mécaniques des films et en particulier leurs modules de Young résultent des interactions entre microfibrilles et ainsi de la densité du film. Les MFC-T-MG permettent ainsi le développement de films plus résistants comme observé Figure 13. Ces valeurs sont comparables avec celles décrites auparavant dans la littérature.

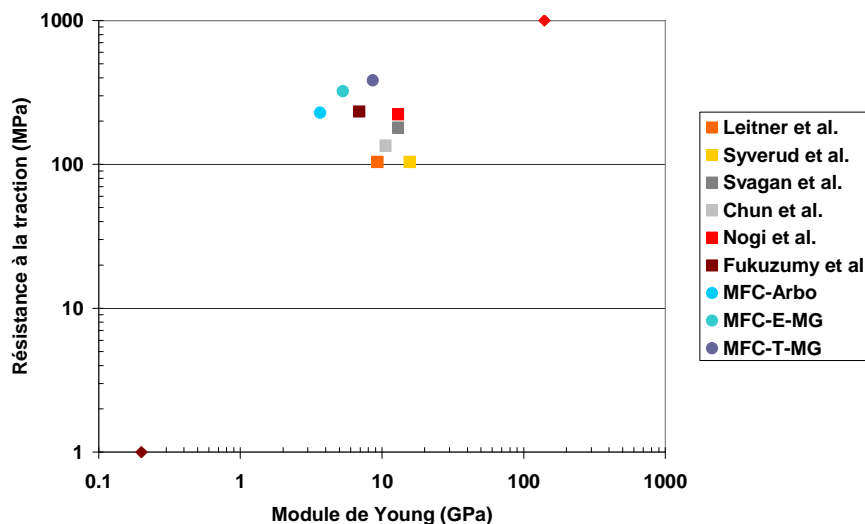


Figure 13: Propriétés mécanique des films de MFC^{10,11,12,13,14,15}.

1.2.2.3. - Propriétés barrières

Concernant les propriétés barrières, deux mesures ont été réalisées sur les films obtenus à partir des trois suspensions de MFC : mesures des coefficients de transmission à la vapeur d'eau (WVTR) à 23°C-50% HR et à l'oxygène (OTR) à 23°C-0% HR. Les valeurs de WVTR 23°C-50% HR montrent que la meilleure performance est obtenue pour les films MFC-E-MG (cf. Figure 14). Le réseau formé à partir des éléments les plus fins permettent en effet de former une couche barrière performante. Cependant, le prétraitement de la pâte influence également cette propriété. En effet, malgré une taille plus fine pour les MFC TEMPO, la modification de chimie de surface des MFC due à l'oxydation augmentant le caractère hydrophile des MFC, la perméabilité à l'eau de leurs films est supérieure à celles des films de MFC prétraitées par enzymes.

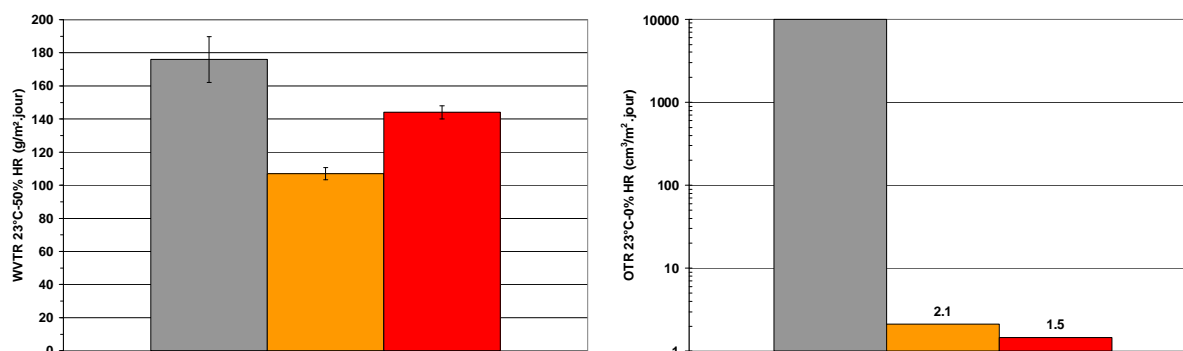


Figure 14 : Propriétés barrières des MFC.

Des écarts importants sont observés pour les valeurs de perméabilité à l'oxygène. En effet, l'OTR du film MFC-Arbo est supérieur à 10000 correspondant à la limite du détecteur. Ceci montrait bien que ce type de MFC ne permet pas d'obtenir de films avec de bonnes propriétés barrières à l'oxygène contrairement aux deux autres grades produits à l'échelle laboratoire qui montraient des valeurs prometteuses inférieures à 2.

1.2.3. - Comparaison des méthodes de production des films de MFC

La méthode par coulée/évaporation est une méthode couramment utilisée pour l'élaboration de films modèles à l'échelle laboratoire. Toutefois, afin d'étudier les possibilités d'un transfert industriel, une deuxième technique a été étudiée pour la production de films. Cette technique, appelée technique formette, utilisant une formette semi-automatique, se rapproche des procédés papetiers et permet la formation rapide de films de MFC.

Les propriétés des films obtenues ont ainsi été comparées avec celles obtenues pour les films produits par coulée/évaporation à partir des MFC-E-MG. Toutes les valeurs sont résumées dans le tableau Figure 15.

	Coulée/ évaporation	Méthode par formette
Densité (g/cm³)	1.05	1.15
Transmittance (%)	91	85
Rugosité (µm)	0.3	0.7
Module de Young (GPa)	5.6	7.7
WVTR 23°C-50% HR (g/m².jour)	107	172
OTR 23°C-0% HR (cm³/m².jour)	1.8	1.7

Figure 15: Comparaison des propriétés de films de MFC-E-MG obtenus par coulée/évaporation et par méthode formette.

Il apparaît ainsi que la technique de film formette permet l'obtention de films plus denses entraînant ainsi un module de Young plus important. Cependant, la transparence est légèrement plus faible avec une rugosité plus importante. Les propriétés barrières à l'oxygène sont équivalentes pour les deux types de film, toutefois les films formette montrent une barrière à la vapeur d'eau inférieure. Ces résultats montrent ainsi l'influence de la technique de production des films sur les propriétés des films.

1.3. - Conclusion

Cette étude a ainsi permis de démontrer l'influence de la taille des éléments sur les propriétés des suspensions puis des films 100% MFC. En effet, la rhéologie des suspensions augmente généralement avec la finesse des fibrilles. De même, les films les plus performants sont produits à partir des suspensions les plus homogènes et des éléments les plus fins. Il a également été observé que le prétraitement utilisé lors de la production des MFC impacte également sur les propriétés. En effet, l'oxydation TEMPO introduisant des groupements carboxyle augmente le caractère hydrophile des MFC entraînant une augmentation de leur sensibilité à l'eau. Enfin la méthode de préparation des films et notamment le séchage joue également un rôle sur les propriétés finales des films.

Les films de MFC ont montré des propriétés intéressantes avec notamment une bonne résistance mécanique et une forte barrière à l'oxygène. Toutefois, des améliorations devront être apportées pour entrevoir la possibilité d'un transfert à l'échelle industriel. En effet, la sensibilité à l'eau des films restent un frein majeur à leur utilisation dans les applications emballages.

2. - Développement de composites polymère/MFC

L'utilisation des MFC à l'échelle industrielle peut être difficile à cause de leur faible concentration (2%) accompagnée de leur forte viscosité. C'est pourquoi, il peut-être intéressant de les coupler avec différentes matrices. Dans cette étude, deux matrices hydrosolubles ont été sélectionnées : un amidon et un alcool poly(vinyle) (PVA_L) afin d'obtenir une bonne compatibilité avec les MFC. L'influence de l'addition des MFC a ainsi été étudiée sur les propriétés des deux matrices. Les propriétés mécaniques et barrières des films composites ont été déterminées en fonction du ratio de MFC allant de 0% à 100%.

2.1. - Matériels et méthodes

2.1.1. - Matériels

Les microfibrilles de cellulose utilisées dans cette étude étaient les MFC-E-MG, produites à partir d'une pâte épicea/pin et utilisant un prétraitement enzymatique suivi de 5 passages dans un masuko grinder. Deux matrices sont étudiées, la première est le polyvinyle alcool (PVA_L) le Mowiol 4-98 (Kuraray) et la seconde est un amidon modifié par des groupements hydrophobe (Cargill).

2.1.2. - Méthodes

Des films composite polymère/MFC de 30 g/m² ont été élaborés avec des ratios de MFC allant jusque 100% par coulée/évaporation.

L'organisation des microfibrilles au sein de la matrice a été observée en utilisant deux techniques : la première est la microscopie électronique à balayage (MEB) et la seconde est la microscopie optique à lumière polarisée.

Les propriétés mécaniques et barrières de ces matériaux ont été déterminées en suivant les méthodes décrites dans la première partie.

2.2. - Résultats et discussion

2.2.1. - Apparence des films de MFC

Les films de PVA_L avec ou sans MFC sont représentés Figure 16. Visuellement, les films paraissent homogènes bien que l'introduction de MFC entraîne une légère diminution de la transparence. Ceci est confirmé par l'observation de la coupe des films en MEB où aucune aggrégation n'est observée indiquant une bonne distribution des MFC au sein de la matrice PVA_L.

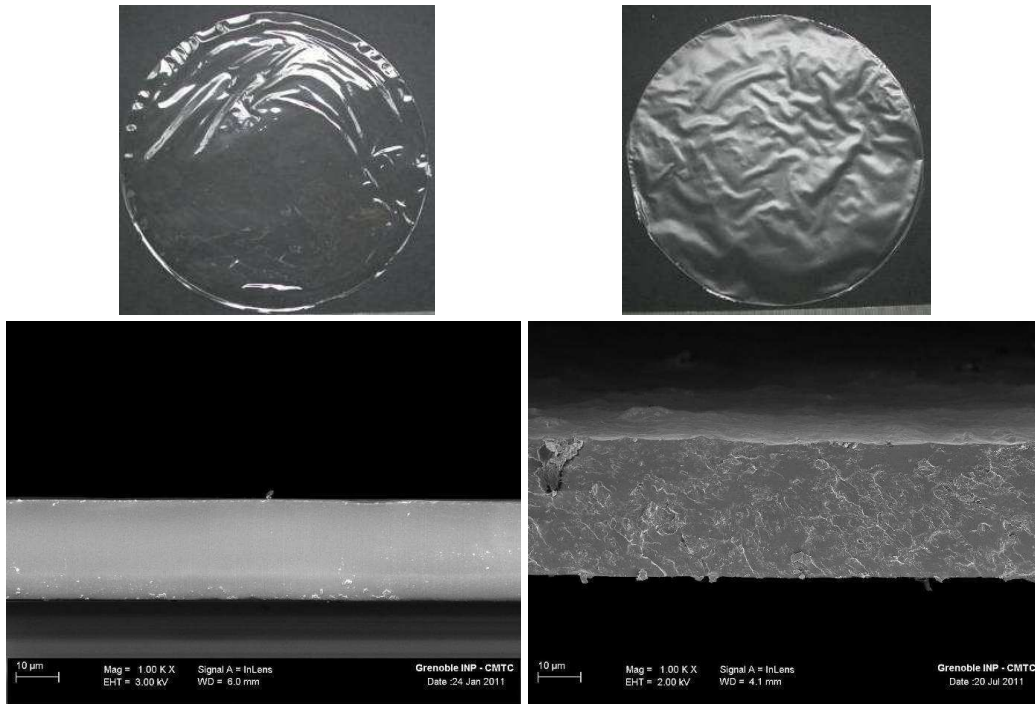


Figure 16 : Photos et image MEB de la coupe de films PVA_L (gauche) et PVA_L/MFC (95/5)(droite).

Les mêmes observations ont été faites avec les composites à base d'amidon (Figure 17). Ici, des images au microscope optique à lumière polarisée permettent la mise en relief des parties cristallines des MFC. Une nouvelle fois, cette technique montre la bonne dispersion des MFC dans la matrice et l'homogénéité du composite.

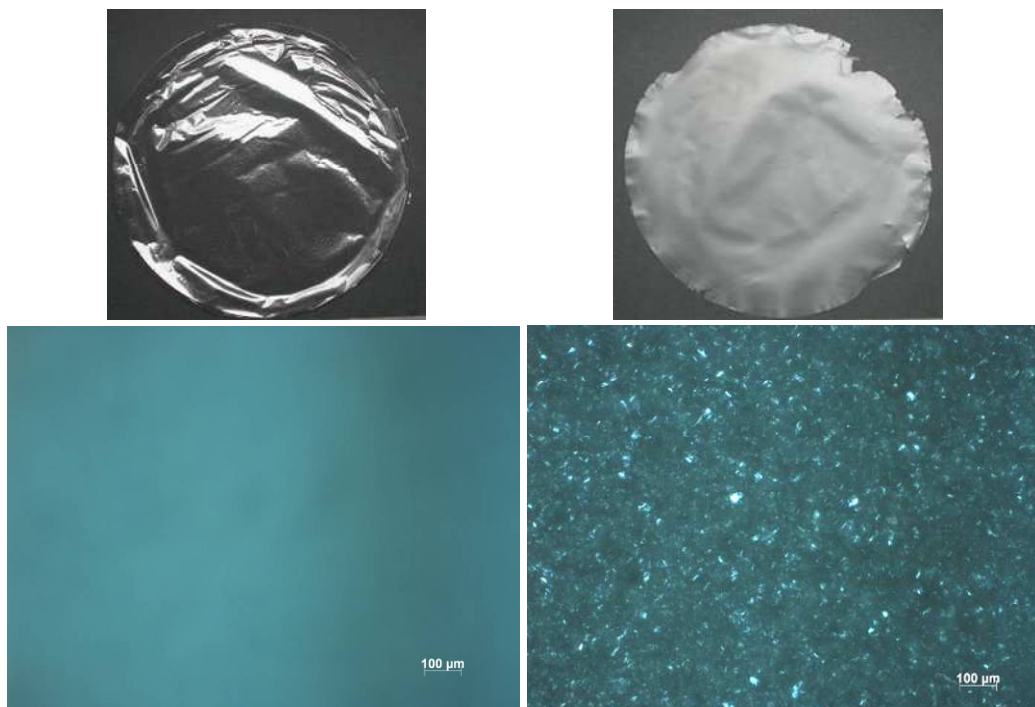


Figure 17 : Photos et image de microscopie optique à lumière polarisée de films d'amidon et d'amidon/MFC (95/5).

2.2.2. - Influence des MFC sur la résistance à la traction des matrices

Les valeurs de module de Young des matrices PVA_L et amidon, décrites Figure 18, sont déterminées en fonction du pourcentage de MFC introduit.

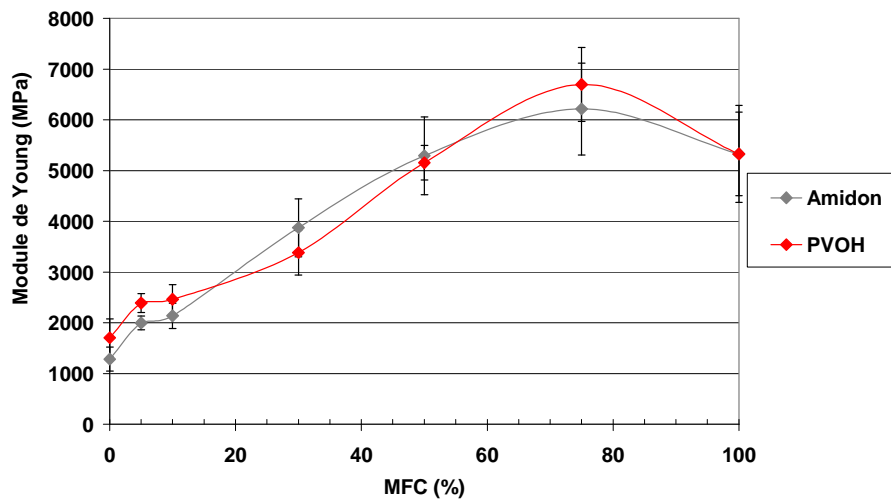


Figure 18: Module de Young des films composite PVA_L/MFC et Amidon/MFC.

Un effet de renfort est clairement observé pour les deux matrices lors de l'ajout des MFC. La résistance mécanique s'accroît en fonction du taux des MFC et quel que soit ce taux. Cet effet est dû à deux phénomènes majeurs : les interactions entre microfibrilles avec la formation d'un réseau et les interactions polymère/MFC.

2.2.3. - Influence des MFC sur les propriétés barrières des matrices

2.2.3.1. - WVTR 23°C-50%HR

Les propriétés barrières à la vapeur d'eau de l'amidon et du PVA_L sont très différentes comme observé Figure 19.

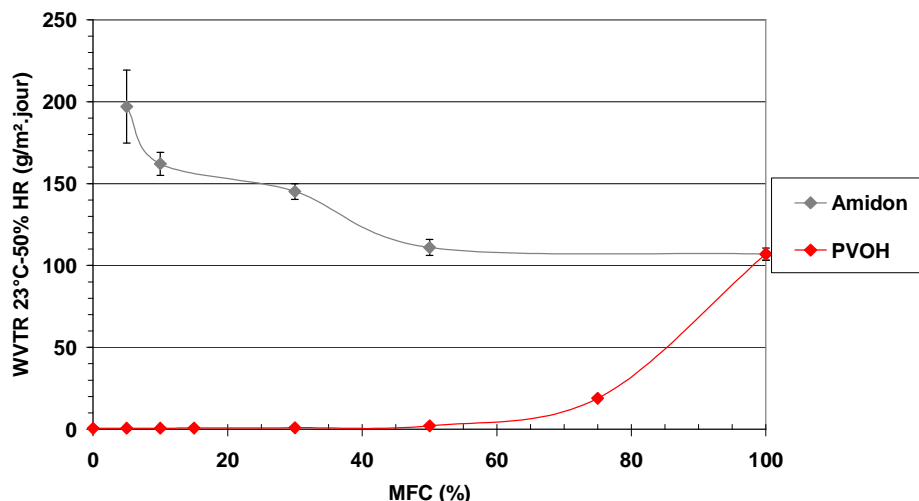


Figure 19: WVTR 23°C-50% RH des matrices en fonction du taux de MFC.

Le PVA_L montre une très faible perméabilité à la vapeur d'eau en condition ambiante. L'introduction de MFC permet de conserver ces valeurs jusqu'à un taux atteignant 30% en MFC. Au-dessus de ce taux, une dégradation des propriétés est observée. La matrice

amidon et sa faible cristallinité montrent des propriétés barrières à la vapeur d'eau plus modérées. L'ajout de MFC montre alors un effet positif en divisant quasiment la valeur par 2 avec un mélange amidon/MFC (50/50).

Le PVA_L est un film barrière sensible à l'humidité et ses propriétés sont dégradées en condition tropicale (38°C-90% HR). Toutefois, l'ajout de MFC permet d'améliorer cette propriété pour un taux de MFC inférieur à 30%. Une nouvelle fois, lorsque le taux en MFC est très important une dégradation des propriétés est observée.

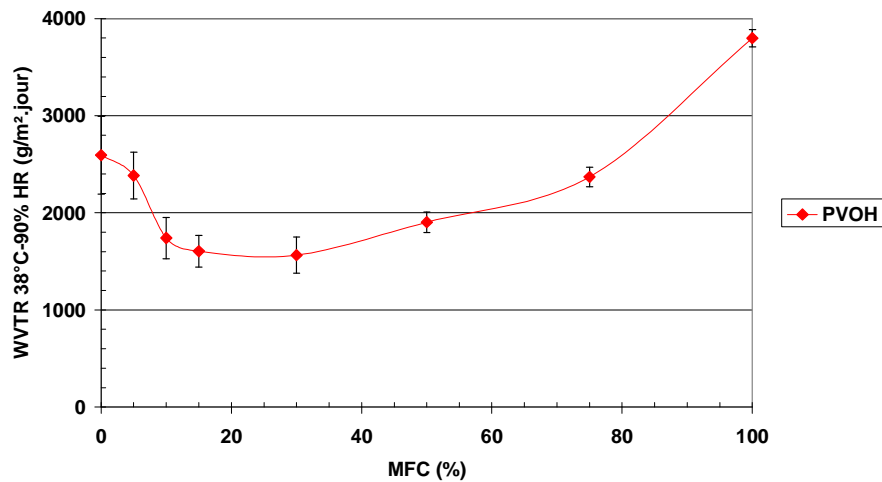


Figure 20: WVTR 38°C-90% RH du PVA_L en fonction du taux de MFC.

Les valeurs de perméabilité à l'oxygène (Figure 21) confirment que le PVA_L permet d'obtenir de meilleures propriétés barrières comparé à l'amidon. L'ajout de MFC dans le PVA_L influence peu les valeurs et permet de conserver les bonnes propriétés barrières tout en améliorant leurs propriétés mécaniques.

Concentration en MFC	Amidon (cm ³ .µm/m ² .jour.bar)	PVA _L (cm ³ .µm/m ² .jour.bar)
0%	-	18 - 27
5%	-	16 - 29
10%	-	19 - 35
50%	125	21 - 45

Figure 21: OTR 38°C-90% RH des matrices en fonction du taux de MFC.

2.3. - Conclusion

Au cours de cette étude, des films composites polymère/MFC ont été élaborés par coulée/évaporation afin d'obtenir une bonne distribution des MFC au sein des deux matrices. L'ajout de MFC a permis d'améliorer les propriétés des deux matrices avec tout d'abord une augmentation de leur résistance mécanique grâce à une augmentation de leur module de Young. Il a ainsi été possible de réaliser des films d'amidons sans plastifiants qui sont généralement néfastes pour les propriétés barrières. Une amélioration des propriétés barrières a été démontrée lors de l'ajout de MFC et notamment sur le coefficient de

transmission à la vapeur d'eau. Concernant la matrice PVA_L, les composites les plus performants restaient ceux ayant un ratio inférieur à 30%.

Le système PVA_L/MFC s'est révélé être le plus performant au niveau de la barrière et a ainsi été sélectionné pour les essais d'enduction afin de développer cette couche à la surface d'un carton et produire un emballage carton barrière.

3. - Développement d'un emballage carton barrière à partir d'un mélange PVA_L/MFC

3.1. - Introduction

L'utilisation des microfibrilles de cellulose dans des procédés de couchage est un véritable challenge à cause de leur faible concentration (2%) associée à une viscosité élevée entraînant des poids de couche déposés très faibles et un coût d'énergie de séchage très important. Comme observé précédemment avec le développement de composite PVA_L/MFC, l'utilisation du PVA_L permet de développer des couches barrières et offre la possibilité d'augmenter la matière sèche initiale des formulations. Cette partie étudie la machinabilité d'enduire des couches PVA_L/MFC à la surface d'un carton afin de lui conférer des propriétés barrières. De plus, un démonstrateur a été produit à l'échelle pilote à partir d'un carton et de deux couches comme décrit (Figure 22): la première est une combinaison PVA_L/MFC correspondant à une couche barrière aux graisses et à l'oxygène, la seconde réalisée à partir d'un latex commercial apportant la résistance à l'eau.

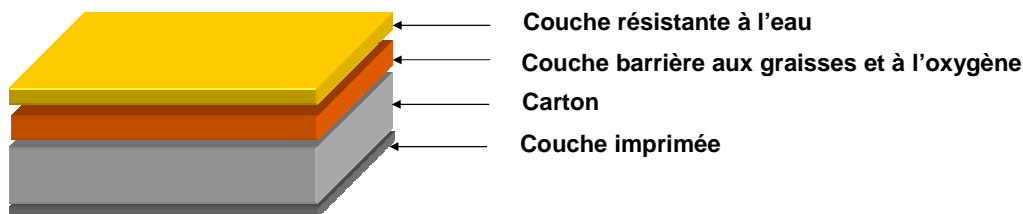


Figure 22: Design du démonstrateur.

3.2. - Matériels et méthodes

3.2.1. - Matériels

Les couches barrières ont été déposées sur des bobines de carton couché fournies par Stora Enso (Ensocoat 182 g/m² sec).

La pré-couche est composée de MFC introduites dans une matrice PVA_L à deux concentrations différentes 5 et 9%. Les MFC sont obtenues à partir d'un prétraitement enzymatique et de plusieurs passages dans un homogénéiseur GEA.

Cette pré-couche barrière étant sensible à l'eau, 5-7g/m² d'un latex commercial sont déposés en top couche afin d'apporter de la résistance à l'eau au matériau final.

3.2.2. - Méthodes

3.2.2.1. - Préparation de la sauce de couchage

L'introduction de MFC à 2% dans une solution de PVA_L entraîne une forte réduction de la concentration finale. Afin d'atteindre la concentration la plus haute possible, la solution retenue fût de dissoudre directement les granules de PVA_L dans la suspension de MFC comme décrit Figure 23.

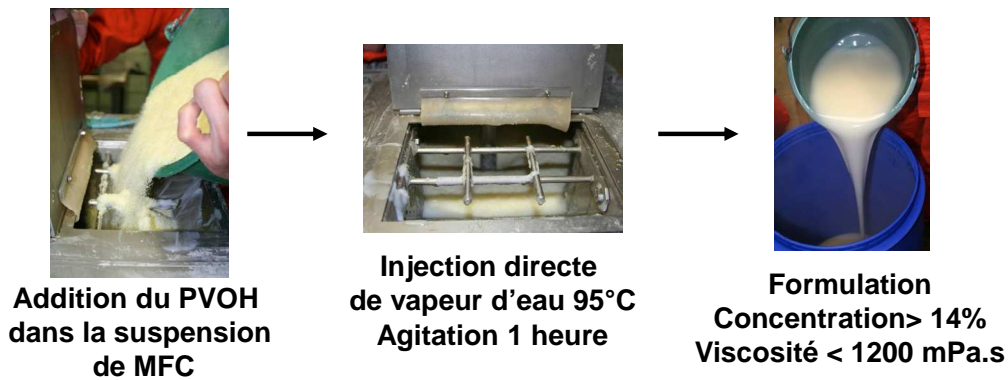


Figure 23: Préparation de la sauce de couchage.

3.2.2.2. - Essais d'enduction à l'échelle pilote

Les échantillons ont été produits sur le pilote de couchage du CTP (Figure 24). Les deux couches ont été déposées en utilisant une Soft-Tip blade à une vitesse de 70 m/min.

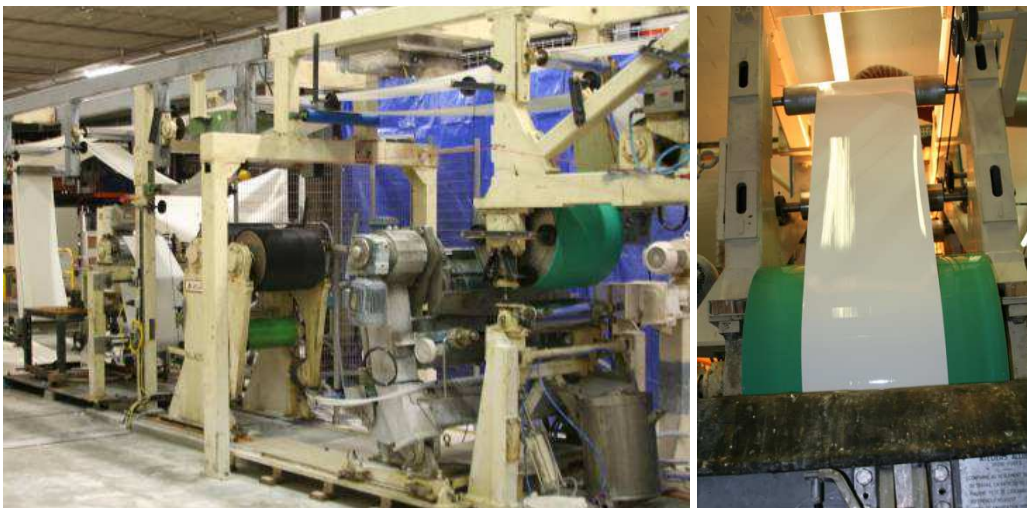


Figure 24 : Pilote de couchage du CTP.

3.2.2.3. - Caractérisation des échantillons

Les propriétés barrières suivantes ont été déterminées pour chaque échantillon :

Le coefficient d'absorption d'eau en utilisant la méthode classique du Cobb60 réalisée suivant la norme ISO535 mesurant l'eau absorbée par 1 m² de papier en 60 secondes.

La résistance à la graisse est évaluée à 23°C-50% HR en utilisant la méthode du Cobb mais en remplaçant l'eau par de l'huile d'arachide colorée. La résistance à la graisse correspond à la masse d'huile absorbée par 1m² de papier en 24 heures.

Les méthodes utilisées pour mesurer la perméabilité à la vapeur d'eau ainsi que la perméabilité à l'oxygène ont été préalablement décrites ci-dessus.

3.3. - Résultats et discussion

3.3.1. - Propriétés barrière de la couche PVA_L/MFC

3.3.1.1. - Photos MEB des cartons couchés

Les échantillons avec une couche barrière de PVA_L seule étaient très difficiles à produire. En effet, le PVA_L est un matériau très filmogène et la stratégie de séchage appropriée est très difficile à obtenir. Des phénomènes de cloquage étaient ainsi observés sur la plupart des échantillons entraînant de faibles propriétés barrières (Figure 25).

Lors de l'ajout de MFC dans la matrice de PVA_L, le séchage de la couche est grandement amélioré et le nombre de cloque est fortement réduit. L'utilisation de MFC améliore ainsi la machinabilité et la productivité.

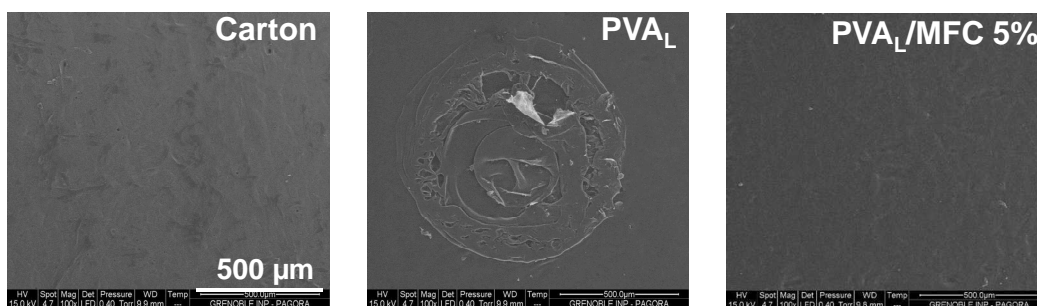


Figure 25 : Photos MEB – Effet de cloquage sur les cartons couchés PVA_L.

3.3.1.2. - Résistance à la graisse

Un exemple de résultat obtenu après mesure de la résistance aux graisses est donné Figure 26.



Figure 26 : Résistance à la graisse des couches PVA_L/MFC.

Après exposition d'huile colorée pendant 24h, le papier support est totalement rouge, montrant que l'huile a largement pénétré à l'intérieur du papier. A l'inverse, tous les cartons couchés PVA_L/MFC restent blancs, prouvant la forte résistance à la graisse de ces couches.

3.3.1.3. - Coefficient de transmission à l'oxygène

Les valeurs de transmission à l'oxygène sont données Figure 27. Les résultats montrent clairement le problème de cloquage rencontré avec les couches de PVA_L seul. En effet, le

PVA_L est connu pour être une bonne barrière à l'oxygène, or ici la valeur obtenue pour 10 g/m² de PVA_L déposés à la surface du carton est vraiment élevée avec une valeur d'environ 600 cm³/m².jour.bar. Dès que les MFC sont introduites dans la couche, la machinabilité, le séchage et ainsi la barrière à l'oxygène sont améliorés avec des valeurs d'OTR d'environ 5 cm³/m².jour.bar.

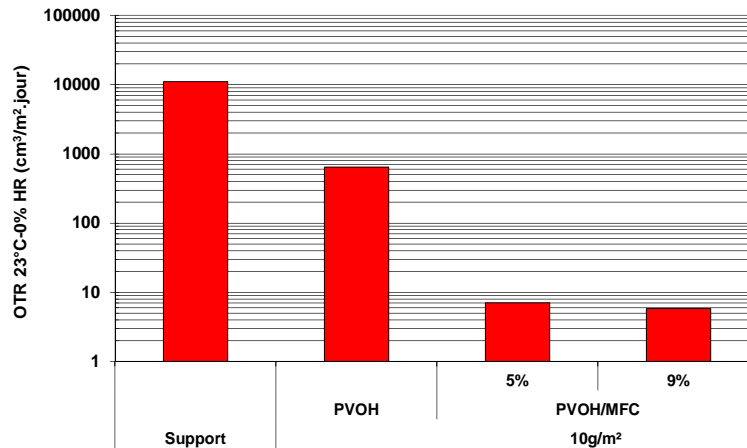


Figure 27: OTR à 23°C-0% HR.

3.3.2. - Propriétés barrières du démonstrateur final

Afin de protéger la couche barrière, un latex commercial est utilisé pour apporter de la résistance à l'eau et à la vapeur d'eau.

3.3.2.1. - Adsorption d'eau

Comme espéré, la couche barrière joue bien son rôle de protection, le coefficient d'adsorption d'eau est fortement réduit après enduction de la top couche signifiant une bonne résistance à l'eau. La valeur du Cobb60 est en effet relativement faible avec une valeur de 1 g/m² comme observé Figure 28.

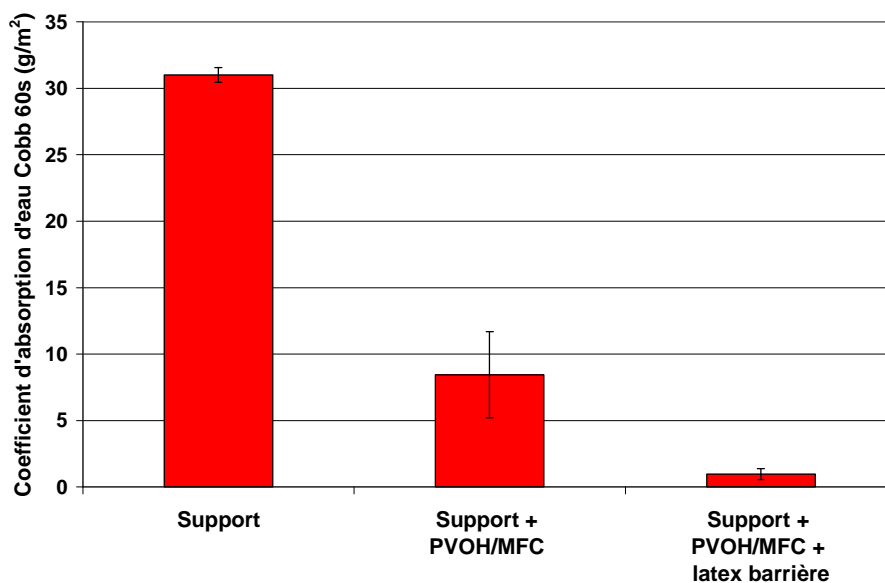


Figure 28 : Résistance à l'eau d'emballage carton final.

3.3.2.2. - Coefficient de transmission à la vapeur d'eau (WVTR)

Tout comme pour la résistance à l'eau, la couche barrière latex joue également un rôle sur la perméabilité à la vapeur d'eau et particulièrement à 90% HR (cf. Figure 29 & Figure 30) .

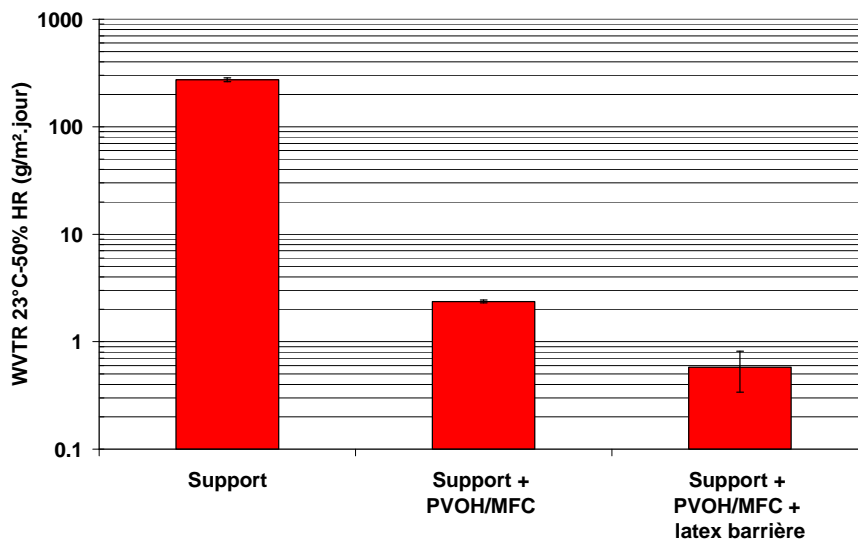


Figure 29 : Coefficient de transmission à la vapeur d'eau à 23°C-50% HR de l'emballage carton final.

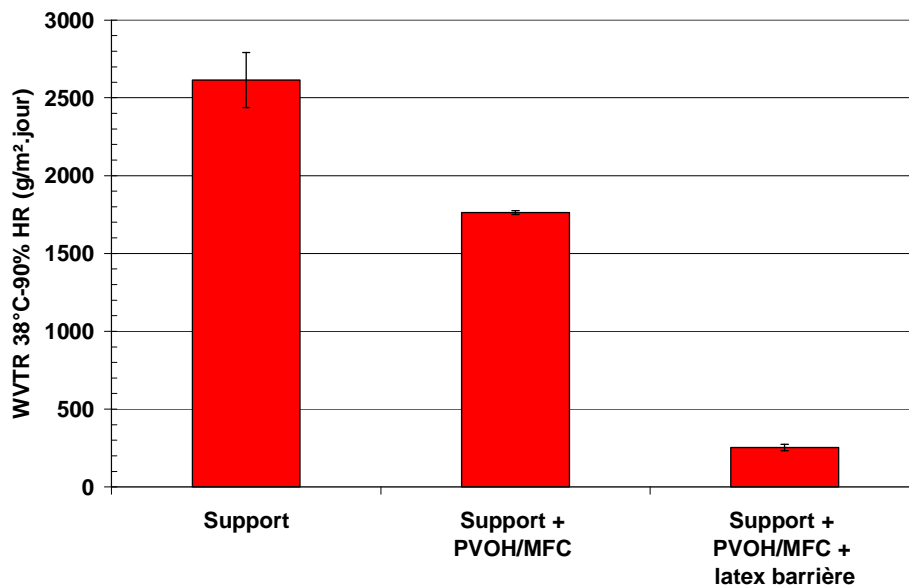


Figure 30 : Coefficient de transmission à la vapeur d'eau à 38°C-90% HR de l'emballage carton final.

La top couche permet ainsi de diminuer le WVTR des cartons précouchés PVA_L/MFC et notamment en condition tropicale où la valeur diminue de 1700 à 250 g/m².jour. Toutefois, les deux couches sont complémentaires et nécessaires pour obtenir une bonne barrière au gaz, à la graisse et à l'eau.

Les travaux réalisés dans cette étude ont ainsi permis de démontrer, à l'échelle pilote la production d'un emballage carton présentant de bonnes propriétés barrières comme résumé dans le tableau .

Propriétés barrières	Carton de référence	Objectif du projet
Coeff. de transmission à la vapeur d'eau @ 23°C-50%RH « Perméabilité »	0.6 g/m ² /jour	<0.5 g/m ² /jour
Coeff. de transmission à la vapeur d'eau @ 38°C 90%RH « Perméabilité »	1250 g/m ² /jour	<100 g/m ² /jour
Solubilité de la couche (exposition à l'eau de 60s)	5%	<1%
Coeff. de transmission à l'oxygène @ 23°C-0%RH « Perméabilité »	6 cm ³ /m ² /jour	<5 cm ³ /m ² /jour
Absorption d'huile (exposition type Cobb 24h)	2g/m ²	<2g/m ²

Figure 31 : Propriétés des cartons couchés produits par enduction.

3.4. - Conclusion

Durant ce projet, la possibilité d'utiliser les MFC dans des procédés de couchage a été démontrée à l'échelle pilote. Dans le domaine des couches barrières, aucune autre étude à l'échelle pilote n'avait été décrite précédemment dans la littérature.

La préparation de la sauce de couchage a été adaptée afin d'atteindre la concentration la plus élevée possible et de garantir des conditions de séchage acceptables sur le pilote de couchage. La solubilisation du PVA_L directement dans la suspension de MFC a permis une sauce de couchage homogène en une seule étape.

Concernant le procédé de couchage, l'utilisation d'une lame Soft-Tip a permis d'obtenir des cartons couchés avec une surface homogène et une bonne couverture. Des différences ont été observées au niveau du séchage en présence ou non de MFC. En effet, l'introduction de MFC réduit fortement les problèmes de cloquage observés lors de l'application de PVA_L seul. Il a ainsi été montré que la machinabilité et la productivité des essais pilotes avaient été fortement améliorées avec l'introduction de MFC dans les couches de PVA_L.

La couche barrière PVA_L/MFC a montré un bon niveau de barrière avec une forte résistance à la graisse, un faible coefficient de transmission à la vapeur d'eau et à l'oxygène. Cependant la couche présentant une sensibilité à l'eau, une topcouche composée d'un latex barrière a été ajoutée afin de protéger la couche PVA_L/MFC. Les propriétés barrières obtenues montrent des résultats proches des matériaux existants comme observé Figure 32.

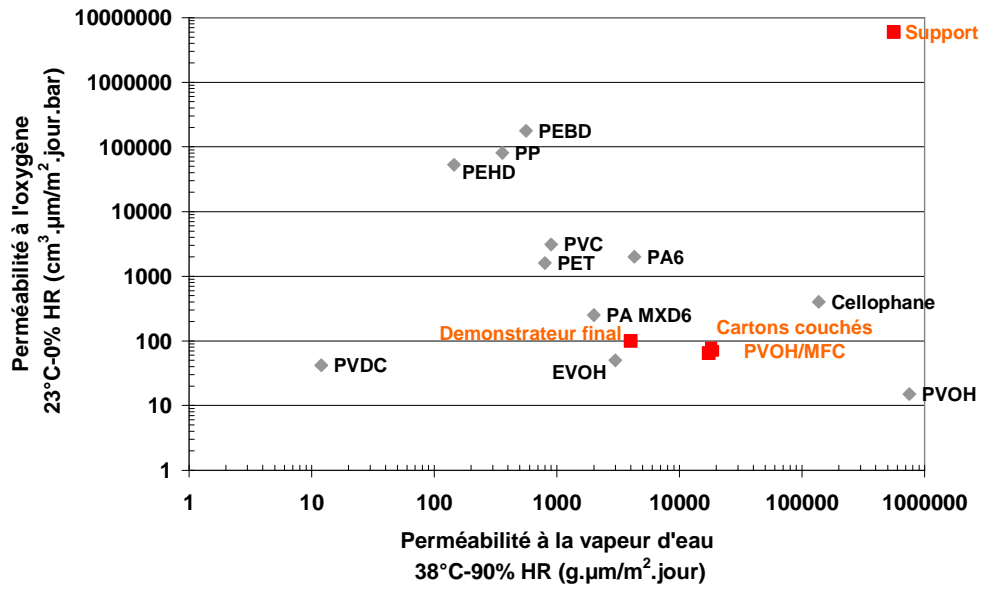


Figure 32: Propriétés barrières des matériaux existants.

Conclusion

Cette thèse a ainsi permis de mieux cerner les possibilités d'utilisation des MFC dans le domaine de l'emballage. Plusieurs grades de MFC ont été dans un premier temps étudiés afin de déterminer l'influence du degré de fibrillation sur les propriétés des suspensions mais également sur celles des films. Pour cela, des méthodes ont été développées afin de produire ces films de manière homogène et reproductible. Concernant les propriétés des films, le module de Young tout comme la perméabilité à l'oxygène montrent des valeurs intéressantes. Cependant, la résistance au déchirement et à l'eau restent leurs points faibles et devront être améliorées afin d'envisager un transfert à l'échelle industrielle. La seconde partie consacrée à l'élaboration de composites polymère/MFC a montré une bonne distribution des MFC au sein du film ainsi qu'une bonne synergie matrice/MFC. L'influence positive des MFC sur les propriétés des matrices a clairement été observée avec un effet renfort et une amélioration des propriétés barrières. De plus, l'association d'un polymère avec les MFC augmente la concentration à 15% permettant ainsi d'envisager une application par procédés d'enduction. Le système PVA_L/MFC montrant une plus grande performance au niveau des propriétés barrières a ainsi été testé dans une troisième partie sur le développement d'un carton barrière. Des formulations PVA_L/MFC ont donc pu être testées sur un procédé d'enduction afin de vérifier leur machinabilité. Une amélioration de la qualité du séchage a ainsi été observée au cours des essais pilote montrant le potentiel d'utilisation des MFC comme additif de séchage. Le démonstrateur obtenu montre des propriétés intéressantes avec une bonne barrière à l'oxygène, à la vapeur d'eau, à la graisse ainsi qu'à l'eau. On obtient ainsi des propriétés équivalentes à celles des matériaux plastique existants sur le marché avec une bonne biodégradabilité et compostabilité.

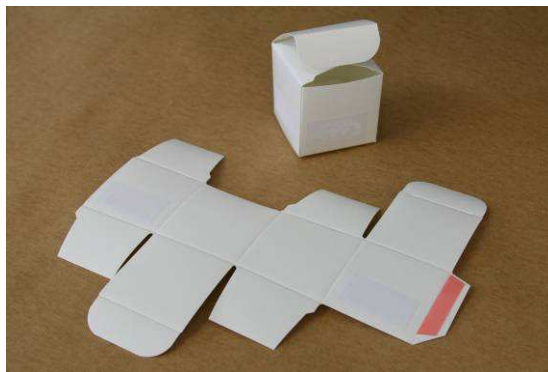


Figure 33 : Démonstrateur.

Des améliorations pourront tout de même être apportées afin de renforcer les propriétés et la résistance à l'eau de la couche PVA_L/MFC. De plus, l'évaluation de la performance après transformation fait partie des perspectives intéressantes à cette étude.

Références

- ¹ Turbak A.F., Snyder F.W., Sandberg K.R., "Microfibrillated cellulose, a new cellulose product: properties, uses and commercial potential", *Journal of Applied Polymer Science: Applied Polymer Symposia* 37 (1983):815-827.
- ² Da Silva Perez D., Tapin-Lingua S., Janodet A., Petit-Conil M., Dufresne A., "Nanofibres: Production of cellulose micro and nano-fibres: state of the art and first results", *5th Intechfibres Research Forum: Centre technique du Papier*, Grenoble (2009).
- ³ Herrick F.W., Casebier R.L., Hamilton J.K., Sandberg K.R., "Microfibrillated cellulose: morphology and accessibility.", *Journal of Applied Polymer Science: Applied Polymer Symposia* 37 (1983):797-813.
- ⁴ Dalle P., Girard F., "Mechanical and barrier properties of films made of cellulose micro and nano fibrils", Centre Technique du Papier: Grenoble (2009).
- ⁵ GEA Niro Soavi, http://www.nirosoavi.com/literature/pdfs/GEA_Niro_Soavi_Profile.pdf (june 2012).
- ⁶ Ultra-fine friction grinder "Supermasscolloider", Masuko Sangyo Co. Ltd., <http://www.masuko.com/English/company/Introduction.html> (june 2012).
- ⁷ Eichhorn S.J. *et al.*, "Review: current international research into cellulose nanofibres and nanocomposites," *Journal of Materials Science* 45, no. 1 (2010): 1-33.
- ⁸ Dufresne A., "Preparation of microfibrillated cellulose", *In Nanocellulose : From nature to high performance tailored materials*, De Gruyter : New-York and Berlin, chap 2 (2012).
- ⁹ Aulin C., Gällstedt M., Lindström T., "Oxygen and oil barrier properties of microfibrillated cellulose films and coatings," *Cellulose* 17, no. 3 (2010): 559-574.
- ¹⁰ Leitner L., Hinterstoisser B., Wastyn M., Keckes J., Gindl W., "Sugar beet cellulose nanofibril-reinforced composites," *Cellulose* 14, no. 5 (2007): 419-425.
- ¹¹ Syverud K., Stenius P., "Strength and barrier properties of MFC films," *Cellulose* 16, no. 1 (2009): 75-85.
- ¹² Svagan A.J., Azizi Samir A.S., Berglund L., "Biomimetic polysaccharide nanocomposites of high cellulose content and high toughness," *Biomacromolecules* 8, no. 8 (2007): 2556-2563.
- ¹³ Chun S.J., Lee S.Y., Doh G.H., Lee S., Kim J.H., "Preparation of ultrastrength nanopapers using cellulose nanofibrils", *Journal of Industrial and Engineering Chemistry* 17, no. 3 (2011): 521-526.
- ¹⁴ Nogi M., Iwamoto S., Nakagaito A.N., Yano H., "Optically Transparent Nanofiber Paper," *Advanced Materials* 21, no. 16 (2009): 1595-1598.
- ¹⁵ Fukuzumi H., Saito T., Iwata T., Kumamoto Y., Isogai A., "Transparent and high gas barrier films of cellulose nanofibers prepared by Tempo-mediated Oxidation," *Biomacromolecules* 10, no. 1 (2009): 162-165.

Développement de nouveaux matériaux d'emballage à base de micro- et nano-fibrilles de cellulose.

Les micro- et nano-fibrilles de cellulose (MFC/NFC) sont des nanomatériaux issus de ressources renouvelables présentant un fort intérêt notamment pour le domaine de l'emballage. En plus des avantages naturels de la cellulose, ces matériaux offrent des propriétés barrières prometteuses (Oxygène, graisse), de bonnes propriétés de résistance mécanique ainsi que la possibilité de produire des films transparents. L'objectif de cette thèse était de développer par des procédés d'enduction un carton barrière aux gaz et aux graisses en utilisant les MFC/NFC. Différentes suspensions de MFC/NFC ont été premièrement caractérisées puis utilisées pour la production de films afin de déterminer leurs propriétés intrinsèques. Des films modèles ont ensuite été développés avec la production de composites polymère/MFC. Une dernière partie était focalisée sur l'introduction de MFC/NFC dans des saucés de couchage afin de développer une couche barrière à la surface d'un carton. Un démonstrateur a ainsi été validé à l'échelle pilote. Le potentiel des MFC/NFC a été démontré comme agent de séchage et comme composant principale d'une couche barrière.

Mots clés: Micro- et nano-fibrilles de cellulose, couche barrières, procédés d'enduction

Development of new packaging materials based on micro- and nano-fibrillated cellulose.

The micro- and nanofibrillated cellulose (MFC/NFC) are nanomaterials from renewable resource with a high interest and partly for the packaging development. MFC combined both interesting properties (high tensile strength, good barrier to oxygen and grease, good transparency) and the advantages of natural cellulose source. The objective of this thesis was to develop a barrier packaging board based on MFC/NFC by coating processes. Firstly, the study focussed on the characterisation of the MFC suspensions, on the manufacturing of MFC self-standing films and on the determination of their properties. Secondly, the development of MFC based composites was studied as model films. The last part was devoted to the introduction of MFC in coating colours in order to develop a barrier layer at the board surface. Trials at pilot scale demonstrated the industrial feasibility of this product. The potential of the use of MFC/NFC was demonstrated to be used as a drying additive and a main component of barrier layer.

Keywords: Micro- and nanofibrillated cellulose, barrier layer, coating processes